INFORMATION TO USERS

The most advanced technology has been used to photograph and reproduce this manuscript from the microfilm master. UMI films the original text directly from the copy submitted. Thus, some dissertation copies are in typewriter face, while others may be from a computer printer.

In the unlikely event that the author did not send UMI a complete manuscript and there are missing pages, these will be noted. Also, if unauthorized copyrighted material had to be removed, a note will indicate the deletion.

Oversize materials (e.g., maps, drawings, charts) are reproduced by sectioning the original, beginning at the upper left-hand corner and continuing from left to right in equal sections with small overlaps. Each oversize page is available as one exposure on a standard 35 mm slide or as a 17″ × 23″ black and white photographic print for an additional charge.

Photographs included in the original manuscript have been reproduced xerographically in this copy. 35 mm slides or 6″ × 9″ black and white photographic prints are available for any photographs or illustrations appearing in this copy for an additional charge. Contact UMI directly to order.

Accessing the World's Information since 1938

300 North Zeeb Road, Ann Arbor, MI 48106-1346 USA

Order Number 8821083

^{31}P NMR studies of anchorage-dependent neural-type cells in tissue culture

Glynn, Paul, Ph.D.

City University of New York, 1988

Copyright ©1988 by Glynn, Paul. All rights reserved.

U·M·I
300 N. Zeeb Rd.
Ann Arbor, MI 48106

PLEASE NOTE:

In all cases this material has been filmed in the best possible way from the available copy. Problems encountered with this document have been identified here with a check mark __✓__.

1. Glossy photographs or pages ✓
2. Colored illustrations, paper or print _____
3. Photographs with dark background ✓
4. Illustrations are poor copy _____
5. Pages with black marks, not original copy _____
6. Print shows through as there is text on both sides of page _____
7. Indistinct, broken or small print on several pages ✓
8. Print exceeds margin requirements _____
9. Tightly bound copy with print lost in spine _____
10. Computer printout pages with indistinct print _____
11. Page(s) _____ lacking when material received, and not available from school or author.
12. Page(s) _____ seem to be missing in numbering only as text follows.
13. Two pages numbered _____. Text follows.
14. Curling and wrinkled pages ✓
15. Dissertation contains pages with print at a slant, filmed as received _____
16. Other _____

_____

_____

U·M·I

^{31}P NMR Studies of Anchorage-Dependent Neural-Type Cells in Tissue Culture

by

Paul Glynn

A dissertation submitted to the Graduate Faculty in Biology in partial fulfillment of the requirements for the degree of Doctor of Philosophy, The City University of New York.

1988

COPYRIGHT BY
PAUL GLYNN
1988

This manuscript has been read and accepted for the Graduate Faculty in Biology in satisfaction of the dissertation requirement for the degree of Doctor of Philosophy.

3/15/88
date

Chairman of Examining Committee
Dr. Richard Chappell, Hunter College

April 27, 1988
date

Executive Officer
Prof. Peter C. Chabora

Dr. Katherine Lyser, Hunter College

Dr. Harvey Ozer, Hunter College

Dr. Seiji Ogawa, AT&T Bell Laboratories

Dr. Truman Brown, Fox Chase Cancer Center

Dr. K. Ugurbil, University of Minnesota

Supervisory Committee

The City University of New York

ABSTRACT

A ^{31}P NMR probe and microcarrier-based life-support system were built to measure NMR spectra of anchorage-dependent cells in a tissue-culture environment and to study development and metabolic processes in N1E-115 neuroblastoma, C6 glioma, dissociated rat brain cells (DRBC) and C3HT10½ fibroblast cells. Development changes were found in the phosphoethanolamine (PEt) and phosphocholine (PCh). Creatine kinase activity was found in DRBC, C6 glioma cells, and in differentiated and undifferentiated cells. The uptake of creatine into these cells was extremely slow under physiological conditions.

A major finding of this work centered around the creatine kinase reaction and the observed changes in the cell Pi, PCr, and ATP when the cells were subjected to an external pH jump. Measurements of these values, and determination of the PCr/Cr ratio from ^{1}H and ^{31}P spectra of the cell extracts allowed the phosphate potential to be calculated. This important parameter had not been unambiguously measured in live, intact cells in tissue culture.

DRBC showed a higher creatine kinase activity in the range of 0.07 to 0.09 S^{-1} comparable to *in vivo* measurements made on rat brains. C6 glioma cells were found to have creatine kinase activity and to take up extracellular creatine. Undifferentiated neuroblastoma cells with high PCr when stressed with an ischemic episode showed that depleted ATP and PCr concentrations recovered to near preischemic value in a fixed pattern dependent on the time of the ischemic episode. Stress of depolarization resulting from addition of

potassium chloride (final concentration 90 mM) to the extracellular medium were also studied.

ACKNOWLEDGEMENTS

I wish to acknowledge Dr. Seiji Ogawa for his insightful comments, his contributions to the NMR aspects of this work, and for his unending patience.

I would also like to thank Dr. Robert G. Shulman for introducing me to NMR, Dr. Kamil Ugurbil and Dr. Truman R. Brown, who taught me NMR in biology, and Dr. Angelo L. Lamola for supporting much of the work presented here, which was done in his NMR facility at AT&T Bell Laboratories.

Thanks to Dr. Harvey Ozer and Dr. Katherine Lyser for their help with cell and tissue culture work, and to Dr. Z. Ahmed for teaching me the brain cell culture techniques which are presented in Appendix A.

I am also indebted to Columbia University for allowing me to use their Bruker 300 wide-bore NMR spectrometer, and to Hunter College for the use of their NMR facility.

Dr. Richard L. Chappell has been far more than an advisor to me. Since my first undergraduate courses, he has shared his knowledge with eagerness; his enthusiasm for science has been a constant source of inspiration. I feel extremely fortunate to have been his graduate student.

DEDICATION

To my wife and children

and

to my parents

CONTENTS

TABLES

FIGURES

^{31}P NMR Studies of Anchorage-Dependent Neural-Type Cells in Tissue Culture

1. INTRODUCTION

High field NMR spectroscopy is just starting to be used in tissue culture systems. This thesis describes the first system which was constructed to allow anchorage-dependent cells to be studied in high-field ^{31}P NMR spectroscopy and the subsequent use of the system for studying four cell strains, C6 glioma, differentiated and undifferentiated N1E-115 cells, and CH3T10½ fibroblast cells, and one primary culture, dissociated rat brain cells (Uburgil, et al., 1981). There have been numerous studies on whole perfused organs (Gadian, et al., 1976) and anaerobic cell suspensions. An effort at keeping aerobic cell systems adequately supplied with oxygen at physiological temperatures was first attempted using hydrogen peroxide and the cell's endogenous peroxidase as an oxygen source (Cohen, S., et al., 1979). This worked well for short periods of time at 20 ° C with rat hypatic cells, but the cells eventually were destroyed by the high concentrations of the hydrogen peroxide. This led to the development of a microcarrier-based system for cell growth and a solenoid coil probe for the spectrometer. The first test of this system used C3HT10½ cells, normal and transformed, in a narrow-bore 360 MHz Bruker spectrometer. Capabilities were improved by using a 300 MHz wide-bore magnet with a better probe design. Additional improvement was achieved by using a wide bore Bruker 360 MHz system.

The microcarriers are spheres made in a variety of materials. They are nominally 150 μm in diameter and have surface properties which are conducive to cell adhesion and growth (Pharmacia, 1981). A small volume of these microcarriers gives a very large surface area for cell attachment. When placed in a suitable container, they may be superfused with nutritive medium conditioned to supply a suitable environment for cell growth. By using a solenoid coil with the cells contained in its core, a ^{31}P NMR probe was constructed to give a two-and-one-half times improvement in signal-to-noise over the conventional Helmholtz coil probe. This proved to be the difference which made the problem tractable on the Bruker 360 narrow-bore spectrometer.

After the system's development with the robust fibroblast, C3HT10½ cell line, the N1E-115 neuroblastoma, C6 glioma, dissociated fetal rat brain cells E16-E21, and rat brain cells P21-P23 were studied. The P21-P23 cells were grown on defined medium which supported neuronal but not glia or fibroblast growth. The N1E-115 and C6 cells were chosen because they can be induced to differentiate morphologically and biochemically into adrenergic type neurons and astrocytes, respectively, and represent a good model system for studying biochemical events in the nervous system. The thought was to initiate a series of studies which would be fundamental to the study of model cell systems, dissociated brain cells, brain slices or minces, and finally surface coil studies of the brain *in vivo*. Starting with the homogeneous model cell cultures it should be possible to progress to the whole animal with each step providing some insights with which to bridge the steps between the experimental systems and

suggesting relevant questions to be answered by the next more complicated system. The initial question asked was: How do these cell systems respond to large energy demands placed on them? Particularly, what happens to the adenosine triphosphate (ATP) levels when the cells are subjected to ischemic episode, global depolarization by the addition of a high concentration of potassium to the medium or the impeding of glycolysis by addition of 2-deoxy-D-glucose (2DG)? The unexpected finding that the N1E-115 cells, C6 cells and dissociated rat brain cells which had been in culture under standard conditions identical to those found in the literature had virtually no phosphocreatine (PCr) in their ^{31}P NMR spectra prompted me to supplement the growth medium with creatine and to study the PCr which was subsequently seen to appear in the cells, in terms of transport of creatine into the cells, kinetics of the creatine kinase reaction and other factors such as pH, glucose and oxygen availability.

The same studies were also made of the N1E-115 cells during and after they were induced to differentiate with dimethyl sulfoxide (DMSO). In addition to changes in the creatine-associated functions, dramatic changes in the phosphoethanolamine (PEt) and phosphocholine (PC) pools were found.

Since a good portion of this thesis is the detailing of a novel experimental technique for tissue culture, the material is divided into two parts. The first portion deals with the principle of ^{31}P NMR presented in a manner to promote understanding of the principles and limitations in general terms. The examples for the most part are drawn from experimental results I have obtained in dealing with bacteria, mitochondria and cells. This section also presents the

design and performance of probes, cell holders and life-support systems used with each of the three magnets used to develop the apparatus. The second part presents the background of the cell systems used, their characteristics on microcarrier systems, experiments performed and results obtained with interpretive discussion.

2. NMR IN BIOLOGY AND TISSUE CULTURE

NMR has made an impact on all areas of biology in solution biochemistry, organelles, cell systems, organs and whole intact organisms. In this section the history of NMR is traced from its inception to its application to tissue culture systems, and then a brief description of NMR principles is presented with a short bibliography aimed at helping the reader to understand the research presented here.

2.1 History

In 1938 Rabi performed the first experiment demonstrating magnetic moments (Rabi, 1938). This was done by having a molecular beam of LiCl molecules traverse a magnetic field. They made the first direct measurement of the nuclear magnetic moments of Li and Cl. The first condensed matter experiments were done almost ten years later on wax by Purcell et al. (1946) and on water by Bloch and coworkers in the same year (See Table 1) (Bloch, et al., 1946).

NMR's entry into biology can best be attributed to Cohn and Hughes (1962) when they showed that a signal could be obtained from 0.1M adenosine triphosphate (ATP) and adenosine diphosphate (ADP) solutions. It was not until 1973, however, that NMR was applied to cell biology. At this time Moon and Richards (1973) showed that 40 MHz spectrum of erythrocytes allowed one to observe the two ^{31}P NMR peaks of 2,3 diphosphoglycerate (2,3 -DPG) as well as two peaks from intracellular and extracellular inorganic orthophosphate (Pi).

It was possible from these two spectral peaks to distinguish the intracellular and extracellular pH's. The next year, Hoult, Busby, Gadian, Radda, Richards and Seeley (Hoult, et al., 1974) showed that ^{31}P NMR spectra could be obtained from intact biological tissue, namely rat hind leg muscle.

The first intact eucaryote, baker's yeast, was looked at in 1975 by Salhany, Yamane, Ogawa, and Shulman (Salhany, et al., 1975). They saw polyphosphate peaks from long chain or cyclic polyphosphates, a result consistent with suggestions that these polyphosphates act as a phosphate store in yeast. They also measured the cytoplasmic pH to be 6.3, a value considerably higher than the acidic environment in which they live.

In 1976, Navon, Ogawa, Shulman and Yamane (Navon, et al., 1976) gave strong support to the chemiosmotic hypothesis by measuring the pH gradient across the E. coli cell membrane during respiration with succinate as a carbon source, in a nitrogen environment and in a glucose-supplemented medium with and without oxygen. NMR allowed observations to be made continuously and in a nonintrusive way. In the same year they demonstrated the utility of ^{31}P NMR in studying cells in suspension – in this case a tumor cell.

In 1976, Gadian, Hoult, Radda, Seeley, Chance and Barlow (Gadian, et al., 1976) reported the first organ, an excised rat heart at 4 °C. In the next year, Jacobus, Taylor, Hollis and Nunnally (Jacobus, et al., 1977) reported results on perfused heart. The first work on isolated organelles was reported in 1977 by Casey, Njus, Radda, and Sehr (Casey, et al., 1977), where they presented

evidence indicating that the chromaffin granule membrane possessed an electrogenic proton pump directed inward.

In 1978 Ogawa showed by synchronizing the NMR data acquisitions with 3-second bursts of oxygen that it is possible to measure the internal pH with a time resolution of 1 second (Ogawa, et al., 1978). Also in 1978, the first ^{31}P NMR experiments with isolated rat liver mitochondria were reported (Ogawa, et al., 1978). The actual phosphorylation of external ADP to ATP by mitochondria in an NMR sample was observed when the mitochondrial suspension was oxygenated in the presence of succinate and ADP via added H_2O_2 and indogenous catalase.

In the rat liver cell suspension, both the mitochondrial and cytosolic pH values in the respiring cells were seen for the first time (Cohen, et al., 1978). These cells were at 4 °C and were oxygenated with H_2O_2 via indogenous catalase. In the same year the first ^{13}C experiment in E. coli cells was also reported (Ugurbil, et al., 1978), and in 1979, Cohen (Cohen, et al., 1979) reported the same in rat liver cells. In 1981, the first experiments with anchorage-dependent cells in tissue culture were reported (Ugurbil, et al., 1981). In 1982, ^{19}F NMR was first used for pH measurements in cells, and protons were used to identify metabolites of cells in suspension (Deutsch, et al., 1982). In 1983, ^{19}F NMR was used to measure intracellular calcium (Smith, et al., 1983), and ^{31}P NMR experiments were done on anchored neuroblastoma cells in tissue culture (Glynn, et al. 1983). In 1984 and 1985 similar data for dissociated rat brain cells were reported as well (Glynn, et al., 1983). In the same year ^{39}K and

^{23}Na and ^{31}P NMR studies of ion transport and intracellular pH in yeast were reported by Ogino, et al. (Ogino, et al., 1983).

The system I have been using was the first reported in the literature in 1981, (Ugurbil, et al., 1981) but is not the only system in use today. There are at least two other systems which have been successfully used and reported, one using a cell and agar/collagen mixture (Foxall and Cohen, 1983). In this case, kidney dialysis fibers are immersed in the solution with cells, and are allowed to solidify with medium pumped through the tubing. Foxall and Cohen used this to study glucose metabolism in chicken embryo fibroblasts. Similarly, in 1983 Karczmar reported a high-density cell system (Karczmar, et al., 1983) where he used spaghetti-like strands of agar in which the cells were embedded.

TABLE 1 FIRST EXPERIMENTS OF THEIR TYPE

HISTORY

1939 *Molecular beam resonance experiment*

Rabi, I. I., Zacharias, J. R., Millman, S., Kusch, P. (1938). A new method of measuring nuclear magnetic moment. *Phys. Rev.* 53:318.

1946 *NMR of wax*

Purcell, E. M., Torrey, H. C., and Pound, R. V. (1946). *Phys. Rev.* 69:37.

NMR of water

Bloch, F., Hansen, W. W., and Packard, M. (1946). *Phys. Rev.*

69:127.

1960 *NMR measurements of chemical shifts of adenosine di- and triphosphate on 0.1 M solutions.*

Cohen, M. and Hughes, T. R., Jr. (1960). *J. biol. Chem.* 235:3250.

1973 *NMR of erythrocytes*

Moon, R. B. and Richards, J. H. (1973). Determination of intracellular pH by ^{31}P NMR magnetic resonance. *J. Biol. Chem.*, 248:276-7278.

1974 *NMR of tissue* (rat leg muscle)

Hoult, D., Busby, S. J. W., Gadian, D. G., Radda, G. K., Richards, R. E. and Seeley, P. J. (1974). Observation of tissue metabolites using ^{31}P NMR nuclear magnetic resonance. *Nature* 252:286-289.

1975 *NMR of yeast cells*

Salhany, J. M., Yamane, T., Shulman, R. G., and Ogawa, S. (1975). High resolution ^{31}P NMR nuclear magnetic resonance studies of intact yeast cells. *Proc. Nat. Acad. Sci. USA* 72:4966,4970.

1976 NMR of non-perfused organ (rat heart)

Gadian, D. G., Hoult, D. I., Radda, G. K., Seeley, P. J., Chance, B., and Barlow, C. (1976). Phosphorus nuclear magnetic resonance studies

on anoxic and ischemic cardiac tissue. *Proc. Natl. Acad. Sci. USA* 73:4446-4448.

NMR of E. Coli

Navon, G., Ogawa, S., Shulman, R. G., and Yamane, T. (1976). High-resolution ^{31}P NMR nuclear magnetic resonance studies of metabolism in aerobic escherichia coli cells. *Proc. Natl. Acad. Sci. USA.* 74:888-891.

NMR of Ehrlich ascites tumor cells

Navon, G., Ogawa, S., Shulman, R. G., and Yamane, T. (1976). ^{31}P NMR nuclear magnetic resonance studies of Ehrlich ascites tumor cells. *Proc. Natl. Acad. Sci. USA.* 74:87-91.

1977 *NMR of organelles*

Casey, R. P., Njus, D., Radda, G. K., and Sehr, P. A. (1977). Active proton uptake by chromaffin granules: observations by amine distribution and phosphorus — ^{31}P NMR techniques. *Biochem.* 16:972-976.

NMR of perfused heart

Jacobus, W. E., Taylor, G. J., Hollis, D. P., and Nunnally, R. L. (1977). *Nature* 263:756-758.

1978 *pH measurements made with one-second time resolution on E. Coli*

Ogawa, S., Shulman, R. G., Glynn, P., Yamane, T., and Navon, G. (1978). On the measurement of pH in escherichia coli by ^{31}P NMR nuclear magnetic resonance. *Biochim. Biophys. Acta* 502:45-50.

NMR with mitochondria

Ogawa, S., Rottenberg, H., Brown, T. R., Shulman, R. G., Castillo, C. L., and Glynn, P. (1978). High-resolution ^{31}P NMR nuclear magnetic resonance study of rat liver mitochondria. *Proc. Natl. Acad. Sci.* 75:1796-1800.

NMR of isolated rat liver cells in suspension

Cohen, S. M., Ogawa, S., Rottenberg, H., Glynn, P., Yamane, T., Brown, T. R., Shulman, R. G., and Williamson, J. R. (1978). ^{31}P NMR nuclear magnetic resonance studies of isolated rat liver cells. *Nature* 273:554-556.

NMR 13C of E. Coli

Ugurbil, K., Brown, T. R., Den Hollander, J. A., Glynn, P., and Shulman, R. G. (1978) High-resolution 13C nuclear magnetic resonance studies of glucose metabolism in escherichia coli. *Proc. Natl. Acad. Sci. USA.* 75:3742-3746.

1979 *NMR 13C of rat liver cells*

Cohen, S. M., Ogawa, S., and Shulman, R. G. (1979) 13C NMR studies of gluconeogenesis in rat liver cells: utilization of labeled glycerol by cells from euthyroid and hyperthyroid rats. *Proc. Natl. Acad. Sci. USA* 76:1603-1607.

1979 *NMR 13C of anchorage-dependent cells in tissue culture*

Ugurbil, K., Guernsey, D. L., Brown, T. R., Glynn, P., Tobkes, N., and Edelman, I. S. (1981) ^{31}P NMR NMR studies of intact anchorage dependent mouse embryo fibroblasts. *Proc. Natl. Acad. Sci. USA* 78:4843-4847.

1982 Deutsch, C., Taylor, J. S., and Wilson, D. F. (1982) Regulation of intracellular pH by human peripheral blood lymphocytes as measured by 19F NMR. *Proc. Natl. Acad. Sci. USA* 79:7944-7948.

1982 *Proton measurement of 12 amino acids and 19 other intermediary metabolites*

Agris, P. F. and Campbell, I. D. (1982) Proton nuclear magnetic resonance of intact friend leukemia cells: phosphorylcholine increase during differentiation. *Science* 216:1325:1327.

1983 *NMR of neuroblastoma in tissue culture*

Glynn, P., Brown, T. R., Ugurbil, K., and Chappell, R. (1983) Intracellular pH, 2 deoxyglucose and sugar phosphate profile changes in morphologically differentiating neuroblastoma NIE-115 cells. *Biophys. J.* 41:72a.

19F NMR calcium measurements

Smith, G. A., Hesketh, R. T., Metcalfe, J. C., Feeney, J., and Morris, P. G. (1983) Intracellular calcium measurements by 19F NMR of fluorine-labeled chelators. *Proc. Natl. Acad. Sci. USA* 80:7178-7182.

39K and 23Na NMR

Ogino, T., den Hollander, J. A., and Shulman, R. G. (1983) 39K, 23Na

and ^{31}P NMR studies of ion transport and intracellular pH in yeast. *Biophys. J.* 41:283a.

1984 *NMR of rat brain cells in tissue culture*

Glynn, P., Ogawa, S., Lee, T. M., Chappell, R., and Ahmed, Z. (1984) ^{31}P NMR Creatine phosphate in dissociated fetal rat brain and N1E115 neuroblastoma cells. 8th International Biophysics Congress (Abstract) p. 316.

1985 ^{31}P NMR *NMR of creatine kinase kinetics in rat brain cells in tissue culture*

Glynn, P., Ogawa, S., Lee, T. M., and Chappell, R. (1985) Developmental changes of creatine kinase and phosphomonoesters in N1E115 neuroblastoma, dissociated rat brain cells, and whole animal rat brains seen with ^{31}P NMR. *Biophys. J.* 47:370a.

2.2 Principles

Magnetic nuclei behave like microscopic bar magnets. In small molecules, in the absence of a magnetic field, spins are randomly oriented. Put them in a magnetic field with a field strength of B_0 and they assume orientations parallel and antiparallel to the field. These are quantum mechanically allowable states (shown in Fig. 1). They are tilted by an angle theta from the magnet use in these experiments and precess much like a top does in the earth's gravitational field. This precessional frequency is called the Larmor frequency. It is proportional to B_0. The proportionality constant is gamma, the magnetogyric ratio, an intrinsic property of each nuclear species. Note that ^{31}P has a ratio of 17.23. The field strength is 8.45 Tesla in our magnet and therefore the ^{31}P in phosphoric acid precesses at 145.8 MHz, and similarly a proton precesses at 360 MHz.

Under thermal equilibrium, the net number of nuclei parallel to the field is slightly greater than the number antiparallel, and the sum of these magnetic vectors can be shown to be along the B_0 direction, as depicted in Fig. 2a - c. The components of the vector in the plane perpendicular to B_0, the X-Y plane, all cancel out Fig. 2-B. For convenience of description and understanding, it is easier to observe the magnetic vectors just described from a rotating reference frame, one which rotates around the Bo or z axies at the Larmor frequency, and not from the laboratory reference frame. If we apply a small magnetic field, call it B_1, perpendicular to B_0, for a short time – on the order of say 30 μs seconds then the net magnetization vector M_0 is rotated into the X-Y plane. In the

Figure 1

a) Nuclei represented by small bar magnets in the absence of an externally applied magnetic field.

b) much like a top precesses in a gravitational field, a nucleus may be thought of as precessing in a magnetic field.

c) The allowable states of the ^{31}P nuclei when placed in a magnetic field B_o are in the general direction parallel or antiparallel to the magnetic field at some angle θ. This figure shows two nuclei N1 and N2 to demonstrate the two cases. The dark arrow represents the direction B_o, the applied magnetic field along the Z direction.

d) In reality, at any instant in time there are many nuclei with their associated magnetic vectors. These vectors have a random distribution around the Z axis and B_o. They precess around B_o much as a top does about the earth's gravitational field, but at a much higher frequency, i.e., 145.8 MHz for P_i.

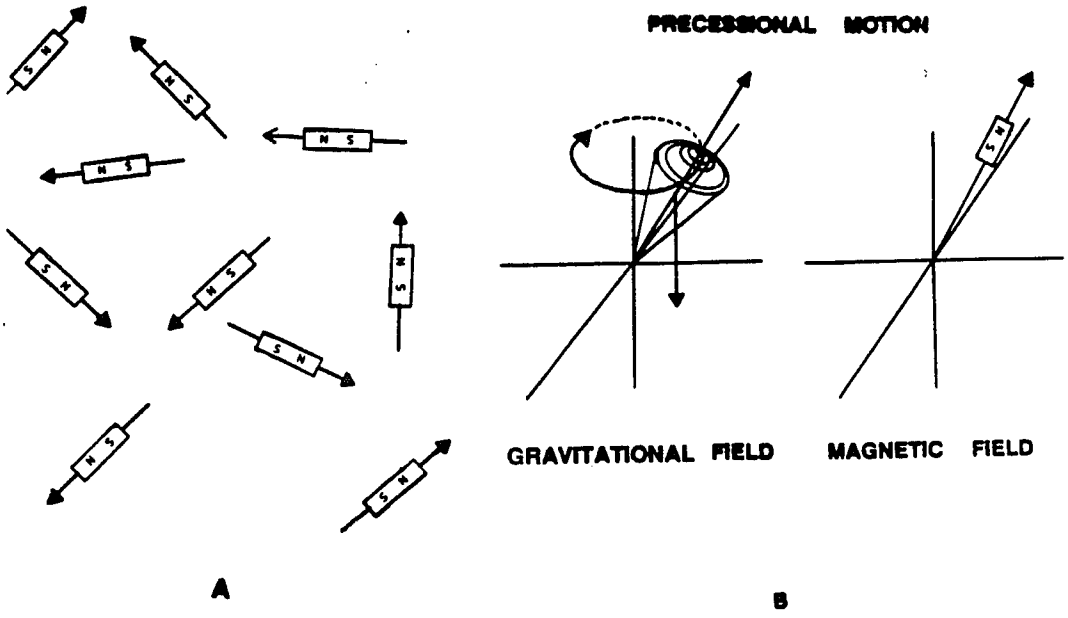
PRECESSIONAL MOTION
GRAVITATIONAL FIELD
MAGNETIC FIELD
A
B

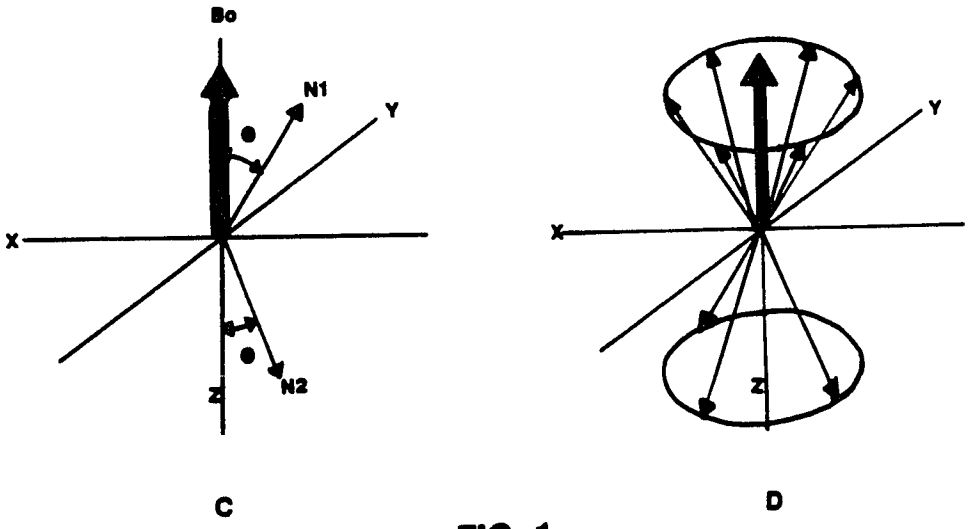
Bo
N1
Y
X
Z
N2
Y
X
Z
C
D

FIG. 1

Figure 2

At thermo equilibrium (a) the vector sum M_1 and M_2 along B_o in the parallel and antiparallel directions are not equal. Thus, the sum of M_1 and M_2, which is M, is in the B_o direction (b). When a small magnetic field B_1 is applied for a short time (30 μS) to this magnetic vector, it is rotated into the X-Y plane of the rotating reference frame as shown in (C).

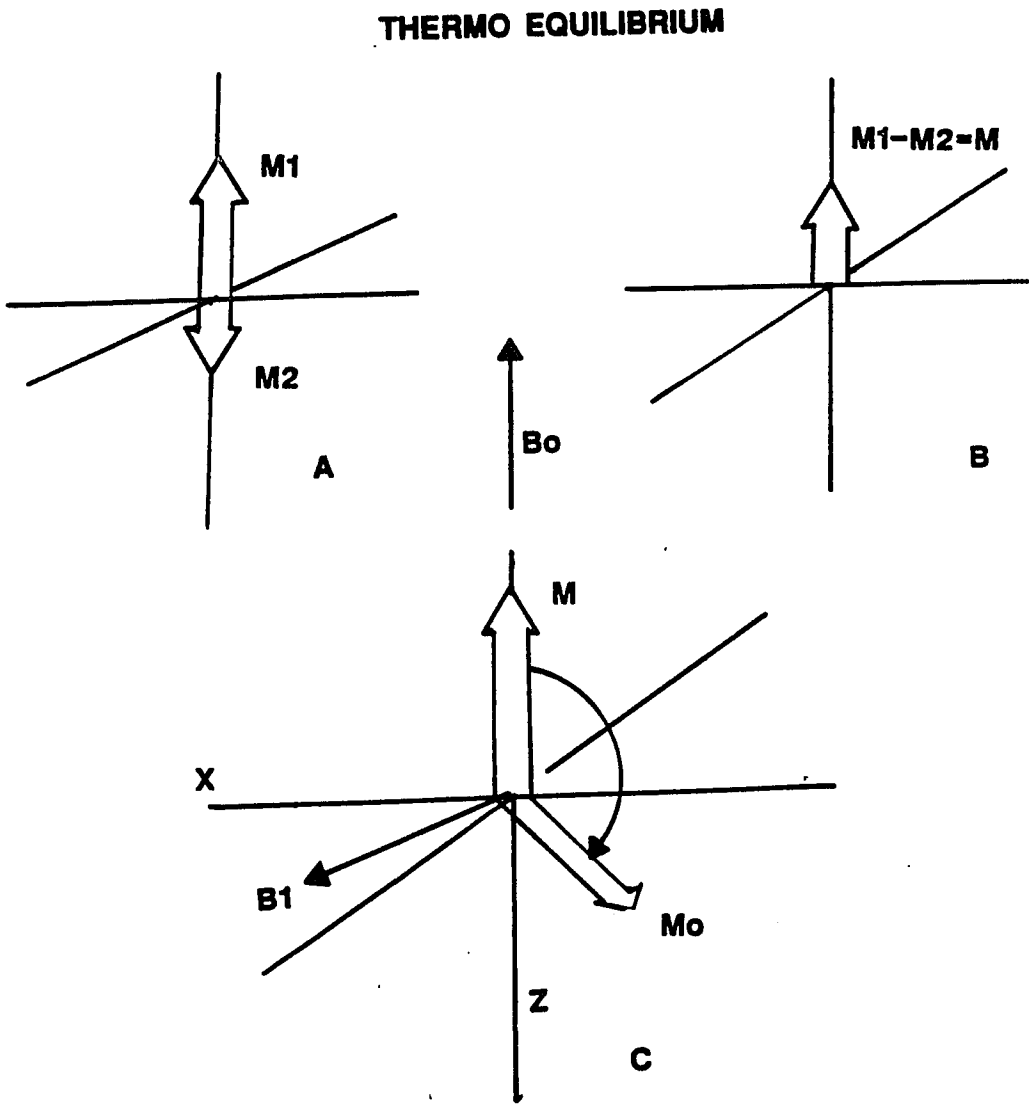

FIG. 2

laboratory frame, this would precess at the Larmor frequency. In the case of ^{31}P this would be 145.8 MHZ for phosphoric acid, but in the rotating reference frame there would be no rotation. If the magnetization vector in this rotating reference frame were to do ^{31}P in some other phosphorylated compound, then the vector could be rotating in a clockwise or a counterclockwise direction at some rate in the kilohertz region.

Since we applied B_0 as a short pulse, after it is over there is nothing to keep the "net magnetization" vector from relaxing, i.e., returning to the normal state of affairs. And as it precesses, the magnitude of the X-Y plane decreases (as in Fig. 3) and can be measured by placing an RF (radio frequency) coil in the X-Y plane (as shown in Fig. 3). This results in a signal shown in Fig. 3, the free induction decay or FID. If our sample had only one species of magnetic nucleus, then taking the FFT (fast Fourier transform) of the FID would generate a spectrum in amplitude and frequency for the nuclei with one peak. This is the case in Fig. 4.

If there are several species of nuclei which have different Lamor frequencies due to increases or decreases in the static magnetic field they see (due to local electron environment) the spectra will have several peaks at different frequencies. These shifts or "chemical shifts" give rise to fingerprints of the interesting molecules in biology see Fig. 4(B).

Figure 5 gives examples of several high-energy phosphate compounds frequently encountered. These spectra were obtained by putting the

Figure 3

As the magnetization vector relaxes back to its normal thermoequilibrium condition, the magnitude of its component in the X-Y plane diminishes in an exponential fashion while the component in the Z direction increases. The magnitude of the $M_{x,y}$ component of the vector, sensed in time by an R.F. coil, is amplified and can be visualized on an oscilloscope in amplitude and time. This is called a free-induction decay (FID).

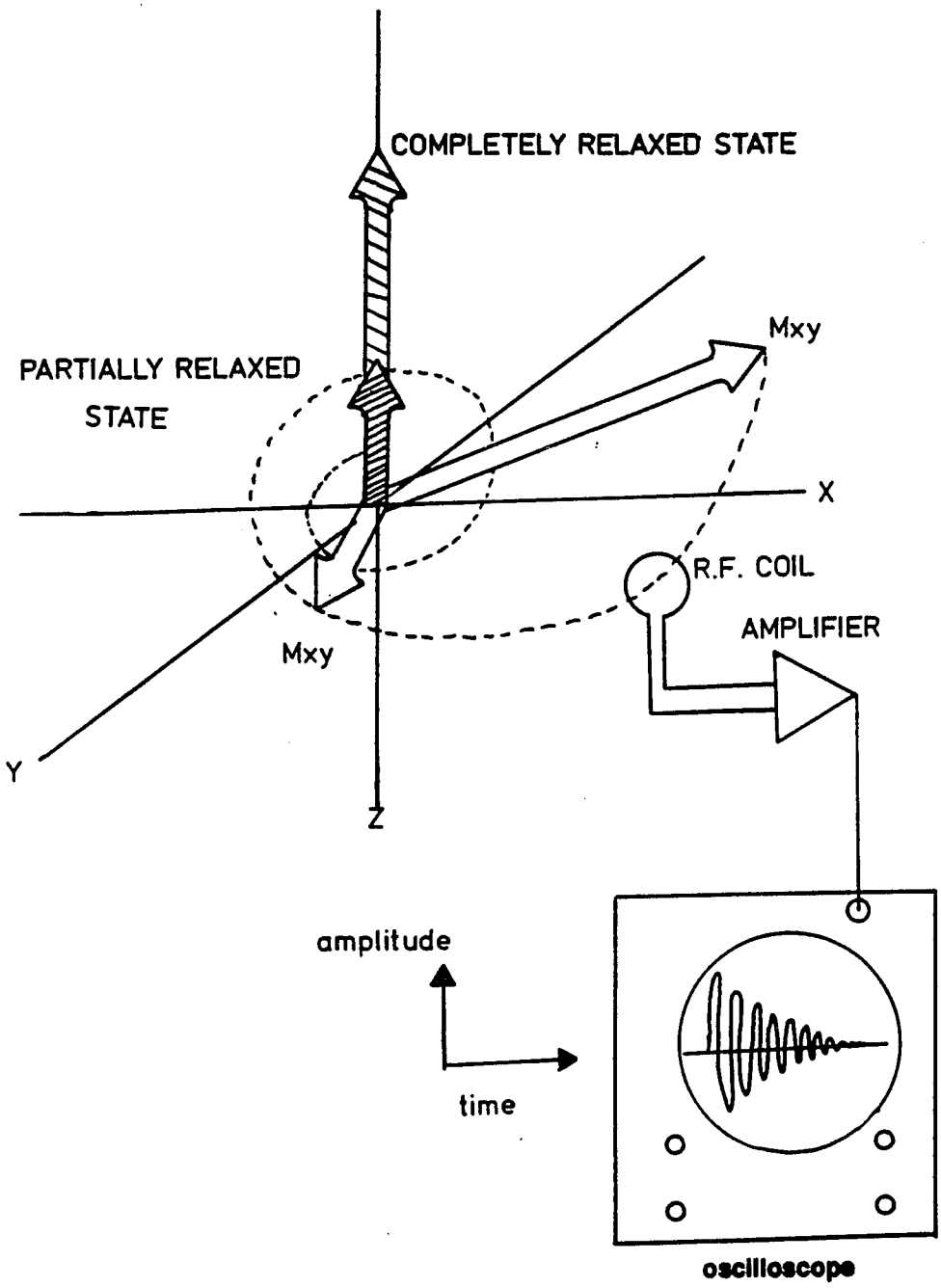
COMPLETELY RELAXED STATE
PARTIALLY RELAXED STATE
Mxy
X
R.F. COIL
AMPLIFIER
Mxy
Y
Z
amplitude
time
oscilloscope

FIG. 3

Figure 4(A)

This is a spectrum obtained from phosphocreatine in a 50 mM salt solution in a sample holder (see C) on a 360 Bruker WB operated at 145.8 MHz. PCr is found inside muscle and brain cells. Its precession frequency did not change with the pH of its environment over the normal physiological range of pH and was thus used as a reference point from which other spectral peaks emanating from the cells may be measured.

Figure 4(B)

In the case where there are four species. In this case three PCr, GPC, Pi pH7.62 are in the cell sample holder (C). In addition there is a capillary in the center of the sample holder. The capillary contained a 50 mM phosphate buffer with the pH adjusted to 7.00±0.01 at 25 C. The bulk of the sample is in 0.9% sodium chloride solution at a basic pH of 7.62. The GPC was assigned a value of 72 HZ (−0.486 ppm) and is used as a secondary standard. The pH values are calculated an expression given in section 2.3.2.2. The areas under the peaks are proportional to the number of moles in the sample holder plus capillary. The difference in the PH value of the standard P_{ii}, 7.00 ± .02 and the calculated value 6.855 can be attributed to the difference in salt concentration and temperature.

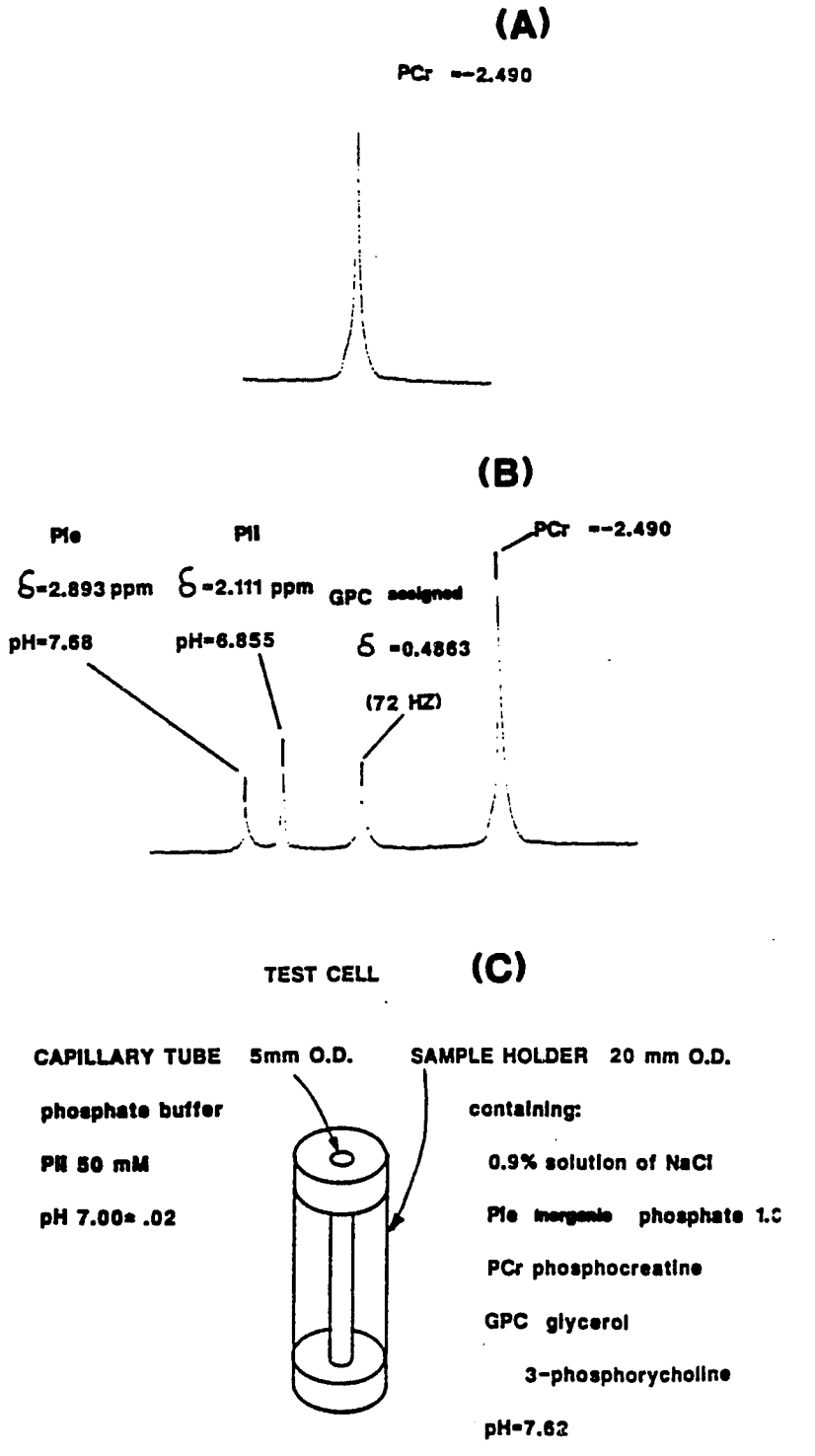
(A)
PCr --2.490
(B)
Pie
Pii
PCr --2.490
δ=2.893 ppm
δ=2.111 ppm
GPC assigned
pH=7.68
pH=6.855
δ =0.4863
(72 HZ)
TEST CELL
(C)
CAPILLARY TUBE 5mm O.D.
SAMPLE HOLDER 20 mm O.D.
phosphate buffer
containing:
PII 50 mM
0.9% solution of NaCl
pH 7.00± .02
Pie inorganic phosphate 1.0
PCr phosphocreatine
GPC glycerol
3-phosphorycholine
pH=7.62

FIG. 4

Figure 5

This is a spectrum of 1 mM inorganic phosphate (P_i), 3 mM (ATP), 4 mM (PCr), 1 mM glycerol-3-phosphorylcholine (GPC) in 10 mM Mops buffer at pH = 6.5. This spectrum was taken on a Bruker 360 wide bore magnet. The numbers refer to the chemical shift of the corresponding peaks in parts per million (ppm) relative to GPC which is assigned a value of -0.4863 ppm.

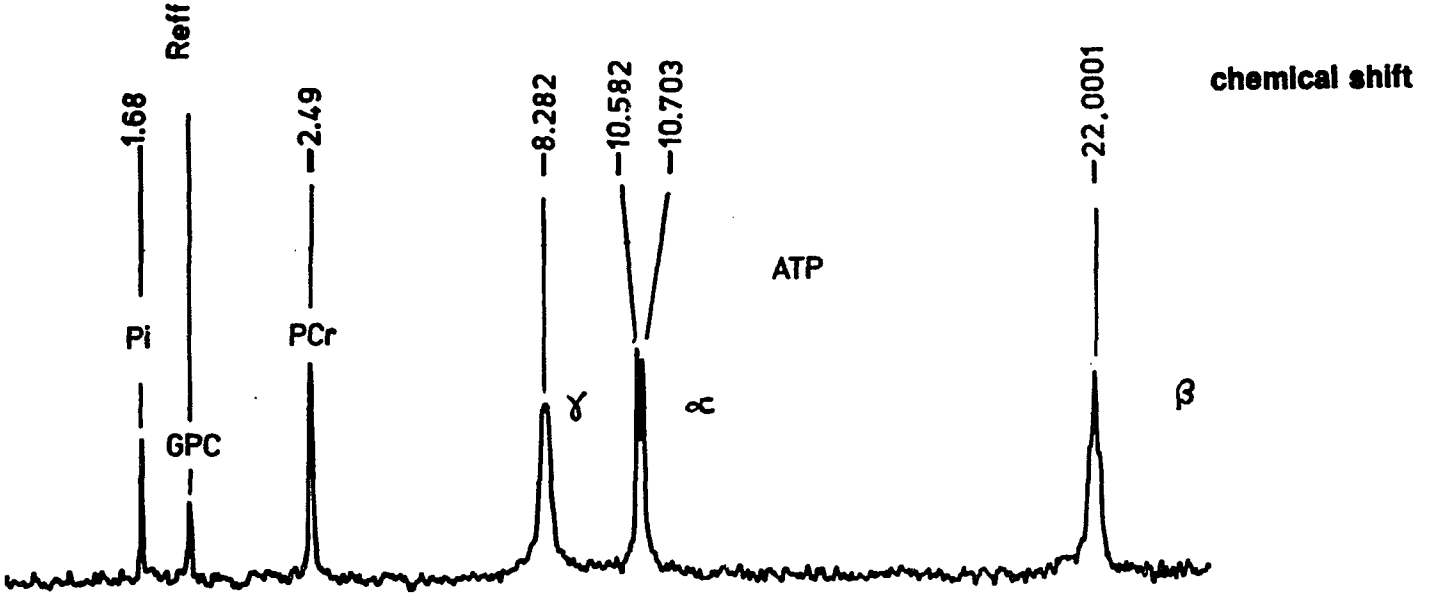
Reff
1.68
2.49
8.282
10.582
10.703
22,0001
chemical shift
Pi
GPC
PCr
γ
ATP
α
β

FIG. 5

compounds in a salt solution similar to that found in cells. Figure 6 is a spectrum obtained from a cell system. Basically one would like to get spectra like these in Fig. 5 for cells, but at the moment those shown in Fig. 6 were obtained. The reason has to do with such things as the heterogeneity of the sample, the inability to spin the sample and variations in the freedom of movement of the molecules.

Looking at Figure 6 in a simplistic way we can list the kind of information one can get:

1. cytosolic pH
2. total concentration of phosphomonoester (PME) such as 2DG, PEt, PC and G6P
3. concentrations of:
    a) ATP
    b) NAD and NADPH
    c) PCr
    d) the ratio of ATP bound to Mg++ to that in the unbound state
    e) the amount of inorganic phosphate (Pi) present

In this experiment (Fig. 6) the cells had a total volume of .6 ml in a sample holder, which had a total volume of 6 ml of growth medium containing 1 mM free Pi. Within the experimental error of $\pm 10\%$ the area under the Pi peak was proportional to 1 mM. With this as a measure one could then obtain the

Figure 6

This is the spectrum of N1E-115 cells in tissue culture made on a Bruker 360 WB spectrometer. This figure shows the major phosphate pools in intact cells in a tissue culture system at 37° C. The intracellular pH is 7.37 and the extracellular pH is 7.5. The abbreviations in the spectra are as follows:

U	=	unknown
PEt	=	phosphoethanolamine
PC	=	Phosphocholine
P_i in	=	inorganic phosphate inside the cell
P_i ex	=	inorganic phosphate outside the cell
PCr	=	phosocreatine
NTP_β	=	nucleoside triphosphate β phosphate
NDP_γ	=	nucleoside diphosphate γ phosphate
NDP_α	=	nucleoside diphosphate α phosphase
NTP_α	=	nucleoside tryphosphate α phosphate
NAD^+	=	Nicatinamide ademine
UDPG	=	uridine diphosphate-glucose
$NTP\beta$	=	nucleoside tryphosphate β phosphate

Most of the area of the nucleotide peaks was due to ATP, ADP and AMP. The measurements were made relative to PCr (i.e., the PCr chemical shift was

assigned a value of −2.49 PPM).

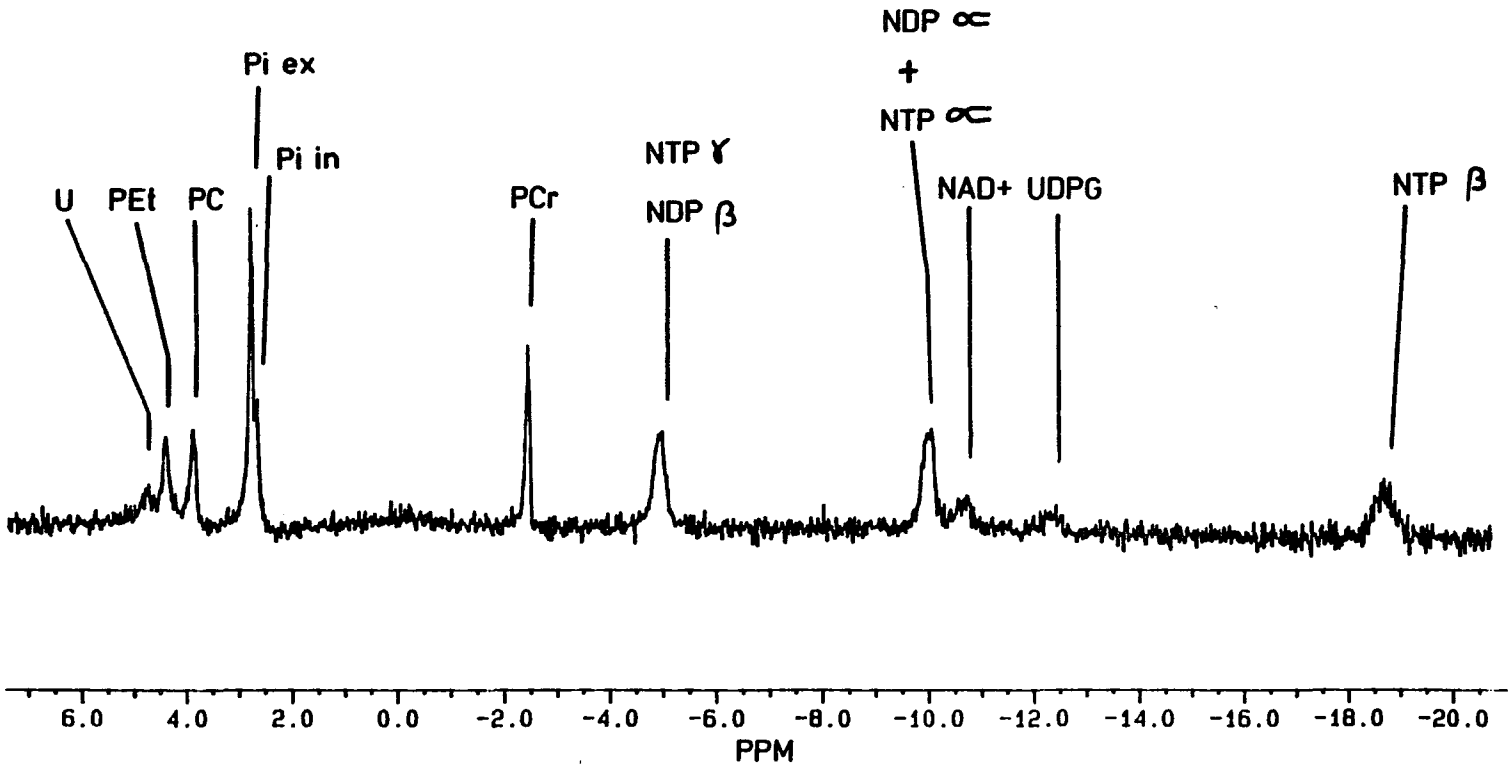
NDP ∝
+
NTP ∝
Pi ex
Pi in
NTP γ
NDP β
U
PEt
PC
PCr
NAD+
UDPG
NTP β
6.0
4.0
2.0
0.0
-2.0
-4.0
-6.0
-8.0
-10.0
-12.0
-14.0
-16.0
-18.0
-20.0
PPM

FIG. 6

concentrations of the various molecules in the sample within an error interval of about 10% for the spatially resolved peaks such as Pi, PCr and ATPβ. In theory the ATPγ peak was the sum of ATP and ADP, so by subtracting the ATPγ area one should get the ADP concentration. In practice, however, the ADP concentration was small and was completely masked by the error of the measurements. So the extent of what could be said in making the area estimates in Fig. 6 was, for example, that the number of moles in the sample is (such and such). If we know the volume of cells as we do in this case, the actual concentrations may be calculated. In practice the cell volume is not known unambiguously and concentrations are generally given in terms of moles/mg protein or moles/mg DNA, a more realistic way since protein profiles can change considerably during a cell's life cycle. These values of DNA and protein were measured after the experiment was finished.

2.2.1 pH

The pH inside the cells can be determined from the chemical shift of 2DG if it is present, or the shift of Pi inside the cell, if it is not masked by extracellular Pi. The choice of pH indicators is in part restricted by the pH range. The Pi peak is the weighted average of the two resonances of the protonated and unprotonated form of Pi which are in fast exchange and appear as one peak because they are not time resolved. They therefore titrate with pH in a sigmoidal fashion shown in Fig. 7. In practice phenylphosphonic acid (PPA) is used as an indicator of the external pH and 2DG for the cells' pH in the low pH region. Internal Pi is used for this measurement under conditions of low or no

Figure 7

The chemical shift of inorganic phosphate (P_i) in a 120 mM sodium chloride solution.

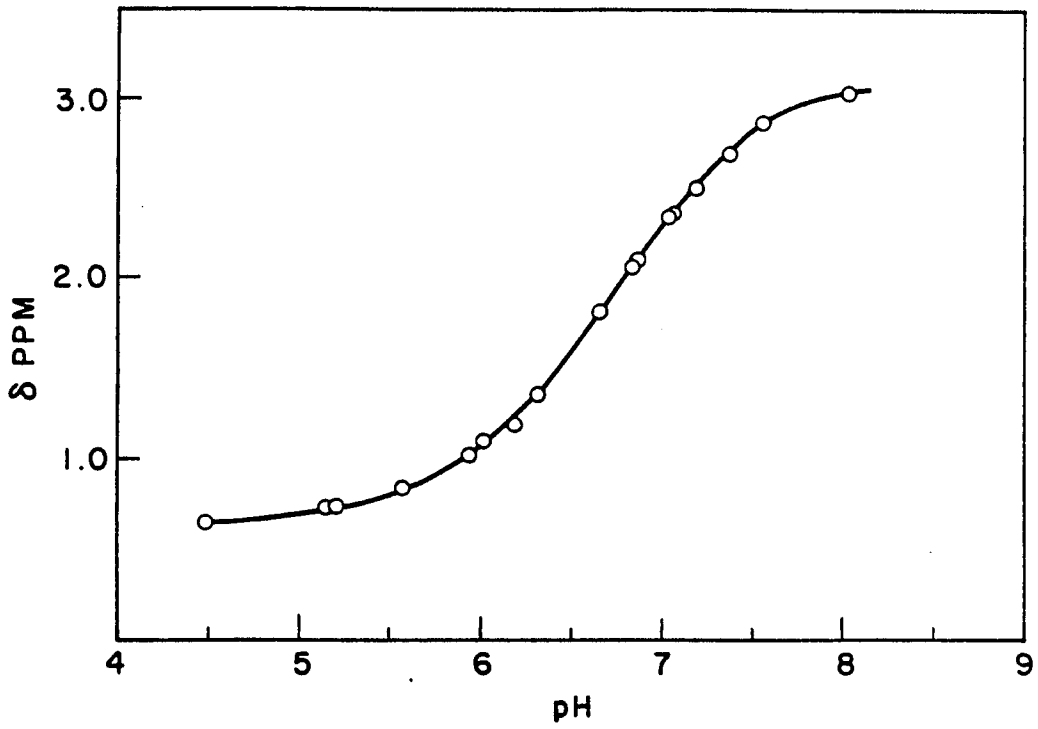

FIG. 7

external Pi, or in the case where there is a pH gradient across the cell membrane. So in principle one can measure pH and the high energy phosphates of cells continuously over some time course. The time resolution is of course dependent on the cell concentration and the concentration of molecules. In the intact heart, for example, where the PCr is in high concentration, one can get an adequate signal with one pulse of R.F. energy lasting 30 microseconds. In theory this times plus the relaxation time could be the time resolution of an experiment. The relaxation time is discussed below. In cells in tissue culture this is not the case. First, the cell density is much lower than that in whole organs. Typically these experiments required several hundred to several thousand pulses.

2.2.2 $T_1 + T_2$

This brings us to the point of looking at two more attributes a nucleus has when interacting with its environment once it has been energized in a magnetic field with an R.F. pulse. Once a 90° pulse is given, and the magnetic vector rotates into the X-Y plane. The term spin-spin is used to describe the interactions between neighboring spins. The form of this relationship is:

$$\frac{dM_{xy}}{dt} = - \frac{M_{xy}}{T_2^*}$$

That is, the exponential decay of the magnetization vector in the X-Y plane, M_{xy} to zero, has a time constant T_2^*. The spreading of precessional frequencies leading to the broadening of the line associated with a particular chemical shift

is related to T_2^* as follows:

$$\Delta \nu_{1/2} = \frac{1}{\pi T_2^*}$$

Where $\Delta \nu_{1/2}$ is the resonance line width at half height. The best value of $\Delta\nu\frac{1}{2}$ obtained for PCr, for example, on any cell sample was 10 Hz.

Of great interest in terms of these experiments is a second relaxation time called T_1, or spin-lattice relaxation time. Prior to the 90° pulse the net magnetization in the z-direction was M_0 and that in the X-Y plane was zero, after the pulse, M_0 is zero and M_{xy} is some finite value. We have just discussed the parameters describing the relaxation of M_{xy} to its equilibrium condition via spin-spin interactions, a process which does not necessitate the return of M_z to its equilibrium state M_0. This return to equilibrium value M_0 or relaxation is due to an interaction between the spin of the nuclei in question and its surrounds. The extra molecular environment is sometimes called the molecular framework and regardless of the physical state of the environment is called the "lattice," hence the term spin-lattice relaxation time. It is characterized by a time constant T_1 and is defined by:

$$\frac{dM_z}{dt} = - \frac{(M_z - M_0)}{T_1}$$

where M_0 is the equilibrium value of M in the z-direction and M_z is the value at the time t after the 90° pulse (Martin, et al., 1980). We should keep in mind

that M_0 is thermodynamically determined and therefore has a temperature dependence. Thus, T_1 can be considered the time for the magnetization vector M_z to return to its original conditions due to its "thermo" interactions and T_2 associated with dephasing of the M_{xy} vector in the X-Y plane.

We can forget about T_2^* for the present. The T_1 values place major constraints on the rate we can pulse the system, that is, make repeated measurements, and in that way places constraints on signal-to-noise values obtainable, say, in a ten-minute period. The T_1 can vary from 12 seconds for Pi in Dulbecco's modified Eagle's medium (DMEM) to 1.5 seconds for ATP in a cell. The measurements of the T_1's reported here were performed on cells.

2.2.3 Saturation Transfer

The value of T_1 is of major importance in measuring reaction kinetics. Using the method of "saturation transfer" we can measure the first order rate constant for the reaction:

$$ATP + Cr \rightleftarrows ADP + PCr$$

which is basically of the form of

$$A \underset{k_2}{\overset{k_1}{\rightleftarrows}} B$$

where A = ATP and B = PCr.

At equilibrium it can be shown that during continuous saturation of M_z with a continuous low-power r-f field:

$$dM_z^A/dt = -(M_z^A - M_0^A)/(T_1^A) - k_1 M_z^A$$

where M_z^A = the magnetization vector of A in the z direction

M_z^B = the magnetization vector of B in the z direction

T_1^A = spin-lattice relaxation time of A in the absence of exchange

k_1 = the rate constant from A going to B

If during an experiment where this low-power r-f field is being applied there is an equilibrium condition, that is:

$$k_1 M_0^A = k_2 M_0^B$$

and if the system is probed with a 90° pulse every T seconds then

$$M_z^A(T) = [M_0^A/(1+k_1 T_1^A)][1 - \exp(-T/T_1 \text{ sat})]$$

where $M_z^A(T)$ is the M_z^A when pulsed every T seconds.

$$T_1^{sat} = T_1^A/(1+k_1 T_1^A) \quad \text{or}$$

$$\frac{1}{T_1^{sat}} = \frac{1}{T_1^A} + k_1$$

Now if T is much larger than T_1^{sat}

$$M_z^A(T) = M_0^A/(1+k_1 T_1^A)$$

now the change in M or ΔM is

$$M_0^A - M_z^A(T) = \Delta M$$

$$\frac{\Delta M}{M_0^A} = \frac{M_0^A - M_0^A/(1+k_1 T_1^A)}{M_0^A}$$

$$= 1 + k_1 T_1^A$$

$$= k_1 T_1^{sat}$$

Now T_1^{sat} can be measured using saturation recovery techniques at the same time the low power r-f radiation is on:

$$\therefore \qquad k_1 = \frac{\Delta M}{M_0^A} \frac{1}{T_1^{sat}}$$

There are several very nice features of this measurement when it is applied to the phosphocreatine reaction.

$$PCr + ADP = ATP + Cr$$

which is of the form $A \rightleftarrows B \rightleftarrows C$. In this reaction C represents a myriad of reactions and possibly a compartmentalization of reactions involving ATP; however when the reaction is considered going in the opposite direction with A as a terminal product, it is reasonable to measure the rate constant of B going to A or k_2 and expect it to reflect the true flux in one direction of creatine kinase, and this is what has been done (see section 4.3.5.). The constant k_1 and k_2 are referred to as pseudo first-order rate constants (Brown and Ugurbil,

1984). I use the f_1, f_2 nomenclature for flux rates.

2.3 Probe Design and System

To study anchorage-dependent cells in tissue culture it is necessary to have a system which will supply a substrate for the cells to attach to, and a system for changing the culture medium in the extracellular space. It is necessary to have a high cell density in order to have a good signal-to-noise ratio. Another consideration in the design of the system is the maintenance of good homogeneous magnetic susceptibility in the sample volume.

For the substrate we considered and tried several materials such as glass wool, agar and several types of microcarriers. Based on a preliminary screening, it was decided that microcarriers would be used. The first experiments using cells on microcarriers in a 10 cm NMR tube at 4 ° C in a conventional probe with a Helmholtz coil gave very poor signal-to-noise in a time interval required to do an experiment. This led to the design of a solenoid coil. In addition to the above condition, a system which could be sterilized, loaded with cells and operated under sterile conditions for weeks was needed. Here I detail the evaluation of the system developed over a period of time, using five cell types, and three different NMR machines.

2.3.1 Probe

There are several coil configurations which can be used for probe design. The solenoid coil was chosen because it gave a better signal-to-noise ratio than other types (Hoult, 1978). The noise in large part comes from Brownian motion

of the electrons in the coil. It has been shown that the root mean square noise is proportional to the square root of the coil resistance among other factors (see Table 2). This expression is for a solenoid, but similar dependence on resistance of the coil is also found for Helmholtz, or as they are also called, saddle-shaped coils. It turns out that for the optimum design of both coil systems, the Helmholtz coil requires a longer wire length, i.e. large coil resistance. Theoretical calculations put an upper limit of a three-times improvement in signal-to-noise ratio when a solenoid is used.

The noise in e.m.f. associated with the Brownian motion of the electrons within the coil is:

$$N = (4K\ T_c\ R_c\ \Delta\ \nu)^{1/2}$$

where R_c = coil resistance

T_c = temperature

$\Delta\nu$ = band width at the resonant frequency

(Gadian, 1982)

It would be good to state at the outset of this section that the single-turn solenoid coil used for most of the work reported here may not be the design of choice in all types of anchorage-dependent cell work, for in addition to a good signal-to-noise ratio, there are several other important design considerations which center on peak resolution, the facility with which the probe can be put in and taken out of the magnet, whether the sample is spinning or not, and whether the symmetry of the sample will be coaxial or normal to the B_0 of the

magnet. These considerations are not independent of one another, and they also depend on the type of cells being looked at, the substrate being used, the conductivity of the milieu of cells, the substrate and perfusion medium in the sample volume. This latter point — conductivity of the sample volume — can lead to an important contribution to the noise as a result of eddy currents generated in the sample volume.

The approach to an optimal design was to pick a reasonable coil configuration and matching network for each cell type and magnet used, and then look for optimal results by varying the parameters, such as the number of turns in coil, wire diameter, diameter of the sample holder, length of the sample, length of coil, matching capacitor configuration, and the type of microcarrier. There are a number of relevant expressions which have been derived with regard to solenoid coils concerning signal-to-noise, magnetic loss due to sample conductivity, electrostatic losses and matching networks. These are summarized in Table 2 along with their sources.

In the first experiments a 15 mm outside diameter sample holder was used with a 3-turn coil, 15 mm diameter by 10 mm length. This turned out to be the best for the Bruker 360 narrow bore at Bell Labs. At Columbia, on the Bruker 300 wide-bore spectrometer, coils with 1, 2, 3 and 4 turns were tried. The single-turn coil, 24 mm long by 25 mm diameter, was selected for these experiments. The sample holder was 25 mm O.D. and 23 mm long. The cells involved in the measurements were CH3T10½ cells. In the Bruker 360 WB, coils of 20, 23, 25 and 27 mm in diameter were tried with comparable sample holder

Table 2 Signal-to-noise ratio after a 90° pulse

$\psi_{rms} = K\eta M_0 (\mu_0 Q \omega_0 V_c / 4FkT_c \Delta f)^{1/2}$

k = a numerical factor $\simeq 1$

η = the filling factor, a measure of the coil volume occupied by the sample

M_0 = the nuclear magnetization which is proportional to the field strength, B_0

μ_0 = the permeability of free space

Q = the quality factor of the coil

ω_0 = the Larmor angular frequency

V_c = the volume of the coil

F = the noise figure of the preamplifier

k = the Boltzman constant

T_c = the probe temperature

Δf_c = the band width in Hertz of the receiver

(Table 2, con't.)

The interaction of terms in the equation above

	T	F	Q	K_n	V_c	B_0
Temperature (T)						S
Preamp. noise figure (F)	S					
Coil quality factor (Q)	S			S_s	S	S
Filling factor and geometry (K_n)					S_s	
Volume of coil (V_c)						S_F
Field strength (B_0					S_F	

an S designates a strong dependence

s and also a dependence on sample

F a dependence on frequency

Taken from (Iles, et al., 1982)

Figure 8

This is the experimental set up for measuring the probe Q and for tuning the probe.

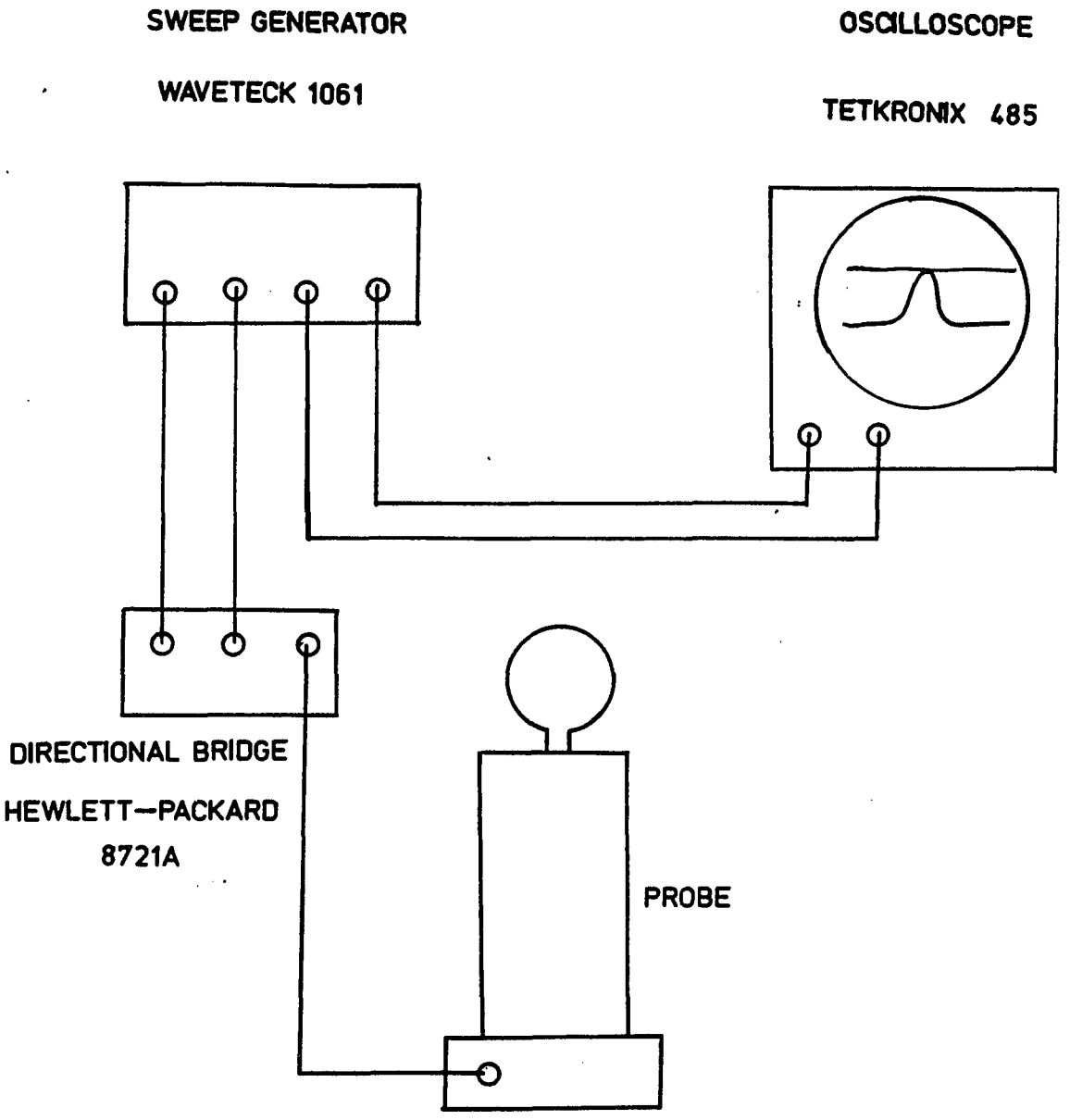
SWEEP GENERATOR
WAVETECK 1061
OSCILLOSCOPE
TETKRONIX 485
DIRECTIONAL BRIDGE
HEWLETT—PACKARD
8721A
PROBE

FIG. 8

lengths. A trade-off was looked for between signal-to-noise and peak resolution. The 20 mm diameter coil was used for N1E-115 cells and the 23 mm diameter coil for CH3T10½ cells. The resolution was evaluated by measuring the line width at one-half peak height. The Q was taken as a correlate of the signal-to-noise. The set up is shown in Fig. 8.

The actual measurement of signal-to-noise (S:N) was measured by the graphic technique where S:N = (S/PP Noise) $\times$ 2.5 or by an automated program in the Bruker computer. The noise as measured by the Bruker method is RMS noise; therefore, it must be multiplied by 0.5 before comparing to the graphic method. It should be noted here that the signal is really proportional to the area under the curve. Now if the curve is Lorentzian, then the signal peak height is linearly related to the area. In general, in cell work, the peaks are not Lorentzian, and a measure of the deviation should be made prior to comparing signals. A good indicator of the Lorentzian quality is the ratio of $\Delta \nu$ at the half peak divided into the $\Delta\nu$ at the one-eighth peak, or one quarter height, which are 2.65 and 1.73 respectively for a perfect Lorentzian line shape. Let us consider specifically the three preferred coil configurations and their parameters.

For the Bruker 360 wide-bore probe, a standard sample holder was used to determine the signal-to-noise characteristics of these solenoid coils under several conditions. The standard holder consisted of a glass cylinder 30 mm long and 21.1 mm in outside diameter. The wall thickness was 1.0 mm. Silicone stoppers (number 2 Thomas Scientific) were cut and fixed in the ends of the cylinder.

Figure 9

This spectrum was obtained from one scan on a 20 mm diameter by 20 mm long sample holder filled with a Fisher standard solution of pH = 7.4, at 25 C. The standard contains 50 mM Pi. This spectrum is presented to give a sense of the type of proton signal one can get using the grossly mismatched ^{31}P resonance circuit. By maximizing the peak height while maintaining the Lorentizian line shape when the magnetic field is shimmed generates a homogeneous field, which gives a good ^{31}P spectrum.

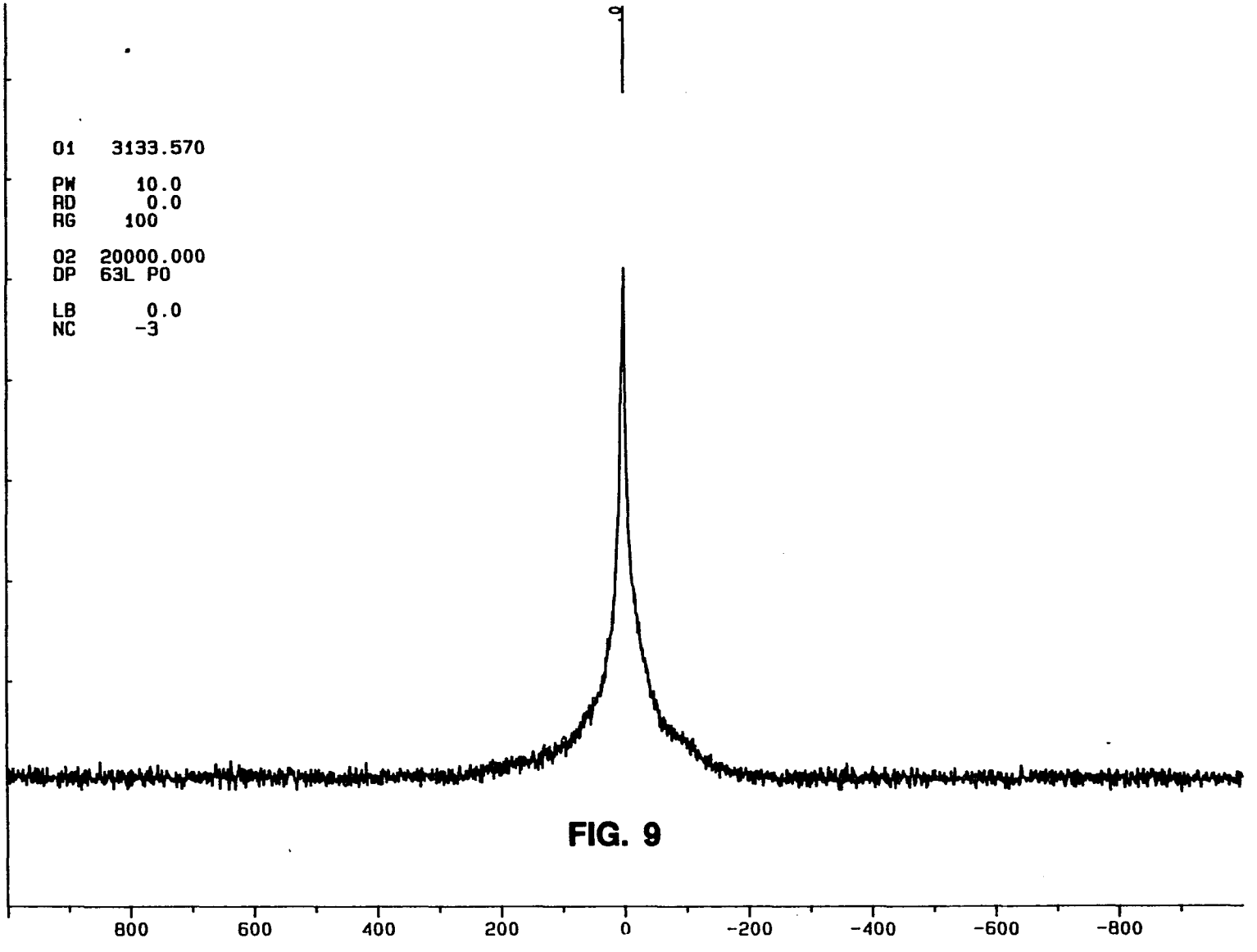
O1 3133.570
PW 10.0
RD 0.0
RG 100
O2 20000.000
DP 63L PO
LB 0.0
NC -3
800
600
400
200
0
-200
-400
-600
-800

FIG. 9

Figure 10

A typical ^{31}P measurement on a 100 mM ^{31}P standard at the values indicated and also those given in Table 3.

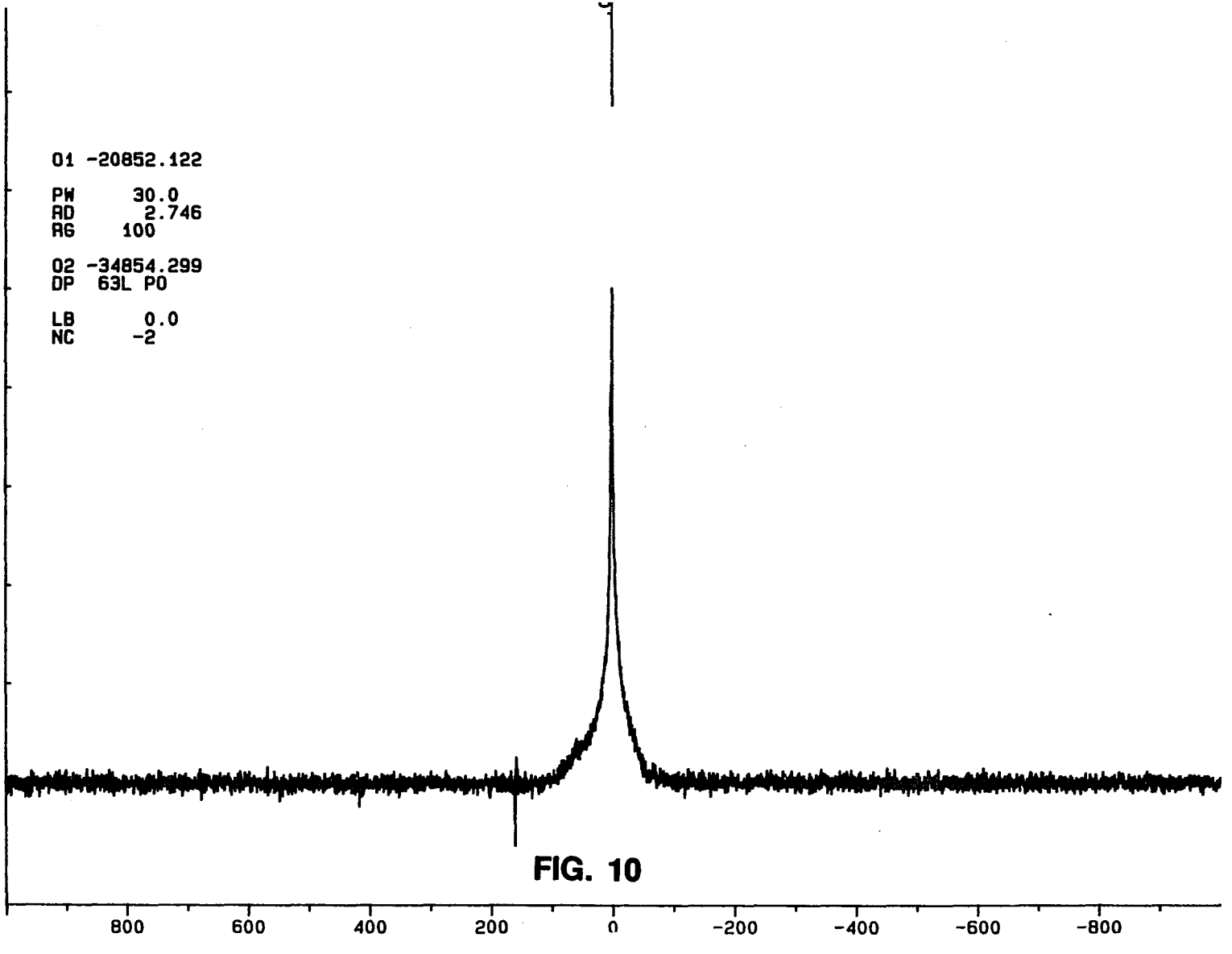
O1 -20852.122
PW 30.0
RD 2.746
RG 100
O2 -34854.299
DP 63L PO
LB 0.0
NC -2
800
600
400
200
0
-200
-400
-600
-800

FIG. 10

TABLE 3

a) Table of conditions used to measure the ^{31}P signal to noise.

b) A typical measurement on a 100 mM ^{31}P standard at the values indicated.

TABLE 3

Standard Conditions for Signal-to-Noise Measurements

A

GRAPHIC

Sweep width f	= +1 KHZ
Number of scans	= 1
Pulse angle	= 90°
Line broadening, LB	= 1 HZ
Temperature	= 37° C
pH	= 7.4
Noise, Npp	= peaks to peak measured graphically, see (B) below
Signal, S	= peak height
Signal to noise S/N	= S/Npp × 2.5

Computer Measurement

Noise	= RMS noise
Peak	= peak
Signal to noise S/N	= (S/RMS noise) × 0.5

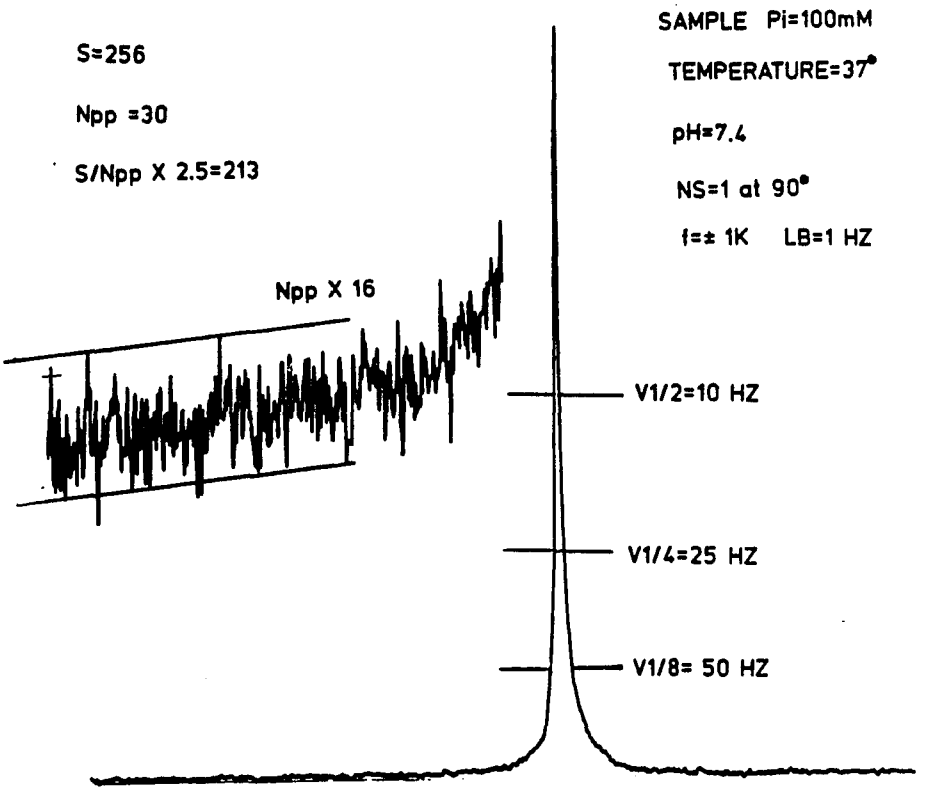
SAMPLE Pi=100mM
TEMPERATURE=37°
pH=7.4
NS=1 at 90°
f=± 1K LB=1 HZ
S=256
Npp =30
S/Npp X 2.5=213
Npp X 16
V1/2=10 HZ
V1/4=25 HZ
V1/8= 50 HZ

TABLE 3 (B)

Standards of 0.1 or 0.05 M solutions were used. Fisher Scientific Catalogue - #S0-B110 pH 7.4 standards, a 50 mM potassium phosphate mono-basic sodium hydroxide buffer, was used for the latter case. The sample holder and standard solution were brought to 37 ° C before filling to minimize the formation of bubbles in the sample holder when it was subsequently placed in the magnet of the spectrometer maintained at 37 ° C. The sample volume was 6 ml. Care was taken to remove air with a hypodermic syringe inserted through the end stopper when filling. With the spectrometer at 37 ° C and the pH standard in the holder, the spectrometer was shimmed on the proton signal, the spectrum of which is shown in Fig. 9. This spectrum was obtained by passing the proton frequency r-f pulse up the channel tuned for phosphorus at 145.8 MHz. Although this channel was clearly mismatched for the proton frequency 360 MHz, sufficient signal got to the protons in the water of the sample, which subsequently generated such a large signal that even with large losses on route to the pre-amp, the signal above was generated with one pulse. The beauty of this was that one can use this substantial signal to shim the spectrometer and obtain a homogeneous magnetic field. This was extremely important in actual experiments because the phosphate signal for free P_i in the cell sample volume in a normal experiment is only 1 mM which is an inadequate amount of material for shimming using the Pi signal. It also turns out that in a solenoid with a multiple turn coil, the field homogeneity obtained by shimming the magnet with the proton signal is no good, and results in field inhomogeneities which are totally unacceptable. This was due to false signal amplitude generated by phase

shifting of the proton signal between portions of the coil at these very high frequencies. With this standard, one has the opportunity to compare homogeneity from shimming, which has been done on the ^{31}P NMR 50 mM signal, to that done using the proton signal. It was found that these values are the same only for the single-turn coil.

The ^{31}P NMR spectrum is shown in Fig. 10. This was the 20 mm sample holder with 50 mM P_i pH 7.5 Fisher standard in it. The peak height was set to ten, and the spectrum was intergrated over an interval of ± 1 KHz around the peak. The spectrum was generated from a signal with line broadening of 1. Table 3 gives the standard conditions under which signal-to-noise was measured with a measurement on a 100 mM Pi standard. Two factors that actually affected the noise measurement were the frequency over which the measurement was made and the line broadening factor (see Table 4). There was an apparent increase of 29% in going from a line-broadening of 1 to a line broadening of 20. However in looking at the width of the spectrum there was little change between a window of 2 KHz and 8 KHz. Values measured in this frequency range were therefore considered comparable without correction. From this it can be concluded that it is important to maintain the line broadening constant in making measurements on different systems which are to be compared. It is also very important to make the measurement using a 90° pulse (see Fig. 14 for typical 90° data and plot for this holder). Here the 90° pulse is 30 μs and if it is off 16%, the peak signal is off 7%, which shows that it is a factor to be controlled.

Table 4

A S:N with Line Broadening

Line Broadening in HZ	1	5	10	20
S:N × .5	136.7	174.5	179.8	176.5
S	10.003	10.002	10.000	9.988
×	3.65 × 10^{-2}	2.87 × 10^{-2}	2.78 × 10^{-2}	2.83 10^{-2}

B $\Delta\nu$ with Line Broadening

	KHZ 2	KHZ 4	KHZ
	136.7	136.2	137.5

Figure 11

Three configurations of cell sample holder tried. a) Teflon end pieces with plugs in the input and output holes. There is a piece of Teflon tubing going from the input port to the left end piece simulating the condition of pumping perfusate into the cell sample holder from the right end, passing it to the left end via the tube and allowing it to come back to the exit port b) the same condition as (a) but with an external connection between input and output ports c) the conventional system used most successfully.

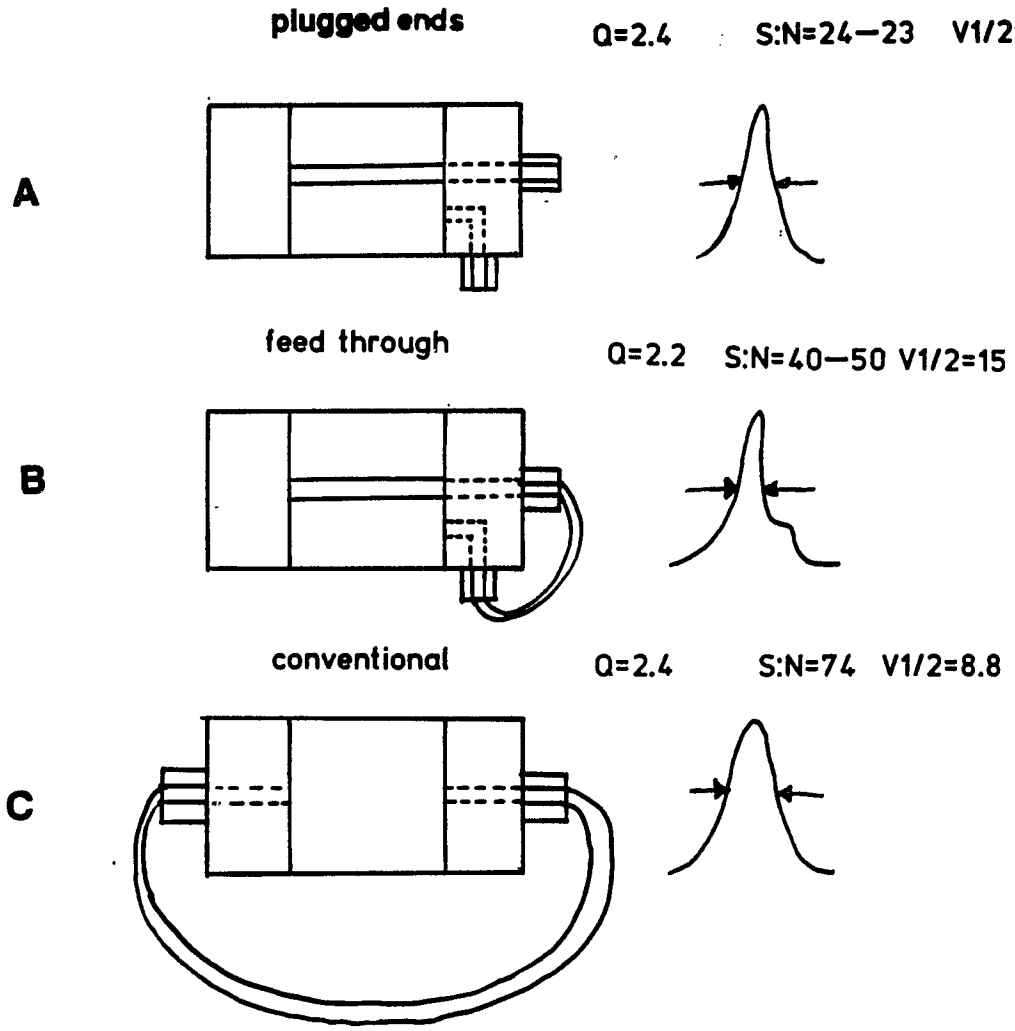
plugged ends
Q=2.4 S:N=24—23 V1/2=58
A
feed through
Q=2.2 S:N=40—50 V1/2=15
B
conventional
Q=2.4 S:N=74 V1/2=8.8
C

FIG. 11

With a good signal-to-noise and the form of the general wave shape to be expected under ideal conditions, three configurations were considered for use with the actual sample holder. What was needed was to have was medium pumped into the sample holder at one end and out the other. The three configurations in Fig. 11 were tried and compared. A and B were made to test the possibility of perfusing the sample holder from one end. The results show that the best configuration was the conventional coaxial one, in one end, out the other. Next, the flow through the cells was checked (see a cut-away drawing in Fig. 12). The microcarriers are not to scale. The experiment performed was to pump medium, (which at basic pH values is red to magenta due to the presence of phenol red, a pH indicator) through the sample holder, then to switch to an acid medium and observe the time and pattern of change in color in the sample holder as the acid medium permeated the space. The object was to see if the flow pattern was good.

The sample consisted of 75% by volume of Cytodex III which slumped in the holder. When the pump was set at three ml/min it took two minutes for the medium to flow from the bubble trap to the sample holder (i.e. a total volume of 6 ml). However, there were still a few inhomogeneous spots at eight minutes. With the pump set to 6 ml/min it took one minute to get to the holder and 2.5 minutes to get a homogeneous flow pattern in the sample holder. One can conclude from this that at a flow rate of 3 ml/min it took at least eight to ten minutes for the chamber to become homogeneous as determined by dye infusion. Therefore, the system at this pump speed should be expected to

Figure 12

A. Cell sample holder

The heart of the system is the sample holder. It now consists of two silicone corks (#2) cut down as shown in the drawing. In one end, a cone is cut out and a hole is made coaxially in the cork with an ice pick. A length of Teflon tubing which has had the last half-inch roughened with sand paper is forced through the hole and held in place with Dow Corning silicone rubber adhesive. The end of the cone is covered with nylon mesh through which the liquid sample passes. It is held in place with silicone adhesive. Air bubbles trapped in the holder can be removed by inserting a hypodermic syringe through the cork. 3 to 4 ml per minute of medium was pumped through the system.

B. Test standard

CELL SAMPLE HOLDER

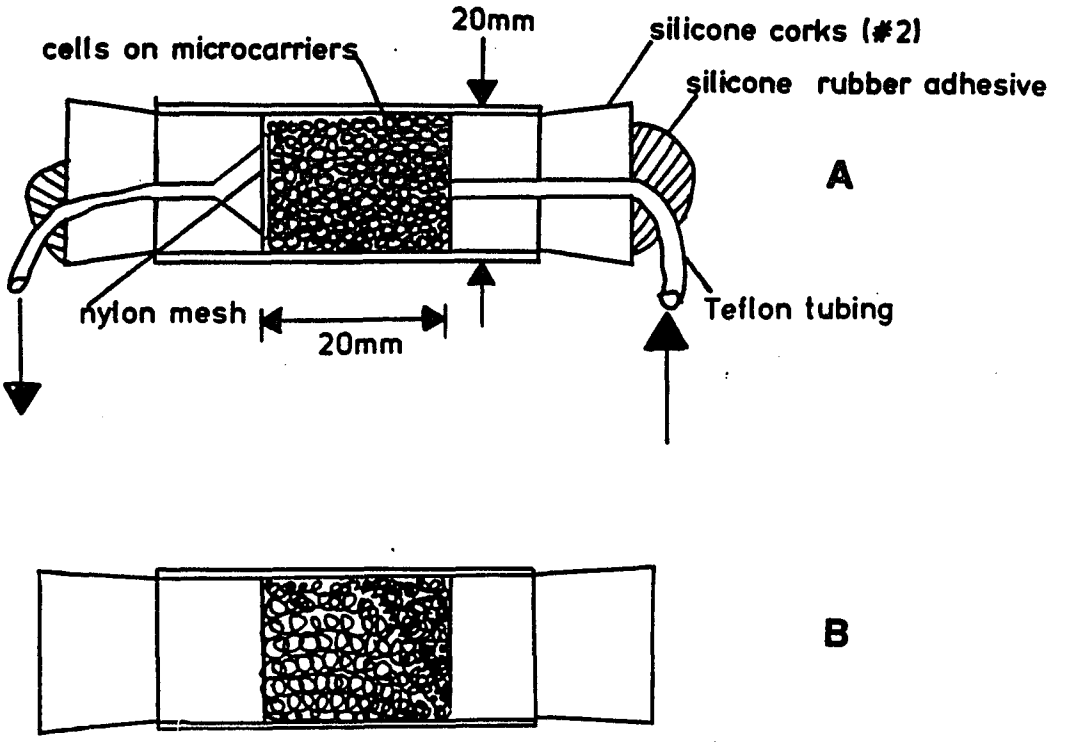

FIG. 12

Figure 13

The width of an r.f. pulse of 145.8 MHZ required to give a maximum signal is called the 90° pulse. The pulse width can be determined by measuring the signal at various pulse widths and plotting the results. This was done for the sample holder containing Cytodex III and DMEM medium supplemented with 50 mM phosphate. The data is in (A) and is plotted in (B). The peak value is calculated to be 35 u seconds.

Time in Seconds	Peak Height
5 μ sec	2.43
10 μ sec	4.77
15 μ sec	6.49
20 μ sec	8.34
25 μ sec	9.26
30 μ sec	10.00
40 μ sec	9.95
45 μ sec	9.26
50 μ sec	8.43
55 μ sec	7.22
60 μ sec	5.72
65 μ sec	4.52
70 μ sec	3.48

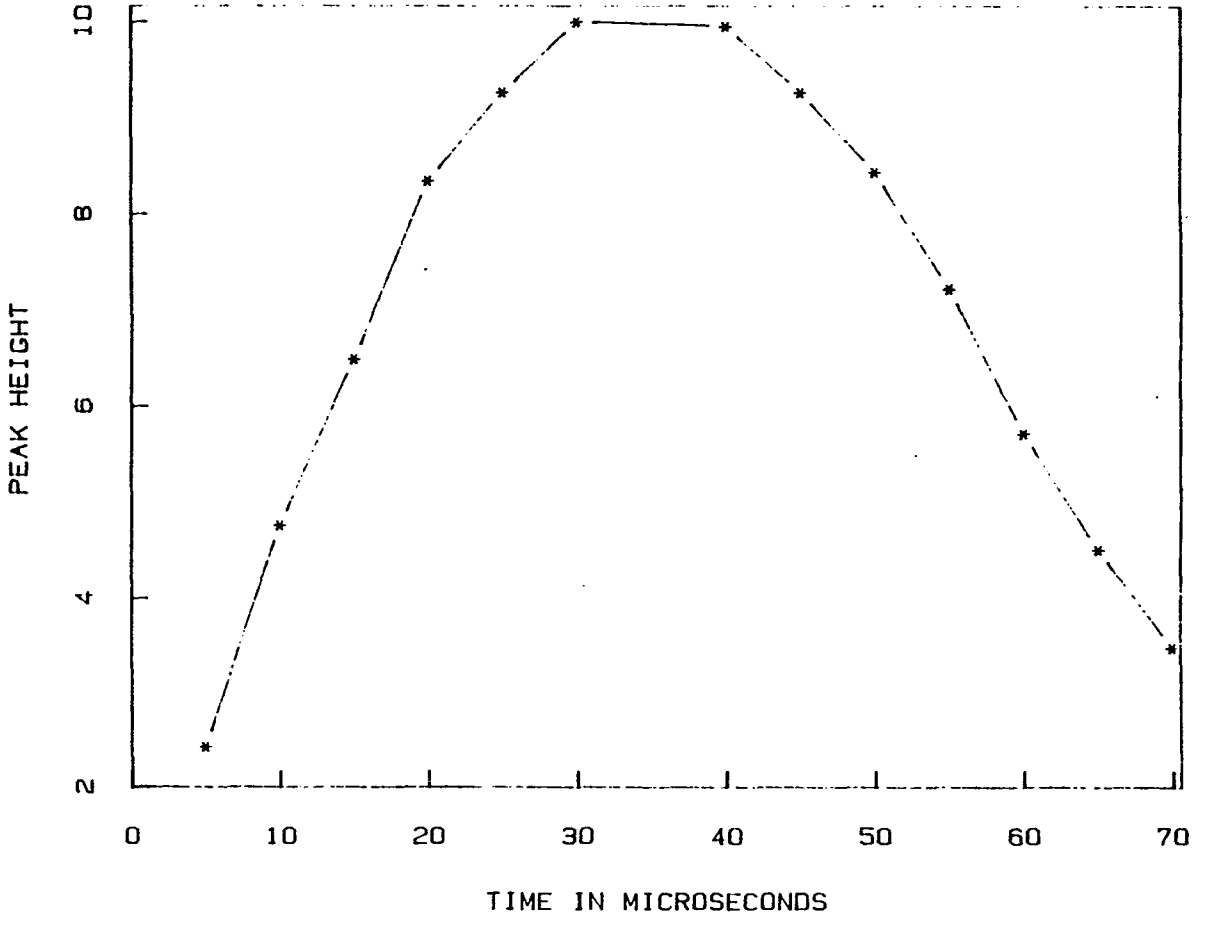

FIG. 13 (B)

Figure 14

This is a spectrum taken of C3HT10½ cells in a Bruker 300 wide-bore magnet operated at a repetition rate of one second and with a 60° pulse. There is a question about the asymmetry on the upfield side of the Pi peak. Is it an artifact or is it due to Pi inside the cells?

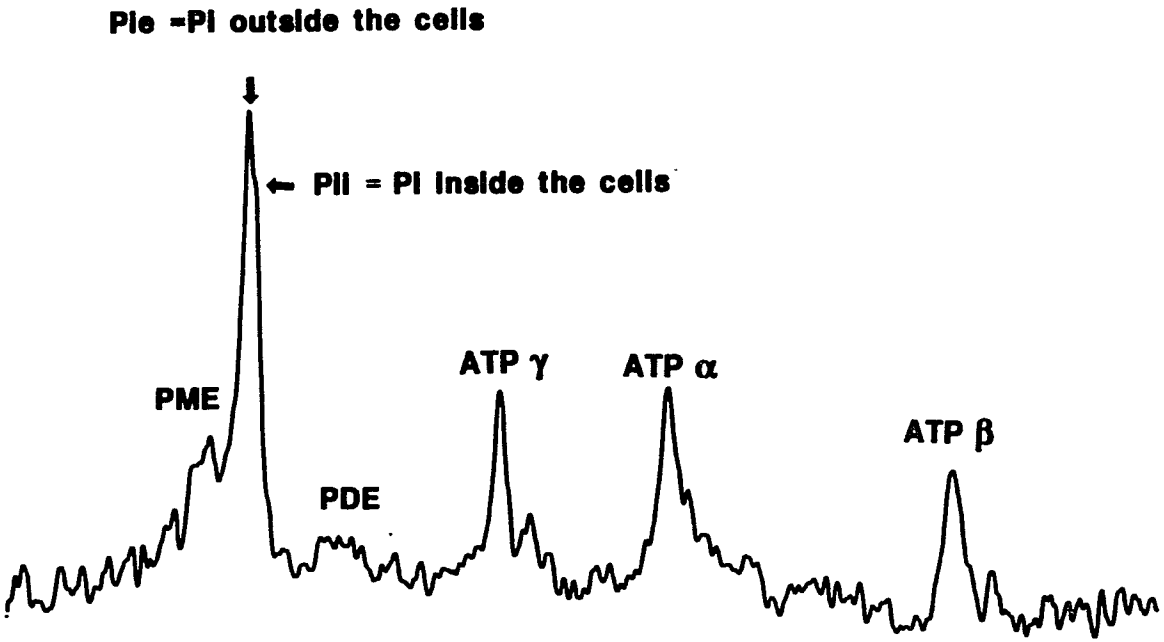
Pie =Pi outside the cells
Pii = Pi inside the cells
PME
PDE
ATP γ
ATP α
ATP β

Fig. 14

deliver drugs or medium changes to the cell surface with a window of no less than ten minutes. When the pump speed is set to 6 ml/min this can be as small as three minutes.

There is some question about the internal P_i in the cells when they are on Cytodex III microcarriers in the NMR perfusion system. Note, for example, the P_i split in Fig. 14. This small peak could be due to several artifacts such as: 1) compartmentalizing — the microcarriers and cells occupy 1.5 cm of the 2 cm compartment length. 2) Cytodex III microcarriers are porous and one phase may be on the inside and one on the outside. 3) Inhomogeneity in the cell — Cytodex III microcarriers vs. pure perfusate due to inhomogeneity of the magnet susceptibility. Therefore these artifacts were studied to decide if they exist.

Protocol:

1) Cytodex 3 microcarriers were put in the sample holder without cells, filling approximately 80% of the sample volume.

2) The bubble trap was filled with Ringers, supplemented with 1.5-2 mM P_i and 1 mM PPA and Hepes buffered.

3) The pH was monitored, but not continuously.

4) 1 ml of 1N HCl or 1 ml of 1N KOH was added to the bubble trap and the system was allowed to recirculate.

5) 250 second blocks of data were taken; i.e. NS = 250 with a

repetition time of 1 second.

From the above, one gets some idea of the wash-out time of the sample holder, but still problems could arise from the heterogeneity of the sample, due to the presence of the microcarriers in the sample space. So it was decided to look at the samples shown in Fig. 15. The coil is an open type which allows a 20 mm NMR tube to be placed coaxially into the Bo field. This allowed one to homogenize the magnetic field without having to concern oneself unduly with radial symmetry problems. Sample inhomogeneities were introduced midway up the sample as indicated in the drawing. For example, in Fig. 15a the volume above the center line of the pick-up coil is a 50 mM phosphate solution only, while that in the lower half contained Cytodex III microcarriers. In both cases using these microcarriers a split was seen (see Fig. 15). In the one case using 1/2 the Cytodex III (Fig. 15a), it was not possible to homogenize out the double peak in the P_i spectrum. When Biosylon microcarriers were used, in case c and d, no double peak appeared after homogenizing. I concluded from these results that Cytodex III microcarriers may lead to peak splitting on the order of 17 Hz, which in turn leads to an artifact in the P_i chemical shift and to possible misinterpretation of peak splitting. Therefore, Biosylon microcarriers should be used whenever other considerations justify it. With care, Cytodex III microcarriers may be used for internal pH determination when PPA is supplemented in the medium. When the upfield shoulder on the P_i peak is due to inhomogeneities of the magnetic field, there is also a shoulder on the PPA peaks. When it is due to a pH difference across the cell membrane, there is no

Figure 15

This is the experiment for testing for effects of heterogeneity of the sample a) the measured volume is filled half with 50 mM P_i solution and half with Cytodex III microcarriers and 50 mM P_i. The microcarriers are added to the 20 mm NMR tube and allowed to pack via gravity. b) the total active volume is filled with Cytodex III microcarriers + 50 mM P_i. c) the same as (a) but with Biosylon® as the microcarrier. d) same as (b) but with Biosylon® as the microcarrier.

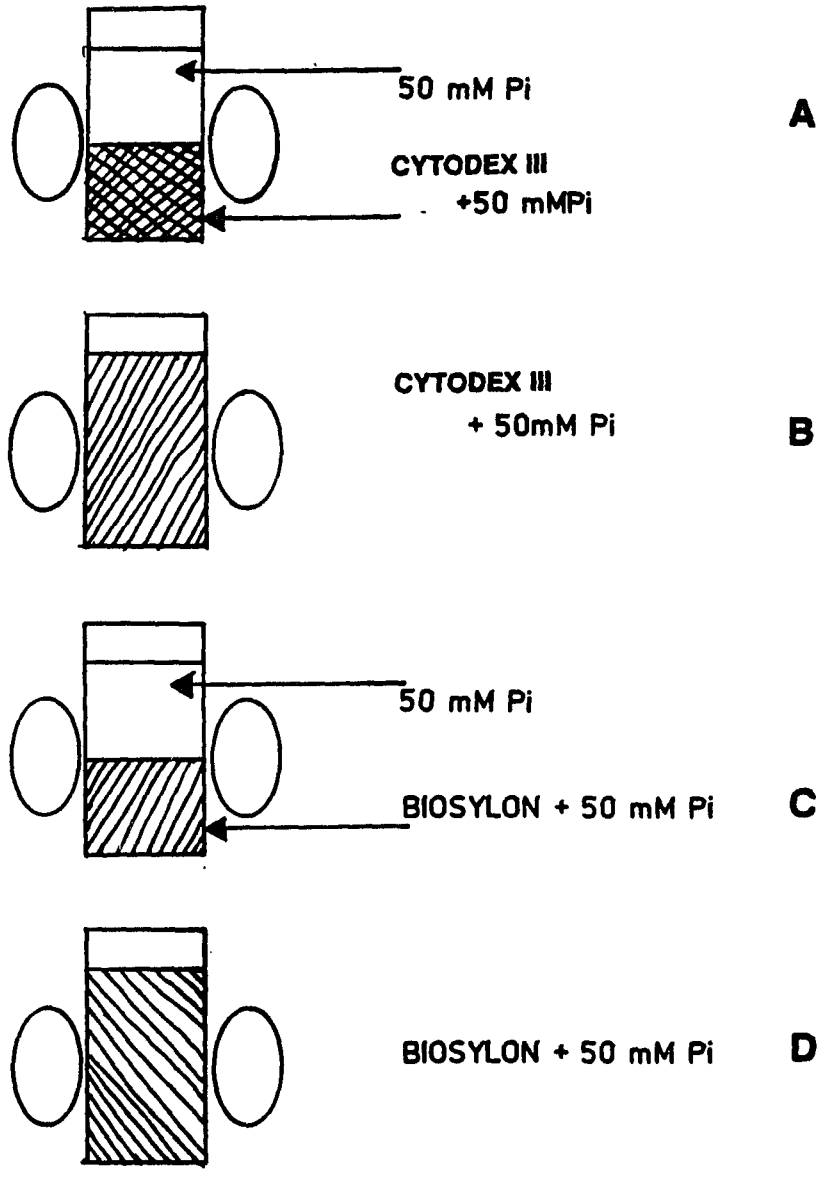
50 mM Pi
CYTODEX III
+50 mMPi
A
CYTODEX III
+ 50mM Pi
B
50 mM Pi
BIOSYLON + 50 mM Pi
C
BIOSYLON + 50 mM Pi
D

FIG. 15

shoulder on the PPA.

2.3.2 Cell holder and support system

2.3.2.1 Pump and exchange system

The basic purpose of the sample holder and support system is to maintain anchorage-dependent cells while in the NMR magnet in an environment comparable to what they would have in tissue culture conditions. The principle conditions of concern are pH, oxygen supply, glucose supply and sterile conditions. To this end, the system shown in Fig. 16 was constructed. Cells to be studied were grown using conventional tissue culture techniques on 100 mm plastic tissue culture plates. When the cells were near confluence, they were mechanically removed from the tissue culture plates and seeded onto microcarriers which had been prepared in one of several ways. Then, when the cells attached to the microcarriers, the microcarriers were pipetted into the sample holder. The entrance and exit ports of the sample holder were covered with a nylon mesh which had a 50 μm pore size. This kept the microcarriers and the cells which were attached to them in the sample holder while medium superfused the cells.

The medium was pumped from a reservoir to the oxygen exchanger, to a bubble trap, and then to the sample holder. After passing through the sample holder, the medium was returned to the medium reservoir or passed through a pH meter, and/or oxygen meter, or it was simply collected in a separate container without recirculating. The specifics of each part of the system are

described here.

The tubing used to connect the system is thick-wall Teflon tubing, 1/8" outside diameter, with a wall thickness of 0.030 inches. This was put together with fittings also made of Teflon and manufactured by General Valve Corporation, Fairfield, N.J. In some places connections were improvised with silastic tubing and nylon ties. Thick tubing was used to minimize oxygen diffusion into or out of the perfusion medium while passing through the tubing in route to the cells. The medium was put into two Gibco 500 ml medium bottles (called A and B). The caps of the bottles were modified. They had three holes drilled in them and tubing was passed through. The joint at the point where the tubing passes through the cap was made air and water tight with RTV General Electric silastic cement. One tube was connected to a 0.2 μm millipore filter as a vent port, a second tube for medium return was connected to a three-way switch, and a third was also connected to a three-way switch for medium outflow. The two three-way switches allowed for selection of medium in bottles A or B, and determined the disposition of the return. The medium bottles were in an ice bath to prevent degradation of the medium and impede possible bacteria growth. The medium was pumped from these bottles by an LKB (model 2120) pump at 3 ml/min into a gas exchanger maintained at 47 ° C by a self-pumping constant temperature bath (MGW LVDA model C3). The gas exchanger was made by wrapping 50 ft. of Silastic® tubing (0.058 in I.D. by 0.077 in O.D. Lot. No. 602-235) manufactured by Dow Corning around a 2-inch diameter glass tube 5 inches long, which in turn was placed

concentrically in a similar length of 3 inch diameter glass tubing with Teflon blocks on either end fitted with 0 rings held in a pressure fit against the end of the glass tubes by a bolt connecting them. Heating water from the water bath passes through the inner cylinder, and the exchange gas passes through the space between the inner and outer cylinder. The silicon tubing, filled with medium which was being pumped through it, was in good thermal contact with the inner tube and was heated to 47 ° C. It is at this temperature that the gas mixture was equilibrated with the superfusion medium across the Silastic tubing, which is highly permeable to gas (Ross, 1972). The net result was that the medium exited the exchanger at a temperature higher than that with which it entered and similarly with a higher O_2 and CO_2 content. The medium contained a sodium bicarbonate buffer, and hence the pH of the medium was modified with a change in the partial pressure of the CO_2 in the medium.

Figures 17 and 18 shows the relationship between the pH, O_2 content and temperature of the medium as it exited the exchanger with changes in the speed with which the medium was pumped through the exchanger. The medium next entered the bubble trap which was also maintained at 47 ° C. The output of the bubble trap passed through five feet of tubing to the NMR probe. This five-foot length of tubing was covered with a one-half inch thick foam hot water pipe insulator which had a half-inch inside diameter. The exit gas of the oxygen exchanger was fed into the space between the insulating tubing and the perfusion tubing. This gas passed through the 5-foot length of insulation tubing and exited at the NMR probe. This reduced the possibility that the CO_2 or O_2

Figure 16

(A) This is a block diagram of the life-support system used for cell growth. Medium is pumped from a reservoir of 500 ml through a heat and gas exchanger from which it exits at 47° C saturated with 10% CO_2, 90% O_2 gas. From the gas exchanger it passes through a bubble trap, which is also maintained at 47° C, then to the sample holder. There is heat loss between the bubble trap and sample holder such that the medium is at 37° C when it enters the cell chamber. The medium superfuses the cells in the chamber at 3 ml per minute, exits and returns to the reservoir. The exiting superfusate can be monitored for O_2 consumption (shown) and/or pH (not shown). The cell chamber is in a single-turn coil of the NMR probe. Only the coil is shown for clarity.

(B) This diagram is a more detailed version of (A) and illustrates a later version of the system in which a heat exchanger was also put in the probe itself, just before the sample holder.

(C) These are photos of the autoclavable system. (2) shows the complete system, including the probe right background which is not autoclaved. (1) and (3) show the gas and heat exchanger center and the two medium bottles right. After autoclaving, these medium bottles are filled with growth medium and

moved into an ice bath before the system is put into operation. (4) shows the sample holder which has cells and microcarriers in it before the cover is placed over the probe head.

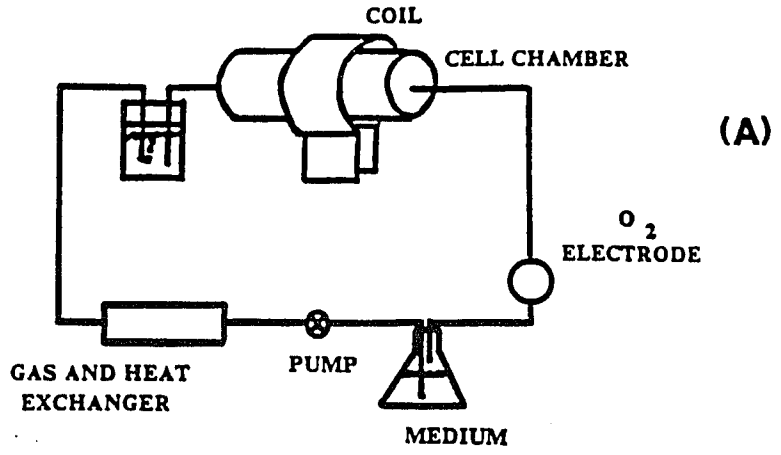
COIL
CELL CHAMBER
(A)
O 2
ELECTRODE
GAS AND HEAT
EXCHANGER
PUMP
MEDIUM

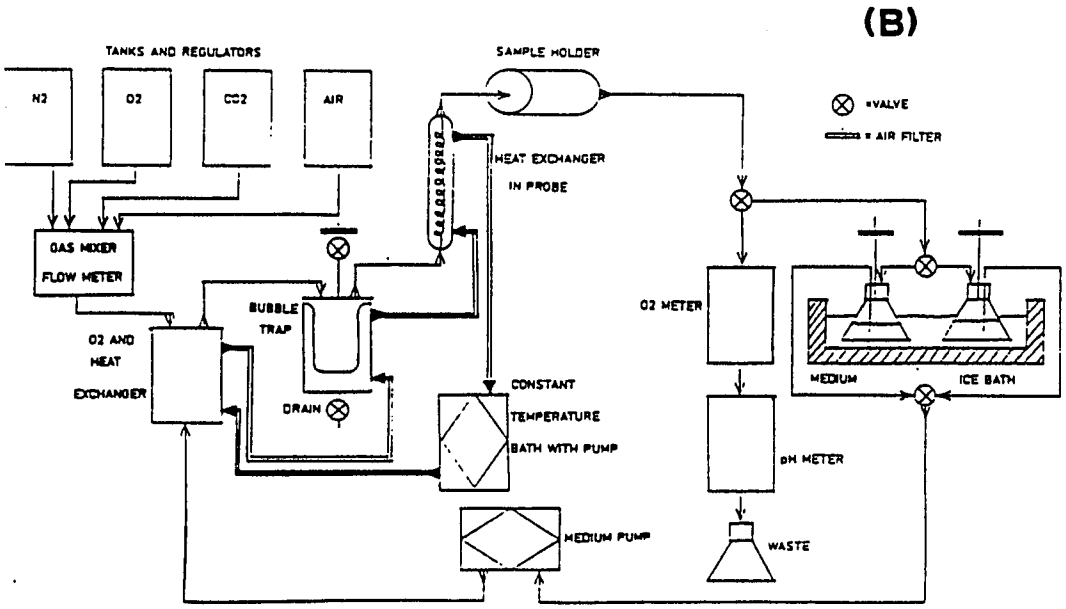
(B)
TANKS AND REGULATORS
N2
O2
CO2
AIR
SAMPLE HOLDER
VALVE
AIR FILTER
HEAT EXCHANGER
IN PROBE
GAS MIXER
FLOW METER
BUBBLE
TRAP
O2 AND
HEAT
EXCHANGER
DRAIN
CONSTANT
TEMPERATURE
BATH WITH PUMP
O2 METER
MEDIUM
ICE BATH
pH METER
MEDIUM PUMP
WASTE

FIG. 16 (A) (B)

(1)

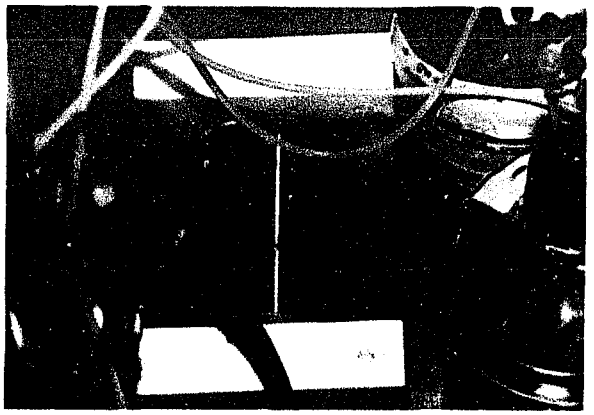

(2)

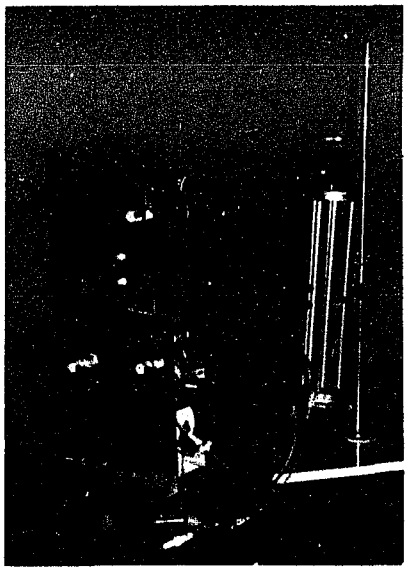

(3)

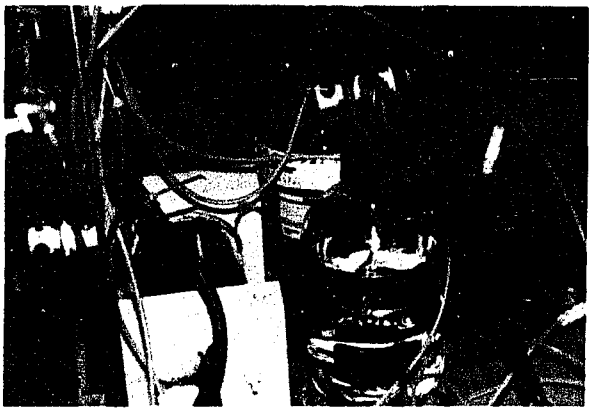

(4)

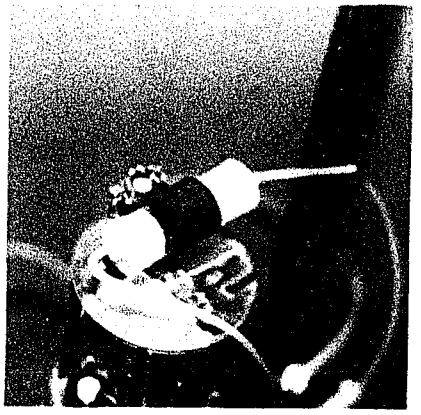

FIG.16(C)

Figure 17

An experiment was run to determine the effect of pump speed on the oxygen content, temperature and pH of the superfusing medium delivered to the sample holder. Under normal experimental conditions, the tubing between the gas and heat exchanger was clad with a larger diameter tubing. The exchange gas as it exists the gas and heat exchanger was forced into the volume between the inner and outer tube, thus reducing the oxygen and CO2 gradient across the tubing which carried the medium to the cell holder. In the experiment reported in this figure this outer tubing was not used in order to obtain a worst case condition for oxygen loss across the line.

(A) The oxygen electrode and meter is a YSI model 54 oxygen meter. It has a calibrated scale from 0 to 20 mg/1 and a voltage jack. The voltage output and scale readings are plotted in this figure. The output of the meter was 337.5 mV when the electrode was put in the medium fully saturated with O_2. The voltage is linear with oxygen content as measured in mg/1 or percent of the saturated content. The conversion factor as measured was 6.15 mgO_2/mV and 3.38 mV per percentage of the saturated value. (B) shows the calibration of the LKB pump in terms of the pump settings vs. the actual flow rate in ml/minute measured.

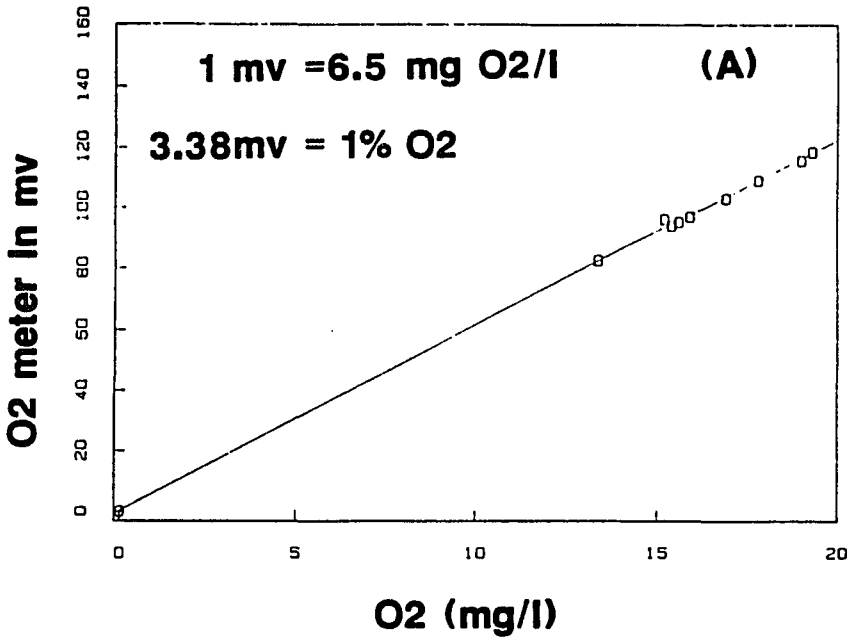
1 mv =6.5 mg O2/l
(A)
3.38mv = 1% O2
O2 meter in mv
0
20
40
60
80
100
120
140
160
0
5
10
15
20
O2 (mg/l)

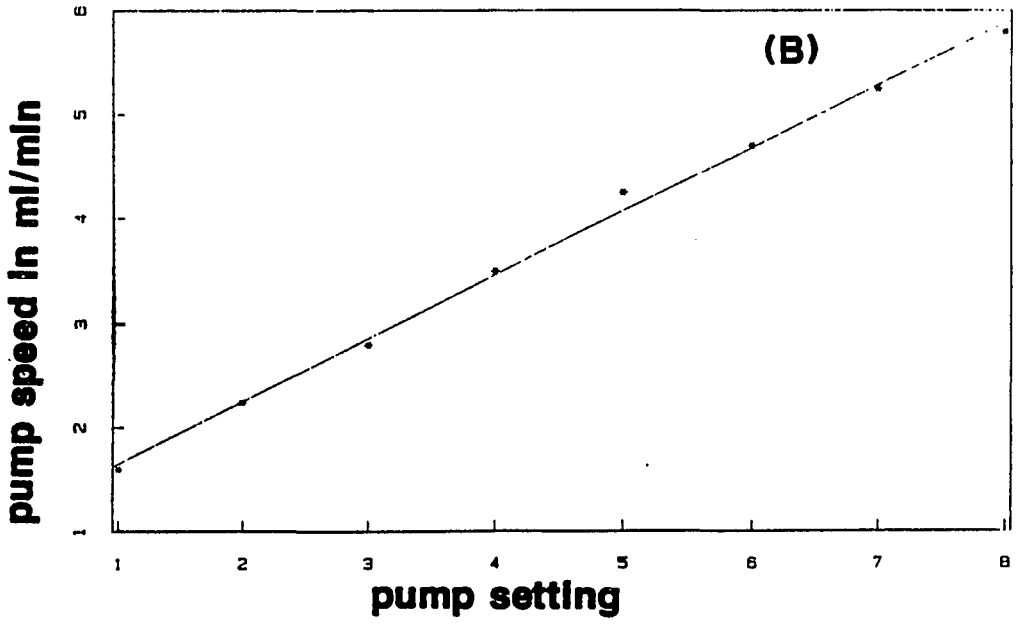
(B)
pump speed in ml/min
1
2
3
4
5
6
1
2
3
4
5
6
7
8
pump setting

FIG. 17

Figure 18

Data obtained as in Fig. 17 except that measurements were made at the entrance to the cell chamber.

Using the calibrated system described in Fig. 17, data obtained are shown in (A) (B) and (C). These are plots of the flow rate through the tubing vs. the oxygen content as a percent of 100% saturated medium at three points in pumped loops. (See (D)). It was measured at a point at the entrance to the NMR probe, (b) at the exit of the NMR probe and (c) eleven feet downstream from the probe just before the medium bottle. The temperature bath was maintained at 48 C for all experiments. The gas-heat exchanger was perfused with 90% O_2 and 10% CO_2. The change in the temperature of the sample holder is plotted as a function of the pump speed in (E) the variation in the pH as a result of changes in the CO_2 content of the cells is shown in (F).

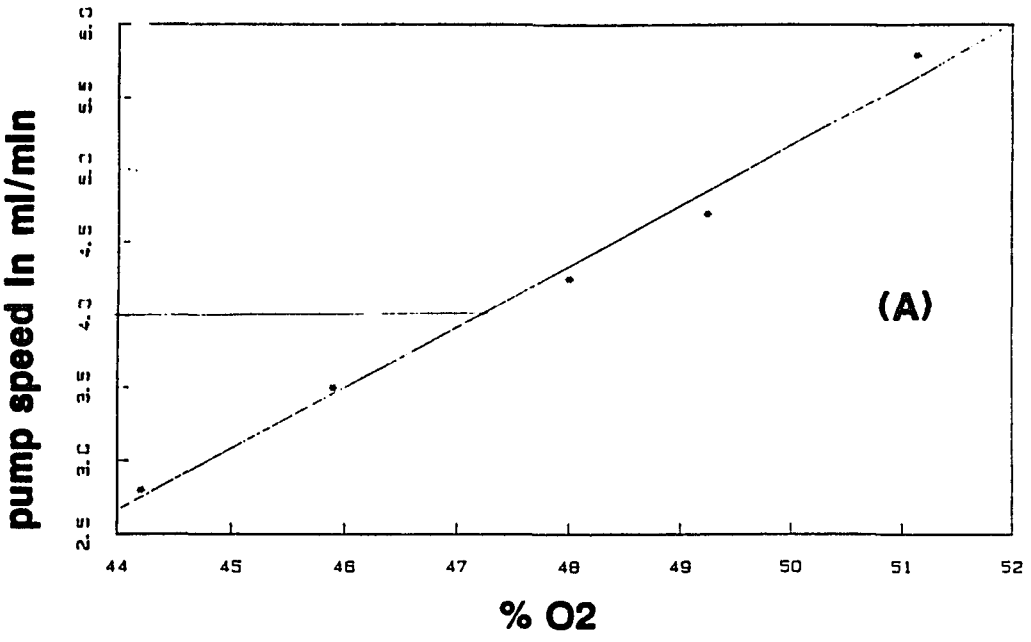
pump speed in ml/min
2.5
3.0
3.5
4.0
4.5
5.0
5.5
6.0
44
45
46
47
48
49
50
51
52
% O2
(A)

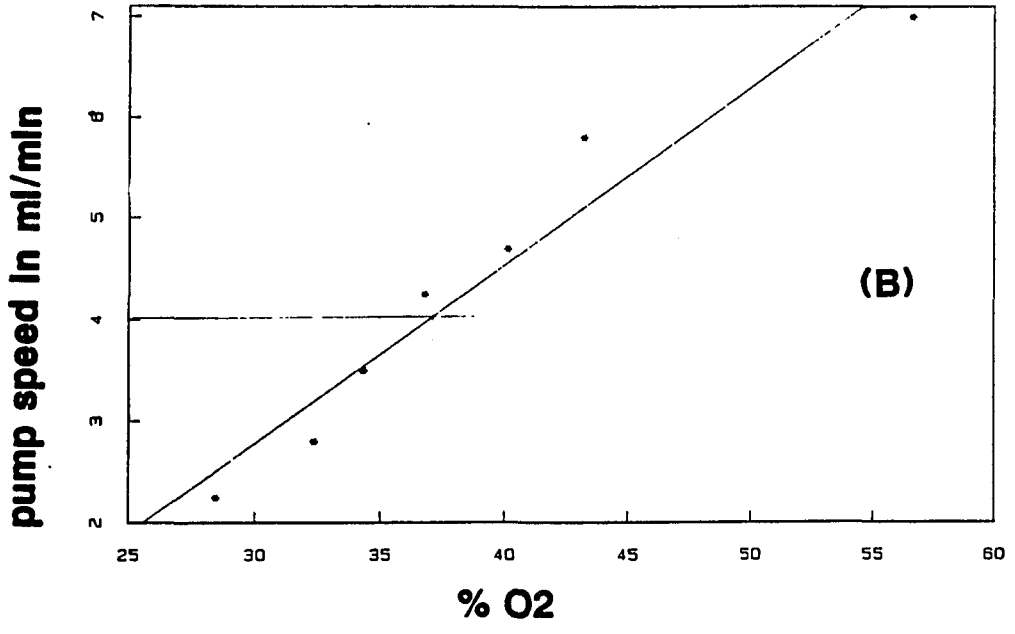
pump speed in ml/min
2
3
4
5
6
7
25
30
35
40
45
50
55
60
% O2
(B)

FIG. 18 (A) (B)

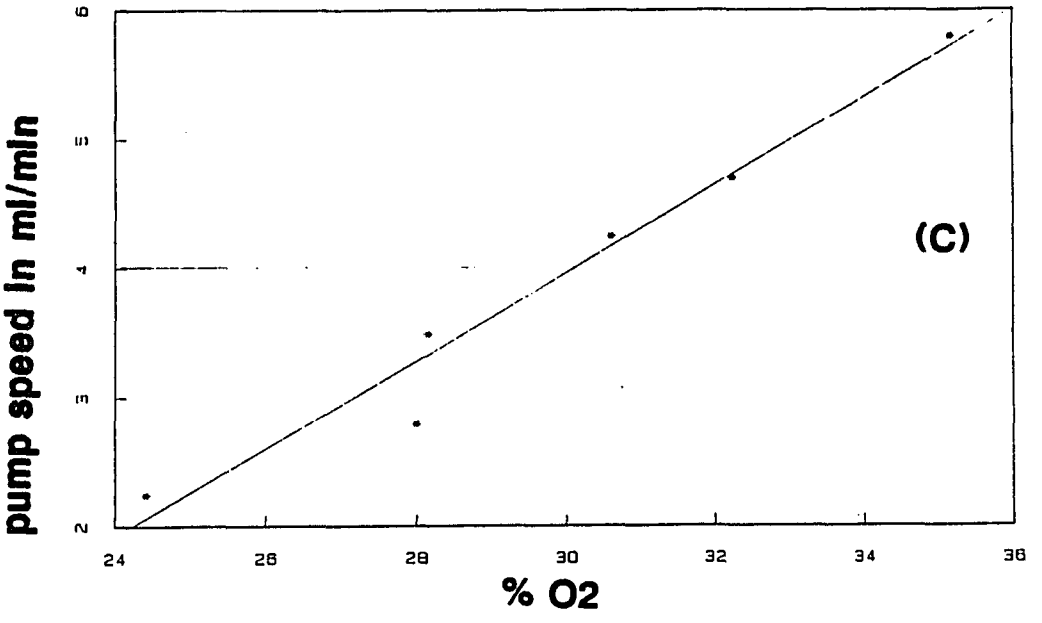
pump speed in ml/min
2
3
4
5
6
24
26
28
30
32
34
36
% O2
(C)

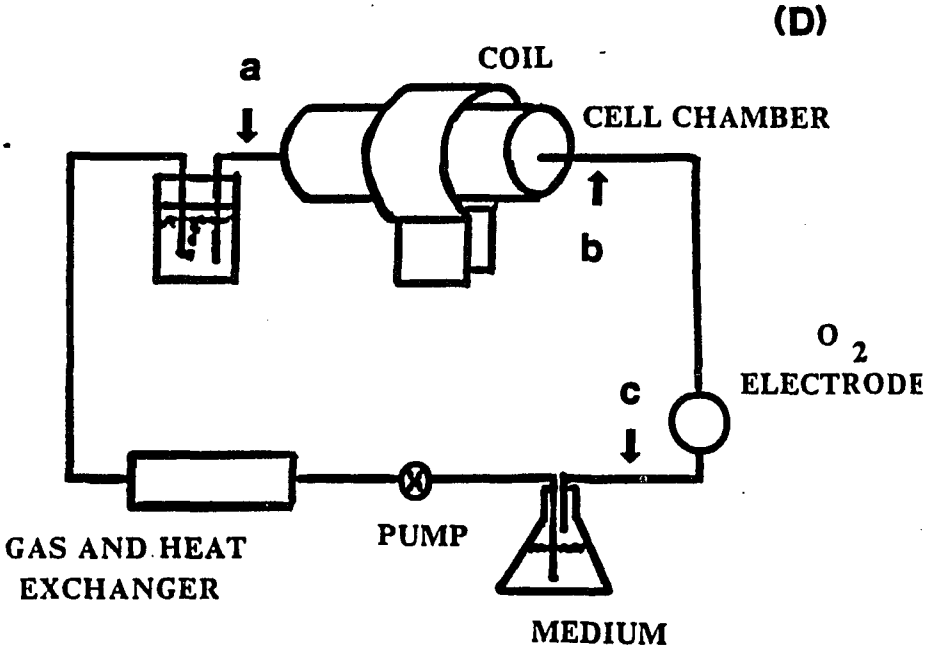
(D)
a
COIL
CELL CHAMBER
b
O 2
ELECTRODE
c
GAS AND HEAT
EXCHANGER
PUMP
MEDIUM

FIG. 18 (C) (D)

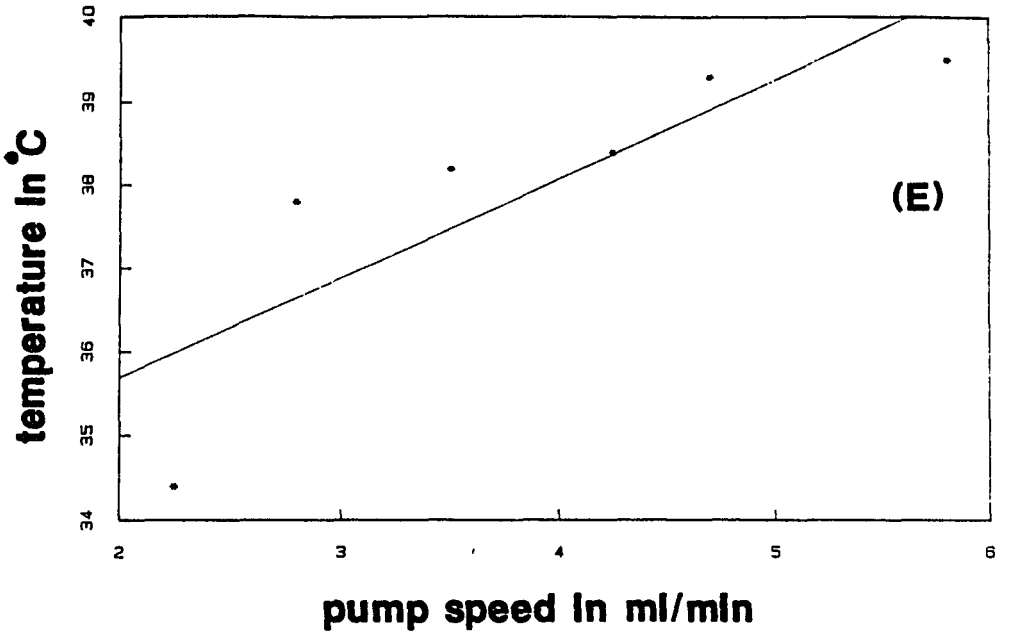
temperature in °C
40
39
38
37
36
35
34
2
3
4
5
6
(E)
pump speed in ml/min

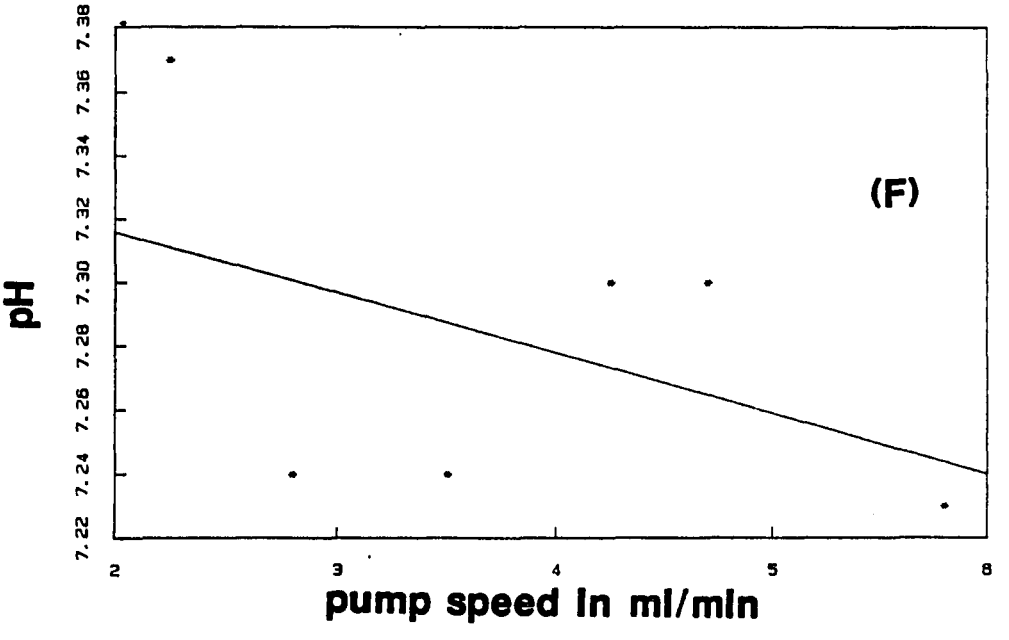
pH
7.38
7.36
7.34
7.32
7.30
7.28
7.26
7.24
7.22
2
3
4
5
8
(F)
pump speed in ml/min

FIG. 18 (E) (F)

content of the perfusion medium could change. Figure 18 shows data obtained at the entrance and exit to the NMR spectrometer probe and also at the oxygen meter. (Note: at the pump speed used in the experiments, the temperature is 37°). The sample holder in the probe was bathed in a 37°C nitrogen gas stream. The gas temperature was maintained by a temperature controller in the Bruker 360 spectrometer. The return trip from the spectrometer was relatively uneventful. It passed out of the probe to a three-way switch, which determined whether or not it returned to the reservoir from which it came, or to the oxygen meter, pH meter and finally to a non-recirculating receptor for spent medium. The sample holder is shown in Fig. 19. Two silicon number 3 corks had a cone cut in the smaller diameter end and a hole was poked through the axis of the cork. The Teflon tubing, whose surface had been abraded with sandpaper, was pushed through the cork to the tip of the cone and cemented in place with a large blob of silicon cement. The nylon mesh was also cemented in place. The corks were easily pushed into the ends of 20 mm I.D. right-circular cylinders. The cork on the feed side can be removed and the cylinder can be passed through the single-turn probe coil, the sample holder loaded with the sample and the cork replaced. In practice, this was found to be the step most sensitive to contamination. In the process of filling the sample holder, the nonrecirculating mode was used and the return receptacle was placed 3 feet below the sample holder to insure a good gravitational flow of medium to allow compacting of microcarriers and cells in the holder. During running in the magnet, the return receptacle and medium bottles were positioned on a table a

Figure 19

This shows the components of the sample holder used in most of the experiments.

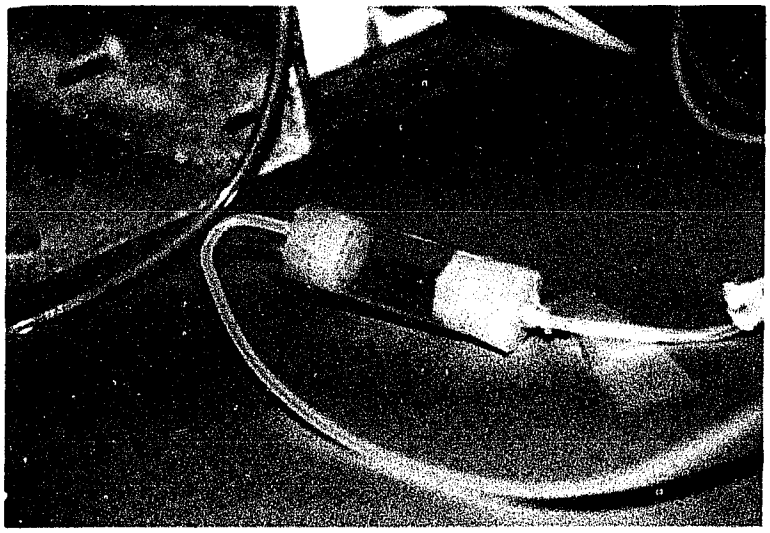

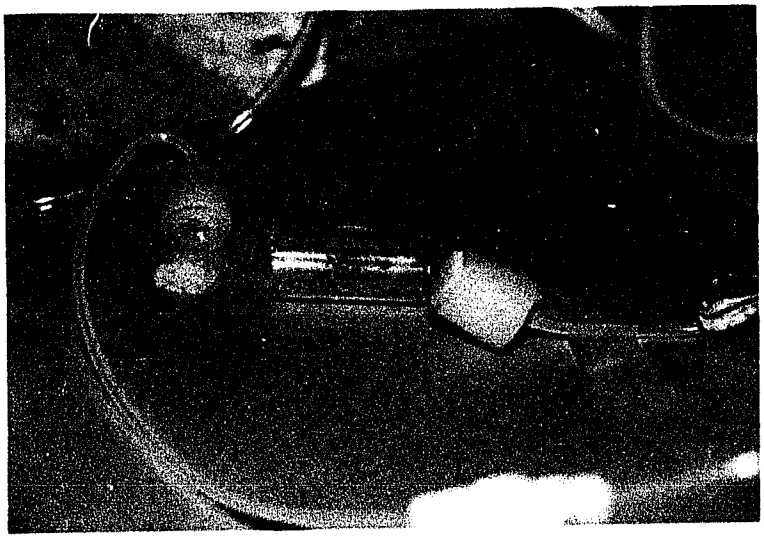

FIG. 19

few inches higher than the sample holder in the magnet. This insured that the sample holder would not be syphoned off in the event of a small air leak in the lines, bubble trap, etc., thus allowing air bubbles to form in the active coil volume and destroying the homogeneity of the magnetic field. The gas mixer was a Matheson gas mixer (model 7-315T) with four flow gauges, two number 603, and two 602. These allowed the gases to be mixed in the right proportions. The O_2 and CO_2 gas tanks were supplied with Matheson regulators (model numbers 8L-296 and 1L-302 respectively); in addition to these a second low-pressure regulator was placed in series with the O_2 and CO_2 regulator. This was done because in the normal mode of operation, when oxygen and carbon dioxide are used, it was found that the pH varied $\pm$.05 pH units due to fluctuations in the partial pressure of CO_2. This was brought down to $\pm$.02 pH units when the low pressure regulators were installed after the two-stage high-pressure regulator. Even this fluctuation was cause for concern in many experiments, and on these occasions, Hepes buffer was used to maintain the pH. The pump which pumped the medium is an LKB (model 2120) which pumped on a Silastic tube that could be removed from the pump without breaking connections. Thus, by removing the insulating arm from the input tube and breaking connections at the points one to five in the drawing, removing the medium bottles from the ice bath and replacing them with empty bottles, the heart of the system, without the medium, can be autoclaved intact. This allowed for sterile operation up to 200 hours, the longest time an experiment has been followed.

Once the system had been autoclaved, the medium bottles were replaced with bottles containing appropriate medium. This was done in a sterile hood. The medium came in contact with the following materials: glass, silicon rubber, Teflon, microcarriers and cells. This also allowed for sterilization by pumping ethanol through the lines, and was the method of choice when the experiment was to be run in less than ten hours. The first experiments were on a system which used 1/8 inch Tygon tubing for connecting the various parts, and nylon valves. This system was good for experiments lasting up to ten hours if the system was thoroughly flushed with medium. This system was not amenable to autoclaving and could not be flushed with ethanol without altering the Tygon tubing. In addition, the Tygon tubing is permeable to gases (Ross, 1972).

2.3.2.2 pH measurements

The pH determinations are made on the basis of the chemical shift of various nuclei (Shulman, 1979; Moon, and Richards, 1973). In these experiments the shifts of phenylphosphonic acid (PPA) and inorganic phosphate (Pi) were used. The phosphate can exist in a protonated form at one pH and an unprotonated form for another pH. Each species resonates at a different frequency. If two species are present, one peak is observed at some intermediate frequency, as a result of the fast exchange of protons between species, which can not be resolved in the time of the NMR observation. The chemical shift is a weighted function of the relative populations of each species, and is affected by temperature and ionic strength of the solvent (Brown and Ugurbil, 1984a). Phosphocreatine has a chemical shift which is constant in biological systems in

Figure 20

PPA is used for determining the extracellular pH and as a marker. The peak is downfield of the PME region. This makes it a good choice for determining the pH when there is little extracellular Pi or when the intercellular Pi is large and the pH gradient across the cell is small. The pH was measured at 47. C wit h a radiometer pH meter model 26 which was calibrated against Fisher pH standards between 4 and 9 pH units. The values presented in (A) are corrected in pH for temperature and meter calibration. The values vs. chemical shift are given for 1 mM PPA in a Krebs Henselett buffer. The data plotted in (A) was fitted to a sigmoidal curve by a least squares approximation from which the pH and end points were obtained (δ acid and δ basic).

These values were used in the following expression

$$\mathrm{pH} = \mathrm{pk} + \left[\log \frac{\alpha}{1+\alpha}\right]$$

were $\alpha = \dfrac{\delta_0 - \delta\,\mathrm{acid}}{\delta\,\mathrm{base} - \delta\,\mathrm{acid}}$ The values were

$$\delta\ \mathrm{acid} = 13.74$$

$$\delta\ \mathrm{base} = 11.88$$

$$\mathrm{pk} = 7.077$$

The calculated values of pH for given δ (B) were plotted and used to determine absolute changes in pH.

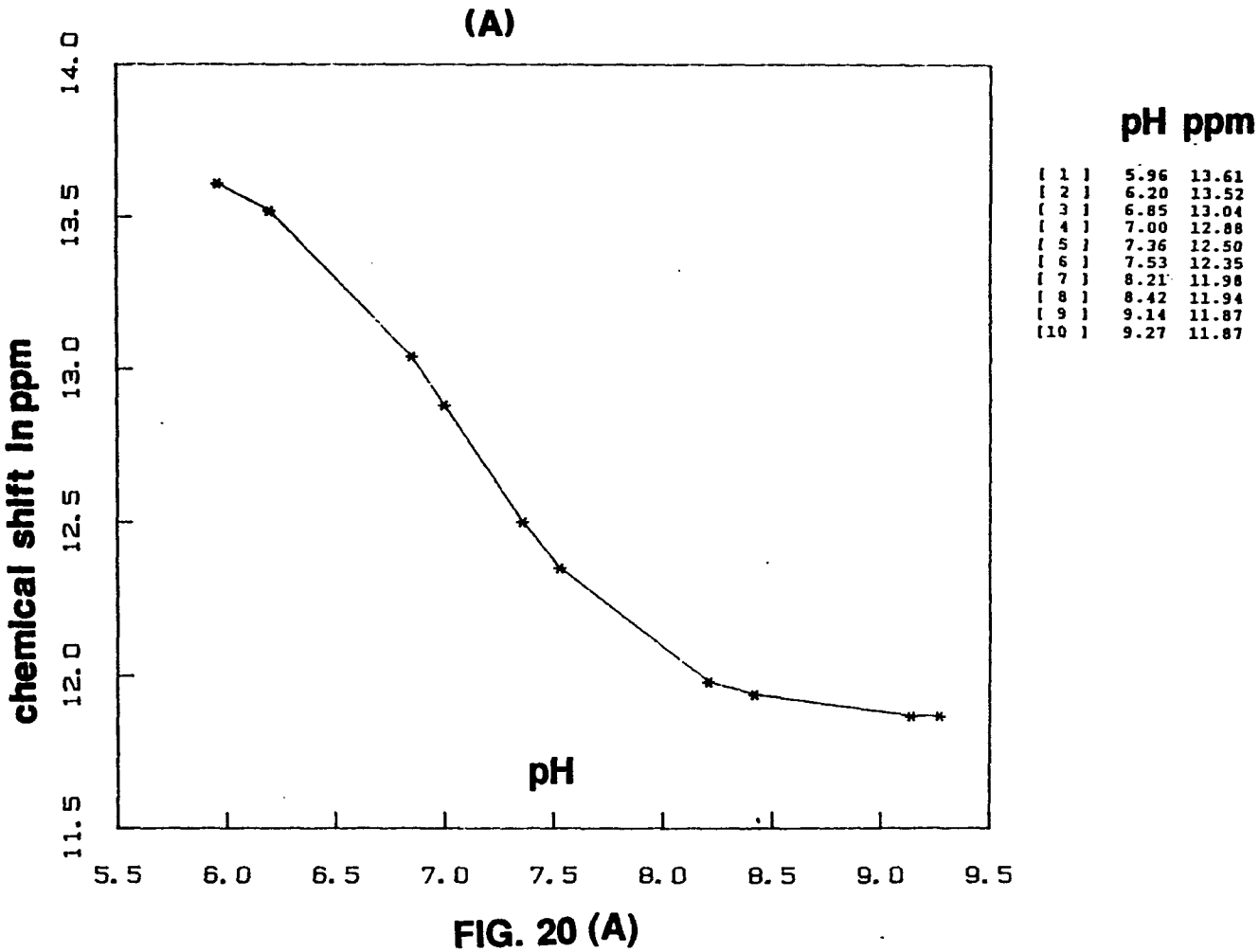
(A)
chemical shift in ppm
14.0
13.5
13.0
12.5
12.0
11.5
5.5
6.0
6.5
7.0
7.5
8.0
8.5
9.0
9.5
pH
pH ppm
[1] 5.96 13.61
[2] 6.20 13.52
[3] 6.85 13.04
[4] 7.00 12.88
[5] 7.36 12.50
[6] 7.53 12.35
[7] 8.21 11.98
[8] 8.42 11.94
[9] 9.14 11.87
[10] 9.27 11.87

FIG. 20 (A)

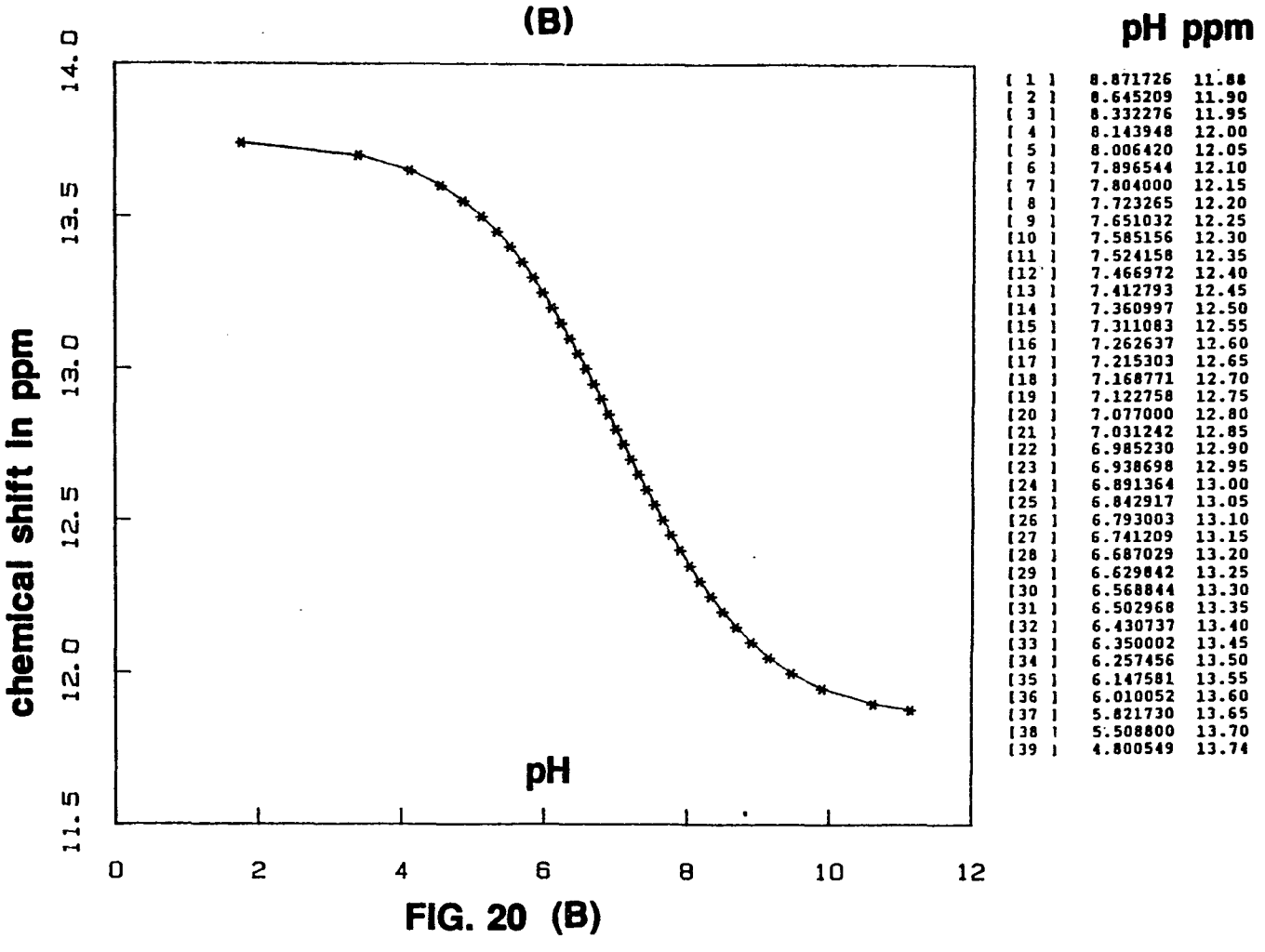
(B)
chemical shift in ppm
14.0
13.5
13.0
12.5
12.0
11.5
0
2
4
6
8
10
12
pH
pH ppm
[1] 8.871726 11.88
[2] 8.645209 11.90
[3] 8.332276 11.95
[4] 8.143948 12.00
[5] 8.006420 12.05
[6] 7.896544 12.10
[7] 7.804000 12.15
[8] 7.723265 12.20
[9] 7.651032 12.25
[10] 7.585156 12.30
[11] 7.524158 12.35
[12] 7.466972 12.40
[13] 7.412793 12.45
[14] 7.360997 12.50
[15] 7.311083 12.55
[16] 7.262637 12.60
[17] 7.215303 12.65
[18] 7.168771 12.70
[19] 7.122758 12.75
[20] 7.077000 12.80
[21] 7.031242 12.85
[22] 6.985230 12.90
[23] 6.938698 12.95
[24] 6.891364 13.00
[25] 6.842917 13.05
[26] 6.793003 13.10
[27] 6.741209 13.15
[28] 6.687029 13.20
[29] 6.629842 13.25
[30] 6.568844 13.30
[31] 6.502968 13.35
[32] 6.430737 13.40
[33] 6.350002 13.45
[34] 6.257456 13.50
[35] 6.147581 13.55
[36] 6.010052 13.60
[37] 5.821730 13.65
[38] 5.508800 13.70
[39] 4.800549 13.74

FIG. 20 (B)

the normal physiological range of pH. It is used as a secondary standard when it is present in cells and assigned a value of -2.49 ppm. When this is not present, the ATPα peak is used and assigned a value of -10.009 ppm. When extracts are measured with phosphorus NMR, glycerophosphorylcholine (GPC) is used and assigned a value of 72 Hz. Experiments were run to establish the chemical shift curves for the various molecules used as pH indicators, and ATP at salt concentrations estimated to be that which is in the cells. Figure 20 shows the plots and listings of calculated numerical values for PPA. The experimental values were fitted to the following expression:

$$\mathrm{pH} = \mathrm{pK} + \mathrm{Log}\left(\frac{\alpha}{1-\alpha}\right)$$

where

$$\alpha = \frac{\delta_0 - \delta_{\mathrm{acid}}}{\delta_{\mathrm{basic}} - \delta_{\mathrm{acid}}}$$

and $\delta_0 =$ the observed chemical shift at a given pH given sufficient experimental data in terms of pH and δ a fitting program can generate pH, δ basic and δ acid.

In practice the terminal chemical shifts remain constant with ionic strength of the solvent, but the pK changes.

PPA is used in a number of experiments where Pi free Ringers is used.

When PCr is present the following expression is used for the Pi chemical

shift which comes from Prichard, et al., 1983:

$$pH = 6.77 + \mathrm{Log}_{10}\left((\Delta - 3.29)/(5.68 - \Delta)\right)$$
where $\Delta = \delta\,\mathrm{Pi} - \delta\,\mathrm{PCr}$.

There is an extensive literature on pH measurements using NMR (Brown, and Ugurbil, 1984).

3. CELL SYSTEM HISTORY AND BACKGROUND

A very large number of cells was used in the microcarrier system. Neuroblastoma cells were chosen because they are a good model cell for the sympathetic nervous system (Augusti-Tocco and Sato, 1969, Schubert, et al., 1969, Haffke and Seeds, 1975). N1E-115 cells were culled from a spontaneously occurring C1300 neuroblastoma by Amano and Richelson while working in Nirenberg's laboratory (Amano, et al., 1972, Blume, et al., 1973). It is one of a number of continuous strains they derived from this C1300 line and it was found to have many of the properties of an adrenergic cell (see appendix D). In particular the tyrosine hydroxlyase activity is high in this cell line. This is a crucial enzyme in the biosynthetic pathway for norepinephrine synthesis. Another attribute which makes the N1E-115 appealing is its rapid doubling time, nominally less than 2 days, thus allowing an NMR sample to be generated from a confluent T25 flask in 5-10 days. The cells can be induced to differentiate in a number of ways (Blume, et al., 1973).

DMEM supplemented with 2% DMSO, and with 2% fetal bovine serum was

used to induce differentiation. This terminates mitosis and induces morphological changes within two days. A typical progression is seen in Fig. 21. At day 2 the cells exhibit the morphology of neurons. These cells also differentiate biochemically and will support an action potential within 3 weeks (Spector, et al., 1973, Chalazonitis, and Greene, 1974, Tuttle, and Richelson, 1974). Complete conditions are not always given. DMEM comes with high glucose 4.5 g/l and low glucose 1.0 g/l. Generally this value is not given. Most people use a bicarbonate buffer system. The specific system used here is detailed below. Cells were generally grown to near confluence in nine days when used in the undifferentiated state. A typical NMR sample currently used is obtained from 25-30 near confluent 100 mm tissue-culture dishes. The cells were mechanically dislodged from the surface of the tissue-culture dish with a jet of medium from a 10 ml pipette, operated with an electric pipetter. Typically five to six pipette-fulls, 10 ml each, were needed to dislodge all the cells. They were then added to the microcarriers, allowed to attach and placed in the sample holder.

To look at differentiated N1E-115 cells, two different procedures were used; in one, undifferentiated cells were placed on microcarriers in the magnet and then the medium was changed to induce differentiation. The second way was to induce differentiation and then to add the differentiated cells to the microcarriers, allowing time for attachment, and then putting them in the sample holder. Glioma, C6 cells, were basically handled in the similar manner.

Dissociated rat brain cells on the other hand were from a primary source. They were obtained from fetal rat brain using the method of Ahmed, (Ahmed, et al., 1983) and maintained in culture for periods ranging from several hours to thirty days prior to being used for NMR experiments.

3.1 N1E-115 Cells

N1E-115 cells were obtained from Richelson of the Mayo Clinic on March 2, 1982. They were in two T25 flasks completely filled with medium, and the tops sealed with paraffin. They were marked passage 12. The medium, except for 5 ml, was decanted from the flasks and used to feed the cells over the next ten days. The cells were split 5:1 on day 9 and subsequently allowed to grow to near confluence, at which time they were passaged again in the ratio of 6:1 using a T150 flask, and passaged again, 2:1. At this point, passage 15, the cells were aliquoted with 5% DMSO in 10% detal bovine serum (FBS) DMEM medium and frozen at 1 °C per minute, and placed in a -80 ° cold chest for storage. The sample holders were Cooke 2 ml cryotubes (Cat. No.235-1) and the DMSO was Gold Label methyl sulfoxide (Aldrich Cat. No. 15493-9). The growth medium used after exhausting the medium supplied with the cells was K&C low-glucose DMEM (Cat. No. DM-324). It was mixed as per instructions with doubly-distilled water, and 4.7 g/l sodium bicarbonate (Fisher Cat. No. S-233) filtered and stored in 500 ml Gibco medium bottles until needed (not more than 6 weeks) at which time 10% K&C heat inactivated fetal bovine serum was added together with 1% penicillin-streptomycin (Gibco Cat. No. 600-5148.) Feedings were Monday, Wednesday and Friday, at which time 80% of the

medium was replaced with fresh medium. When the passage number reached 25, a new sample was cultured up from frozen cells. These cells were not checked for PPLO. Yeast and fungus contamination required no special analysis for their presence in tissue culture, and when contamination occurred in the spectrometer, it became apparent because of an appearance of a phosphorus resonance peak at 22 PPM, one which is associated with polyphosphate for yeast (Barton, et al., 1980). The appearance of this resonance in fungus is my observation.

3.2 Dissociated Rat Brain Cells

Dissociated rat brain cells were obtained from rat fetuses. The method was basically that reported by Ahmed (Ahmed, et al., 1983) with slight modifications. The unique aspect of this preparation was its high yield of neuronal-type cells (90%) and the complete control of medium content. In all other systems with completely defined medium, the cells come in contact with serum at some time during the plating process. In this procedure, the cells never came in contact with serum. It was never used.

Three first-pregnancy Sprague-Dawly pregnant females (E 17-20 days); plug time ±12 hours) were anesthetized with diethyl ether. Fetuses were removed via abdominal laparotomy to an isotonic buffer solution (IBS). The whole brains were removed and placed in fresh IBS. The meninges and all visible blood vessels were removed using a dissecting microscope. The cleaned brains were put in isotonic buffer at 10 ° C. Brains pooled from 30-36 fetuses were minced

and placed in 25% trypsin-supplemented buffer (Worthington Biochemical Corp., Freehold, N.J.) 180 to 220 units/mg. There was approximately one brain per ml with the total sample being divided into three 75 ml Erlemyer flasks. There followed a series of steps of incubation, trypsinization and filtrations which yielded a large number of dissociated cells. These cells were then used to seed microcarriers or for other experiments. (See Appendix A for details.)

When the DRBC were put in Petri dishes which did not have a polysine coating, they started to aggregate and form small irregular clumps within one day, and formed spheres in a few more days, which grew in diameter with time. Similar findings have been reported by others (Guroff, 1980). It should be possible to utilize these spheres of cells in a perfusion system. I did not.

When the cells were plated onto a substrate which had been coated with polylysine, they attached and sent out processes. These cells did not attach well to collagen-coated substrates. The procedure is outlined in Appendix (A).

4. EXPERIMENTS WITH CELL CULTURE

Several experiments were undertaken to see how the neuroblastoma cells and dissociated rat brain cells behaved in various culture conditions. These conditions contain a constraint of using an incubator maintained at 7.5% CO_2. Other conditions involved growing the cells on plates, spinner bottles, serum-supplemented medium, and on ZAM, a completely defined serum-free medium. Growth conditions vary slightly from laboratory to laboratory. These

experiments were designed to establish cell growth in order to establish time requirements for obtaining the large number of cells required for an NMR experiment.

4.1 Cell Growth Characteristics

4.1.1 Cell growth on plates with DMEM

Growth estimates were made for N1E-115 cells on tissue culture plates with DMEM low glucose medium, 5.5 mM supplemented with 10% FBS and 1% PS with and without 0.2 mM Cr supplement, DMEM with 10% FBS, 1% PS, 0.2 mM Cr, 1 mM PPA, and 1% Penicillin-Streptomycin Solution (10,000 units Penicillin/ml, 10,000 mcg Streptomycin/ml in normal saline). Some experiments in the later part of this research used high-glucose medium (Gibco Cat. No. 196G) which has 25 mM of glucose in it. Growth estimates were also run on cells with this medium (see Fig. 21).

4.1.2 Spinner bottles

Since a larger number of N1E-115 cells are needed for each experiment, spinner bottle growth was investigated. A 250 ml spinner bottle with 150 ml of DMEM low glucose (as described above) was inoculated with 2.7×10^6 cells and placed on a spinner-bottle table in an incubator with 100% humidity, and 7.5% CO_2 and 92.5% air. Aloquats were taken every 48 hours, and a growth curve obtained. The results are shown in Fig. 22. The results indicated that this was a good way to obtain a large number of cells when undifferentiated cells are required. This system was not good, however, when differentiated cells are

needed as it has been shown that N1E-115 cells develop a different protein profile when they are induced to differentiate in the absence of a substrate (Akeson, and Herschman, 1974). There is an advantage in growing cells in a spinner bottle over growing cells in plates, in that they are not handled as many times between seeding and harvesting.

4.1.3 ZAM

Ahmed reported a defined medium which I call ZAM (Ahmed, et al., 1983), (see appendix A for details) for maintenance and growth of dissociated cells from cerebrum, cerebellum, and brain stem of 20-day gestational fetal rat. This medium is similar to Sato's defined medium which has been used on neuronal cell systems. ZAM was tested on N1E-115 cells. The 10^5 cells were plated at mid-log phase into Corning 100 mm plates on day zero. On day 1, all the medium was replaced with ZAM. By day 3, the cells appeared morphologically 100% differentiated. Because of this result, ZAM was not used for experiments with N1E-115 cells at this time; however this result was interesting in itself and should be investigated further.

4.1.4 Growth on microcarriers

The heart of the system used for experiments reported here is the cell-microcarrier complex. A tightly-coupled complex keeps the cells in the sample holder during perfusion; on the other hand, poor cell attachment results in the cells sluffing off the microcarriers and clogging the exit port. When the flow of the exiting medium is impeded, the pressure builds up, doing damage to

Figure 21

(A) These are photographs of undifferentiated cells grown in high glucose. Growth curves were not made for cells grown on substrate. This was because the cells do not adhere well during the cell cycle and near mitosis they round up and barely adhere. The result is that during refeeding many cells are sucked off. A more meaningful measure is the splitting ratio and the time between splittings. Cells grown on high glucose and split 5:1 require splitting every 3.7 ± 1.6 days, ($n = 6$) and 4.1 ± 1.4 days ($n=9$) for a 6:1 split. Cells grown on low glucose take better than twice as long to grow.

(B) When 2% DMSO was added to the growth medium and the FBS was reduced to 2% they differentiate morphologically with time as depicted here.

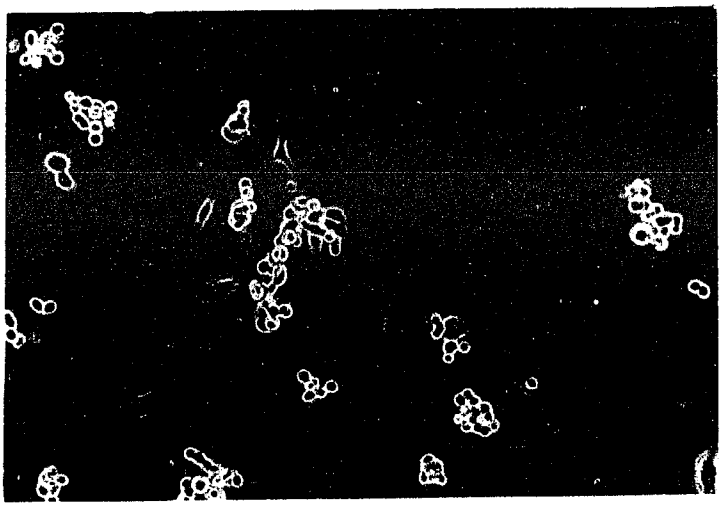

<↔> 100µm

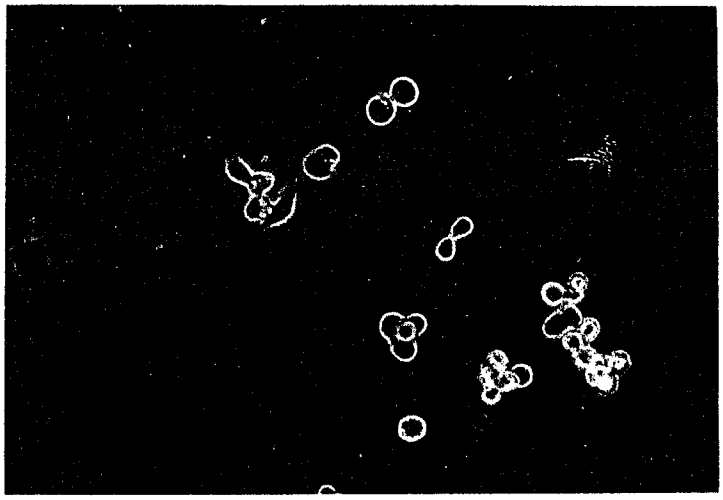

<——> 100µm

FIG. 21(A)

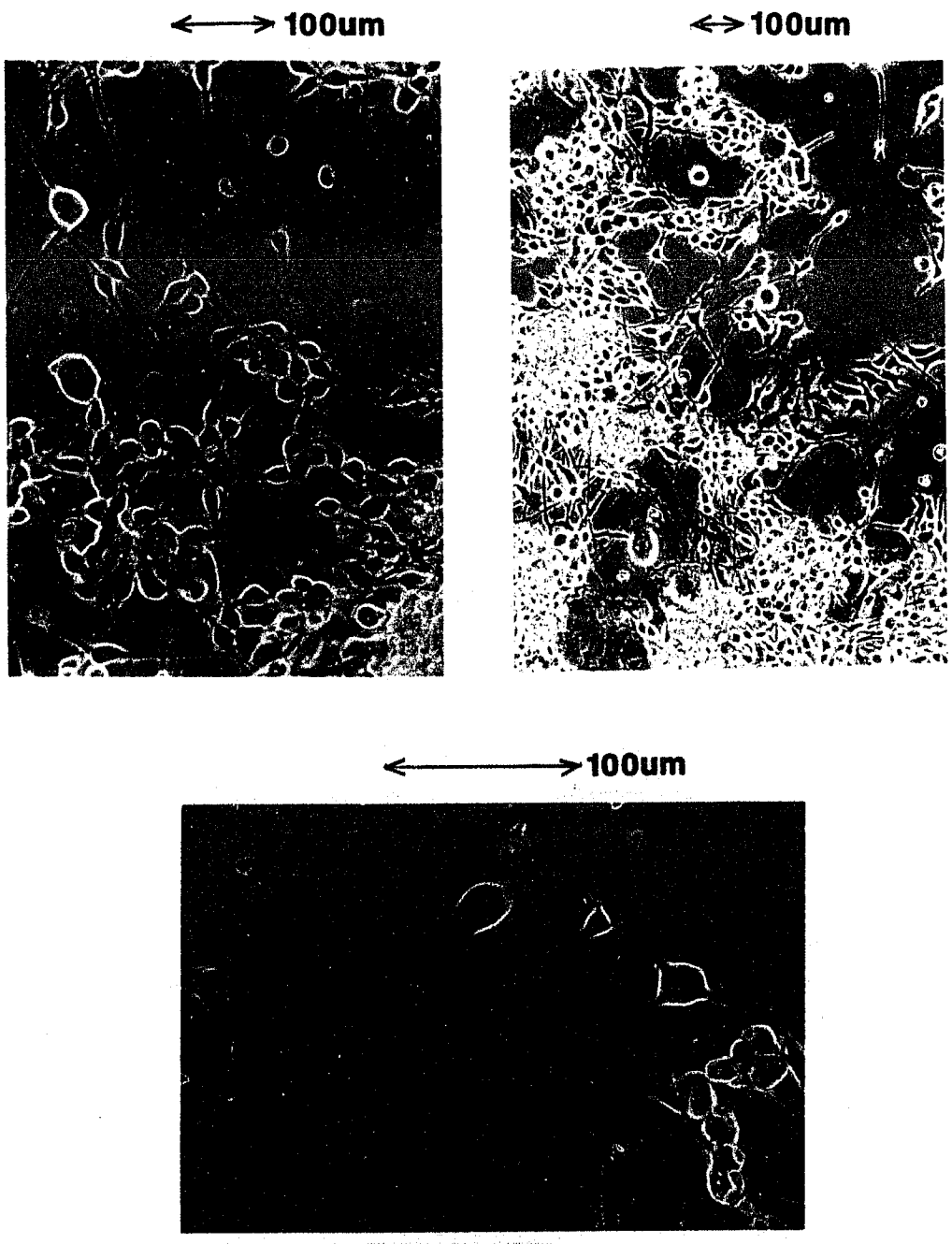

FIG. 21(B)

Figure 22

Cells were grown in a 250 ml spinner bottle (Bellco #1969-00250) containing 150 ml of medium and cells. The inoculation was made from mid-log phase cells dislodged hydrostatically by pipetting. No trypsin was used. 14.5 ml of 2×10^5 cells per ml were used to give a final concentration of 2×10^4 cells/ml. The growth medium is DMEM with low glucose supplemented with 10% fetal bovine serum and 1% penicillin-streptomycin in 7.5% CO_2, 92.5% air at 100% relative humidity.

These results showed that an NMR sample could be grown in 200 ml of medium in 8 to 10 days in a 500 ml spinner bottle to yield the 10^8 cells needed.

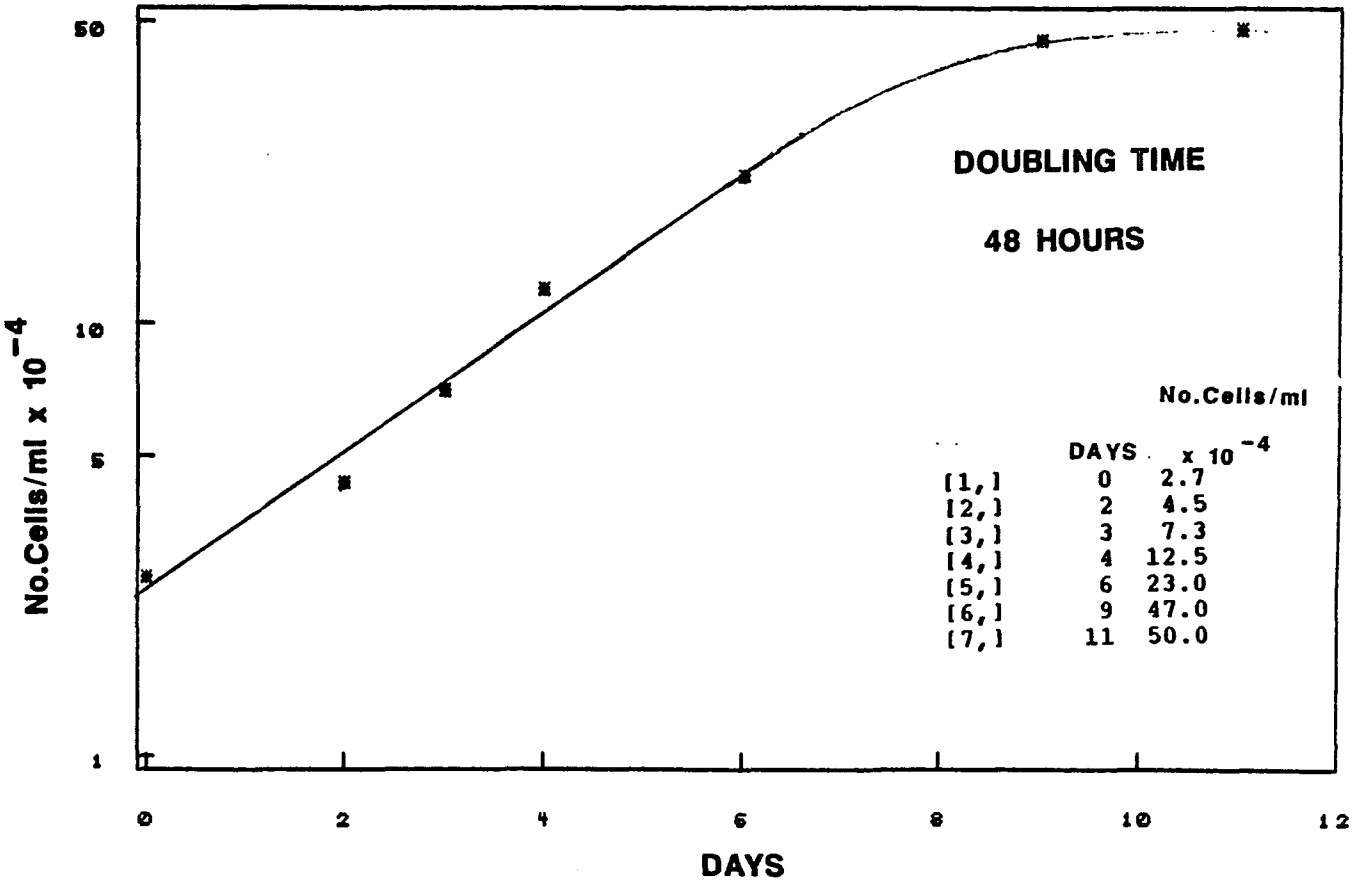
50
10
5
1
No.Cells/ml x 10^-4
0
2
4
6
8
10
12
DAYS
DOUBLING TIME
48 HOURS
No.Cells/ml
DAYS x 10^-4
[1,] 0 2.7
[2,] 2 4.5
[3,] 3 7.3
[4,] 4 12.5
[5,] 6 23.0
[6,] 9 47.0
[7,] 11 50.0

FIG. 22

the cells and eventually forcing the end stoppers off the sample holder. It is therefore important to use the right cell-microcarrier system. The carrier systems available at the start of these experiments were Biosylon, and Cytodex I and II. During the course of the research Cytodex III became available.

The Cytodex III microcarrier system is collagen-coated and is the preferred system for N1E-115 cells. Polylysine-coated Biosylon microcarriers turned out to be the best for DRBC.

4.1.4.1 Cytodex, II & III

The first step in the procedure for growing N1E-115 cell in tissue culture requires the dislodging of the cells from the substrate on which they are growing. In general this is done with a trypsin solution; however when N1E-115 cells are in an exponential growth phase "mid log" they can be dislodged from a 100 mm tissue culture plate hydrostatically by pipetting a 10 ml stream of medium at the substrate surface several times. The cells are not strongly attached. This is convenient for passaging, but poses a problem for a perfusion system. Attempts to get N1E-115 undifferentiated cells to attach to Cytodex II microcarriers yielded poor results. The procedure used was to put the microcarriers into siliconized 150 mm glass Petri dishes, add 30 ml of complete medium and then put the plates in the incubator over night. This allowed any attachment factor present in the serum or in the medium to adhere to the microcarrier surface. After this, cells were harvested from the 100 mm tissue culture plates and seeded onto the microcarriers and placed in the incubator.

Every fifteen minutes for the first hour and a half, the Petri dishes were moved in the pattern of small figure eights in order to get the unattached cells to come into contact with microcarriers. The result at two hours or two days was the same, only a very few cells attached to the microcarriers, so this effort was discarded.

Better results were obtained using Cytodex III microcarriers. These microcarriers have collagen covalently bonded to their surface. Using the same procedure described above, the N1E-115 cells were seeded onto the Cytodex III microcarriers. The results obtained here were usable, although not ideal. The cells attached in two major ways. In the first way, groups of cells formed clumps and these clumps attached to one or more microcarriers. In the second way, single cells attached to single microcarriers. The hoped for homogeneous coating of the microcarriers with cells was never obtained, but when the cells grown in this fashion were put into the sample holder, a good signal was observed and the systems could be maintained for weeks. Many of the earlier experiments were run on cells which were seeded onto the microcarriers and then maintained in the tissue-culture culture incubator for periods of 5 to 20 days, the procedure originally developed for C3HT10½ cells. It became apparent that prolonged growth on the microcarriers was not necessary; on the contrary, it may have been detrimental. The cells on microcarriers which were kept in the tissue culture incubator and fed once every 24 to 36 hours had a pronounced peak in the Phosphodiester (PDE) regions at +0.21 PPM of their ^{31}P NMR spectra when they were finally put into the spectrometer, a peak

associated with dead cells. Experiments were run with cells kept for shorter and shorter periods of time in the tissue culture incubator before putting them into the sample holder of the life-support system. In all the cases when the cells on microcarriers were being fed daily and kept in the tissue culture incubator, it was apparent that the cells were dividing, but the number of cells on the microcarrier itself did not increase beyond a certain point. The extra cells of the division process seem to be left floating in the medium and were sucked off when the medium was changed. The best results were obtained when the cells were seeded onto the microcarriers, left for approximately 40 to 60 minutes in the tissue culture incubator and mechanically agitated every 10 minutes. These cells had little or no phosphodiester peak and appeared to be robust as judged by ATP concentrations. The best results were obtained when thirty 100 mm confluent or near-confluent tissue-culture plates with a total of approximately 10^8 cells were used. These were seeded onto a total of 0.54 g (dry weight) of Cytodex III microcarriers. These were distributed into three 150 mm siliconized glass Petri dishes containing a total of 50 ml of cells, microcarriers and medium per dish. This gave approximately 50 cells per microcarrier.

DRBC were not grown on the Cytodex III microcarriers because collagen supports attachment and growth of glial cells over neuronal cells where polylysine-coated Biosylon microcarriers support neuronal growth over glial growth. Glial cells are a major contaminant of the DRBC preparation.

C3HT10½ cells were grown on Cytodex I microcarriers. The seeding was $1.5 \times 10^6 - 2.6 \times 10^6$ cells per 10 cm Petri dish containing 0.1g (dry weight)

and 25 ml of Basal Medium Eagle (BME) supplemented with 10% FBS, 5% newborn calf serum (NCS) (GIBCO), and penicillin-streptomycin. It took 48 hours for attachment of the cells to the microcarriers. The cells became confluent on the microcarriers in 5-7 days, at which time they were used for experiments. This cell-microcarrier system worked well.

4.1.4.2 Biosylon

N1E-115, C3HT10½ and DRBC were tested on Biosylon microcarriers. The same general procedure was used for these microcarriers as was used for Cytodex carriers.

C3HT10½ cells were seeded onto Biosylon and kept in tissue culture conditions for 10 days before experiments were run. These cells attached and grew on the microcarriers in the 10 days. This cell-microcarrier system is the one of choice for C3HT10½ cells. With the N1E-115 cells, however, there were mixed results. Approximately 20% of the microcarriers formed good attachments with cells; another 40% formed moderate to poor cell attachment and the remaining 30% showed poor to no attachment. Since Cytodex III worked for these cells, additional experiments with these microcarriers were not performed with N1E-115 cells.

Because the preparation of DRBC requires the substrate to be polylysine, the Biosylon microcarriers were coated with polylysine (Sigma P 0899). This was done by putting Biosylon microcarriers under sterile conditions in 25 ml of 0.15 mM polylysine, leaving them overnight and then washing them five times

with Hepes-buffered saline. Before using them they were washed 2 times with ZAM and left to sit in the incubator in 150 mm siliconized Petri dishes until the preparation was completed (approximately seven hours). The cells were obtained as previously described and seeded onto the microcarriers. The microcarriers were manually agitated at 20 minute intervals for two hours by moving the dish in a small figure eights. The cells and microcarriers attached in three ways. First, there was a cell-microcarrier association. This was found on most microcarriers. Secondly, there was a great deal of clumping of these microcarriers with cells already on them. In the third case, cells formed clumps and then associated with microcarriers to form clumps of cells with ten to twenty microcarriers associated with each of them. No quantitative experiments were run to determine what conditions such as cell density, microcarrier density and agitation rate have on obtaining what would be the ideal configuration for the life-support system. DRBC's are much smaller than N1E-115 cells, having a diameter of approximately 10 μm as compared to that of the N1E-115, which is 25-35 μm. There is no question that the Biosylon-DRBC combination is good. When the cells were transferred to the life-support system they tended to clump, but from all external appearances the system perfused well.

4.1.5 Maintenance and growth in the life support system

When C3HT10½ cells were put into the life-support system, there were increases in the ATP, protein and DNA levels. This suggests that the cells were growing in the life-support system.

When undifferentiated N1E-115 cells were put into the life-support system, the ATP levels did not increase when the cells were maintained for 24-72 hours at normal pH, superfusion rates and 90% oxygen in the exchanger. Protein and DNA were not measured. When cell samples were kept in the life-support system for long periods of time, the phosphodiester region showed an increase. There are several possibilities for these findings. One is that the cells could have been growing, dividing and dying in such a way that the total viable cell count and volume stayed the same with the dead cells disintergrating and almost, but not completely, washing out of the sample holder. Thus, the membrane organelles or vesicle debris could have accounted for the build-up in the phosphodiester region. It is also possible that in this very compacted cell-microcarrier system, the cells have an extremely long doubling time equivalent to a confluent state in tissue culture, and I saw no change in the ATP because I did not look at the system for a long enough time. There were a few experiments, when the cells showed a small increase in ATP, but these were also accompanied with increases in the PME region which suggested that the cells may have been responding to a shift in pH (discussed later). No single experiment was run under completely normal physiological conditions from beginning to end. In every experiment the cells were subjected to various experimental conditions, thus no realistic quantitative measure was made of the cell count before and after the experiment, although the cells and microcarriers were studied at the beginning and end of the experiment for their general physiological character, and to make a qualitative measure of their number and

condition. I believe it is some combination of cell growth and death, and therefore treat and refer to these cells as undifferentiated cells in a confluent state.

4.2 Induced differentiation

N1E-115 cells induced to differentiate have different biochemical, morphological and electro-physiological properties (Appendix D). As a model cell for neurons, this cell system offers an interesting way to look at a homogeneous population of neuronal cells and ask probing questions about their development, questions relevant to normal neuronal systems. As a tumor cell, it is interesting because in differentiating it loses its major tumor-like proprieties, and its ability to multiply without bound: properties that if understood and controlled, would have far-reaching implications. Using ^{31}P NMR at the cellular level does not allow one to study micromolar or nanomolar concentrations of phosphorylated compounds which may be involved in the primary control of differentiation and development, but it does let one look at changes in the larger concentrations of PME and ATP, for example. As it turns out, there is a gross change in the PEt and PC concentrations when these cells change to a differentiated state. What is presented here is a comparison between spectra obtained from N1E-115 cells which are undifferentiated when placed in the spectrometer, and those spectra obtained from cells induced to differentiate in tissue culture using DMSO for periods ranging from 3 days to two weeks before being put into the spectrometer. The results of a second experimental protocol are also presented. This protocol is to put undifferentiated cells into the

spectrometer, obtaining a control spectrum, and then following the ^{31}P profile as the cells were induced to differentiate in the spectrometer by adding DMSO to the perfusate. This second protocol resulted in showing a transition from the undifferentiated state to the differentiated state.

4.2.1 Cells induced to differentiate in tissue culture.

N1E-115 cells were grown for 3 passages in DMEM supplemented with 10% FBS, 1% PS and 0.2 mM Cr. Each passage was a 5:1 split with the final passage made to thirty 100 mm tissue-culture plates. They were fed every other day until a near-confluent state was reached, at which time the medium was completely replaced with fresh DMEM supplemented with 2% DMSO, 2% FBS, 1% PS and 0.2 mM Cr, and fed with the same medium every other day (Kimhi, et al., 1976). Within three days these cells had stopped dividing and differentiated morphologically to form neuron-like cells. Within 5 more days these cells had lifted off the surface of the tissue-culture dish and formed clusters or clumps. The clumps were roughly spherical but were irregular and for the most part not attached to the substrate. The cells were grown for thirteen days on DMSO supplement medium before they were seeded onto Cytodex III microcarriers, allowed to sit in the incubator for one hour, and then transferred to the sample holder. The ^{31}P NMR spectrum Fig. 23 shows the cells after differentiation as compared to cells which have not been induced to differentiate (Fig. 24). Aside from the PCr peak at -2.49 PPM which is discussed in section 4.3.4.2, the major difference was in the PME region.

In the undifferentiated cells, the PME region is broad and small, and in the differentiated cells it appears to be the same base line with two large and one small peak added to it. The small peak is at 4.72 PPM and the origin is unknown but it is probably glucose-6P. It is at the same chemical shift as 2D6P. The two larger ones, PEt and PCh, are at 4.373 PPM and 3.858 PPM respectively. These values are for cells with an intercellular pH of 7.34 and an extracellular pH of 7.45, that is, the cytosol is 0.1 pH units more acidic than the environment. It is important to take the pH into consideration because these peaks titrate with pH as was originally shown by Navon when he identified them (Navon, et al. 1972). The ratio of PEt to PCh is approximately equal to one. The T1's were measured and found to be large for PEt (see Fig. 25). From these values, the multiplication factors for normalizing spectra peaks and areas taken with a repetition rate of 3 seconds to those of the fully relaxed state were calculated (see table 5). Assuming the internal ATP is 3.9 mM (Ogawa, et al., 1986) the PEt concentration is calculated to be 2.2 mM and the PCh is 1.8 mM. Because of ambiguity in the base line and general experimental error, these values can be considered to be approximately the same. Not having a good measure of T1 for the 4.72 ppm peak, only a lower limit of 0.5 mM can be put on its concentration. These findings are in keeping with other findings in the literature, namely, that in dog (Bolinger, et al., 1984) and rat (Ogawa, et al., 1986) PEt concentrations are high in late prenatal and early postnatal developing brains.

Figure 23

This is the spectrum made on differentiated N1E-115 cells which had been induced to differentiate by supplementing the medium with 2% DMSO and 2% FBS. The spectrum is the sum of 1200 FIDs taken with a repetition time of 3 seconds and line broadening of 5Hz. The prominent peaks in the PME region are PEt and PCh. The peak at -2.49 ppm is due to PCr. In a fully relaxed spectrum, this peak would be much larger than the ATP peaks. When the cells are maintained in tissue culture for many days (15-25) this peak is prominent. The Cr concentration in the medium is due to an endogenous constituant of the FBS and is 0.2 mM or smaller. The presence of this large peak suggests that the cells take up creatine slowly over a long period of time.

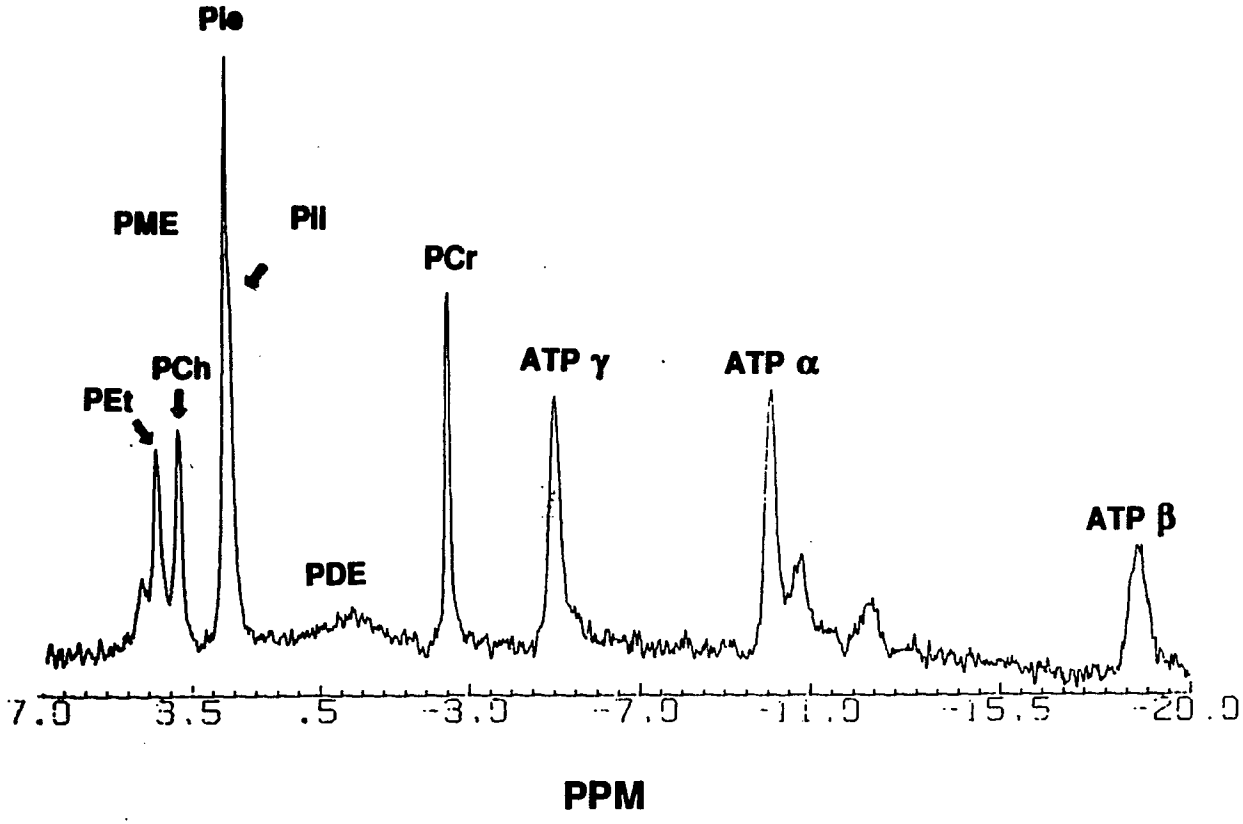
Pie
PME
PII
PCr
PCh
PEt
ATP γ
ATP α
ATP β
PDE
7.0
3.5
.5
-3.0
-7.0
-11.0
-15.5
-20.0
PPM

FIG. 23

Figure 24

This spectrum is from N1E-115 cells which are undifferentiated. The spectrum is the sum of 1200 FIDs collected with a 3-second repetition time and processed with a line broadening of 2.5 Hz. The cells had been maintained in the sample holder for many hours, being superfused with medium containing 20 mM Cr. When the cells first were put on the microcarriers and put in the magnet they had no PCr peak. Large amounts of PCr do not accumulate in undifferentiated cells which are continuously passaged in normal tissue culture conditions. This is in contrast to differentiated cells shown in the previous figure. Notable in this profile are the two peaks associated with PEt and PC. Note that these peaks are small in comparison with those of the differentiated cells. These cells are at a basic pH and thus the Pi peak is seen to be split. The large downfield peak (the one to the left) is due to the extracellular Pi called P_{ie}, while the small upfield peak is due to the Pi within the cells and is labelled P_{ii}.

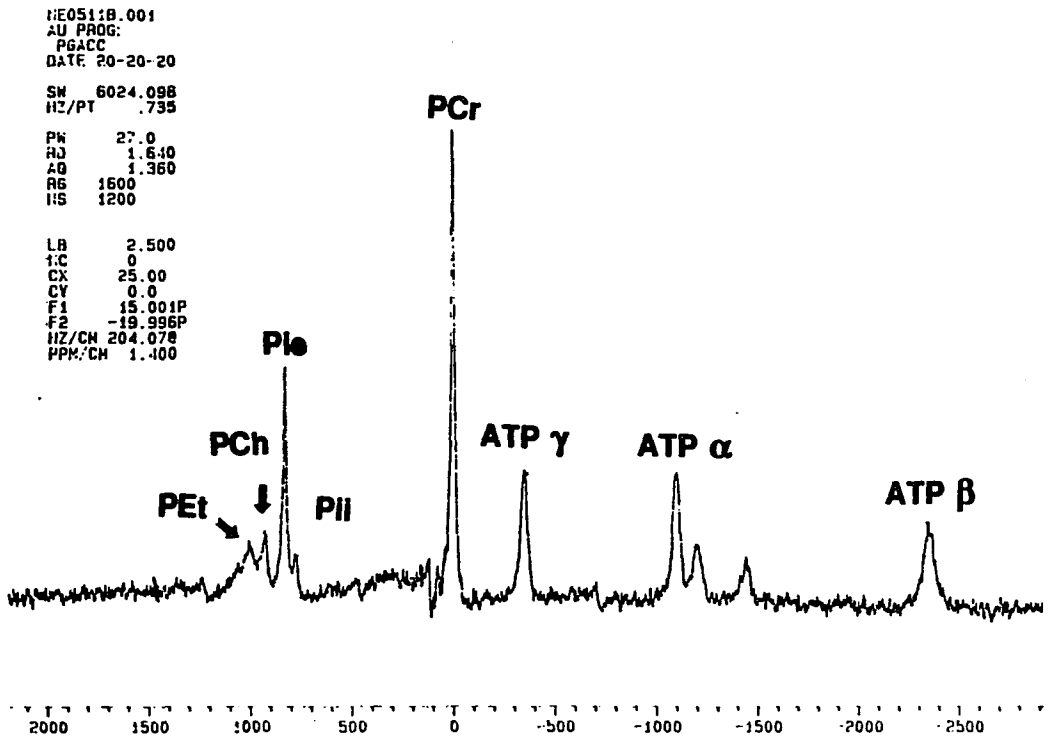
NE0511B.001
AU PROG:
PGACC
DATE 20-20-20
SW 6024.098
HZ/PT .735
PW 27.0
RD 1.640
AQ 1.360
RG 1600
NS 1200
LB 2.500
TIC 0
CX 25.00
CY 0.0
F1 15.001P
F2 -19.996P
HZ/CM 204.078
PPM/CM 1.400
PCr
Pie
PCh
PEt
Pii
ATP γ
ATP α
ATP β
2000
1500
1000
500
0
-500
-1000
-1500
-2000
-2500
HERTZ

FIG. 24

In rat brains, PEt concentrations drop in the first 30 days postpartem to 50% of their original levels (Ogawa, et al., 1986) and presumably are zero when the neuronal cells are in a very early developmental phase.

4.2.2 Cells induced to differentiate in the life-support system.

In the previous experiment only two points in the cells' transition from neuroblast to a functioning neuron where measured. In order to follow the time course of the transition, cells were induced to differentiate in the sample holder while on the microcarriers in the magnet. These changes were reflected in the ^{31}P profile before, during, and at the end of the period of differentiation. The PEt and PCh peak increases continuously during this period.

4.3 Experiments in the NMR Spectrometer

4.3.1 The effects on observable phosphate profiles in cells cultured in the long run

In order to do long-term experiments, it is necessary to establish the behavior of the cells while being superfused under controlled conditions. To this end C3HT10½ cells and N1E-115 cells were maintained in their normal medium and in Ringers solution with and without Pi, glucose, and sodium in different concentrations, and with different buffers, during which time their phosphate profiles were measured in order to see if the cells would be able to do well in, for example, a sodium-free medium. If so, studies on the effects of the phosphate profile of the amiloride-sensitive sodium transport system (Moolenaar, et al., 1983, Boonstra et al., 1982) and/or the oubain-sensitive Na-K ATP-ase transport system on development could be done. If they also do well

Figure 25

A) Stack plot of data obtained on differentiated cells using the saturation recovery method.

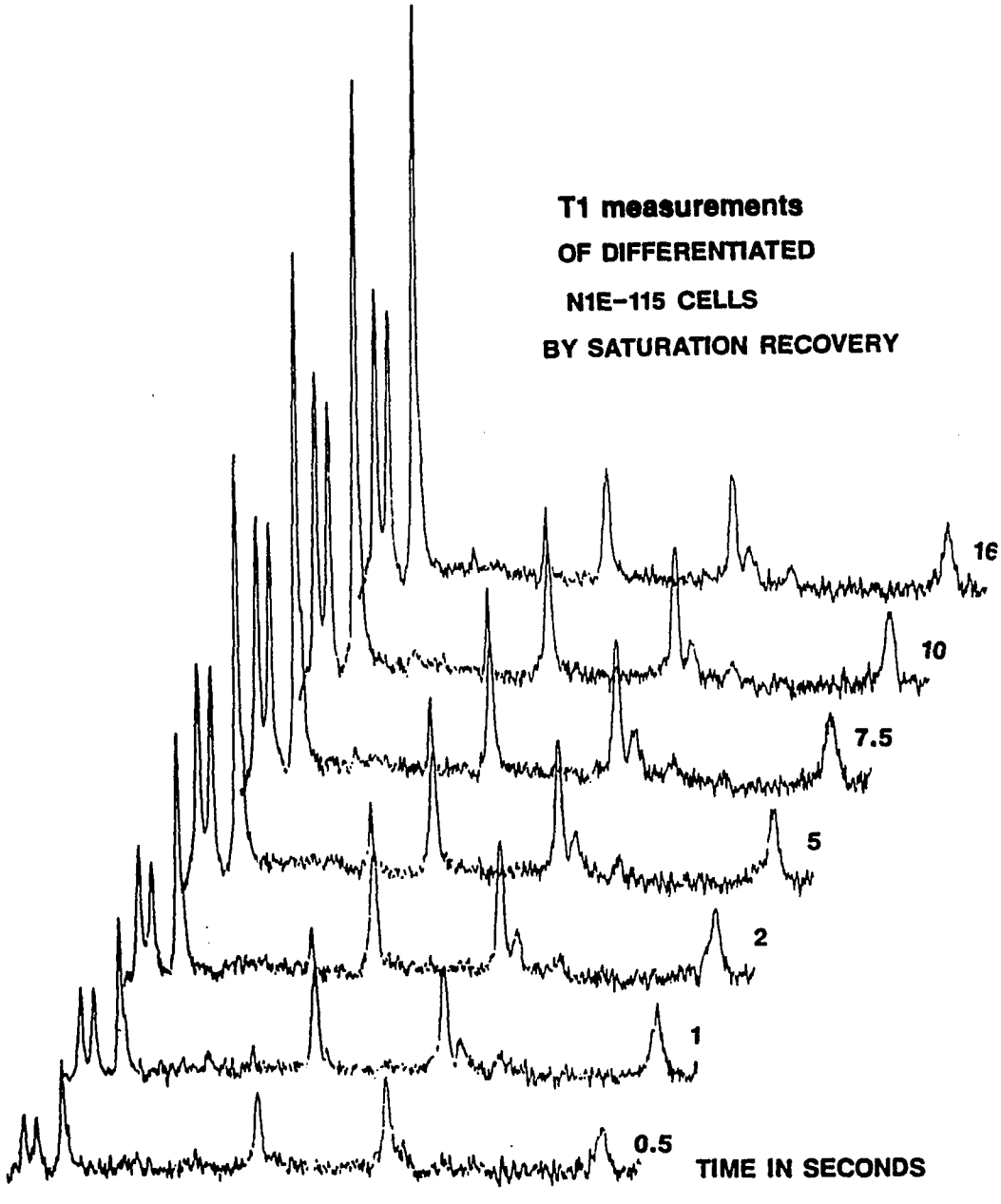
T1 measurements
OF DIFFERENTIATED
N1E-115 CELLS
BY SATURATION RECOVERY
16
10
7.5
5
2
1
0.5
TIME IN SECONDS

FIG. 25

TABLE 5

This table lists the factors which must be used to multiply the peak height of the indicated phosphates obtained when spectra are collected with a 3-second repetition time in order to obtain the corrected value for the completely relaxed form.

TABLE 5

ATPβ	1.1
P_{ie}	extracellular 1.8
P_{ii}	intracellular
PPA	1.89
PCr	1.5
ATPα	1.0

in low Pi, one could make an unambiguous shift of the internal free Pi, which would not be masked by the external free phosphate of the medium.

4.3.1.1 Cell health index (CHI), medium, and Ringers

There is considerable difference between the microenvironment of a cell in the NMR perfusion system, and that which it sees in normal tissue culture conditions. Experiments were performed with the aim of getting some understanding of how long the cells remain in good condition, and to come up with some criteria based on ^{31}P NMR spectral profile, which could be used to judge their condition. With good criteria, the effects of replacing normal growth medium with various Ringers could be assessed.

The first experiments were run on C3HT10½ cells. These cells, as previously mentioned, are robust and were used to develop the perfusion system. Semi-sterile conditions were used during these investigations, that is, the system was washed with distilled water, but was not autoclaved. Because of this, experiments were limited in time to between four and ten hours. For the discussion which follows, refer to Fig. 26.

Spectrum A shows the profile of cells (C3HT10½) grown on BME supplemented with serum and buffered with 95% air, 5% CO_2. These were the control conditions for this cell line, and this spectrum represents a stable condition and was virtually identical to others seen over a three-hour period. The orthophosphate, Pi, was due to the sum of the 1 mM Pi in the BME medium, and the intracellular Pi. It was previously determined that the

Figure 26

The ability of the cells (C3HT10½) to maintain themselves in different media was tested and judged by comparing the ^{31}P NMR spectrum obtained at the beginning and end of the time spent in the medium. There was no difference in the spectra with the different media presented here. The spectra are obtained from 1000 or 3000 free induction decays with a 60 degree pulse and a 1 second repetition time.

A. Spectrum of cells in BME supplement with serum buffered with air, 5% CO_2. The spectrum is from 3000 free induction decays.

B. Spectrum of cells in same medium as above but buffered with 15 mM Hepes and without CO_2. The spectrum obtained after 3 hours in this medium is the result of 3000 free induction decays.

C. Spectrum of cells in serum-free sodium Ringers A solution (see table 6A) buffered with Hepes at pH 7.4 at the end of 2 1/2 hours. The spectrum is from 1000 free induction decays.

D. Spectrum of cells in sodium-free Ringers solution buffered at a pH of 7.4 at the end of 2 hours. The spectrum is from 1000 free induction decays.

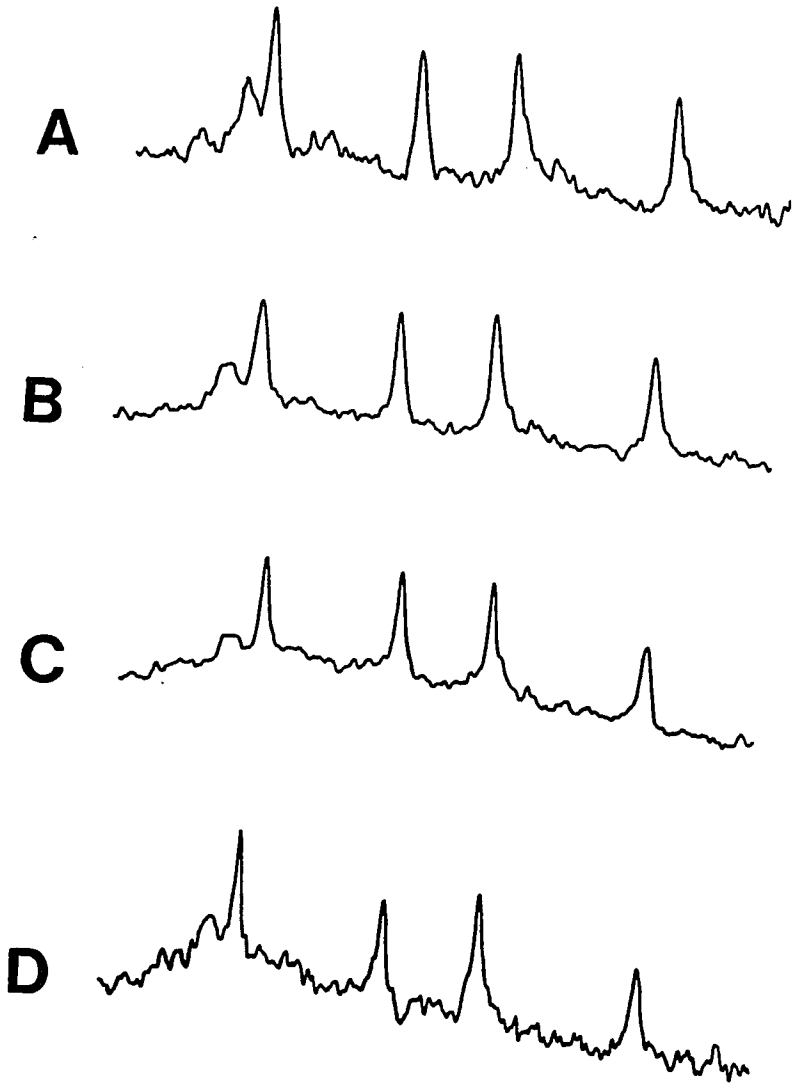

FIG. 26

extracellular Pi contribution was 90% (Ugurbil, et al., 1981). This meant that to a first approximation it could be used as a standard concentration calibration point for the sample holder. The ratio of the peak height at –10 PPM to the Pi peak height is defined here as the cell health index or CHI. The peak at -10 PPM was due to contributions from the nucleotide triphosphate alpha, nucleotide diphosphate alpha, and UGDP resonances. The relative contributions and total contributions were dependent upon the metabolic state of the cells and the number of cells. It turned out that this measure gave a good indication at the onset of any experiment of how healthy the cells were, if you also took into consideration the number of cells in the sample. For example, when thirty 100 mm tissue culture dishes of healthy near-confluent N1E-115 cells were used to seed Cytodex III microcarriers, which were then placed in the sample holder, within one or two minutes one could expect to have a CHI near one for a pulse repetition rate of one second. Cells with this CHI can be expected to do well for more than two weeks, the longest that they had been kept. On the other hand, when the same number of cells had a CHI of 0.2, they frequently lost all of the ATP within an hour or two after being loaded into the sample holder. This index can be more rigorously applied to experiments using the same set of cells.

The spectra in Fig. 26 are from four different sets of cells, all of which were in excellent condition and remained so for the duration of the experiment. The previous two sets of spectra have the same CHI. Cells used in B were with 15 mM Hepes as a buffer instead of the normal 5% CO_2 sodium bicarbonate

Table 6A

Ringer's A
Sodium Ringer's Solution

130 mM	Na++
5 mM	K+
0.5 mM	Mg++
1 mM	Ca++
138 mM	Cl-
1 mM	H2 PO4
15 mM	Hepes pH 7.4
10 mM	glucose

for sodium-free 130 mM choline chloride pH with KOH was used.

Table 6B

Ringer's B

130 mM	TMA*
5 mM	KCl
2 mM	CaCl2
1 mM	MgCl2
20 mM	Tris HCl

*TMA is tetramethylammonium choloride.

buffer while in the holder. The phosphate profiles looked very good, with a CHI of 0.7, and the cells looked good under the microscope at the end of the experiment. These encouraging results led to a test of first glucose supplemented Ringer A, (see Table 6) with and without sodium. For the sodium-free Ringers, choline chloride was substituted for sodium. Both cases with Ringers perfusing the sample holder gave good results. The phosphate levels were robust and did not alter over the two to two-and-a-half hours that they were monitored. The conclusion from these experiments is that the size of the large phosphate pools was not altered in the short run of two hours when the perfusate of the sample holder was switched from standard growth medium conventionally buffered with CO_2 to Hepes buffered medium or to glucose-supplemented Ringers with sodium, or with choline substituted for sodium. Now in fibroblast cells, this opens the way to doing a large number of experiments which normally would be compromised by the constituents of the medium, or the conventional serum-supplemented medium which had a large number of hormones present.

4.3.1.2 Is there any measurable internal Pi?

The above results were encouraging, but it is important to put more stringent requirements on the Ringers used for neuronal experiments. For example, it would be convenient to use a Pi-free Ringers exposing the 9% or more of Pi thought to be endogenous to the cells, and thereby allowing the monitoring of the cytosolic pH by monitoring the chemical shift of Pi. Under normal conditions in all cell types studied, there was only one Pi peak with the

Figure 27

A pH gradient was maintained under inhibition of glycolysis and respiration.

A. The P_i chemical shift of the P_i resonance(s) were monitored to measure pH. "(A)" shows the shift of the P_i peak as a function of time in C3HT10½ cells. The extracellular pH was regulated 5% CO_2 buffered BME serum supplemented medium (balance air). When Antimycin A was added to a concentration of 4 μg/ml, a separation between the internal and external P_i was not observed. When 2 DG was added to a final concentration of 35 mM, a pH gradient was generated and maintained across the cell membrane as indicated by the two separate P_i resonances. The cell chamber was perfused at 4.0 ml per min with medium. Each datum point was from a spectrum of 1000 free induction decays obtained with a 60 degree pulse and a 1 second repetition time.

B. The pH gradient generated by the inhibition of glycosis and respiration was maintained when the external pH is changed from 7.2 to 8.6.

A pH gradient was generated by the addition of KCN (10 mM final concentration and 2-DG (50 mM final concentration) to a 7.4 pH air, 5% CO_2 buffered BME serum-supplemented medium. When the same medium buffered to pH 7.2 with 15 mM Hepes and without CO_2 was pumped through the cells the pH gradient was maintained and tracked the external pH. Upon changing the pH first to 8 and subsequently to 8.6,

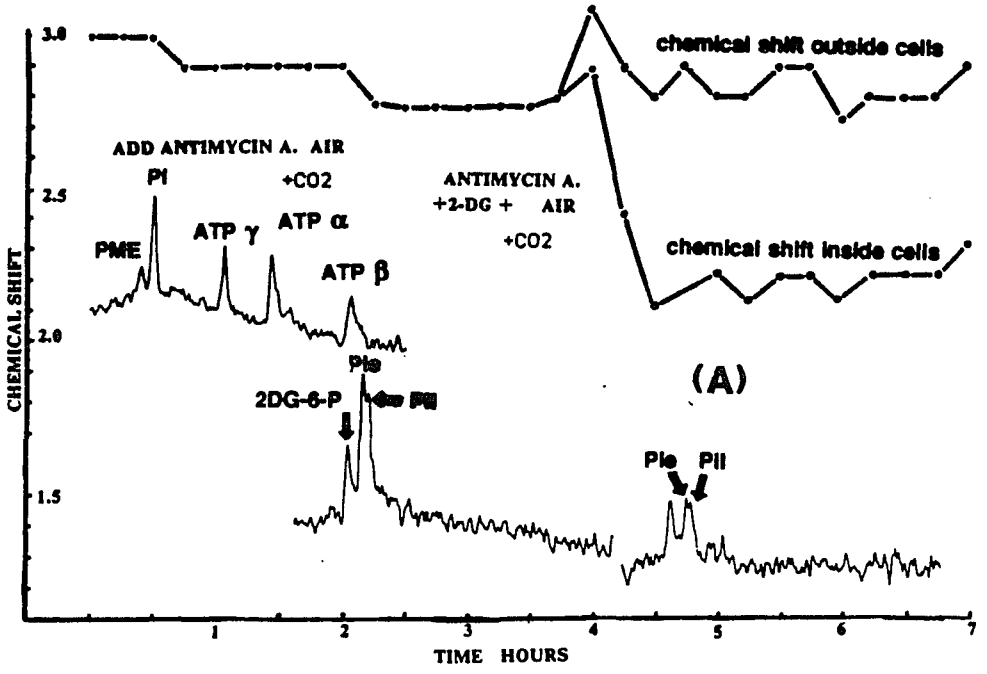
chemical shift outside cells
ADD ANTIMYCIN A. AIR
Pi
+CO2
ANTIMYCIN A.
+2-DG + AIR
+CO2
PME
ATP γ
ATP α
ATP β
chemical shift inside cells
Pie
(A)
2DG-6-P
Pie Pii
CHEMICAL SHIFT
3.0
2.5
2.0
1.5
1
2
3
4
5
6
7
TIME HOURS

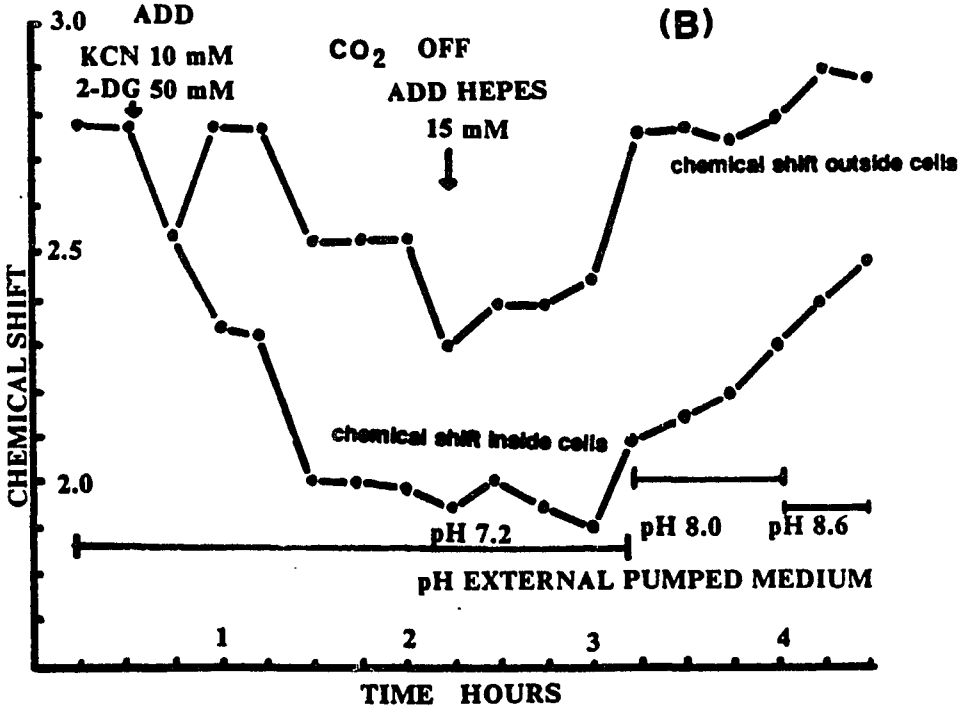
(B)
3.0 ADD
KCN 10 mM
2-DG 50 mM
CO_2 OFF
ADD HEPES
15 mM
chemical shift outside cells
2.5
chemical shift inside cells
2.0
pH 7.2
pH 8.0
pH 8.6
pH EXTERNAL PUMPED MEDIUM
CHEMICAL SHIFT
1
2
3
4
TIME HOURS

FIG. 27

the pH gradient was still maintained and the internal pH increased with external pH.

1 mM Pi of the medium masking the intracellular peak. In addition to measuring the chemical shift, a measurement of the concentration was important in evaluating equilibrium conditions of certain reactions involving Pi.

Several experiments were run on N1E-115, rat brain cells, and C3HT10½ cells. Fig. 27A shows the results for C3HT10½ cells which exhibited an internal Pi upfield of the perfusion medium 1 mM Pi peak. In both cases 2DG was used to inhibit glycolysis, and either antimycin A or KCN was used to block oxidative phosphorylation. In both cases there was a distinct splitting of the Pi peak as a result of acidification of the cellular cytosol, which persisted four hours. The important observation made here was that even in the absence of ATP, the internal Pi was observable over a period of many hours. To a first approximation, no Pi leaked out or into the C3HT10½ cells. In a number of experiments with N1E-115 cells, the intracellular Pi, was resolved from the extracellular Pi, but in these cells the Pi leaked out (see section 4.3.1.4) at least at the basic pH value of 7.5 to 8.0.

4.3.1.3 Changes in phosphomonoesters (PME)

Experiments were performed on N1E-115 cells to elucidate the effects of Pi removal in cells superfused with various ringers supplemented with and without glucose, sodium, and FBS in various combinations and sequences.

In all, a number of experiments were run which show a sequence of conditions which led to a large increase in the PME region (see appendix C for details). The conclusion at this point is that there was a PME pool of

unidentified origin, which was induced to increase a number of fold when the cells were subjected to conditions of low glucose in the presence of serum in substrate-free Ringers. This finding, although very interesting, was not investigated further at this time, and is now the subject of a separate study.

4.3.1.4 Intracellular-extracellular exchange

The existence of internal Pi has been demonstrated above. The next question concerned how freely Pi left or entered the neuronal type cells, and under normal conditions, whether there was a concentration gradient across the cell membrane. The most clear-cut results came from experiments with DRBC, and these are presented first. Dissociated rat brain cells, cultured as previously described, were seeded on polylysine-coated Biosylon microcarriers, placed in the sample holder, put in the magnet, and a control spectra was obtained over a number of hours, while cells were superfused with 30 mM creatine supplemented ZAM. At the end of the control period, the cells were switched to a Ringers C solution supplemented with glucose and PPA, and also supplied with oxygen. At the end of two-and-a-half hours, the Ringers was switched to a Ringers D, which was oxygen, glucose and creatine-free. This constituted an anaerobic and hypoglycemic condition calculated to reduce the phosphate stores, which it did to an amount of 50%. The cells were then superfused with complete ZAM and allowed to recover. The Ringers solution was Pi free, and the Pi peak left in the spectrum was judged to be intracellular. This was based on the belief that all extracellular Pi had been washed out, a belief based in turn on the presence of PPA at its maximum value thirty minutes after being switched from ZAM,

which was PPA-free to ringers with PPA, and the fact that PPA washed out completely in the same amount of time.

A second spectrum was collected in the hour and a half just before switching to ZAM. The ratio of Pi to the ATP alpha peak was 1:4, the same ratio as was found in neonate brains *in vivo*, as seen with a surface coil. During the period of stress, 50% of all PCr and all of the ATP hydrolized while the Pi peak increased. The difference between these profiles and area of nine units compared to the total loss in the areas of the nucleosides and PCr due to hydrolysis, fourteen units, can be considered to be approximately equal, since the T1's of Pi, nucleoside phosphates and phosphocreatine were different. The important point is that the hydrolized Pi product stayed in the cells for two and a half hours at concentrations better than three times greater than their normal values. The cells partially recovered, indicating that they were still viable. This was a very graphic demonstration that the Pi was not in free exchange with the external medium.

N1E-115 cells were looked at next. The first question asked was: Is there a Pi peak which cannot be washed out with Pi-free ringers? The answer was no at basic pH.

4.3.1.5 Effect of extracellular sodium concentrations on the free Mg++ concentration on undifferentialed N1E-115 cells

It has been demonstrated that changes in extracellular sodium concentrations have a marked effect on the intracellular proton concentration

(Moolenaar, et al., 1983; Boonstra et al., 1982). This knowledge, and the experience of successfully culturing cells for limited periods of time on sodium-free Ringers prompted an experiment to see what response the cells would have to various concentrations of extracellular sodium. The results and details are presented in Fig. 28, and 29. The cells were supplied with normal medium for eight hours and then switched to a sodium-free Ringers supplemented with glucose for 60 minutes, and subsequently for similar periods of time to 10, 20, 30, 40 mM sodium-supplemented Ringers, and finally back to sodium-free Ringers again. The most obvious result of this set of experiments was the degradation of the various phosphate peaks, most strikingly during the seventy-five minute period, at the end of the experiment when there was no sodium present. From these results it could be concluded that in a sodium-free Ringers, cells did not fare as well as they do in normal medium, and that the degradation was relatively slow if sodium was present in the medium, and faster if absent. A subtler and interesting observation was made about the effect of changing the extracellular sodium concentration on the concentration of Mg++ bound to ATP. The chemical shift of the ATP β and ATP α peaks at constant pH and temperature are determined by the amount of Mg++ in the system. As the amount of magnesium in the cell increases, the amount of magnesium-bound ATP increases, and the chemical shift of ATP β moved downfield from –21 to –18 ppm, and that of ATP α also moved downfield from approximately –7 to –5 ppm (Gupta and Gupta, 1984; Wu, et al., 1981). It was just such a shift that was observed with the increase in Na+. The shift was found to be a function of

Figure 28

N1E-115 cells were incubated in normal growth medium at pH 7.65, and a control spectrum was obtained which had chemical shifts for Pi and ATP as indicated. The superfusate was then changed to a sodium-free Ringers supplemented with glucose for 60 minutes. The spectra obtained here were superimposed on the control to determine the number of points of the digitalized signal the various peaks were sifted. The technique of continuously subtracting the spectra from the control while shifting the spectra relative to the control results in a difference spectra whose undulations result in a determination of peak separation to within less than one half a data point. Shifts to the left are given negative values and those shifted to the right of the control are given positive values, line (A) in the figure reflects these values. Similarly, 60 minute experiments were run at 10 mM Na^+ (B), 20 mM Na^+ (C), 40 mM Na^+ (D) and finally back to 0.0 mM Na^+ again (E).

Figure 28

	Pi	γ	α ATP	β	[Na] *Condition* 140 mM
Control Chemical Shift (ppm)	$\delta = 2.913$	$\delta = -4.895$	$\delta -10.00$	$\delta = -18.656$	

Shift (-) ← → (+) in points pH

A	−4	−6	−2	−16	7.71	0 mM
B	−6	−3	+1.5	−17	7.90	10 mM
C	−7	−2	+1	−14	7.92	20 mM
D	−5	0	+3	−9	7.92	40 mM
E	−3 but noisy	−2	−1	−16	N.M.	0 mM

1 pt = 1.471 HZ
1 pt = 0.01 ppm

ph of control = 7.65

Figure 29

The data of Fig. 28 is plotted here. The shifts were relative to the ATPα peak.

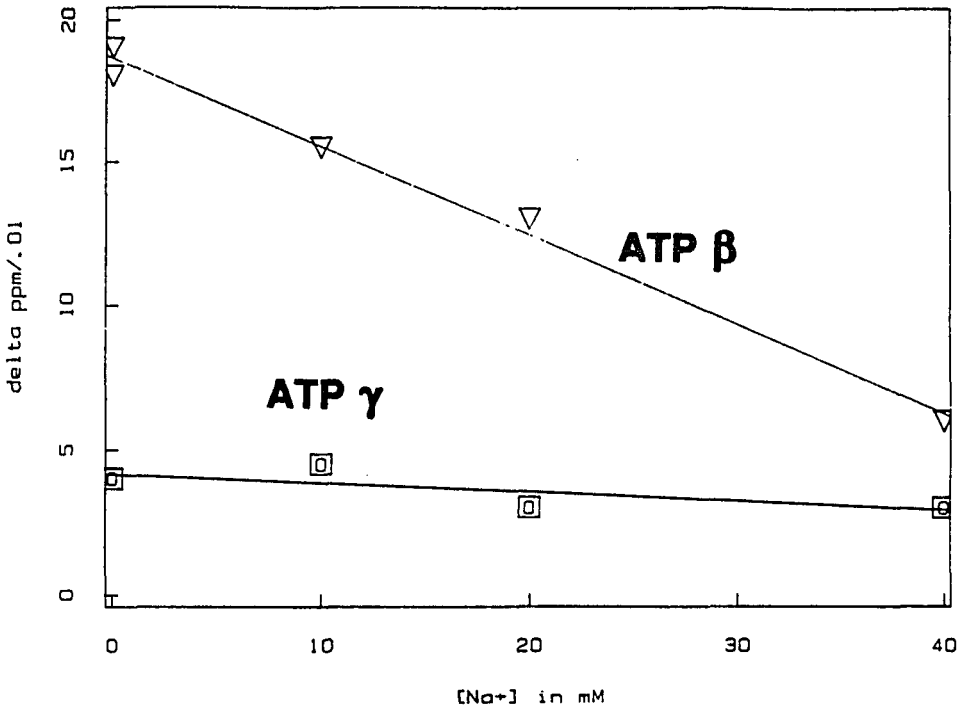

FIG. 29

the sodium concentration and suggests the concentration of ATP-Mg increases with an increased extracellular sodium. A more detailed discussion and experimental details are presented in section 4.3.9. For the present, it is important to note that the concentrations of sodium in the extracellular medium appeared to have an indirect effect on the concentration of Mg++ bound ATP. Since the concentration of magnesium bound to ATP in the cells played such an important roll in so many enzymatic reactions, it was obvious that attention must be paid to this fact when experiments were planned, in which extracellular sodium concentrations were being manipulated.

4.3.2 Effects of ischemic insult on cells in culture without creatine supplement

The effect of an ischemic insult was studied on N1E-115 cells in tissue culture. In the first experiments the cells were grown to late log phase, that is, to near confluence on 10 cm plates and transferred to Cytodex III as described above. They were cultured on the microcarriers for 12 days. This technique had been successfully used on the C3HT10½ cells. Figure 30(A) shows a plot of the spectra "a" during the control period of 2.73 hours followed by an ischemic episode, "b", of 2.5 hours, which in turn was followed by a recovery period (not shown) of ten hours. The ischemic episode was generated by turning off the pump and closing the return line valve. This insured that the medium stayed in the holder and was not syphoned out.

The CHI of the control was 0.44, indicating a good sample. Note the substantial peak at approximately –0.5 ppm. This peak was found in all

Figure 30(A)

(A) is N1E-115 cells under normal conditions (control) the 17 minutes just before the ischemic episode. The line broadening was 25 Hz and an FID was accumulated every second. (B) was obtained at the end of a 2-hour ischemic episode. (C) was a spectrum of the cells take in a 1-hour period starting 1 hour after the resumption of normal conditions. (D) was the final recovery exhibited by the cells. It was obtained in a 17-minute interval seven hours after the resumption of normal conditions. The cells used in this experiment were grown on Cytodex III for two weeks before the experiment was run. The large peak at $-.56$ ppm lying between the Pi and ATPγ peak is attributed to dead cell membrane attached to the microcarriers.

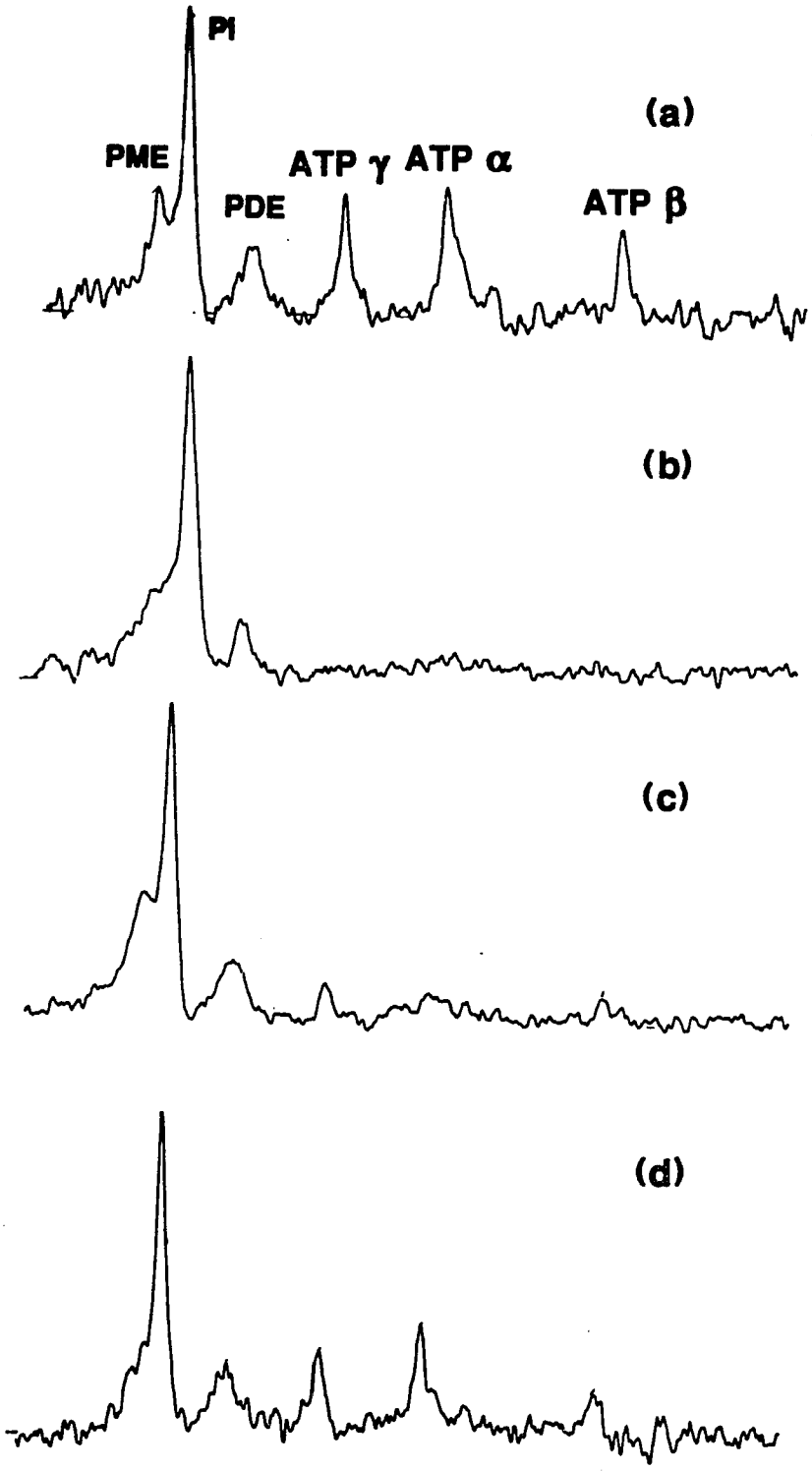

FIG. 30 (A)

Figure 30(B)

Dissociated rat brain cells were subjected to ischemic episode induced when the pump of the life-support system was shut off. This happened between files 4 and 5 and resulted in a decrease in the Pi peak in part due to the difference in the decrease in the pH of the cells and in the extracellular space in the sample holder. This resulted in a broader, shorter Pi peak, which eventually split into a distinguishable external and internal component. Associated with this was a decrease in the ATP peak. (A) is the sum of the control files (B) is the sum of the ischemic period files. (D) is the difference between (A) and (B). Note that the PME and ATP regions went down.

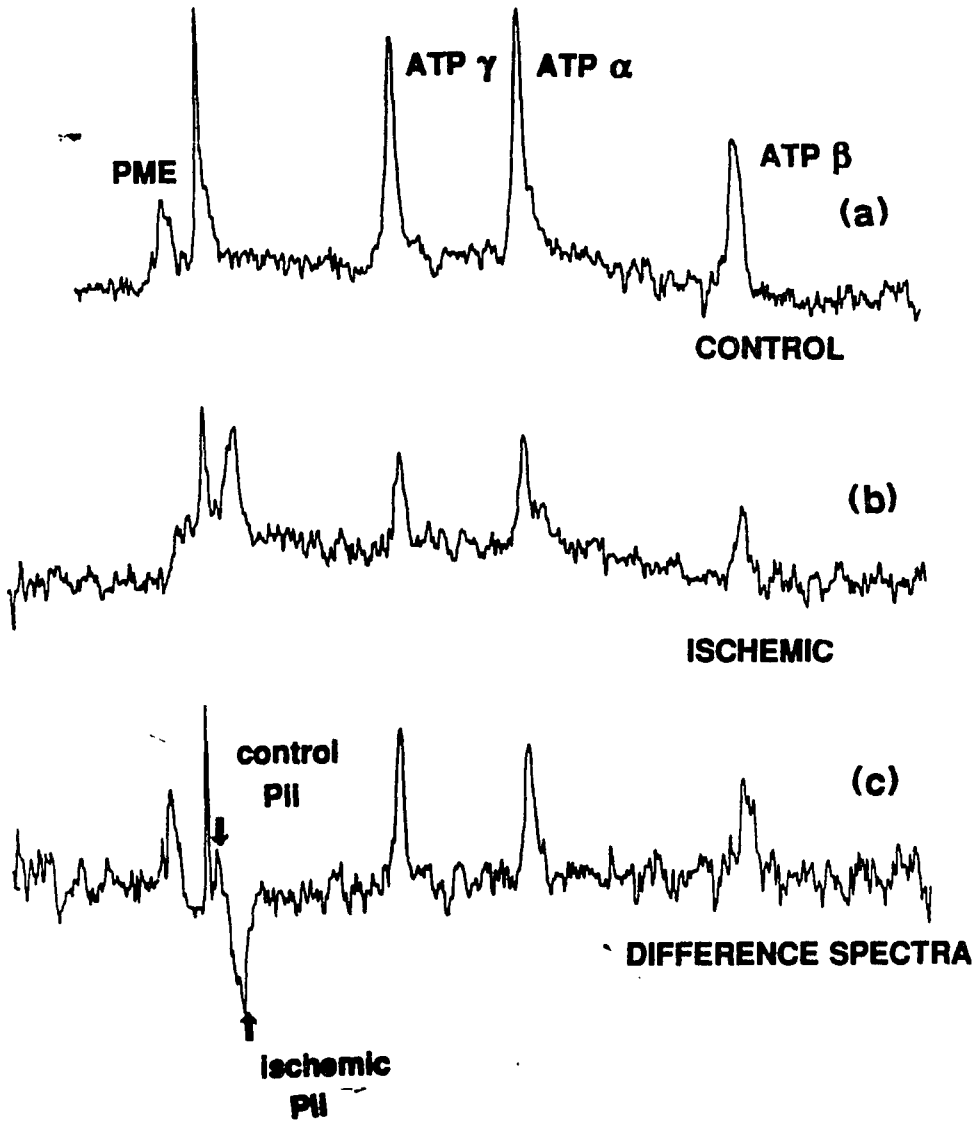
ATP γ
ATP α
PME
ATP β
(a)
CONTROL
(b)
ISCHEMIC
control
PII
(c)
DIFFERENCE SPECTRA
Ischemic
PII

FIG. 30 (B)

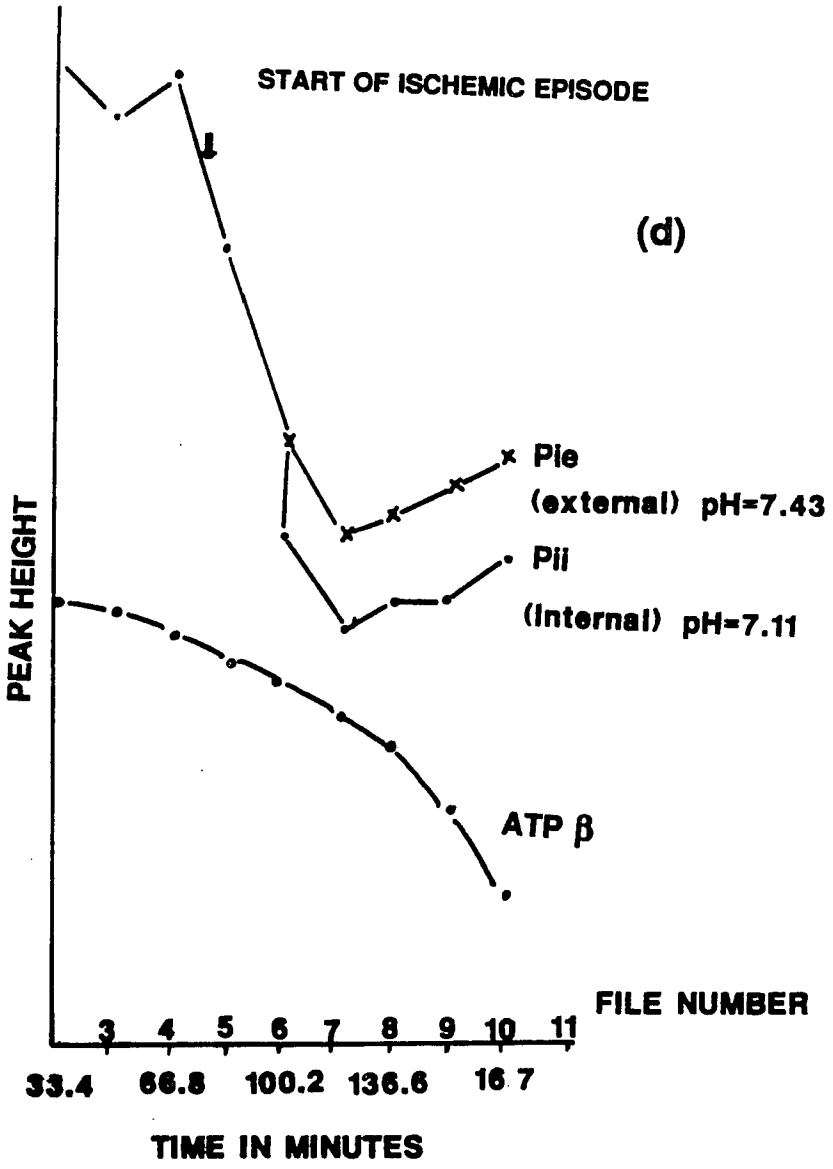
START OF ISCHEMIC EPISODE
(d)
Pie
(external) pH=7.43
Pii
(Internal) pH=7.11
ATP β
PEAK HEIGHT
FILE NUMBER
3 4 5 6 7 8 9 10 11
33.4 66.8 100.2 136.6 16 7
TIME IN MINUTES

FIG. 30 (B)

samples which had been cultured on microcarriers for long periods of time. It was not found on samples which had been grown in large quantities using standard tissue culture techniques, seeded on microcarriers, and used immediately for an experiment. A number of experiments verified what we saw here, that is, this peak did not go away when the cells were subjected to adverse conditions. This same peak had been found in isolated mitochondria which were considered to be in poor condition (Ogawa, personal communications). This suggests that this resonance was associated with phosphorylated components, such as a membrane lipid phosphate left attached to microcarriers after the cell's death or subcellular vesicles formed from cells which broke up.

This region of resonance is where pholpholipids and lysophospholipids are seen in micelles (Dennis, et al., 1984, Dennis, and Pluckthun, 1984). The region is called the phosphodiester region, and includes resonances from serine ethanolamine phosphodiester and glycerol phosphorylinositol. From my experience the ratio of this phosphate peak at 0.5 ppm to the ATP α can also be used to give a qualitative idea of the state of the health of the cells, i.e., a ratio of healthy to dead ones with the passage of time in any given experiment.

A second interesting peak is in the phosphomonoester region. This region, in other cells looked at, is normally a broad shoulder on the downfield side of the Pi peak. Candidates for this sharp peak at 4.2 ppm are AMP, IMP, monophosphate sugars or phosphoethanolamine and phosphocholine for example. This peak, in contrast to the diester peak, diminishes to near zero within fifteen minutes after the onset of ischemic conditions for these

undifferentiated cells. This could be due to pH dependent shifts of the PEt, PC and possibly other compounds with pH dependents.

The major effect of applying the ischemic condition was the resulting disappearance of all the nucleoside phosphate peaks and an upfield shift in the Pi peak from –2.875 to –2.310, indicating a pH shift from 7.4 to 6.97 pH units. The flow was off for 2.3 hours and then was turned on again. Within a half hour, the CHI was up to 0.135 and eventually went to 0.32 ten hours after the resumption of pumping. This was approximately 70% of the original condition. The phosphodiester (PDE) region remained constant through this time, while the PME region returned to its original shape and size. From this, one can conclude that no new cells had grown and that 33% of the cells were lost.

Similar effects were seen in DRBC. Figure 30(B) shows an ischemic response resulting from a pump failure lasting almost two hours, during which time the ATP level fell, the Pi peak dropped and split the downfield peak at 2.7987 ppm corresponding to a pH of 7.48, substantially the same as the extracellular peak prior to the ischemic episode. The upfield peak, on the other hand, had a chemical shift corresponding to a pH of 7.11. This peak is believed to be the intracellular pH, therefore there was a pH gradient across the cell which was .32 units. This gradient was maintained for 84 minutes, at the end of the experiment at which time the cells were superfused with fresh medium. The cells eventually returned to a CHI of 0.95, ostensibly the same condition started with. These cells behaved more like C3HT10½ cells than N1E-115 cells in regard to maintaining a pH gradient for several hours. In the case of the

C3HT10½ cells, this pH gradient persisted in the absence of high energy phosphates, thus the pH gradient was not maintained by an energy demanding pump. It might have been due to a Donna equilibrium, or to a proton impermeable membrane. This might also have been the case for DRBC, but it was not proven here for the DRBC cells because the ATP concentration did not go to zero. It definitely was not the case for N1E-115 where the ATP dropped precipitously to zero within minutes of the onset of an ischemic condition. Although the previous section demonstrated the existence of an internal peak, it could not be conclusively argued here that the upfield peak was intracellular Pi. However, the difference spectra argue in favor of this peak being the intracellular one. First it was noted in the difference spectrum that the sum of the areas of the ATP peak was 95 units and that the increase in Pi was 45 units. When we take into consideration the fact that the repetition pulse frequency was one second and the T1 of Pi was long compared to the T1's of ATP, it all fits. The second point is that the upfield peak was broader than the downfield peak, a condition expected for Pi in the interior of the cells.

Another observation to be made here is that there is a general decline in signal-to-noise, which most probably can be attributed to a change in Q of the coil, resulting, for example, from changes in the cell's volume. The cells seemed to change volume when subjected to ischemic conditions with a concomitant change in magnetic susceptibility. The fact that the system returned to its original pre-ischemic condition in terms of its peak sharpness and signal-to-noise, lends merit to this possibility.

4.3.3 2DG

Glucose metabolism of the brain accounts for 35% of the glucose consumption of the body (Guroff, 1980). The brain does not have much carbohydrate reserve and depends on a constant supply from the blood. The brain also uses 20% of the oxygen consumed by the body under normal conditions. In periods of intense brain activity, anoxic or ischemic conditions, glucose consumption can be up by a factor of 20, and during convulsions by a factor of 20 to 100 times. The point is that glucose transport and consumption is extremely important in the brain. What happens when the glucose supply is interfered with has been studied in many ways, one of which is the partial substitution of 2DG for glucose in the blood. The results of doing this in mice, rats and monkeys have been reported by Horton, (Horton, et al., 1973) where they use a dose of 3g 2DG/Kg body weight, which gives a ratio for 2DG to glucose of approximately 2-3. Between five and ten minutes after intravenous injection the animal become atoxic; in fifteen minutes no movement is seen, and after 25 minutes respiration become slower, with most of the animals dying within 45 minutes (Horton, et al., 1973). 2DG gets transported into the cells, phosphorylated but not metabolized via the glycolytic pathway which metabolizes glucose. In the intact animal, hyporglycemia and an increase in fatty acid concentrations are seen with 2DG injections. This results in provoking the release of adrenaline from the adrenal medulla. At the cell level the action is thought to center around the following (Horton, et al., 1973):

a) carrier: mediated transport – a competition between 2DG and glucose for the carrier.

b) hexokinase: substrate competition between 2DG and glucose for this enzyme.

c) hexose phosphate isomerase: inhibition by 2DG-6-P

d) hexokinase: non-competitive inhibition by G-6-P.

Horton (Horton, et al., 1973) showed that of these, c accounts for the greatest inhibition in the glycolytic flux, and that it comes into dominance only when high intracerebral concentrations of 2DG-6-P have been attained. Thus, a and c account for the dramatic effect in the first three minutes of cerebral functional depression observed in Rhesus monkeys (Meldrum and Horton, 1973). This suggested that using 2DG in an experiment would have a strong but less devastating effect than a total ischemic insult, and that it might give some insight into the rate of appearance of 2DG-6-P and its lifetime in the cells.

4.3.3.1 Rate of uptake of 2DG

The N1E-115 cells were grown on 5 mM glucose DMEM serum-supplemented medium in 10 cm tissue culture dishes as described above, and were used to seed Cytodex III microcarriers. The cells on the microcarriers were put in the cell holder and then into the spectrometer for the experiment. Figure 31a is a reference which is the result of 9000 free induction decays taken with a one-second repetition time immediately after the cell holder was put in the spectrometer then 10 mM 2DG was added. At the end of this time two

Figure 31

Cells were grown on 10 cm tissue culture dishes and used to seed Cytodex III microcarriers in a ratio of 2.5 confluent dishes to one with microcarriers. The microcarriers were immediately loaded into the cell holder and then into the spectrometer for the experiment. Inset (A) is a reference which is the result of 9000 free induction decays taken with a one-second repetition time immediately after the cell holder was put in the spectrometer. At the end of this record, 2-DG was added to the final concentration of 10 mM. At this time two observations were made: First, the ATP levels dropped appreciably and remained constant for the rest of the experiment. Second, the sugar phosphate level started to increase due to the appearance of 2-DG-6 phosphate in the cells. The difference in area (in the sugar phosphate region) between the reference and subsequent records taken over a 20-hour period is graphed here. After 10 hours of perfusion, the cells were switched to a 2-DG-free perfusion medium. Insert (B) shows the spectrum from 3000 free induction decays taken during the time interval indicated. Insert (C) shows the spectrum from 10,000 free induction decays taken in the period indicated.These are N1E-115 cells.

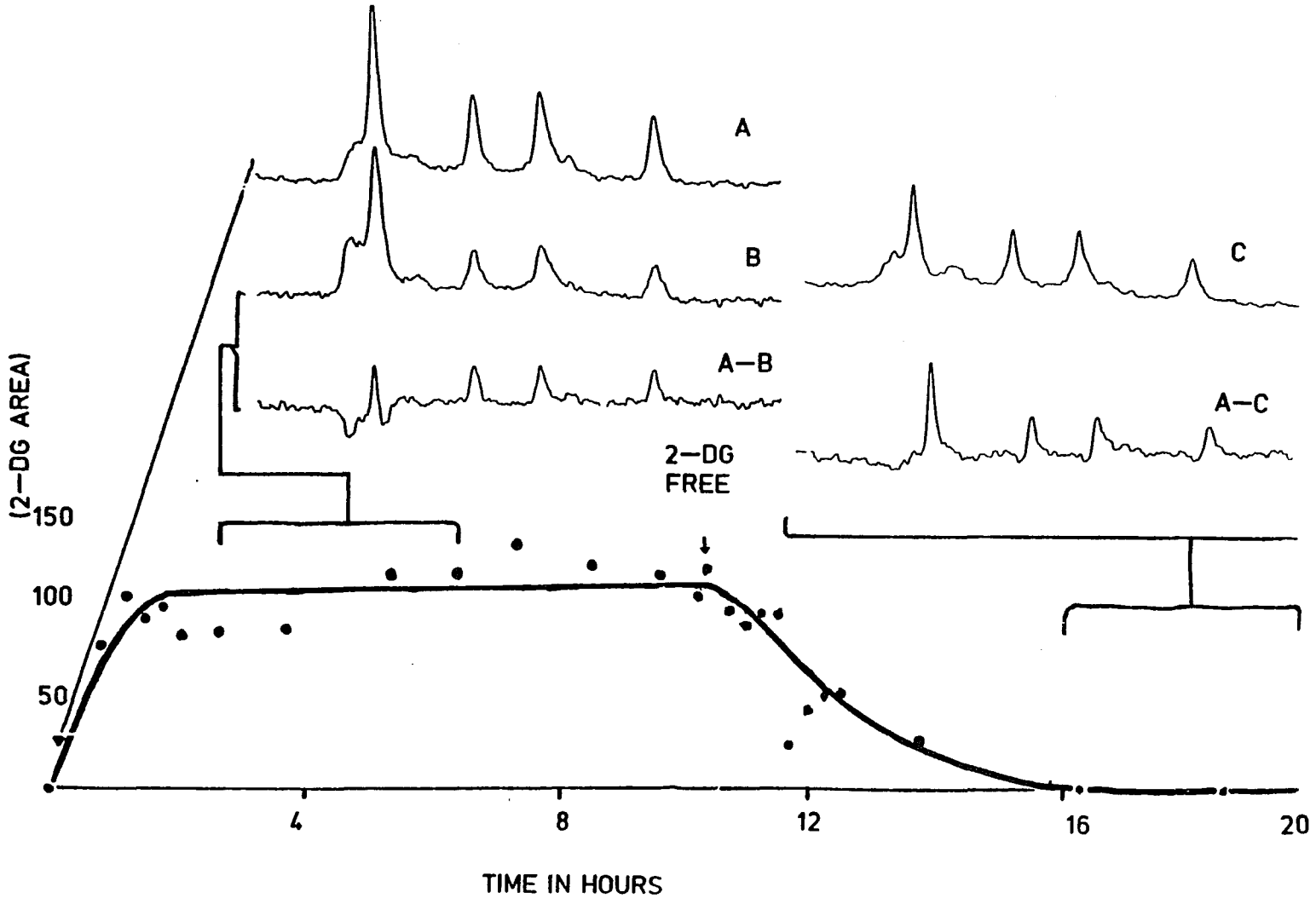

FIG. 31

observations were made: first, the ATP levels dropped appreciably and remained constant for the rest of the experiment. Second, the sugar phosphate level started to increase due to the appearance of 2DG-6-P phosphate in the cells. The difference in area (in the sugar phosphate region) between the reference and subsequent records taken over a 20-hour period are graphed here, and is taken to be proportional to 2DG-6-P. After ten hours of perfusion, the cells were switched to a 2DG-free perfusion medium. Insert (B) shows the spectrum from 3000 induction decays taken during the time interval indicated. Insert (C) shows the spectrum from 10,000 free induction decays taken in the period indicated. Figure 32 shows the results of a similar experiment, where the final concentration of 2DG added was 4.5 mM. The time for the PME region to reach 50% of its final maximum value is concentration dependent, it took 32 minutes with 10 mM extracellular DG and 77 minutes for 4.5 mM. Within the error limits, this shows that the rate of appearance of DG-6-P was directly dependent on the external concentration of 2DG.

Horton found that in mice which had been given 2DG (3g 2DG/kg body weight), the ratio of 2DG/glucose in the brain was 2.65 on the average, at which time the rate of glucose uptake was $.51 \pm .1$ μ mol/g/min, and 2DG was $.688 \pm .06$ μ mol/g/min. This shows that the competition of 2DG with glucose was not one on one, but when 2DG/glucose = 3:1, 2DG was transported evenly with glucose into the cell. He concluded that the concentrations of 2DG-6-P at 30 minutes was 5.5 μ mol/g wet weight of brain. The estimate made here for 2DG-6P in the neuroblastoma is 6 μ mol/g wet weight. The rate of loss of

Figure 32

Graph of difference in the area of the sugar phosphate region after the addition of 4.5 mM 2-DG. Cells which had been growing on Cytodex III microcarriers for 20 days were loaded into the cell holder, put in the spectrometer, and a reference spectrum was taken. These are N1E-115 cells.

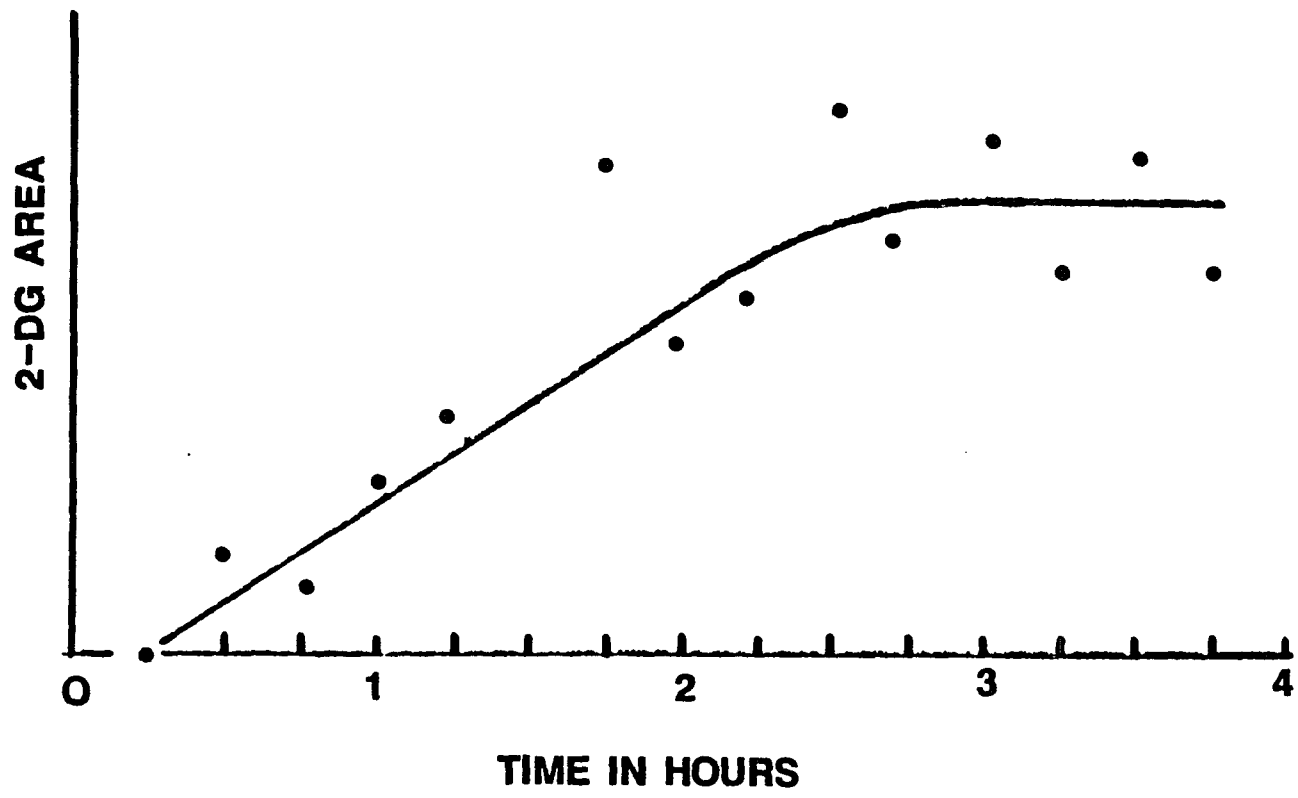

FIG. 32

2DG-6-P when the extracellular 2DG was removed was .02 μmol/g/min. Where could the 2DG-6-P be going? According to Sokoloff, (1984) the only known route open to 2DG-6-P is via phosphoglucomutase to DG-1-P and UDPDG and eventually into deoxyglycogen glycolipids and glycoproteins. This is thought to be a very slow reaction. It is also possible that 2DG-6-P is transported out of the cell, or that the equilibrium of the reaction sets the new value. ^{13}C labeled 2DG could answer this question very nicely. The rate of disappearance of 2DG-6-P, one-tenth that of the appearance, may very well represent the flux through phosphoglucomutase. Whatever the reason, the important point is that the 2DG-6-P reaches a maximum value.

4.3.3.2 Long term recovery of ATP levels

A very interesting point of the above experiment was the drop in the ATP pool to about 50% of the original value. This happened within minutes after introducing 2DG. The pool stayed there throughout the 10 hours of DG treatment, and did not recover within the eight hours post-treatment period, of which the last 4 hours were DG-6-P free. We know from Horton's *in vitro* work on guinea pig cerebral cortex that at 5 mM 2DG-6-P, hexokinase was inhibited to a point of being 60% functional with respect to phosphorylating glucose, and hexose-phosphate isomerase was inhibited 71% by the presence of 20 mM 2DG-6-P a huge concentration (at 5 mM DG-6-P does not inhibit it at all). There was no way of distinguishing between, say, the total death of half the cells and alteration of enzymes or other regulatory functions, which effect the pool size in the experiments in tissue culture. Looking at the Pi peak (Fig. 31)

we can see a distinct broadening on the upfield side which is more clearly shown on the difference spectra. This was attributed to the intracellular Pi, which reflects a decrease in intracellular pH during the time 2DG was present in the medium. This shift disappeared in the 2DG-free recovery period.

There were several things happening here which should be studied further, but what can be concluded from the above is, first, that the ATP pool in cells did not respond in a graded way to interference with their glycolytic enzymes, but instead abruptly changed state to a lower steady-state size pool (50% of that of the original). Secondly, this condition is irreversible upon restoration of original conditions.

4.3.4 Creatine kinase reaction

Creatine kinase is a phosphotransferase which plays an important role in regulating the pool size of ATP and, thus, in the basic metabolic processes of the cell. The enzyme is a dimer. Each dimer is 360 amino acids long with a total molecular weight in the range 79-81d. It was first crystallized from rabbit skeletal muscles by Kuby, et al. (1954), and has since been isolated in three isomeric forms in brain and muscle tissue from a number of animals. The forms are referred to as BB, BM, and MM for brain, hybrid and muscle types, respectively. The isoenzyme BB is found in early developmental stages in muscle cells and brain tissues studied. As the animal develops, the BB isoenzyme continues to be the only one found in the brain, as is the case with chick heart and mammalian smooth muscle. The latter two also have a trace of

BM hybrid, however, in mammalian heart, and red and white striated muscle fibers, the muscle-type gradually predominates as development progresses (Watts, 1973). The enzyme E.C.2.7.3.2 catalyzes the reaction:

$$\text{Mg ATP2}- + \text{creatine} \rightleftarrows$$

$$\text{Mg ADP} + \text{phosphocreatine} + H^+$$

The forward reaction by convention proceeds from left to right. The specific activity of the purified protein for brain is in the range of 250 μ mol/g−protein/min, and that of chick muscle of 720 μ mol/g−protein/min, a value approximately three times as fast.

Solution chemistry with the purified enzyme at 30 ° C has shown a strong dependence of enzyme activity on pH and only a slight temperature dependence. There are several analogues of creatine, which when fed to the live animal, act as substrates for creatine phosphokinase (CPK), get phosphorylated and are hydrolized in a fashion similar to PCr during an ischemic episode (see for example cyclocreatine Watts, 1973). Experiments with these materials have given some insight into the enzymatic process. Noda originally defined the "apparent equilibrium constant" K′ in terms of the total concentration of each substrate (Noda, et al., 1954):

$$K' = (PCr)(ADP)/(ATP)(Cr) \qquad A$$

They found K′ to be greatly affected by Mg++ (or Mn++) concentrations and

by pH. This led to the acceptance of:

$$MgATP + Cr \rightleftharpoons MgADP + CrP + H^+$$

as the reaction which is catalyzed by the enzyme with an equilibrium constant K'b defined by Kuby and Noltmann (Kuby and Noltmann, 1962) as:

$$K'b = (MgADP^-)\,(\text{free phosphocreatine})/(MgATP2^-)\,(\text{creatine}) \qquad B$$

and

Kb as a "pH independent equilibrium constant"

$$Kb = K'b(H^+) \qquad C$$

They found an average value of Kb was $2.81 \pm 0.4 \times 10^{-10}$ for the pH range 7.4 to 9 at 30° C. This was a magnesium activated *in vitro* measurement. Morrison (Morrison and White, 1967) measured the apparent equilibrium constant as defined above (eq. A) at 30° C and pH8 of rabbit muscle creatine kinase *in vitro* buffered with 100 mM triethanolamine HCl and initial concentrations of reactance as follows:

ATP 1mM, ADP 5 mM, phosphocreatine 5 mM

They titrated this mixture in three separate experiments with magnesium, calcium and manganese in the range of 1 to 10 mM. In the range of 6 mM and above (note the sum of ADP and ATP initially was 6 mM) the apparent equilibrium constant is approximately 0.3. However at 1mM concentrations, the

value is near .4, an increase of thirteen times in all cases. They also calculated the "effective equilibrium" constant K'b from the apparent equilibrium constants and stability constants for the metal substrate complexes of Morrison (Morrison and White, 1967) Mg++, Ca++ and Mn++ ADP, (Perrin and Sharma, 1966) MnATP2-, (O'Sullivan and Cohn, 1986) MnPCr. They found a constant value of K'b .030 over the range 1 to 10 mM for Mg2+ which is consistent with theory. However for Ca^{++} the value of Kb' went up with increased Ca++ from .035 to .049 or 40% with a minimum value at 3 mM in the range 1 to 10 mM. The same range of manganese causes Kb' to vary from .037 to .027 dropping to 37% of the original value.

These findings are of most interest when assigning an equilibrium constant to *in vivo* systems, i.e. whole animal, minces, and tissue culture samples. *In vitro* measurements using purified enzymes have given similar results from different investigators for the independent equilibrium constant of 0.28×10^{-9}, (Kuby and Noltmann, 1962) and 0.30×10^{-9} at ph=8.0 (Morrison and White, 1967). This is not the case for *in vivo* experiments. Kass and Lipton (1982) found for *in vivo* rat hippocampal slices a value of 28×10^{-9}, i.e. two orders of magnitude larger than in *in vivo* results and reports a finding of 7.09×10^{-9} as calculated from *in vivo*, and from *in vitro* results. In whole animals Mabe et al., (1983) reported a finding of $7.09\ 10^{-9}$ as calculated from *in vivo* data of MacMillan and Siesjo (1973). The *in vitro* experiments were done in a completely defined solution system and as expected yielded a rate constant consistent with that expected from thermodynamic principles from equations B

and C. It seems appropriate to consider how Kb was determined. Mabe et al. (1983) measured PCr, Cr, ATP, and ADP using an HCl-methanol procedure at −22C° and the flurometric analytical techniques of Folbergrova et al. (1972) from brain tissue that was frozen *in situ* with liquid nitrogen. They derived pHi, the intracellular pH, in the brain cells from the HCO_3- H_2CO_3 buffer system theory and measurements of the arterial and cerebro-venous CO_2 tensions, and estimates of VECF, Bbl and Vi. The volumes (as volume fractions) occupied by extracellular water and solved for Kb using equations B and C. The distribution of the weak acid DMO was used to measure the pH in *in vitro* rat hippocampal slices. The metabolites were extracted with 3N cold perchloric acid and analyzed using standard spectrofluormetric techniques. The pH was found to be 7.2.

4.3.4.1 Rate of uptake of Cr

The uptake of Cr and appearance of PCr were looked at with a view to determining how the extracellular concentration of Cr and the pH affected the appearance of PCr in the cells. The cells were grown, seeded onto microcarrieres, loaded into the sample holder and magnet, where the system was allowed to equilibrate in terms of pH and temperature.

After a control spectrum was taken, the creatine was added to the recirculating reservoir, and the appearance of PCr was followed. Controls showed no PCr present in the cells at all.

The ratio of the PCr peak to the ATPα peak has been used to characterize

the PCr content of the cells. This was chosen after considering alternatives such as the PCr to Pi ratio, which would give good absolute values of PCr, since the Pi in general is mostly due to the 1 mM Pi in the perfusing medium. The advantage of taking the ratio of PCr to the ATPα peak is that the changes in the PCr are tied to a cell parameter. Experience has shown that the ATPα peak remains relatively constant over very long periods of time when the cells are not dividing and are in good health. The ATPα peak is therefore considered to be proportional to the cell number. This ratio thus provides a measure which can be used to compare different experiments on different sets of cells.

In the process of doing these experiments, a strong pH dependence was observed on the appearance of PCr which prompted experiments to measure the rate of appearance at two or three pH values for a particular concentration of extracellular creatine. These results were plotted in Figure 33 for 4, 10, and 30 mM extracellular creatine. These values were used to interpolate and obtain the rate of appearance of PCr at pH7.4 for the three concentrations indicated. These results are presented in Table 7. The rate of uptake is plotted for four concentrations is plotted in Figure 34, and a Lineweaver-Burk plot shown in Figure 35. It has been suggested that the uptake may be heterogeneous and in part transport mediated (Daly, M. and Seifter, S., 1980). The Lineweaver-Burk plot gives a Km of 100 mM and a V max for d $(\frac{PCr}{ATP})$/dt of 1.1 hours -1.

The experiments done at 10 mM are detailed here more extensively to demonstrate how the pH effects the rate of appearance of PCr and how the

Figure 33

The rate of appearance of PCr normalized to ATPα (d(PCr/ATPα)/dt) is plotted for three extracellular concentrations of Cr at several pH values. This data is obtained as described in table 7 and the text; these are undifferentiated cells. Time is in hours.

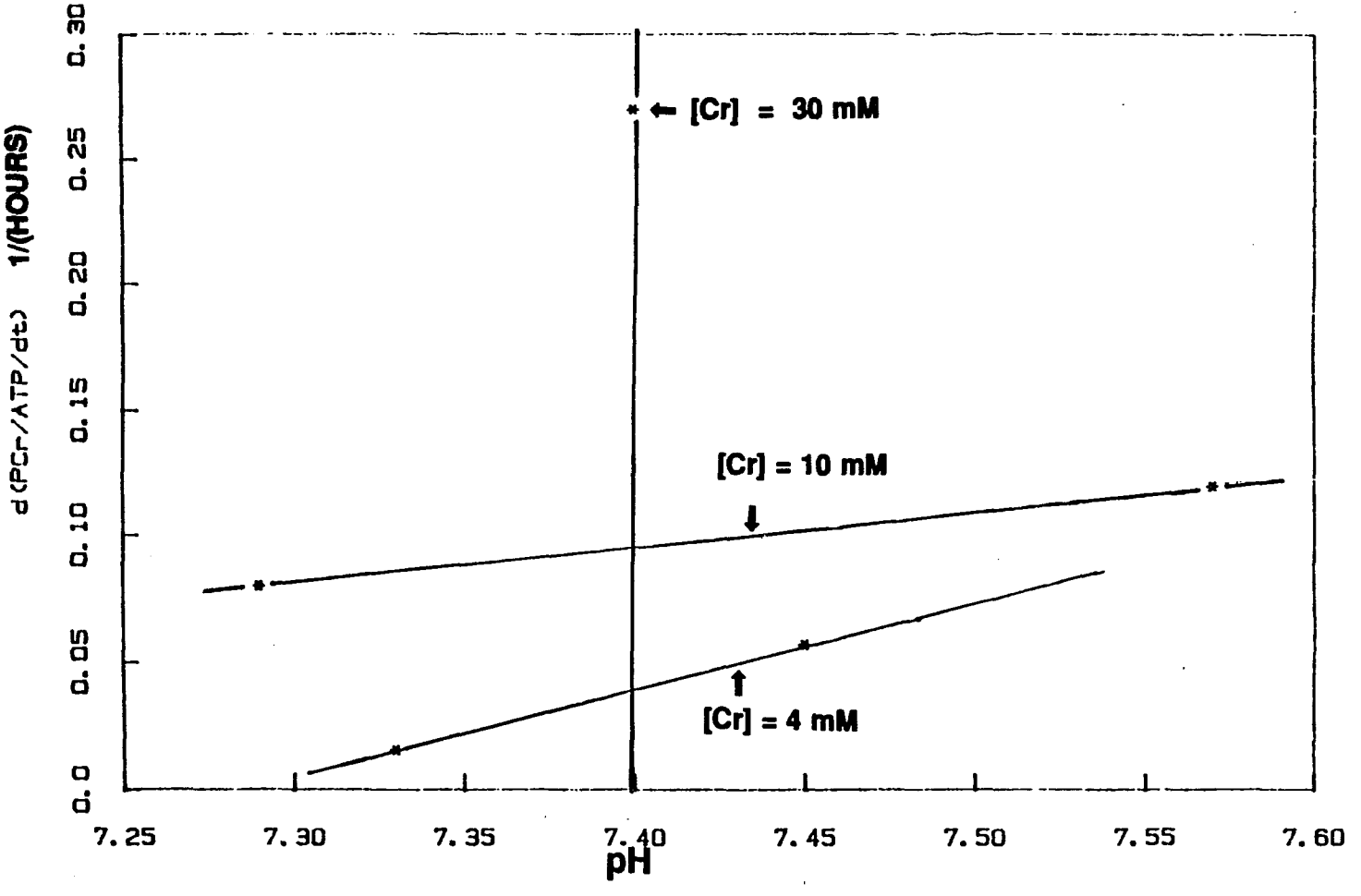
d(PCr/ATP/dt) 1/(HOURS)
0.0
0.05
0.10
0.15
0.20
0.25
0.30
7.25
7.30
7.35
7.40
7.45
7.50
7.55
7.60
pH
[Cr] = 30 mM
[Cr] = 10 mM
[Cr] = 4 mM

FIG. 33

Figure 34

The rate of PCr appearance as a function of extracellular concentration of Cr. The rate of PCr is normalized to ATPα and is plotted as $V = d(PCr/ATP\alpha)/dt$ vs. concentration. The pH is 7.4 (undifferentiated cells). Time is in hours.

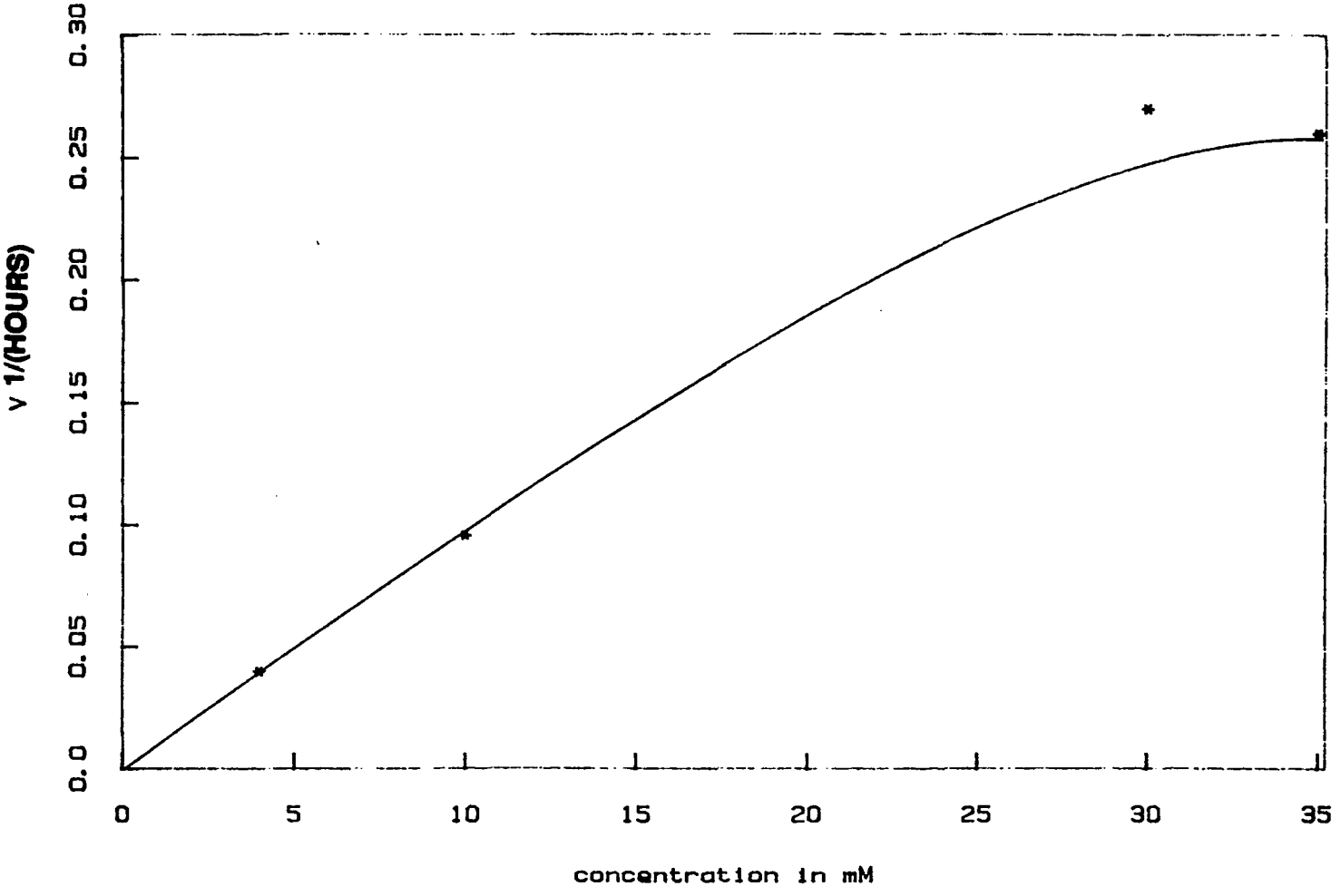
v 1/(HOURS)
0.0
0.05
0.10
0.15
0.20
0.25
0.30
0
5
10
15
20
25
30
35
concentration in mM

FIG. 34

TABLE 7

The rate of appearance of PCr normalized to the ATPα peak $V = d([PCr]/[ATP\alpha])/dt$, is listed against the pH at which it was measured for several different concentrations. Since PCr and ATPα have different T1's it is important to compare values measured at the same pulse repetition rate. In this case, all values were measured at a 3 second repetition rate or normalized to it.

Concentration of extracellular Cr	Extracellular pH	d(PCr/ATPα)/dt (hours -1)
30	7.40	0.27
10	7.29	.08
10	7.57	0.12
4	7.45	0.057
4	7.33	0.016

Figure 35

The values in table 7 given for V and PCr peak height were plotted here as 1/V and 1/[PCr]. The value plotted at 1/[PCr] = 0.1 and indicated as pH 7.4 was estimated by linearly interpolating between the values obtained at pH 7.29 and 7.57. All points but this one were used to obtain the line in a regression analysis.

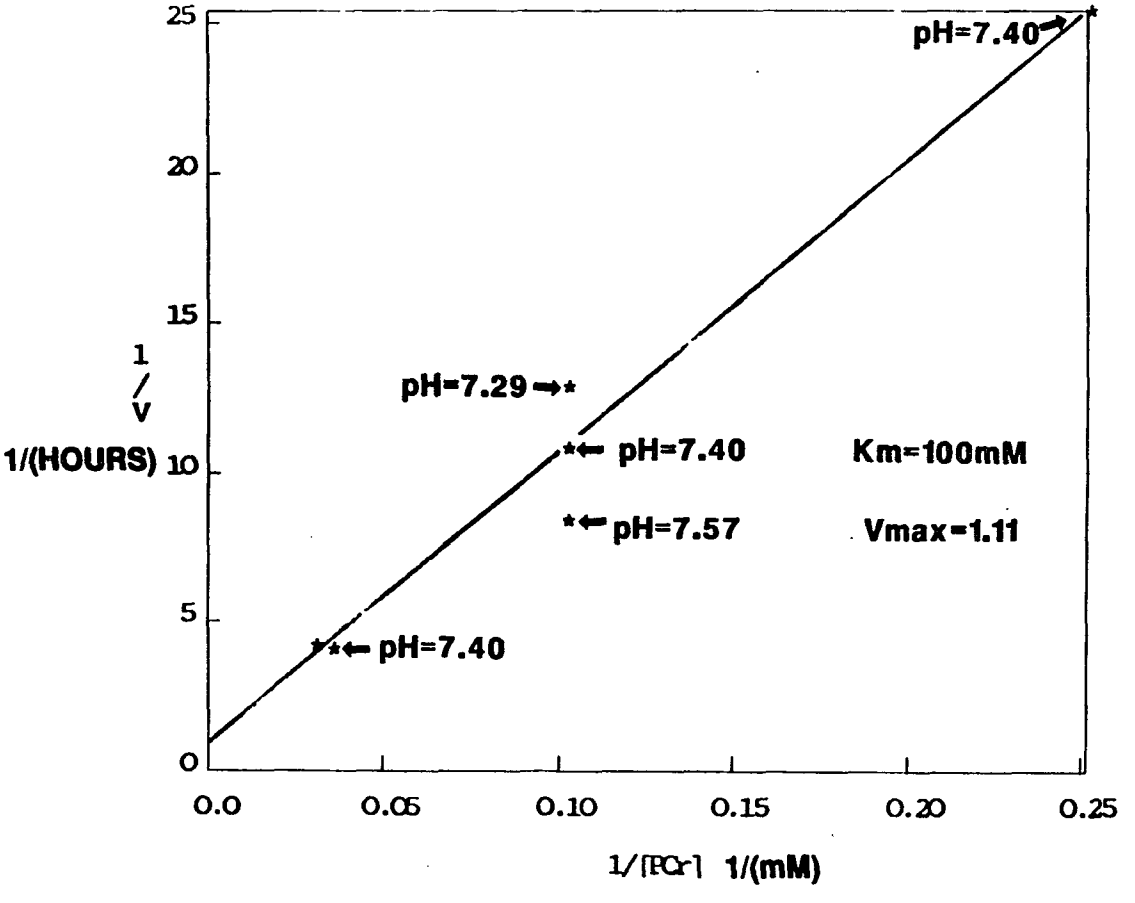
25
20
15
1
/
V
1/(HOURS)
10
5
0
pH=7.40
pH=7.29
pH=7.40
Km=100mM
pH=7.57
Vmax=1.11
pH=7.40
0.0
0.05
0.10
0.15
0.20
0.25
1/[PCr] 1/(mM)

FIG. 35

Figure 36

The time course of PCr uptake when the extracellular concentration of Cr was 10 mM. The pH values were from the best measurement of the intracellular pH. The pH values were calculated from the chemical shift of the intracellular Pi for the higher pH values where intercellular Pi was resolvable from the extracellular value and from the chemical shift of the unresolved peak at the lower pH values. (A) the plot of the peak height versus time. (B) a stack plot of the spectrum of the 10 mM Cr experiment.

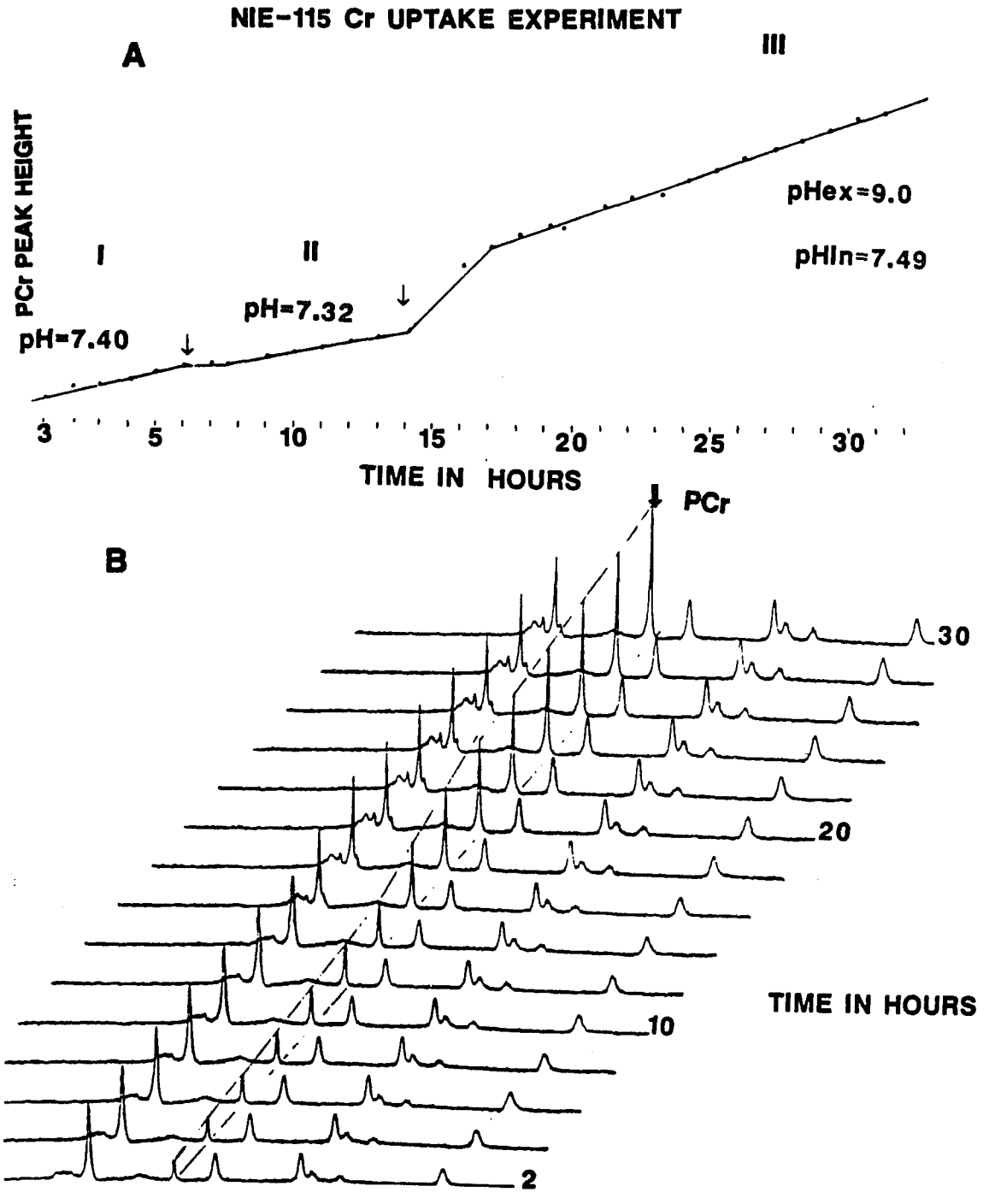
NIE-115 Cr UPTAKE EXPERIMENT
A
III
PCr PEAK HEIGHT
I
II
pH=7.40
pH=7.32
pHex=9.0
pHIn=7.49
3
5
10
15
20
25
30
TIME IN HOURS
B
PCr
30
20
10
2
TIME IN HOURS

FIG. 36

internal Pi can be resolved using spectra obtained at high pH values. Figures 36 shows the time course of cells in 10 mm creatine where the pH of the superfusing medium has been switched from 7.39 $\pm$0.1 to 7.36 $\pm$.01, and then to 9 at 6 and 14 hrs, respectively. This figure also shows a stack plot of the spectra at two hour intervals. There are several interesting features to note here. First, is the slow change and emergence of peaks in the PME region. Second, and a most striking feature, is the change in the rate of PCr appearance, with a shift in pH and the shift in the nominally linear slope. The shift can best be understood by referring to Figure 37. From the period "a" to "b", (labelled on the Figure t1 to t2) the pH changed 0.3 pH units. Now in order for Eq. 2 to remain balanced either the ATP/ADP ratio or the Cr/PCr ratio or both in some combination must change. From the experimental evidence, ATP did not change in the period around the pH jump but the PCr did, and we could measure it. Now if the free creatine does not leak out of the cells, (which is the case in this short time interval), i.e., if the total creatine, the sum of the free unbound and the phosphorylated creatine, remained constant, then the PCr/Cr ratio increases. Thus, by knowing the total Cr concentration or PCr/Cr ratios at a given pH, and the ATP concentration, then by measuring PCr and the slope with a change in pH value, one could calculate the ADP concentration in the cells, given K, and thus calculate the phosphate potential.

Figure 38 gives internal and external pH values during the experiment. Note that at normal physiological pH values, the pH gradient across the cell membrane was in the range of 0.1 pH units, but when the extracellular pH is 9,

Figure 37

This figure depicts the relationship between the various components of the phosphocreatine reaction before, during and after the pH jump.

t_1 = The time the pH of the superfusate was switched from a low pH to a high pH

$t_2 - t_1$ = the time the extracellular pH was equilibrating

t_3 = represents the time the experiment was stopped and an extract was made.

ADP_1 = The concentration of ADP in the cells before they were subjected to the increase in pH.

ADP_2 = The value of ADP in the cells after the pH jump.

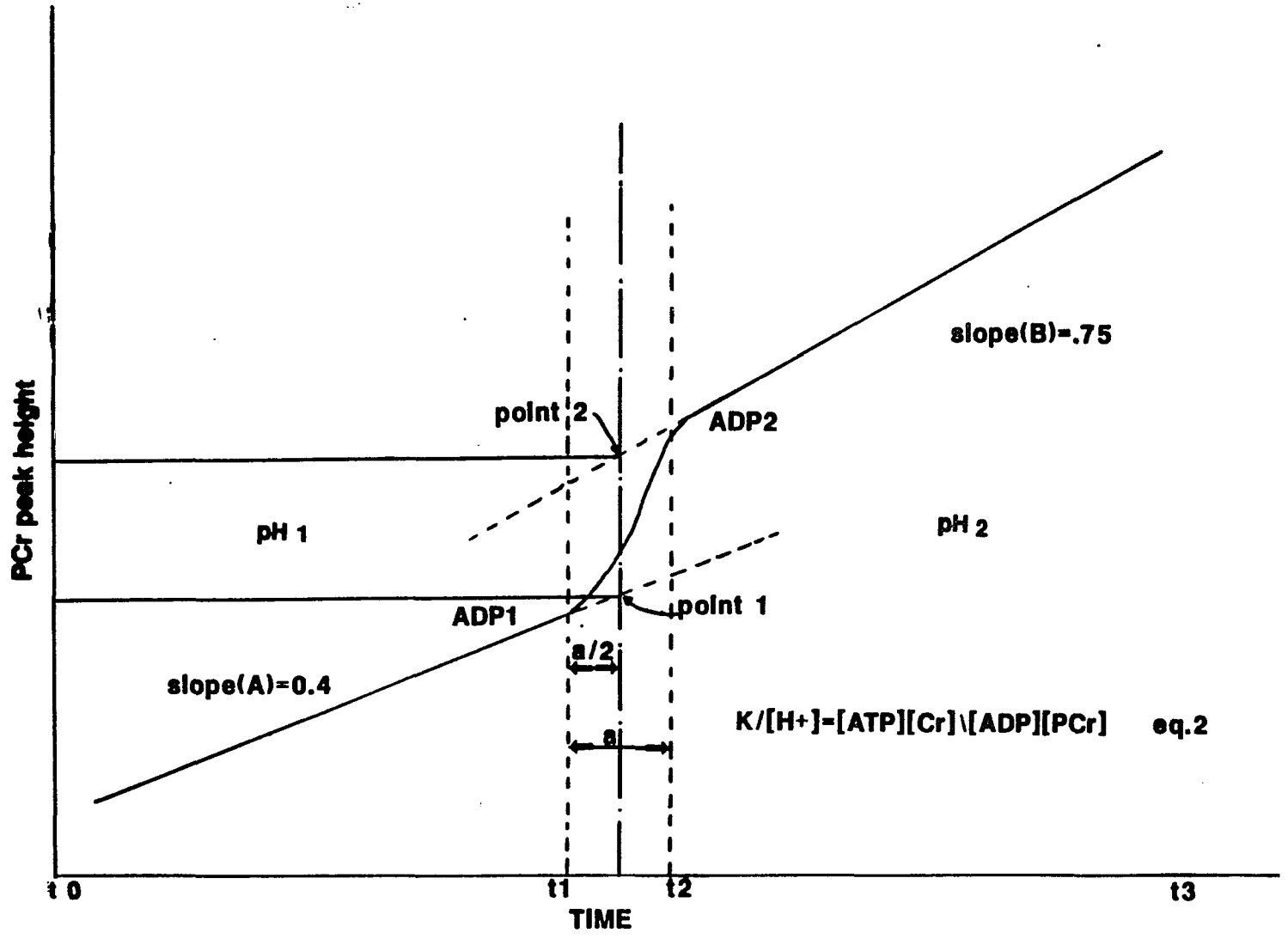
PCr peak height
slope(B)=.75
point 2
ADP2
pH 1
pH 2
ADP1
point 1
a/2
slope(A)=0.4
K/[H+]=[ATP][Cr]\[ADP][PCr] eq.2
a
t 0
t1
t2
t3
TIME

FIG.37

Figure 38

This figure shows the values of slope, interval and external pH for all three pH conditions. The pH value of 9 was calculated from the chemical shift data of the external Pi. At these extreme values of the titration curve for Pi, a 0.01 pp error resulted in 0.3 difference in pH. These large errors should be considered for this particular value. Others can be taken at face value.

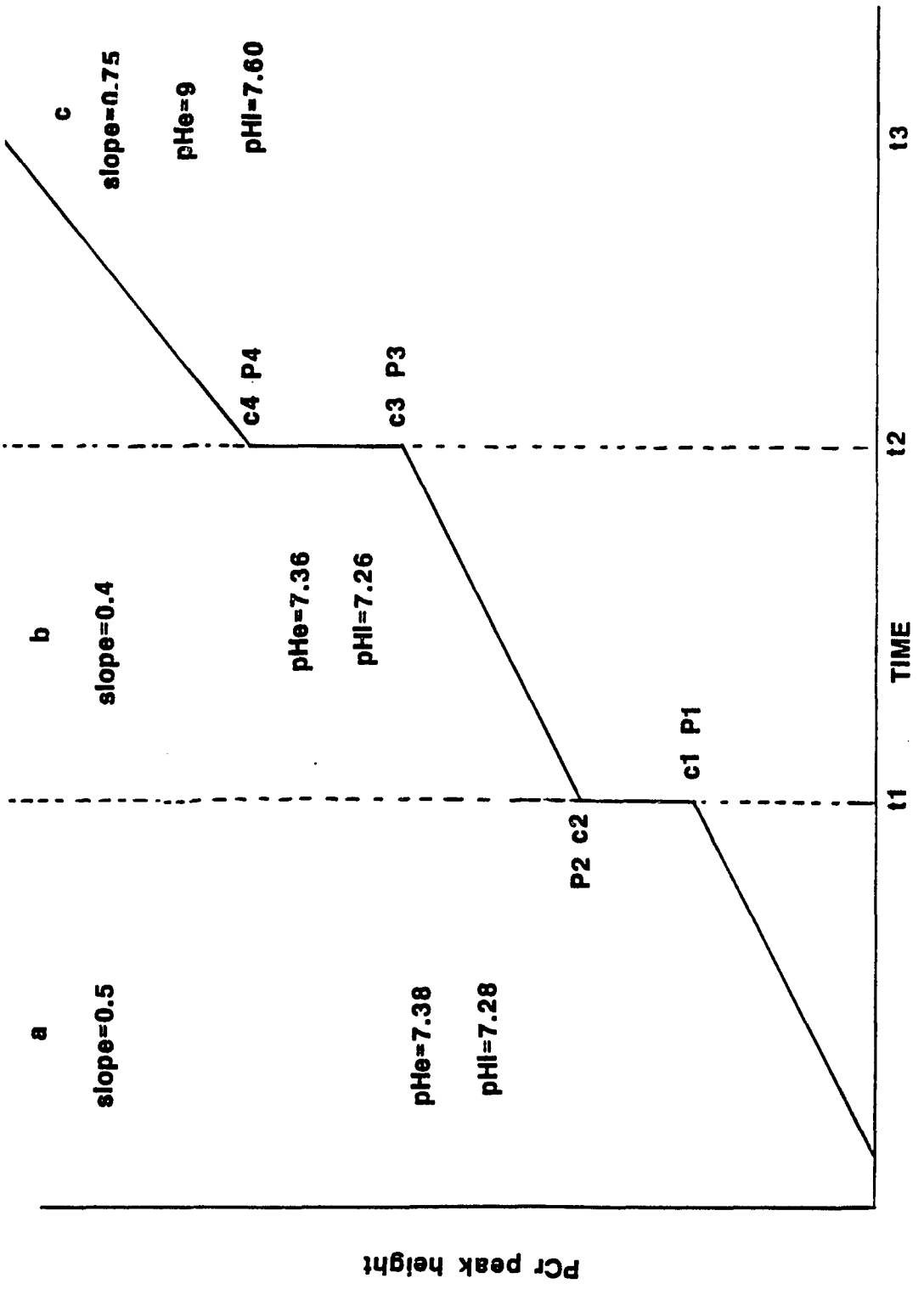
PCr peak height
TIME
t1
t2
t3
a
slope=0.5
pHe=7.38
pHI=7.28
P2 c2
c1 P1
b
slope=0.4
pHe=7.36
pHI=7.26
c4 P4
c3 P3
c
slope=0.75
pHe=9
pHI=7.60

FIG. 38

Figure 39

(A) Spectrum of cells in high pH medium. Note that the small upfield internal Pi is almost resolved. This spectrum has been multiplied with a line-broadening factor of 2.5 Hz. (B) The same spectrum as in (A) but resolution enhanced by the convolution difference method using a broadening factor of 25 Hz. (C) This is a spectrum of cells at a lower extracellular pH similarly resolution-enhanced where the internal and external Pi peaks are not resolved. By subtracting the resolved spectrum of (B) from the unresolved of (A) after superimposing the external portions of the Pi peak (D), the internal Pi of the unresolved spectra can be obtained (E).

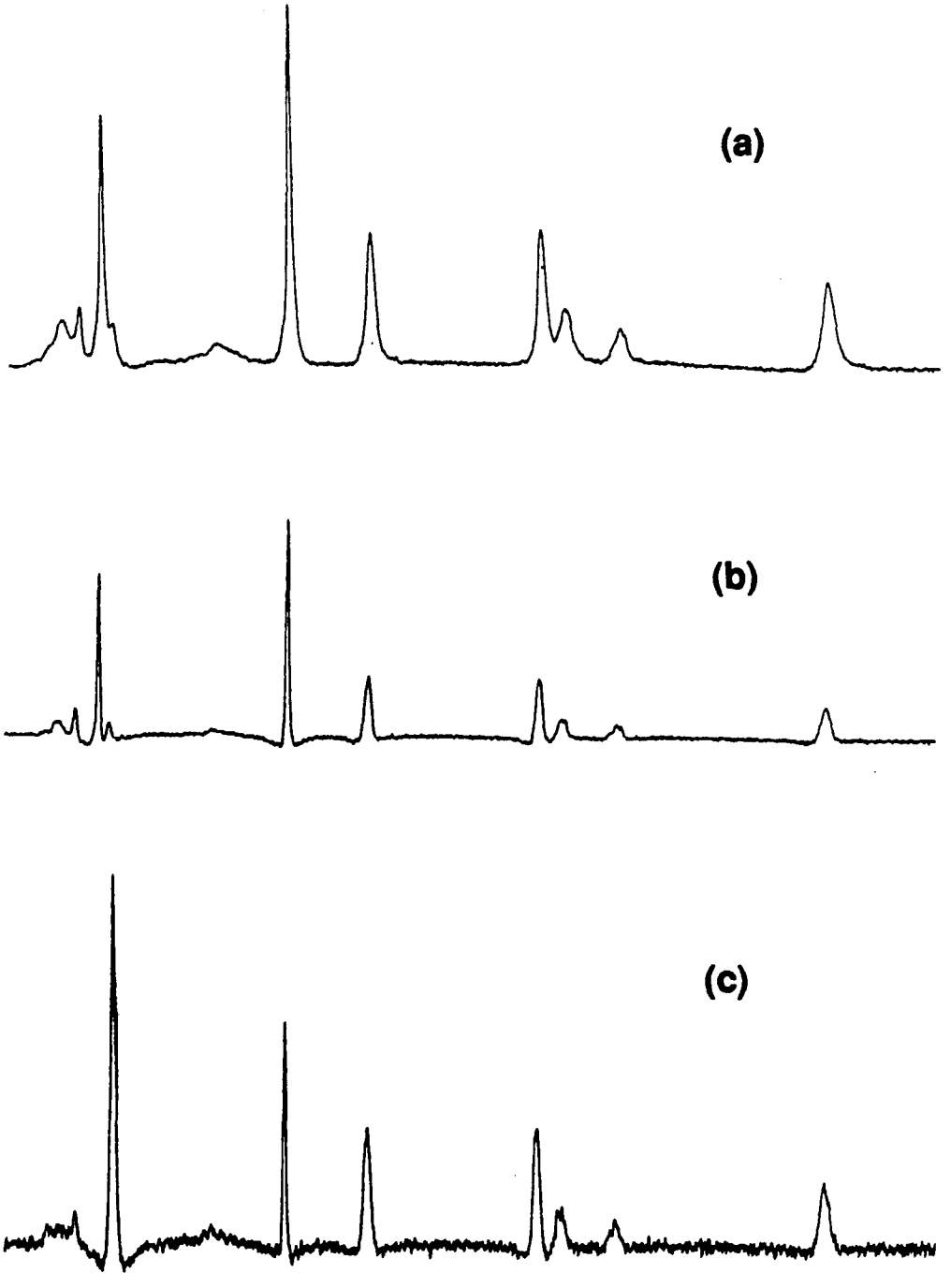

FIG. 39 (A) (B) (C)

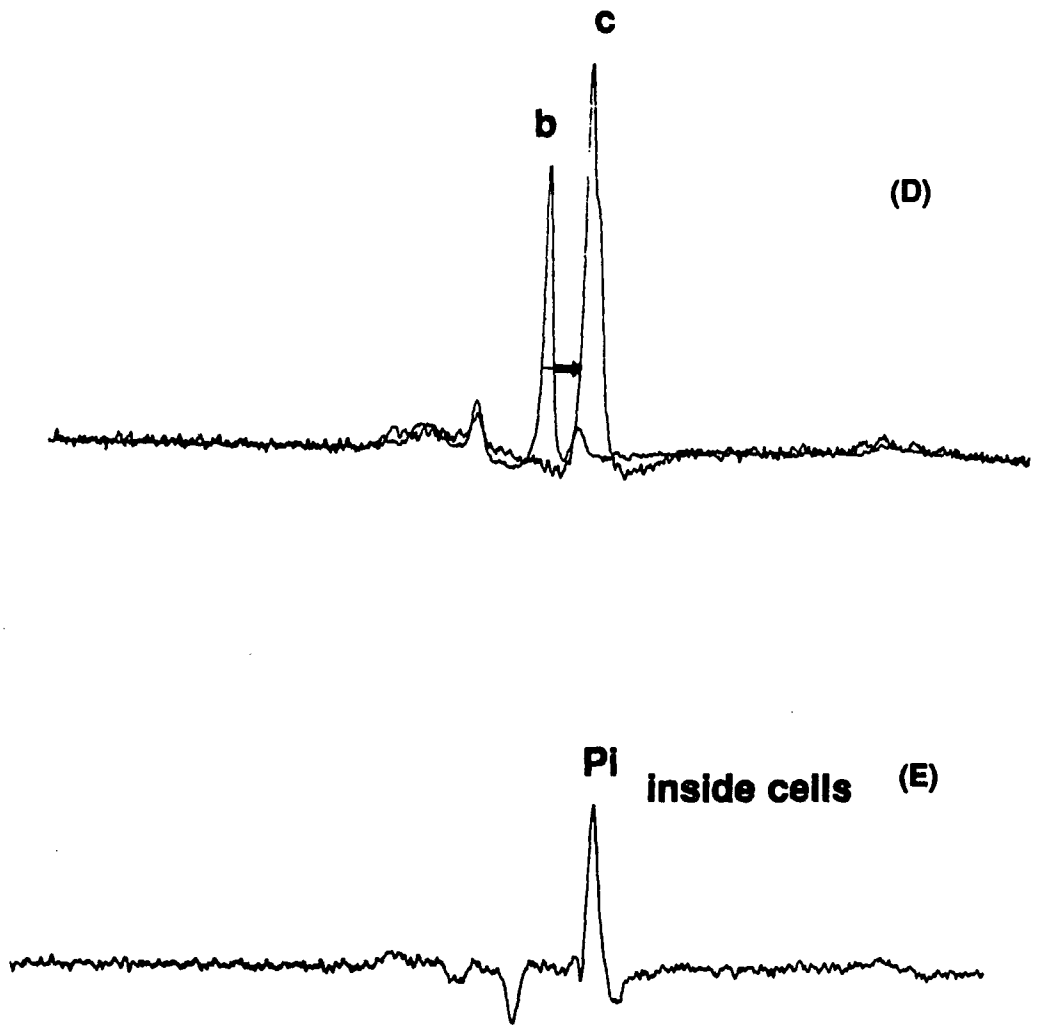

FIG. 39 (D) (E)

the intracellular pH rose only to 7.57 and a gradient of 1.69 pH units was generated and maintained for the 10 hrs duration of the experiment.

The method used to make these internal pH measurements is depicted in Figure 39. The peak associated with the internal pH of 7.57 when the external pH is 9, was 43 Hz upfield from the extracellular inorganic phosphate peak and was not completely resolved when line-broadening of 2.5 Hz was used (see Fig. 39a). However, when the FID was first resolution-enhanced by the method of convolution difference using a line-broadening factor of 25 Hz (Martin, M., 1980b, Gadian, D. G., 1982b, Campbell, I. D., et al., 1973, p. 90) the peak was completely resolved (see Fig. 39b) thus leaving the larger downfield peak, due to extracellular Pi, also completely resolved. This extracellular peak was then subtracted from each of the previous spectra, which were less well resolved but which had similarly been resolution-enhanced, and the chemical shift of the internal pH was obtained (see Figs. 39D and E).

The above method allowed for pH determinations, however the wave shape was distorted too much to be useful for intergrating areas and determining concentrations. For internal concentrations the following manipulation of the data was employed. The FID was first line broadened with a factor of 2.5 Hz and FT. The resulting spectrum was subtracted from itself after shifting the subtrahend so that the PCr peak was under the external Pi peak, then the peak height was adjusted so that the resulting difference of the two spectra was of a symmetric shape. The resulting peak was that of the internal Pi. This method worked well under specific conditions, but not under all conditions. It would

not work when there was no difference in pH between the inside and outside of the cell. This method generated ambiguous results when the field homogeneity was poor. In general, when the pH gradient across the cells was greater than 0.1 pH units and was in a homogeneous field, good results could be obtained.

A third interesting feature in this experiment is the change in the rate of appearance of PCr with pH. The rate of appearance of PCr was dependent on the rate at which creatine was transported to the interior of the cell and also on all the factors in the equilibrium equation for the creatine kinase reaction. Consider Fig. 4.3-18b. There was an external concentration of 10 mm Cr. During the time interval t0 to t1, the rate of appearance of PCr was plotted. During this time period the temperature, pH and oxygen supply were constant, and the cells were not under stress conditions; in addition to this, the ATP concentrations were seen to be constant. It is reasonable to assume, therefore, that the oxygen consumption and ADP levels were constant, that is, $dADP/dt = 0$. In the period t2 to t3, except for the fact that the pH was different, the above considerations were also true. With this one assumption in mind, the question can be asked: is this abrupt change in slope due to a change in the rate at which creatine was being taken up, or to some rearrangement of the equilibrium equation, or both? If we let C1 be the total creatine in the cell just prior to the pH transitions, and take C2 to be the total concentration just after the pH transition, then with the assumption that the total creatine is a constant in this short time interval, we have:

$$C = Cr + PCr \tag{1}$$

then

$$C_1 = Cr_1 + PCr_1 \tag{2}$$

$$C_2 = Cr_2 + PCr_2 \tag{3}$$

where Cr_1 and PCr_1 are the concentrations of creatine and phosphocreatine the moment before the transition, and Cr_2 and CrP_2 for the concentrations just after the transition to pH_2. From the equilibrium conditions, we know:

$$K = \frac{PCr \times ADP \times H}{Cr\ ATP} \tag{4}$$

$$Cr = \frac{H}{K} \times \frac{ADP}{ATP} \times PCr \tag{5}$$

let $A_1 = \frac{H_1}{K} \frac{ADP_1}{ATP}$ and $A_2 = \frac{H_2}{K} \frac{ADP_2}{ATP}$ rewriting Eq. 4 gives

$$Cr = A\ PCr \tag{6}$$

Equations 6 and 1 give:

$$C = APCr + PCr \tag{7}$$

or

$$C = PCr(1 + A) \tag{8}$$

One can therefore write:

$$\frac{C_1}{C_2} = \frac{PCr_1(1 + A_1)}{PCr_2(1 + A_2)} \tag{9}$$

where C_1 = total creatine in cells at t_1

C_2 = total creatine in cells at t_2

But

$$C_1 = C_2 \tag{10}$$

therefore

$$\frac{PCr_2}{PCr_1} = \frac{1 + A_1}{1 + A_2} \tag{11}$$

taking the derivative of Eq. 8 gives:

$$\frac{dC}{dt} = \frac{dPCr}{dt}(1 + A) \tag{12}$$

given:

$$\frac{d}{dt} A = 0$$

$$\frac{d}{dt} (ADP) = 0$$

because the ATP and ADP do not change let:

$$\frac{dPCr_1}{dt} = a$$

$$\frac{dPCr_2}{dt} = b$$

We can therefore write:

$$\frac{dC_1}{dt} \Big/ \frac{dC_2}{dt} = \frac{a}{b} \frac{PCr_2}{PCr_1} \tag{13}$$

Thus, if the rate of change of creatine going into the cells at the lower pH is the same as that at the higher pH then:

$$\frac{a}{b} = \frac{PCr_1}{PCr_2} \tag{14}$$

Using the experimental data from Fig. 4.3.4.1-5 we get:

$$\frac{PCr_2}{PCr_1} \Big/ \frac{b}{a} = .91 \tag{15}$$

This result is very close to one and lets us conclude first that the rate of Cr uptake by the cells changed by less than 10% over the range of external pH values from 7.38 to 9.58 with their corresponding range of internal pH values of 7.28 to 7.6. It can also be concluded that if there was a small change it was in the direction of a decrease in creatine uptake with an increase in extracellular pH, a result which is counterintuitive after a cursory look at the plot of PCr

appearance with pH. An interesting product of this result was that when an extract of the cells in the experiment was made at the end of the experiment and the creatine and phosphocreatine concentrations were determined, one could calculate back and get the creatine concentration prior to the pH jump. And with this value, one can then calculate the ratio of ADP_1/ADP_2 as follows:

Rearranging 4:

$$Cr\left(\frac{K\ ATP}{PCr\ H}\right) = ADP_1 \tag{16}$$

$$\text{Therefore} \qquad \frac{ADP_1}{ADP_2} = \frac{Cr_1}{Cr_2}\left(\frac{PCr_2\ H_2}{PCr_1\ H_1}\right)$$

In the actual experiment reported here, the ATP level remained fairly constant throughout the transition in pH and then started to increase. The underlying assumptions for the argument above were valid through the short transition period, but not in the long term after the transition during this period from approximately 15 hours to 23 hours it increases at about 6% per hour (the transition time of the internal pH jump was less than ½ hour.) It was therefore necessary to make an extract for Cr determination immediately after the pH jump. The fact that ATP went up invalidates the assumption that in the long-term post pH jump period, $\frac{dA}{dt}$ of Eq. 12 was zero. It is interesting to note that the ATP was seen to increase during the period when the gradient of the pH across the cell membrane was increasing and reached a maximum and constant value while this time the gradient of the pH across the cell membrane

was constant. In order to estimate the behavior of this cell system in the post-pH jump period, it would be necessary to determine the Cr concentration during this period, and then to calculate the ADP concentration. At this point it is sufficient to show the pH dependence of the appearance of PCr and to demonstrate the importance of the timeliness in making the extract measurements for creatine determination and the ability to determine the Cr concentration and phosphate potential at specific points.

Figure 40

(A) ^{31}P spectra of N1E-115 cells maintained on 0.2 mM supplemented medium for 5 days prior to loading onto microcarriers and being put in the NMR spectrometer. (B) ^{31}P spectra of N1E-115 cells maintained in the NMR spectrometer for 14 hours with 10 mM creatine supplemented medium. The signals in both cases was derived from approximately 7×10^7 cells. The spectra were from 1000 scans taken in 50 minutes at 145.8 MHz and 37° C and were processed with 2.5 Hz line broading, PCr creatine phosphate, Pi, inorganic phosphate; $ATP_{\alpha\beta\gamma}$, ATP α, β, and γ phosphate resonances.

A

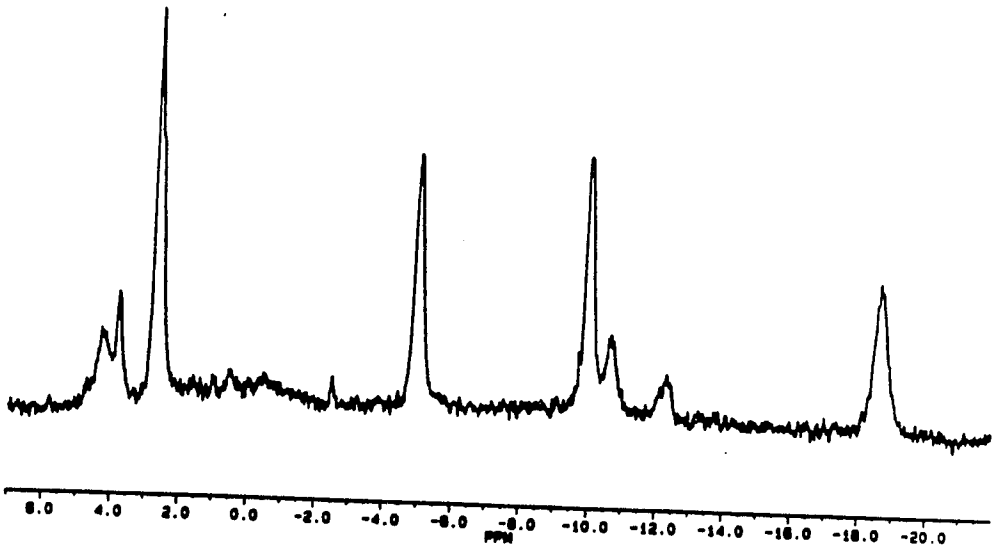
8.0
4.0
2.0
0.0
-2.0
-4.0
-6.0
-8.0
PPM
-10.0
-12.0
-14.0
-16.0
-18.0
-20.0

B

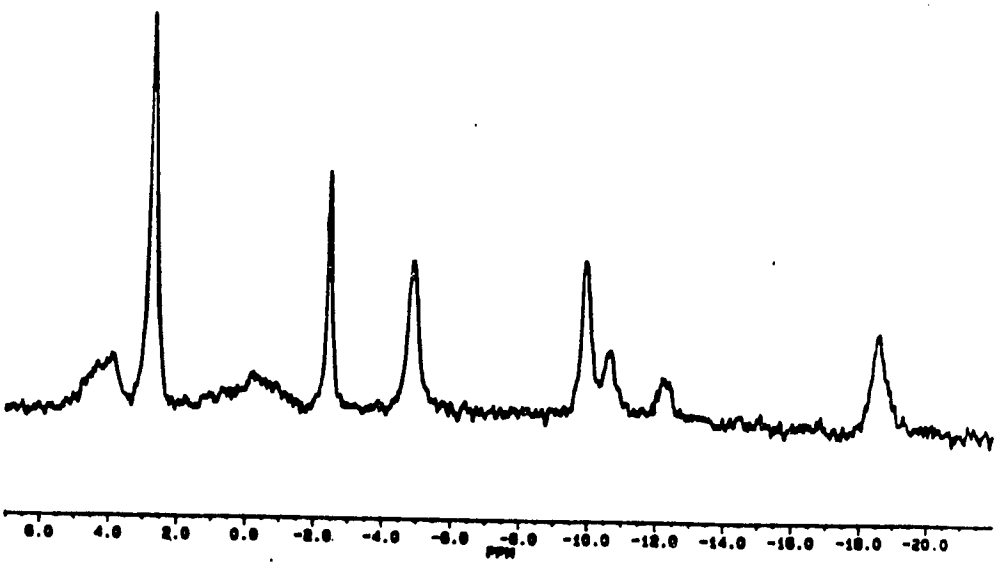
8.0
4.0
2.0
0.0
-2.0
-4.0
-6.0
-8.0
PPM
-10.0
-12.0
-14.0
-16.0
-18.0
-20.0

FIG. 40

Figure 41

(a) ^{31}P spectra of cells with an internal pH (pH_{in}) of 7.3. Note that the phosphomonoester region, PME, is relatively small. There is a split in the Pi peak. The shoulder on the upfield side is due to the intracellular orthophosphate (Pi_{in}), and the large downfield peak is due to the 1 mM orthophosphate in the superfusion medium. With suitable gaussian enhancement this separation is prominent, reproducible and well out of the noise. (b) ^{31}P spectra of cells with a pH inside of 7.5 and an external pH of 8 to 9. In this spectra Pi_{in} is well resolved and smaller than the lower pH case. The PME region is larger with prominent peaks at 3.83 ppm and 4.4 ppm (relative to PCr assigned −2.49 ppm). These spectra were from 1000 scans taken in 50 minutes at 145.8 MHz and 37° C. They were processed with 2.5 Hz line broadening. The captions are the same as in Fig. 40.

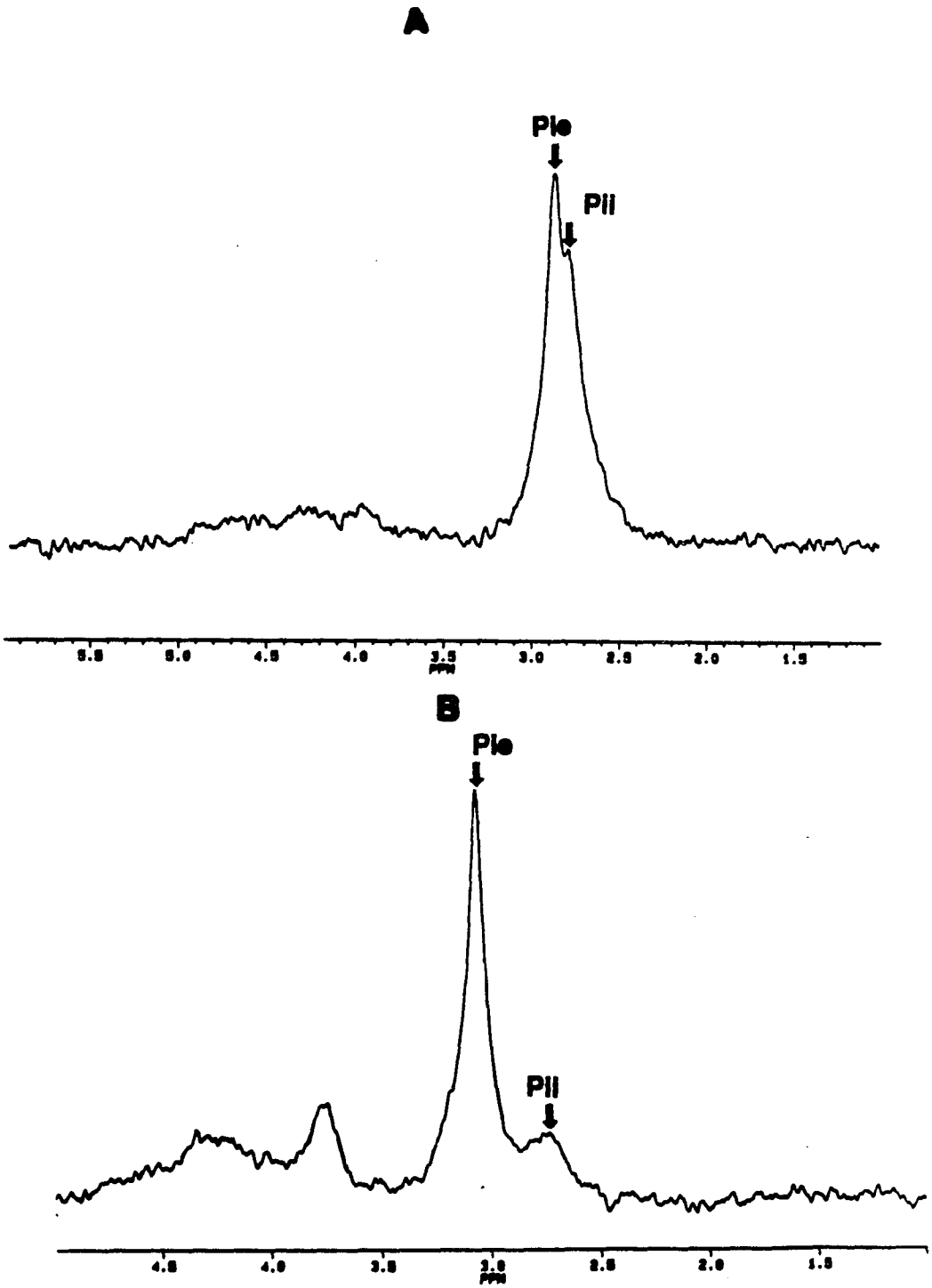

FIG. 41

Figure 42

(A) The pH inside the cells, pH_{in} Δ and outside ○ calculated from the Pi chemical shift relative to PCr (this method is relatively inaccurate above pH 8 and the external values plotted here should be considered as an estimate). (B) The phosphocreatine in the cells. (C) The orthophosphate □ and the ATP Δ in the cells. These results are from a continuous run over a 30 hour period. The absolute concentration are calculated assuming the ATP concentration in the cells is 4 mM at normal physiological conditions.

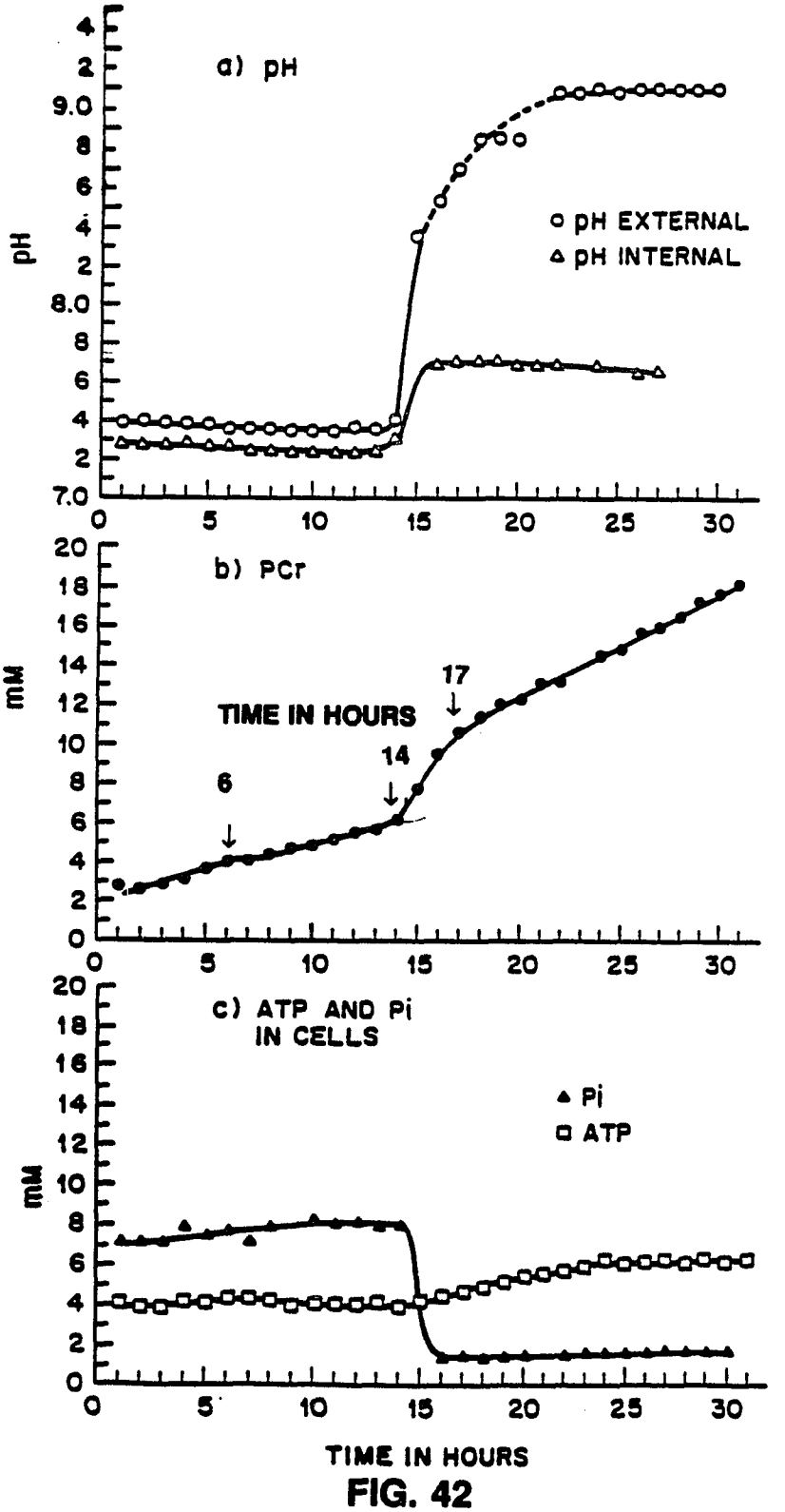
a) pH
pH
9.0
8.0
7.0
o pH EXTERNAL
Δ pH INTERNAL
b) PCr
mM
TIME IN HOURS
6
14
17
c) ATP AND Pi
IN CELLS
▲ Pi
□ ATP
mM
TIME IN HOURS

FIG. 42

Figure 43

(A) ^{1}H NMR spectrum of a perchloric acid extract of N1E-115 cells which had been incubated with 10 mM Cr for a number of hours, then washed with 100 μM Cr medium immediately before the extract was made. The chemical shift scale was referred to trimethylsilapentane sulfonate (TMS). (B) The ^{31}P extract of the same sample as in (A).

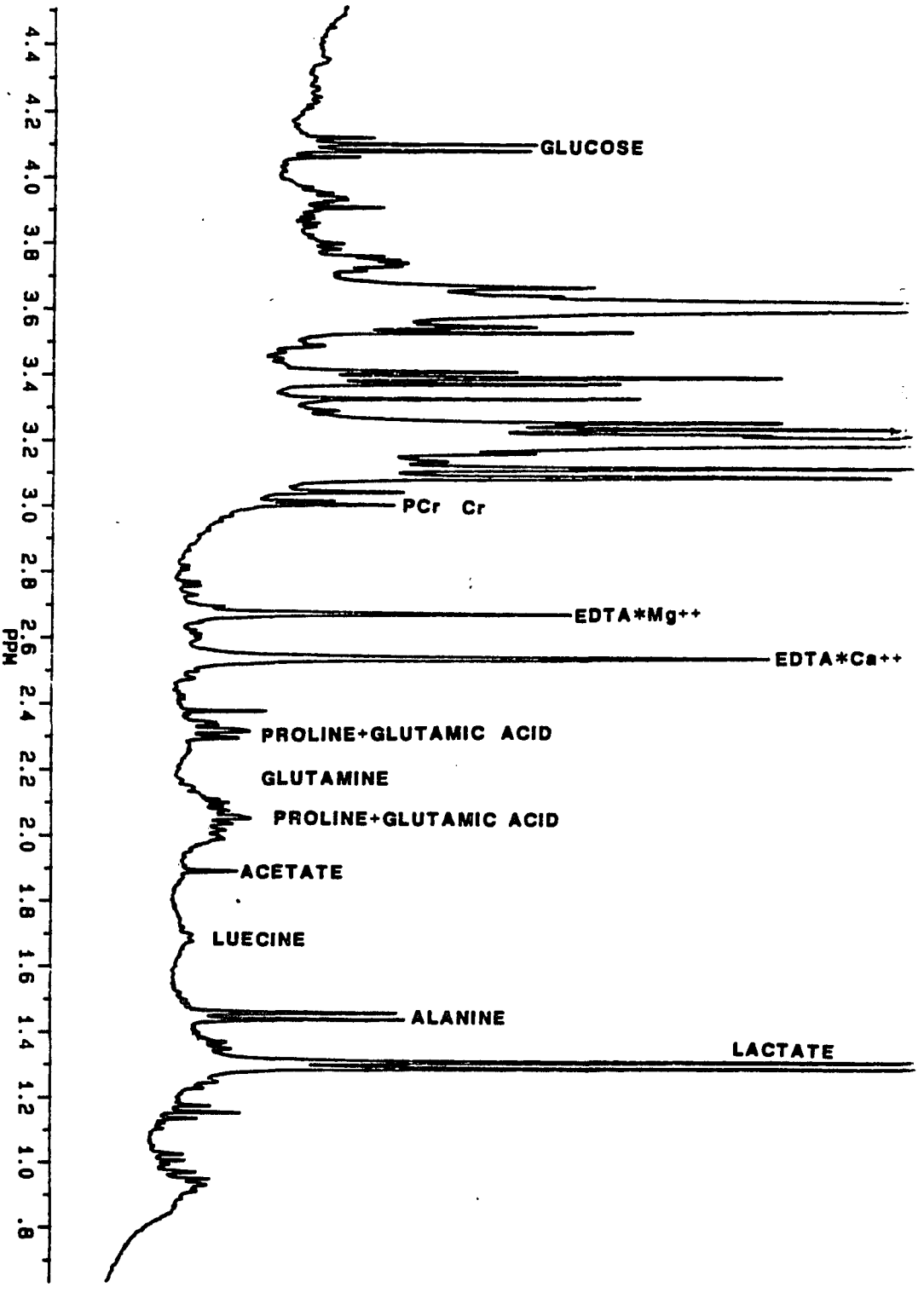
GLUCOSE
PCr Cr
EDTA*Mg++
EDTA*Ca++
PROLINE+GLUTAMIC ACID
GLUTAMINE
PROLINE+GLUTAMIC ACID
ACETATE
LUECINE
ALANINE
LACTATE
4.4 4.2 4.0 3.8 3.6 3.4 3.2 3.0 2.8 2.6 2.4 2.2 2.0 1.8 1.6 1.4 1.2 1.0 .8
PPM

FIG. 43 (A)-1

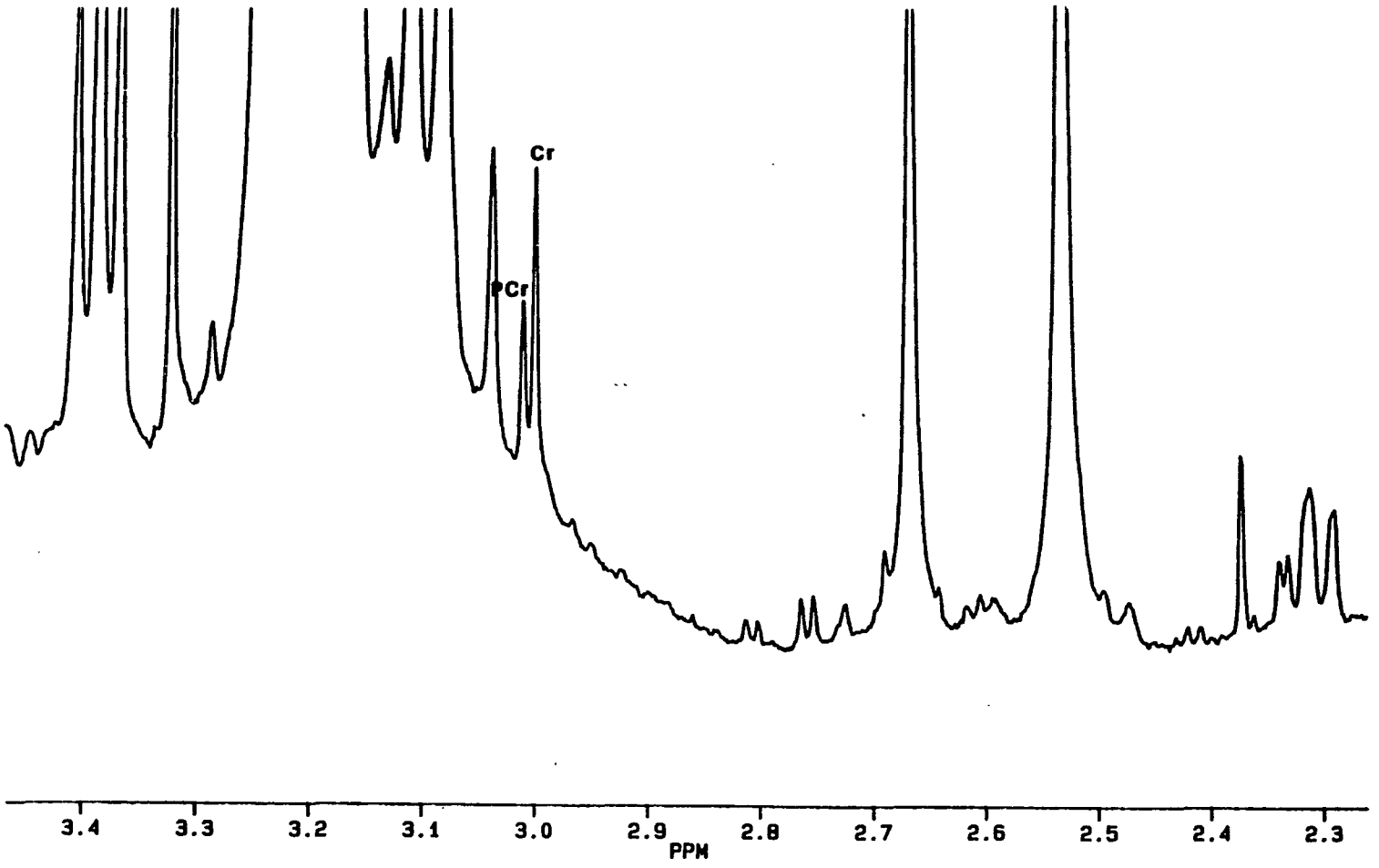

FIG. 43 (A) -2

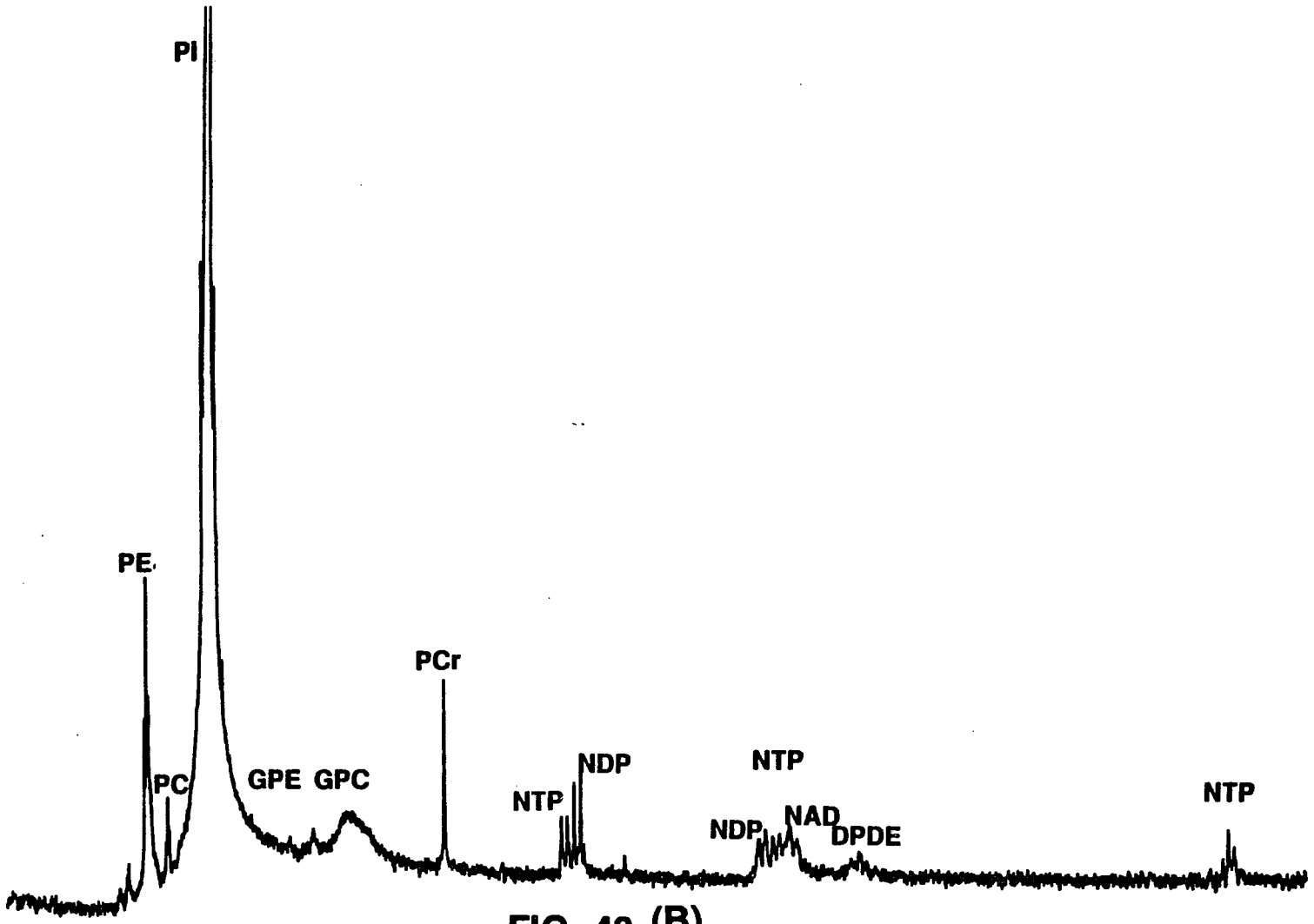

FIG. 43 (B)

An experiment was run at a low pH which allowed for the above calculations to be made. PCr was loaded into the cells by incubating them in a medium with 10 mM of Cr, the cells were washed with a medium with a few tenths of 1 mM of Cr, while the cells were kept well energized. Note that PCr at about 10 mM cellular concentration decreased by only 20% in 22 hrs of washout. This was described (see Figure 48). From this Cr wash-out experiment and also from the Cr uptake experiment shown before, one can see that these cells accumulated a higher concentration of (Cr + PCr) than was present in the medium.

The ratio Cr/PCr, (R), was estimated by comparing ^{31}P NMR spectra of the cells which were washed with Cr free medium as above with the spectra of their acid extracts Fig. 43. The method to estimate the ratio R *in vivo* was previously described (Ogawa, S. et al. 1986). It assumes that the ratios of the pool of (Cr + PCr) to the pool of (ATP + ADP) in intact cells and that in their extracts is the same.

$$[(Cr + PCr)/(ATP + ADP)] = [(Cr + PCr)/ATP + ADP)]$$

$$\text{intact} \qquad\qquad \text{extract}$$

$$= [(PCr)/(ATP + ADP)](1 + R) \qquad (16)$$

The terms PCr/(ATP + ADP) and R in extract measurements can be estimated from ^{31}P NMR and ^{1}H NMR spectra respectively. From ^{31}P NMR spectra of intact cells, the ratio PCr/(ATP + ADP) can be measured, and then R in intact

cells can be estimated from the above assumption. One can modify the assumption by taking into account the contribution of the ADP component, which is measurable in ^{31}P NMR spectra of extracts, but silent in those of intact cells. It could amount to 10% of the ATP. In the experiment the external Cr was washed away to less than 100 μM, the measured parameters for the relationship (16) were 1.0 for R and 3.0 for the ratio of (Cr + PCr)/(ATP + ADP) in the extract and therefore R = Cr/PCr in intact cells was 1.4 under the standard medium condition. It seems strange that the value of R in the extract was smaller than that of the intact cells and in the opposite sense to what one might expect. This might have been due to a change in conditions during the extract making procedures, such as a lower temperature or a shift to a higher intracellular pH due to loss of CO_2. Even so, the ratio of (Cr + PCr)/(ATP + ADP) should have remained the same and equation (16) can still be used.

In the spectra in Fig. 40, the internal Pi resonance was covered by 1 mM of Pi in the medium, but the amount of the internal Pi was substantial. Its peak intensity was estimated by subtracting the external Pi peak intensity from the total Pi resonance intensity. At high pH, the two Pi resonances were fairly well separated. Two spectra at two different pH values are shown in Fig. 41. The peaks of the medium Pi in both cases were at lower field positions than the Pi inside the cells, showing the presence of pH gradients across the cell membrane with a more acidic pH inside. During the periods of constant pH when PCr was being accumulated in the presence of Cr in the medium, the Pi resonances

(inside and outside the cells) stayed constant. Therefore, Pi used for the Cr phosphorylation must have been supplied from the flowing medium. This uptake of Pi should be much faster than that of Cr. Actually the internal Pi was washable with Pi free medium. The level of the internal Pi, as seen in Fig. 41, was not dependent on the presence of Cr or PCr, but rather appeared to depend on pH's (inside and/or outside) and on the external Pi concentrations ($[Pi]_{ex}$). In the experiment shown in Fig. 41, the intracellular Pi concentration ($[Pi]_{in}$) and pH_{in} were 6.5 mM and 7.25 when $[Pi]_{ex}$ and pH_{ex} were 1 mM and 7.50 respectively. When the pH_{ex} was raised to near 9, the pH_{in} became 7.7 and $[Pi]_{in}$ was about 1 mM which was close to $[Pi]_{ex}$.

The creatine kinase reaction is a dead-end reaction, and under the condition of constant PCr, Cr, H and ATP, the reaction would be near equilibrium. In that case

$$Cr/PCr = (H^+ /K)(ADP/ATP) \qquad (17)$$

where K is the equilibrium constant. From this assumption of near equilibrium and also from the knowledge of the ratio $[Cr/PCr]_{in}$, one can estimate the ATP/ADP ratio in the cytosol where the kinase activity is present. The Cr/PCr ratio inside the cells was determined in an experiment where the external Cr was washed away to less than 100 μM. The measurement in the cells was 1.3 for the PCr/(ATP + ADP) ratio. In the extract, the measurements were 1.0 for the Cr/PCr ratio and 1.5 for the PCr/(ATP + ADP) ratio. The *in vivo* ratio R = Cr/PCr at pH_{ex} 7.4 was calculated from the above to be 1.31 under

standard conditions, and the ATP/ADP ratio was estimated to be 63 with pH_{in} at 7.3. When pH_{ex} was raised to near 9 with a concomitant increase of the pH_{in} to 7.7 as in Fig. 42 one would expect the values of the Cr/PCr and ATP/ADP ratios to vary. With this pH change, the Cr/PCr ratio immediately after the transient period could be shown to have changed from 1.4 to 0.3 and the estimated change in the ATP/ADP ratio was a 30% increase.

The cellular concentration of Pi under the standard medium condition was calculated to be 6.5 mM, assuming 4 mM as the ATP concentration. This value of 6.5 mM was consistent with the estimate based upon the peak intensity ratio of the Pi resonances and the volume ratio of the cells to the medium in the sample that was between 1/10 and 1/15. Using this value of the cellular Pi concentration, the phosphate potential in the cytosol was calculated. The value of $\frac{ATP}{ADP}\ \frac{1}{Pi}$ is $2 \times 10^4\ M^{-1}$. These values of ATP/ADP and ([ATP]/[ADP])/[Pi] are lower than those reported for young adult and neonate rat brains. (Ogawa, et al., 1986) and larger than those reported in adult rat brain (Veech, et al., 1979).

The effect of changing the ADP concentration on metabolism is profound (Guroff, 1980; Siesjo, 1978). The fact that the ADP ratio changes in this way gives us insight into respiratory control. What is happening is that an increase in the pH eventually shifts the ADP to a higher level which exerts itself on the respiratory control system, stimulating respiration and a concomitant ATP production. In subsequent experiments it will be interesting to monitor oxygen

uptake while running the experiment in an attempt to get quantitative collaboration.

4.3.4.2 Differentiated N1E-115

The next logical step was to look at differentiated cells.

N1E-115 cells were grown for three passages on DMEM supplemented with 10% FBS, 1% PS and 0.2 mM creatine, then 2% DMSO was added (see section 4.2.1). Within three days, these cells stopped dividing and differentiated morphologically to form neuron-like cells. In the following five days these cells had lifted off the tissue culture dishes and formed clusters or clumps. The clumps were roughly spherical, but were irregular, and for the most part not attached to the substrate. The cells were grown for an additional 13 days with DMSO, and then seeded on Cytodex III microcarriers, allowed to sit in the incubator for one hour or less, and transferred to the sample holder.

The PCr peak was observed to be very large, with areas of 2.49 compared to that of the ATP areas, 1.56, and the total Pi area of 3.9. (see Fig. 44).

The rate of appearance of PCr was measured at two different extracellular concentrations of creatine and the rate of disappearance of PCr charged cells was measured in medium containing no creatine. Fig. 44 shows the spectra of the cells as they appeared when first placed in the magnet. The creatine supplement was changed from 0.2 mM to 10 mM after the temperature and extracellular pH had equilibrated to 37 °C and 7.38, respectively. After the

Figure 44

These spectra are from cells that have been induced to differentiate with medium supplemented with 2% DMSO and maintained on tissue culture plates for an additional 13 days in medium supplemented with Cr, then transferred to Cytodex III microcarriers and put in the NMR magnet. The spectra are obtained from 1200 FID with a repetition time of 3 sec, and an R.F. pulse width of 27.0 μsec. (A) FFT using 2.5 HZ line broadening. (B) the same as (A) but using convolution difference of 25 Hz and line broadening of 2.5 HZ. (C) an expanded portion of (B) shown the enhancement in separation in the PME region and Pi region. This split in Pi corresponds to a pH difference of 0.13 pH units.

PME	*Chemical Shift PPM*	
A Unknown	+4.693	
PCh	+4.3298	
PEt	+3.825	
Pi external (Pie)	2.7357	(ph = 7.40)
Pi internal (Pii)	2.6146	(ph = 7.27
PCr		−2.49 assigned

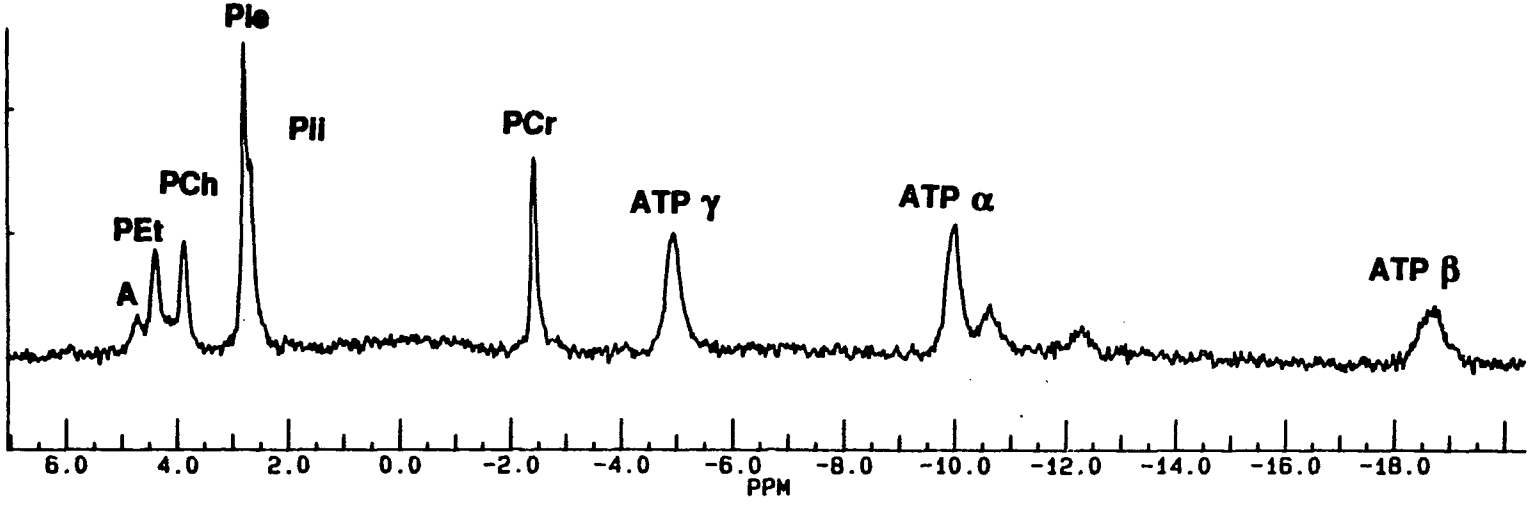
Pie
PII
PCr
PCh
PEt
A
ATP γ
ATP α
ATP β
6.0
4.0
2.0
0.0
-2.0
-4.0
-6.0
-8.0
-10.0
-12.0
-14.0
-16.0
-18.0
PPM

FIG. 44 (A)

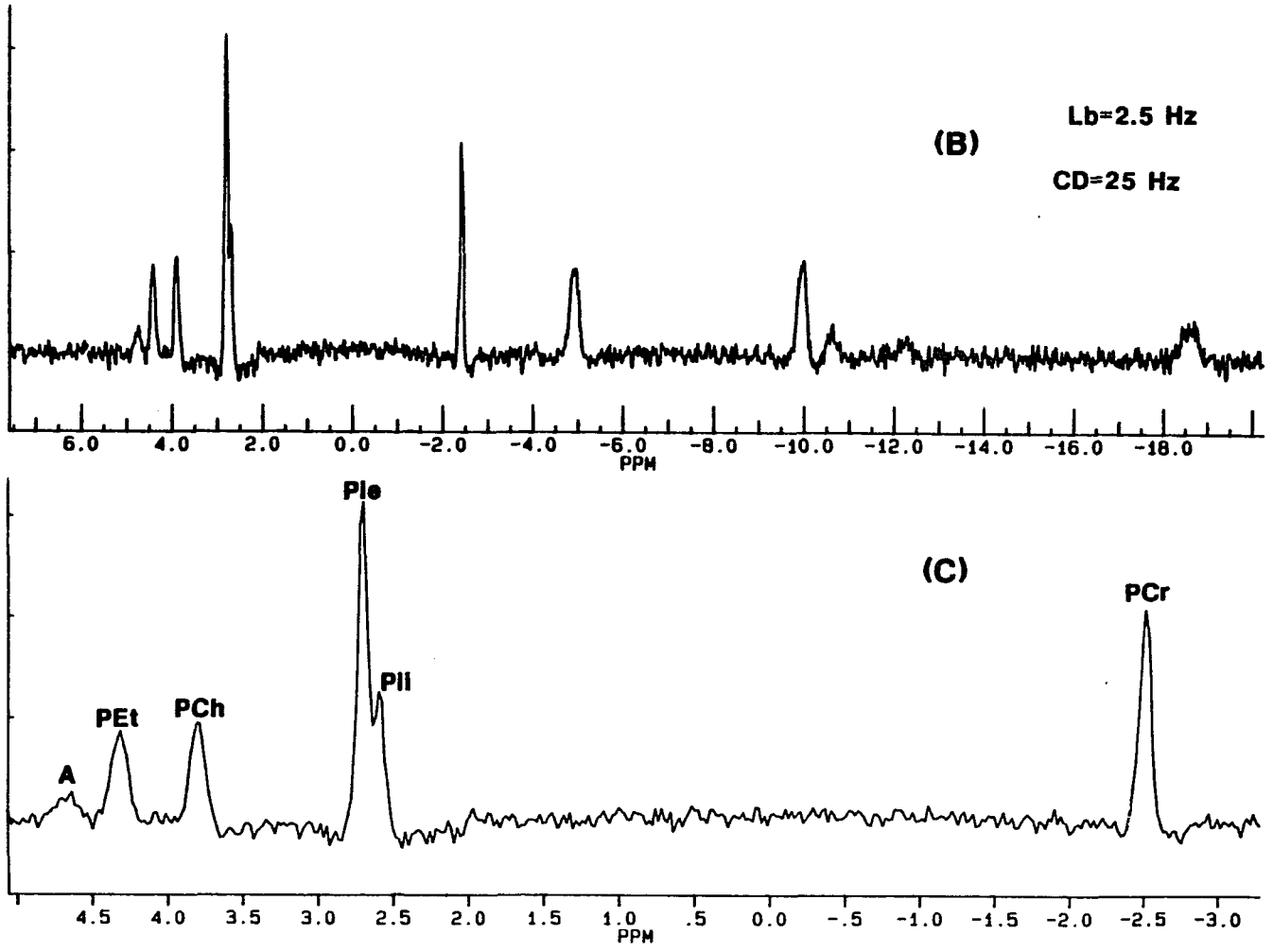
(B)
Lb=2.5 Hz
CD=25 Hz
6.0 4.0 2.0 0.0 -2.0 -4.0 -6.0 -8.0 -10.0 -12.0 -14.0 -16.0 -18.0
PPM
(C)
PIe
PII
PCr
PEt
PCh
A
4.5 4.0 3.5 3.0 2.5 2.0 1.5 1.0 .5 0.0 -.5 -1.0 -1.5 -2.0 -2.5 -3.0
PPM

FIG. 44 (B) (C)

extracellular creatine concentration in the cell sample holder was changed, the creatine phosphate concentration in the cells was monitored in time by observing the changes in its peak over a four-hour period, during which time the internal pH was 7.28_6, and the external pH was $7.39_5 \pm .018$. (n = 4).

Figure 45a shows a plot of the ratio of the peak heights of $\frac{PCr}{ATP}$ plotted against time when the outside Cr concentration was 10 mM and the extracellular pH was 7.38, intracellular pH was 7.28. The slope was 0.063. Compare this to the rate in undifferentiated cells in the previous section at pH 7.29, where the rate was 0.080. Thus, within experimental error, these can be considered equal. The slope is plotted in Fig. 46 for an experiment, using 10 mM Cr at pHi = 7.38 and in Fig. 47 for one using 18 mM Cr at pH 7.59 $\pm$.01 external pH. The results of this experiment suggest that the rate of appearance of PCr in these cells saturated at a lower value of extracellular Cr than that of the undifferentiated cells.

4.3.4.3 Creatine washout experiments on undifferentiated cells

The question naturally arises as to what happened to the high PCr concentrations, which had been induced in the cells by the addition of high concentrations of extracellular Cr. To answer this question the following experiment was done on undifferentiated cells.

The cells, which had been superfused with a 10 mM creatine medium for 25 hours, were switched to a 0.2 mM creatine medium, and the PCr peak was monitored for 20 hours. After an initial sharp decrease in the first five hours,

Figure 45

Plot of the PCr/ATP peak height ratio during the 4-hour period after the superfusate was changed from one containing 0.2 mM Cr to one containing 10 mM Cr. The extracellular pH was 7.38, intracellular 7.28 and the temperature was 37° C. The slope in 0.063 hours^{-1}.

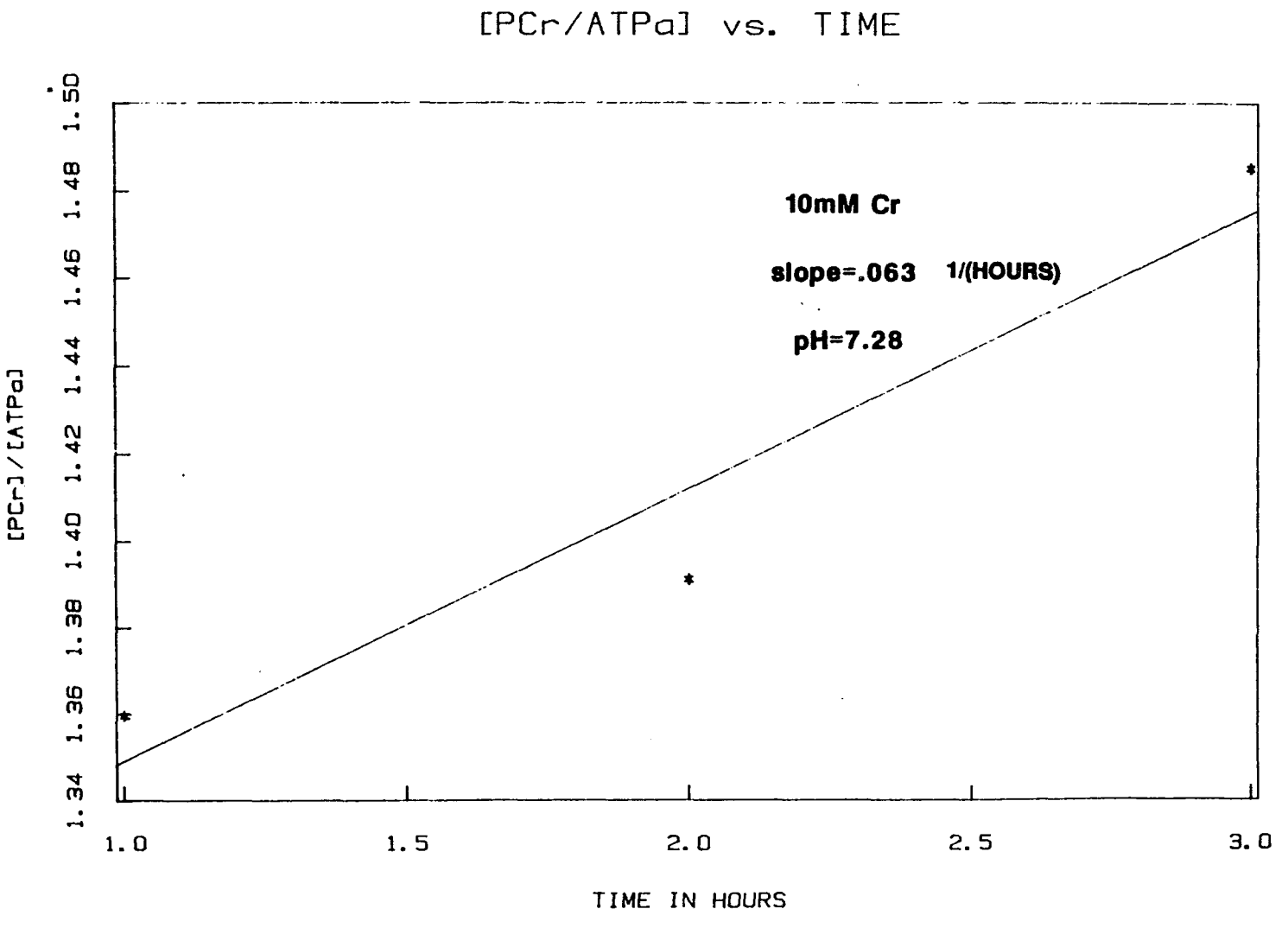
[PCr/ATPa] vs. TIME
10mM Cr
slope=.063 1/(HOURS)
pH=7.28
[PCr]/[ATPa]
1.34
1.36
1.38
1.40
1.42
1.44
1.46
1.48
1.50
1.0
1.5
2.0
2.5
3.0
TIME IN HOURS

FIG. 45

Figure 46

This is a plot of the appearance of PCr in differentiated cells when the extracellular Cr concentration is 10 mM and the pH inside the cells is 7.38. The slope here is 0.067, hours^{-1}.

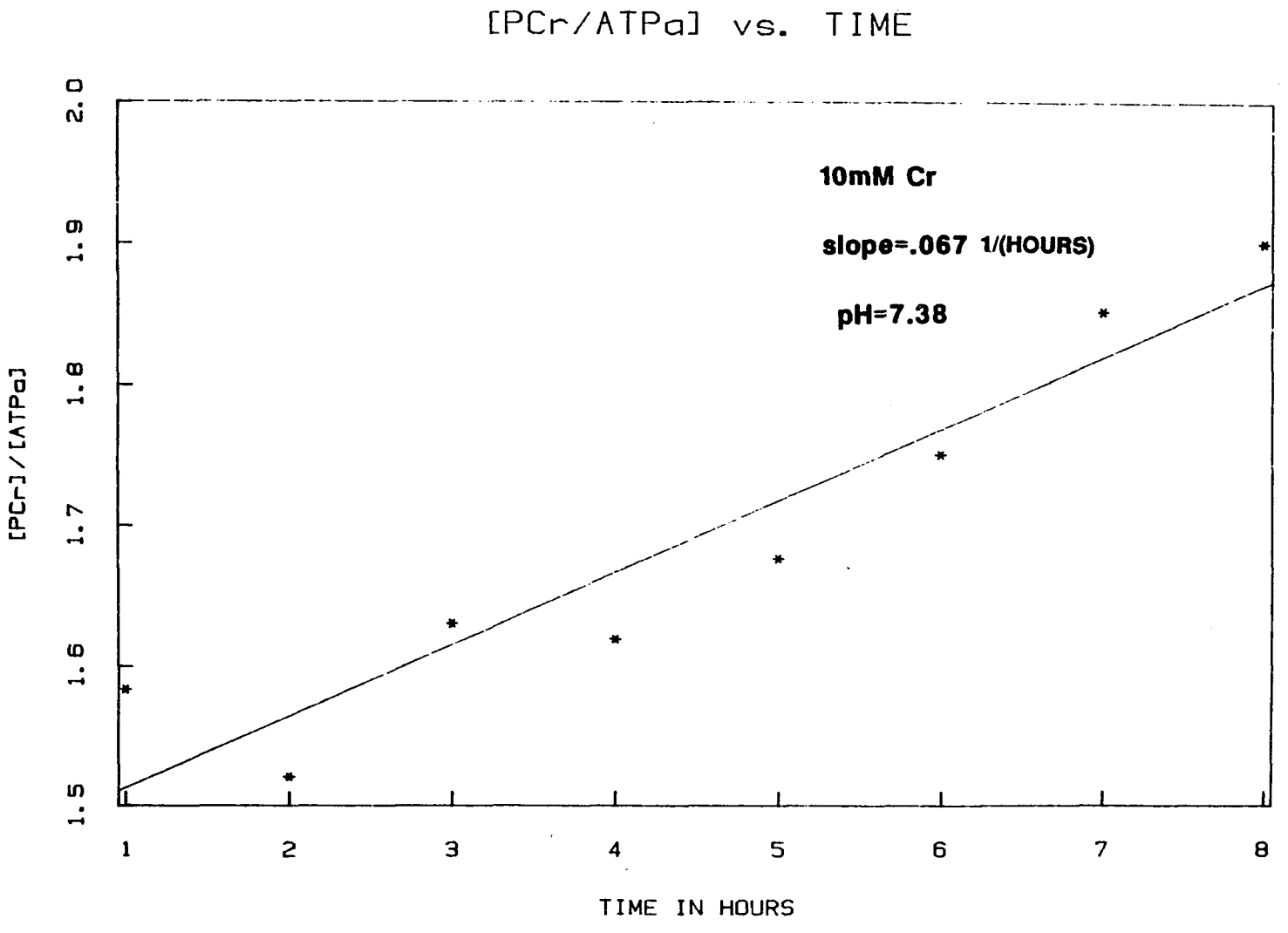
[PCr/ATPa] vs. TIME
10mM Cr
slope=.067 1/(HOURS)
pH=7.38
[PCr]/[ATPa]
2.0
1.9
1.8
1.7
1.6
1.5
1
2
3
4
5
6
7
8
TIME IN HOURS

FIG. 46

Figure 47

This is a plot of the appearance of PCr vs. time in differentiated cells when the outside creatine concentration is 18 mM and the extracellular pH is 7.56. The slope is 0.053 $hours^{-1}$.

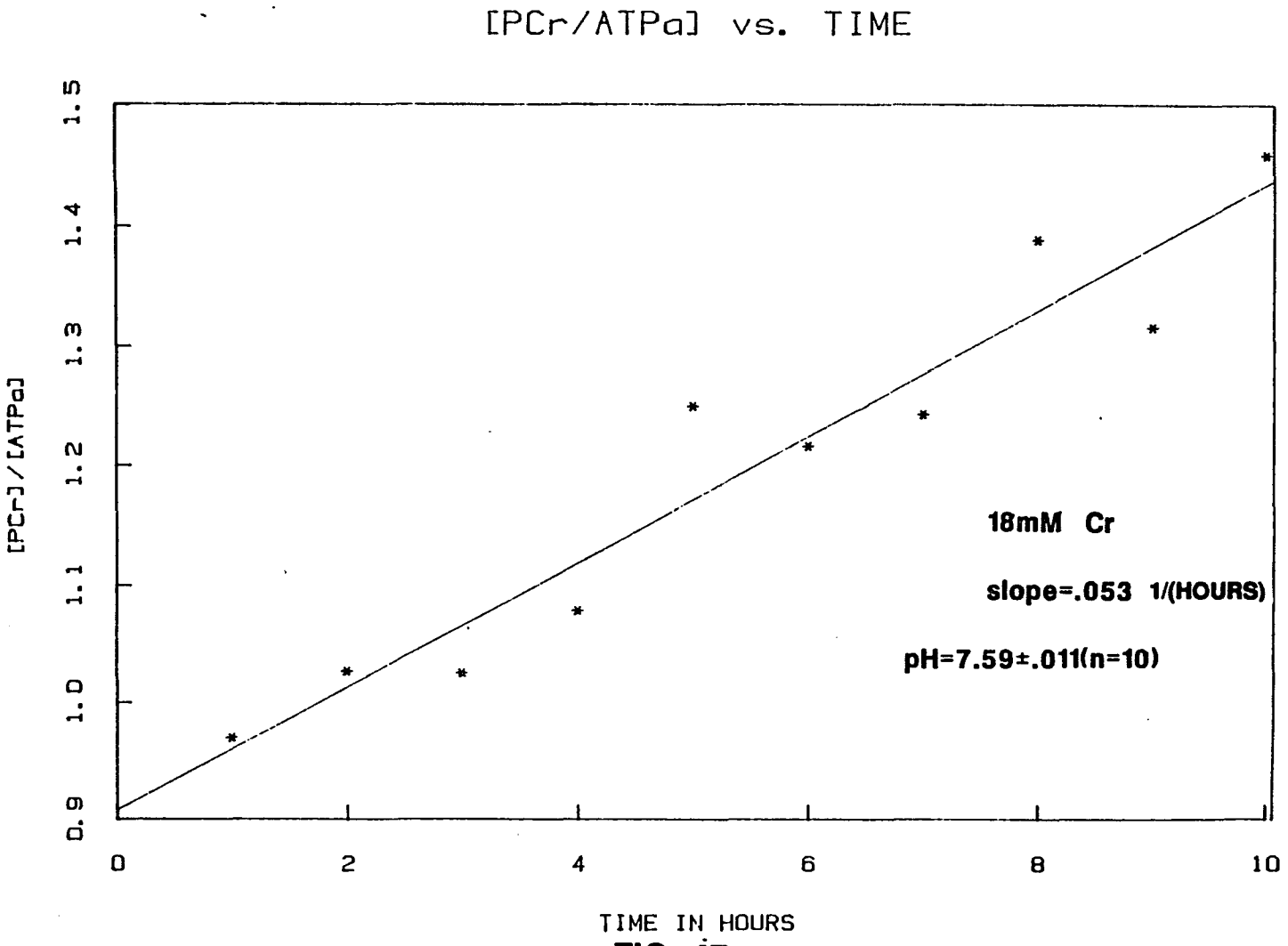
[PCr/ATPa] vs. TIME
[PCr] / [ATPa]
0.9
1.0
1.1
1.2
1.3
1.4
1.5
0
2
4
6
8
10
TIME IN HOURS
18mM Cr
slope=.053 1/(HOURS)
pH=7.59±.011(n=10)

FIG. 47

Figure 48

Undifferentiated cells superfused for 25 hours with medium containing 10 mM Cr were switched to medium containing 0.2 mM Cr at time zero, and the rate of disappearance of the PCr was monitored for 25 hours. Variations in extracellular pH account for some of the irregularities of the curve (see text).

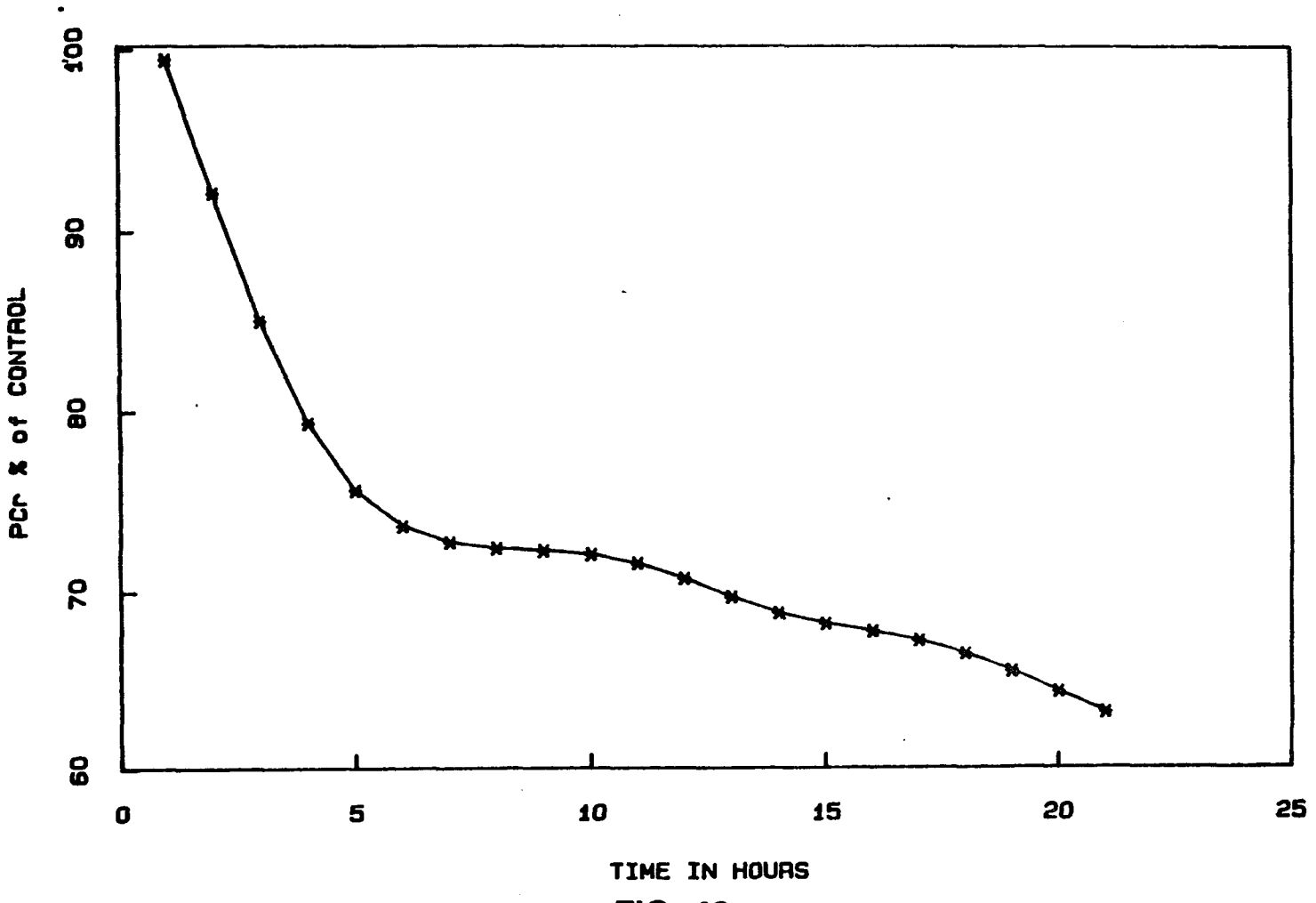
[PCr] vs. TIME
PCr % of CONTROL
100
90
80
70
60
0
5
10
15
20
25
TIME IN HOURS

FIG. 48

Figure 49

Plot of the ATPα peak during the same 25 hour period the undifferentiated N1E-115 cells were in the 0.2 mM superfusate medium depicted in Fig. 48

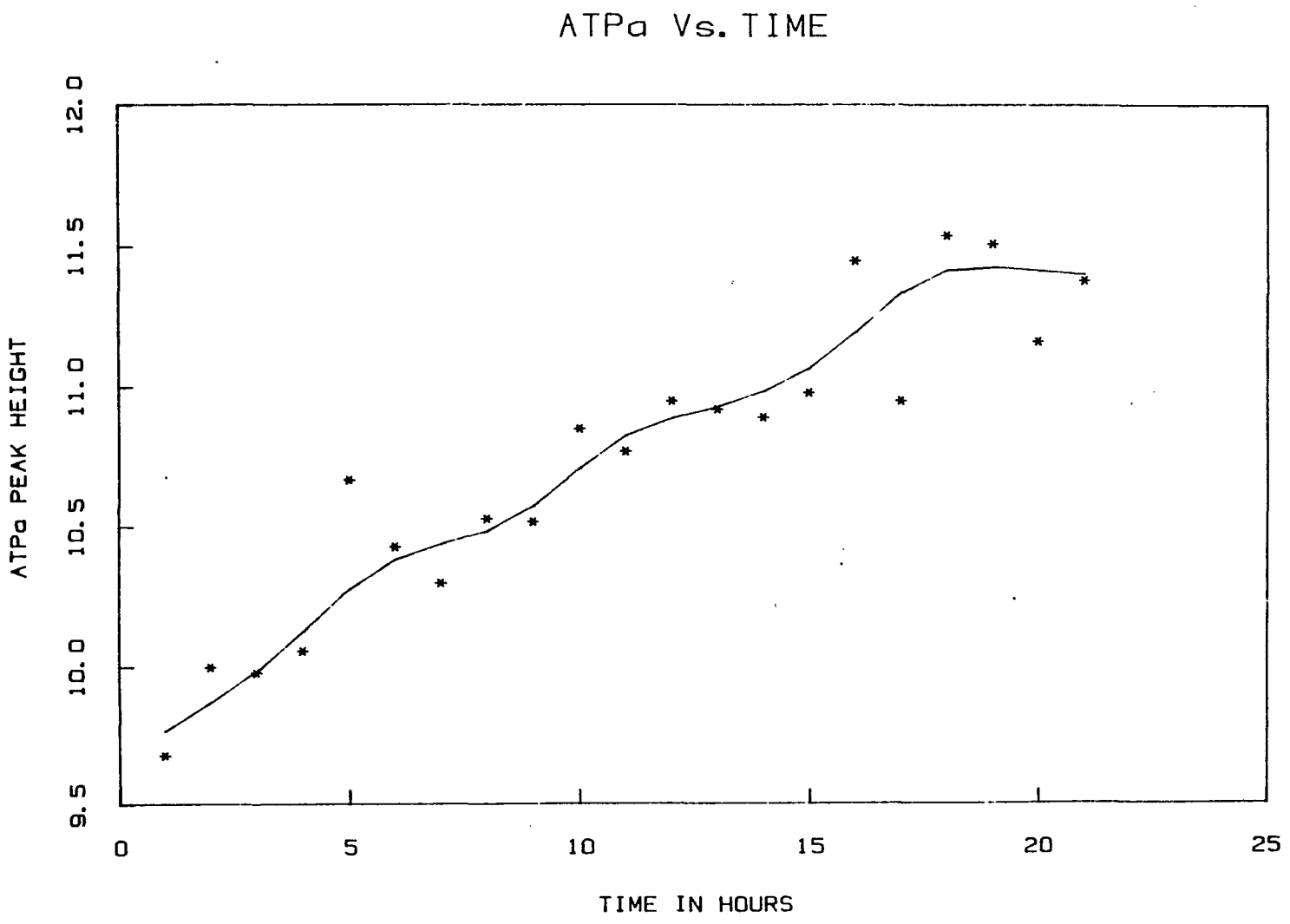
ATPa Vs. TIME
ATPa PEAK HEIGHT
12.0
11.5
11.0
10.5
10.0
9.5
0
5
10
15
20
25
TIME IN HOURS

FIG. 49

the peak declined at a rate of 1.7%/hour. The results are plotted in Fig. 48. The result was complicated to some extent by the fact that the ATPα peak increased (see Fig. 49) and the pH decreased 0.04 pH units from 7.55 at the beginning, to 7.51 at the end, with a short period of stabilization between 7 and 10 hours (see Fig. 50). In this case it was a poor choice to choose the PCr/ATPα ratio (Fig. 51) because of the changing ATPα. This curve gives the impression that there were two slopes which describe this event. In reality, by looking at the PCr peak vs. time, we can say that for a period up to four hours, the PCr and most likely the Cr in the cells remained constant as long as the pH was maintained at a constant value, and when the pH is lowered, the amount of PCr in the cells was also lowered. This is all consistent with what was found for the undifferentiated cells in the previous section. Again we see here that small changes, as little as .005 pH units, had a substantial effect on the PCr concentration, and that when the system was not in equilibrium, it became difficult to interplate.

4.3.4.4 DRBC

With a reasonably good idea of how differentiated and undifferentiated neuroblastoma cells behave with high concentrations of extracellular creatine, experiments were run to examine the behavior of dissociated rat brain cells at two extracellular creatine concentrations, namely 10 and 30 mM. The cells were obtained and put on Biosylon microcarriers as previously described, section 4.2. Figure 52 shows the control. Rate data from different sets of cells were plotted in at extracellular pH values of 7.7 and 7.53 respectively. The slope of 0.06 for

Figure 50

This is a plot of pHex vs. time for the experiment depicted in Fig. 48 Note that there are two four-hour periods starting at 7 hours and at 12 hours which are at constant pH.

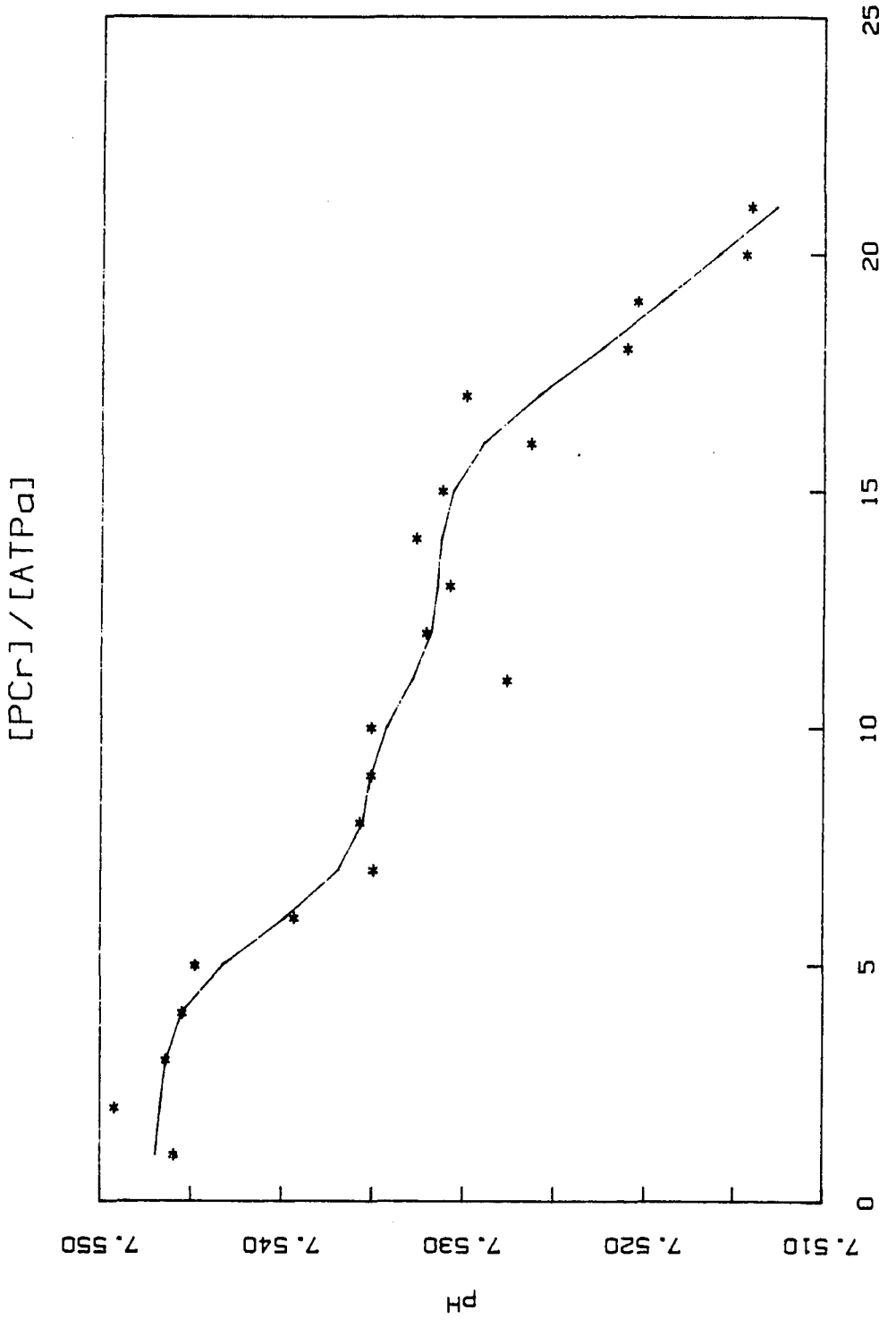
[PCr] / [ATPa]
pH
7.510
7.520
7.530
7.540
7.550
0
5
10
15
20
25
TIME IN HOURS

FIG. 50

Figure 51

This is a plot of the PCr/ATPα peak heights during the 25 hours of the experiment depicted in Fig. 48.

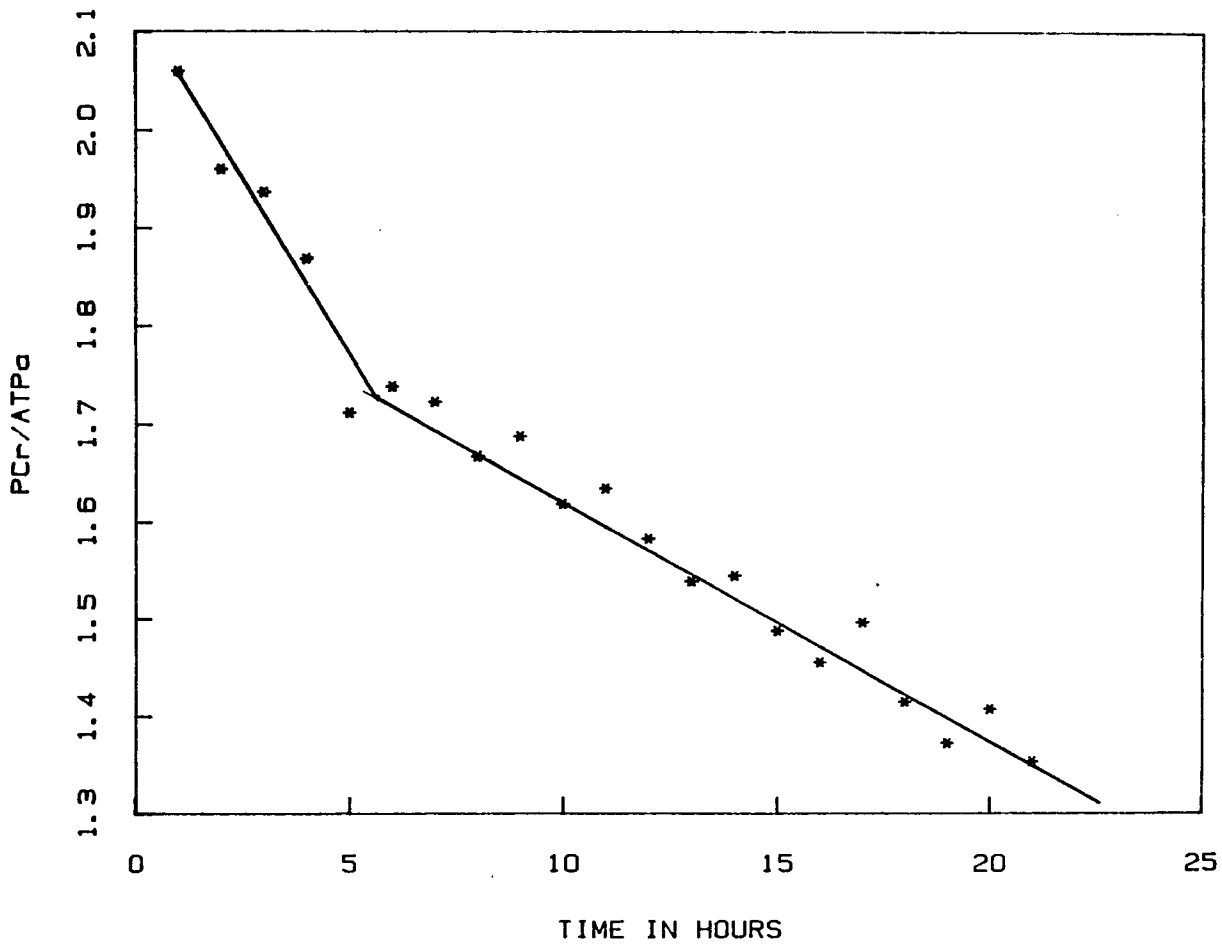

FIG. 51

Figure 52

This is a spectrum from dissociated rat brain cells. This spectrum was obtained from 1000 FID with a repetition time of one second. The spectrum has been processed with a line broadening of 25 HZ. The spectrum represents a control to which no Cr has been added. The small peak at −2.748 is most likely noise and not PCr which would be at −2.49 relative to ATP at −10.00 ppm.

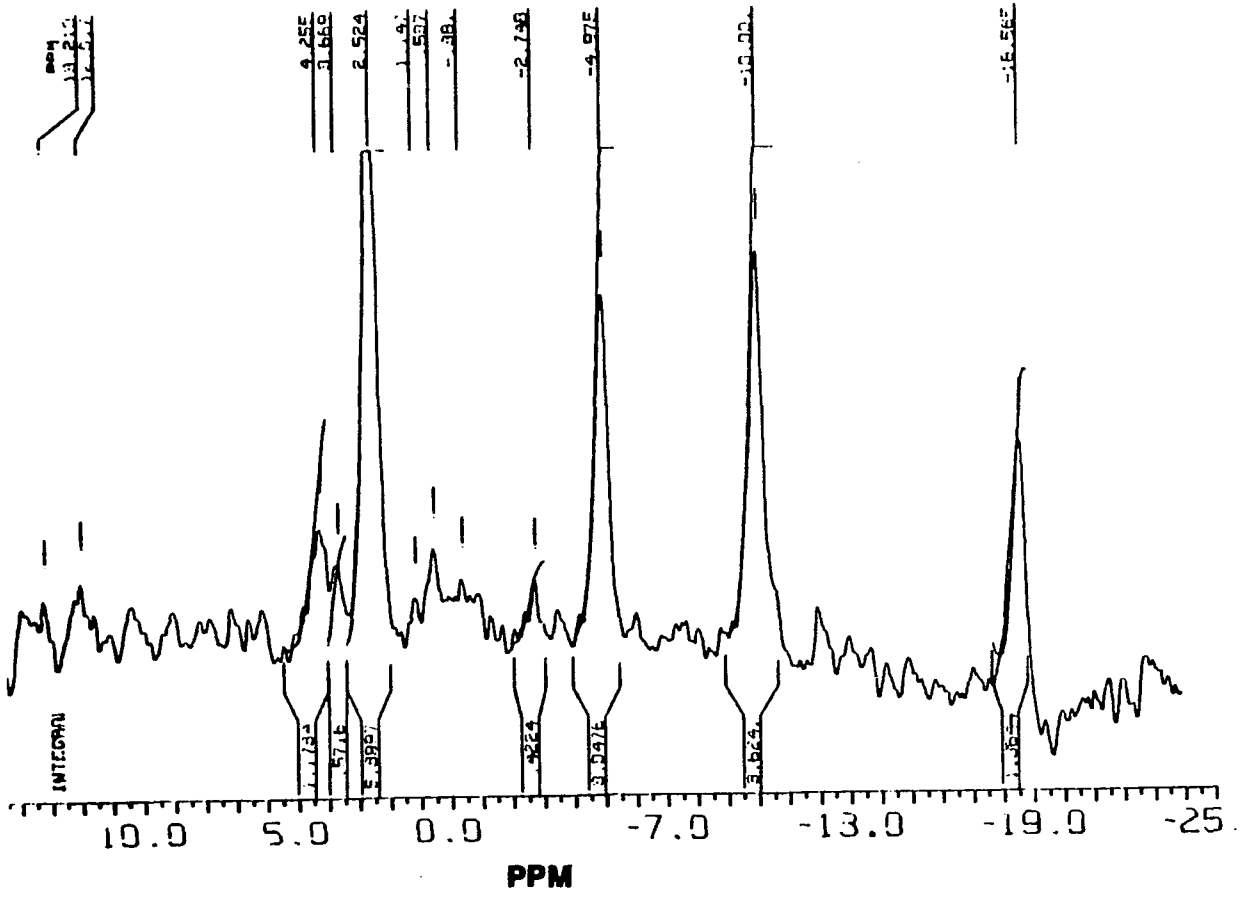

FIG. 52

Figure 53

The ratio of the PCr/ATPα peak heights in DRBC vs time in hours for cells superfused with medium containing 10 mM Cr is plotted. The extracellular pH is 7.71 $\pm$.01 and the slope is 0.06. The repetition time is 3 seconds.

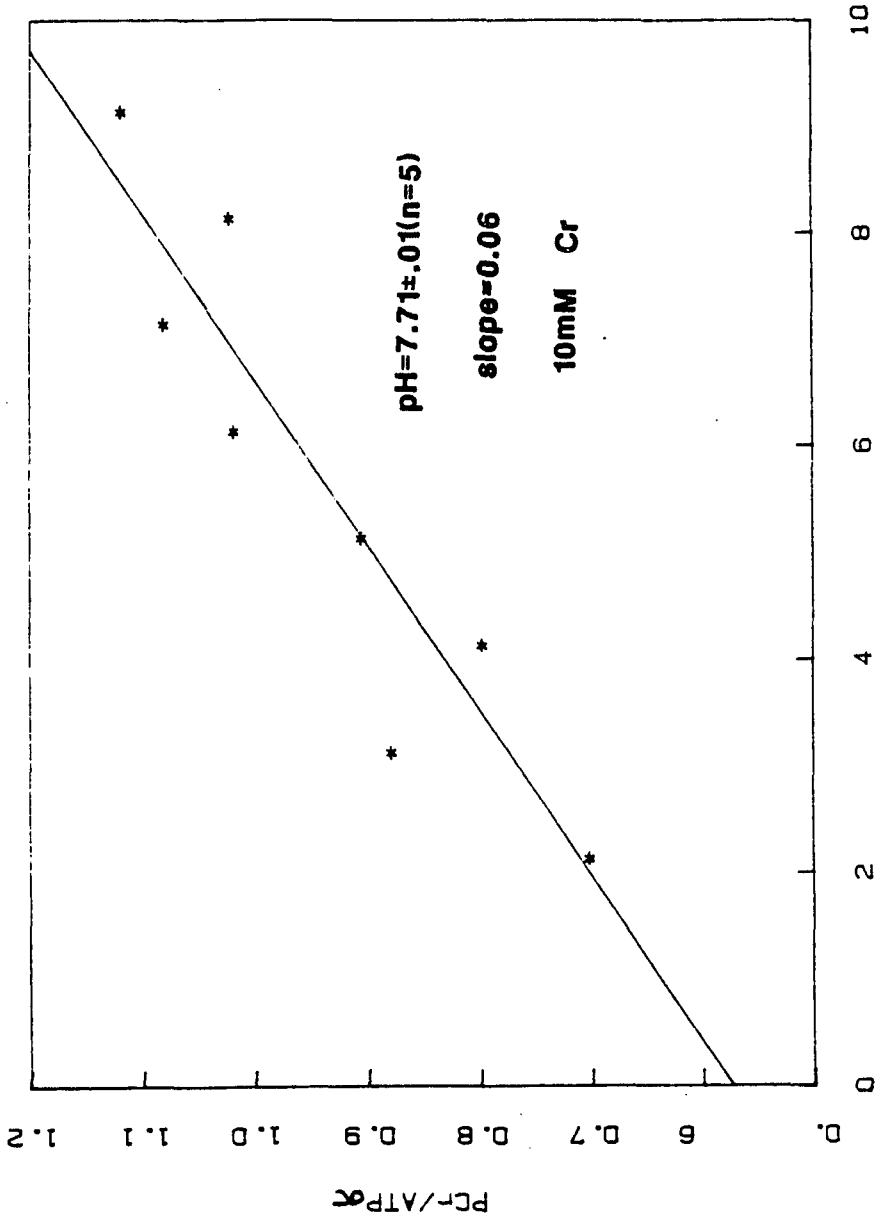
pH=7.71±.01(n=5)
slope=0.06
10mM Cr
PCr/ATPα
TIME I HOURS
0.
.6
0.7
0.8
0.9
1.0
1.1
1.2
0
2
4
6
8
10

FIG. 53

Figure 54

The ratio of the PCr/ATPα peak heights in DRBC vs. time in hours for cells superfused with medium containing 30 mM Cr is plotted. The extracellular pH is 7.53 $\pm$0.084 (n=5).

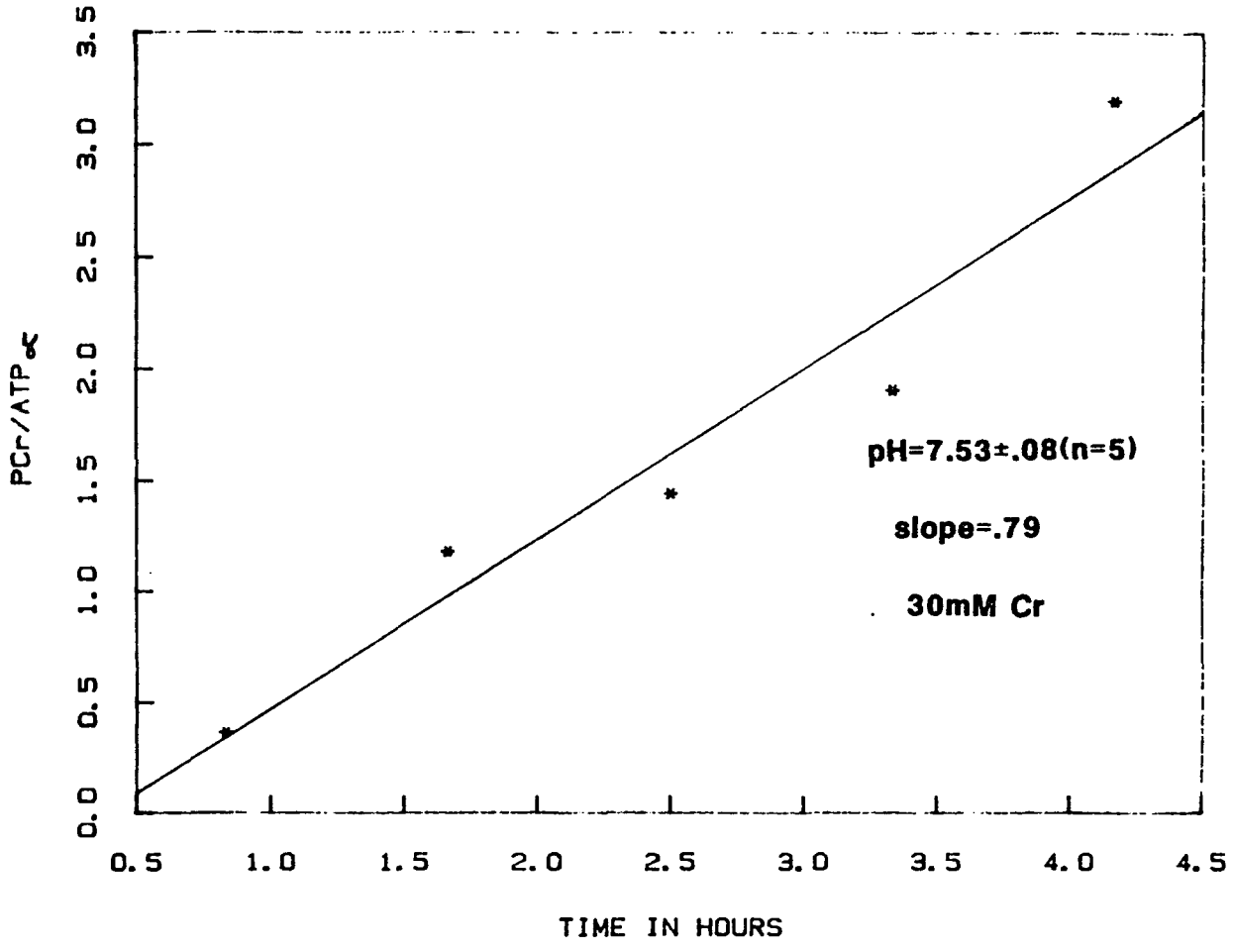
PCr/ATP∝
0.0
0.5
1.0
1.5
2.0
2.5
3.0
3.5
0.5
1.0
1.5
2.0
2.5
3.0
3.5
4.0
4.5
TIME IN HOURS
pH=7.53±.08(n=5)
slope=.79
30mM Cr

FIG. 54

10 mM extracellular Cr is comparable to the slope of differentiated neuroblastoma cells, 0.08, C6 cells undifferentiated 0.07 (see next section), but not to undifferentiated neuroblastoma cells, which is 0.14, almost twice the value of the others. No further experiments were done at various pH's to establish the trends of the slope of PCr appearance at these abnormally high extracellular concentrations of Cr and various pH values in DRBC. With these results one can only stipulate what the values of transport of Cr are at these two diverse pH concentration conditions.

4.3.4.5 Undifferentiated Glioma C6 cells

C6 cells were tested to see if they had any creatine kinase activity. The cells were grown as in 4.2. above, seeded onto Cytodox III and immediately put into the magnet. The results shown in Fig. 55 and Fig. 56 show that they did have activity, and that the rate of appearance of PCr in cells in medium at pH 8 was 0.023. The data are scattered and basically one can only say with certainty that the cells took up Cr and phosphorylated it. This result suggests that further study of C6 cells induced to differentiate into astrocytes could give interesting results, which could be compared to similar experiments on astrocytes from primary cultures.

4.3.5 Kinetic studies

It has been suggested that the flux rate or the true flux in one direction (see section 2.2.4) through creatine kinase changes with development, with the flux being smaller in fetuses and increasing with age. (Ogawa, et al. 1986.) By using

C6 Glioma Cells

Figure 55

(A) This spectrum is the sum of 13,000 scans made with a repetition time of 1 second. It was taken over a 3.6 hour period with a 90 degree pulse. The pH of the medium was 6.96 and the ratio of the PCr to ATPβ peak is 0.39, a value corrected for T1 relaxation so as to be comparable with a 3-second repetition time. This is a control reference.

(B) This stack plot of seven files was made after the medium was supplemented with 5 mM Cr and 1 mM PPA. Each file consists of 1500 FID's with a 3-second repetition time. During this 9 hour period the PCr to ATP peak ratio went from 0.39 to 1.1, an increase of almost three fold. The spectra, although somewhat noisy, clearly demonstrate the uptake and phosphorylation of PCr. pH of the medium was $7.27 \pm .026$.

(C) This is a plot of the peak heights of PCr over ATPβ. The slope is a result of a regression analysis. The slope is 0.023 at this external pH of 7.26.

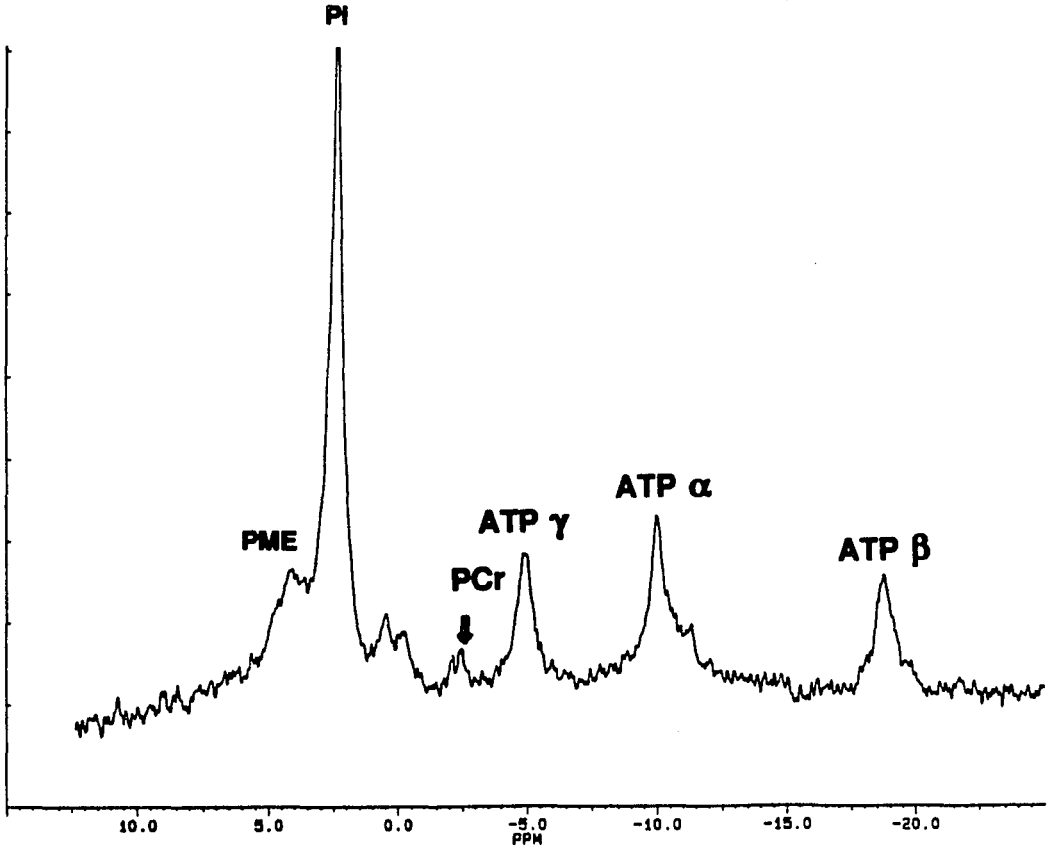

FIG. 55 (A)

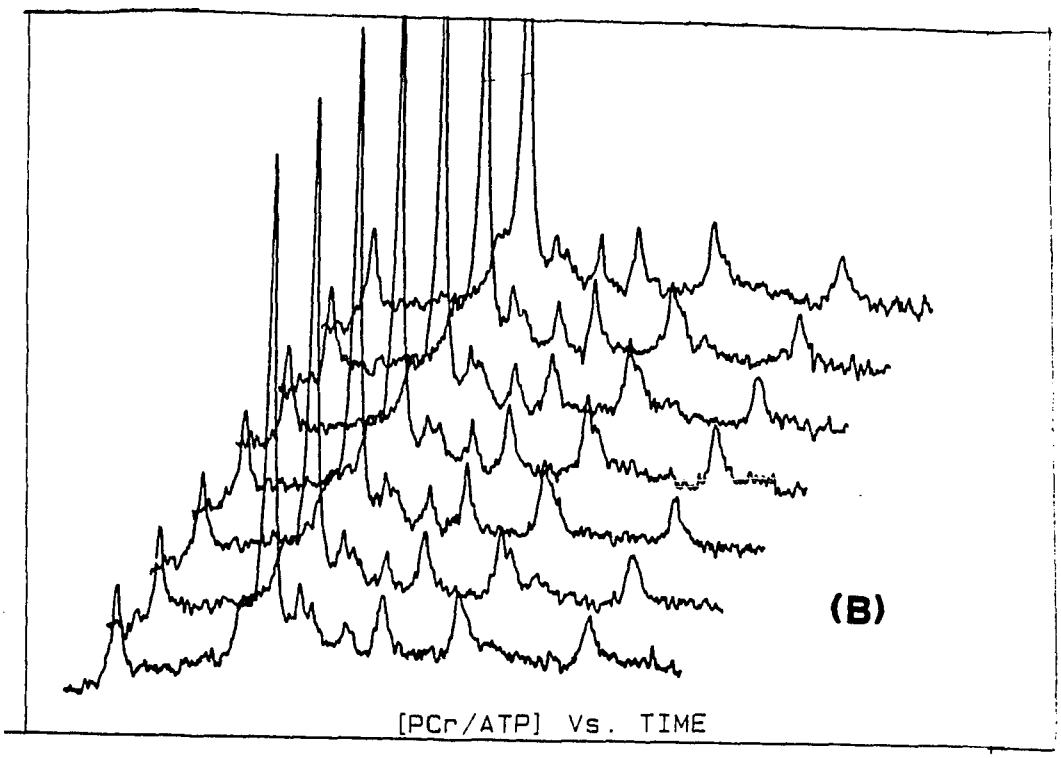
(B)
[PCr/ATP] Vs. TIME

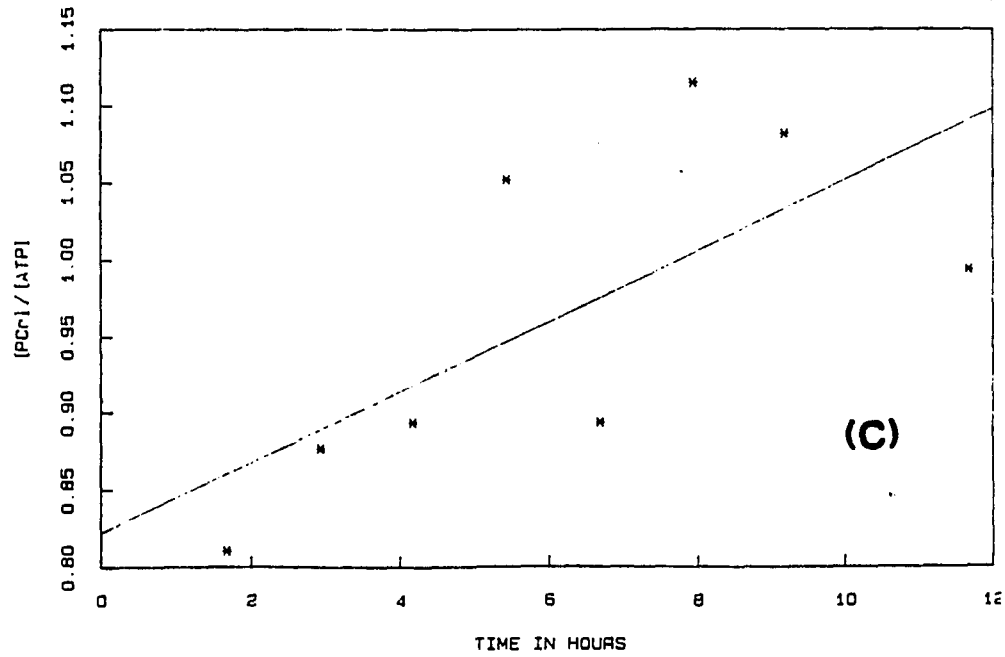
[PCr]/[ATP]
0.80
0.85
0.90
0.95
1.00
1.05
1.10
1.15
0
2
4
6
8
10
12
TIME IN HOURS
(C)

FIG. 55 (B) (C)

C6 Glioma Cells

Figure 56

After the experiment at pH 7.27 shown in the previous figure, the cells in the same medium were switched to a basic pH condition 8.8 and again the PCr/ATP ratio was followed. A) shows the sum of all the files in the series or the average of the 10-hour period. B) shows the stack plot at the times indicated. Each file is the sum of 3000, 3 second FID. C) shows a plot of the peak height ratios together with linear least-squares fit to the data the slope of which is 0.073.

The purpose of the experiment represented in figure 4.3-32 and this one was to demonstrate that there was creatine kinase activity in C6 glioma cells and that in the presence of 5 mM external creatine was transported into the cells and phosphorylated. The fact that the slopes were the same for both pH conditions may be fortuitous and should be taken as such.

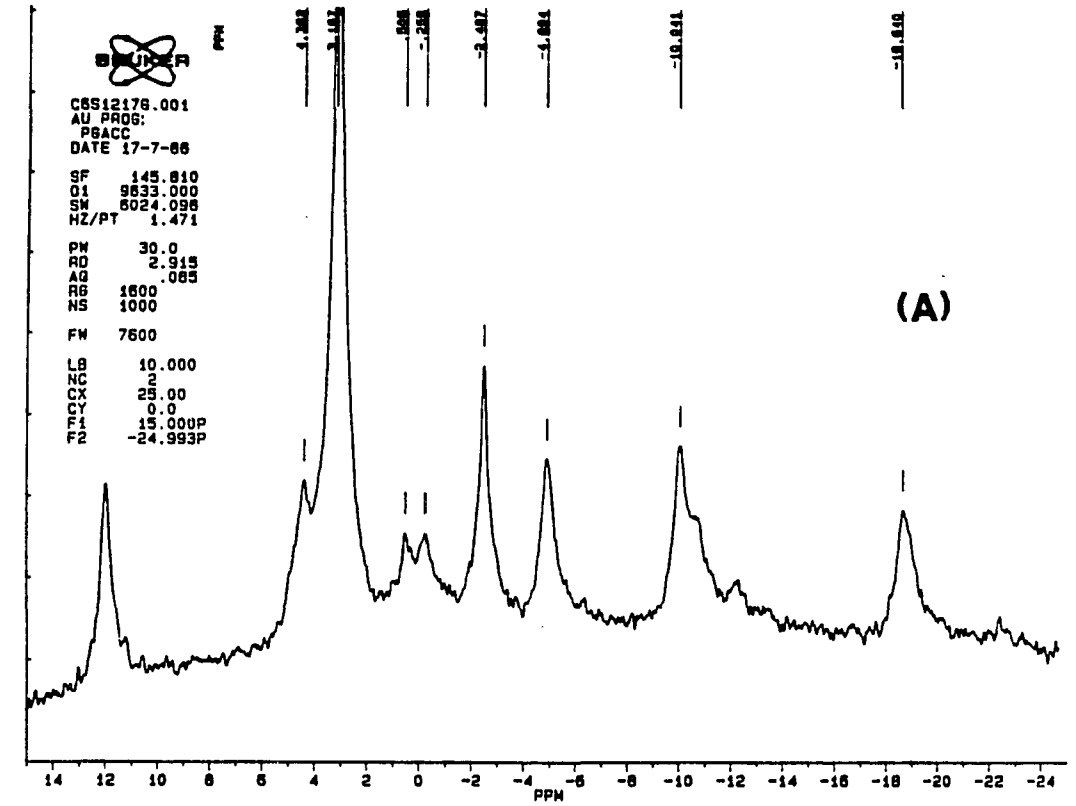
C6S12176.001
AU PROG:
PSACC
DATE 17-7-86
SF 145.810
O1 9633.000
SW 6024.096
HZ/PT 1.471
PW 30.0
RD 2.915
AQ .085
RG 1600
NS 1000
FW 7600
LB 10.000
NC 2
CX 25.00
CY 0.0
F1 15.000P
F2 -24.993P
(A)
PPM

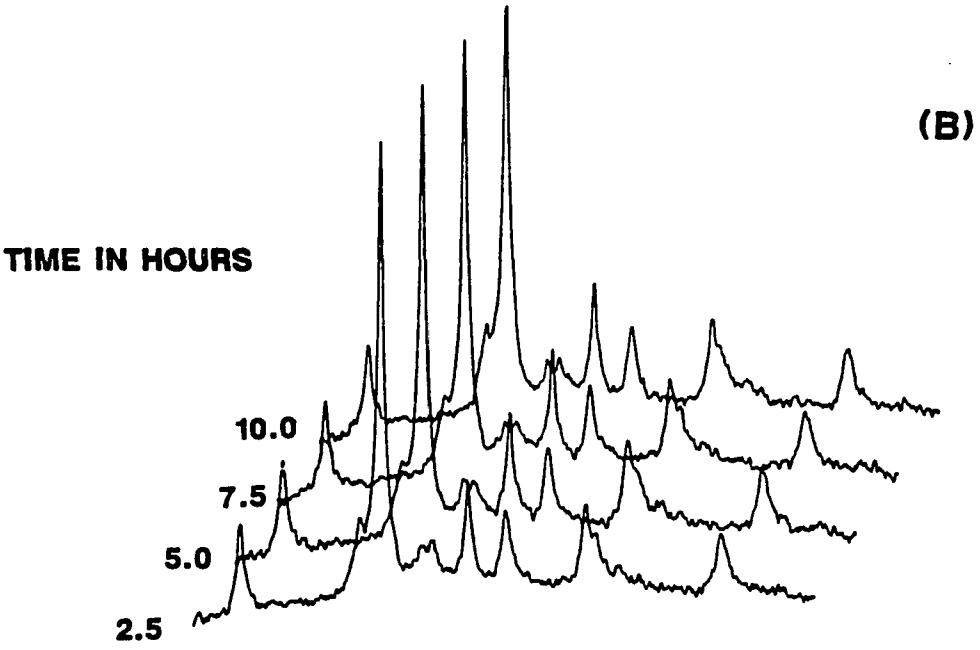
(B)
TIME IN HOURS
10.0
7.5
5.0
2.5

FIG. 56 (A) (B)

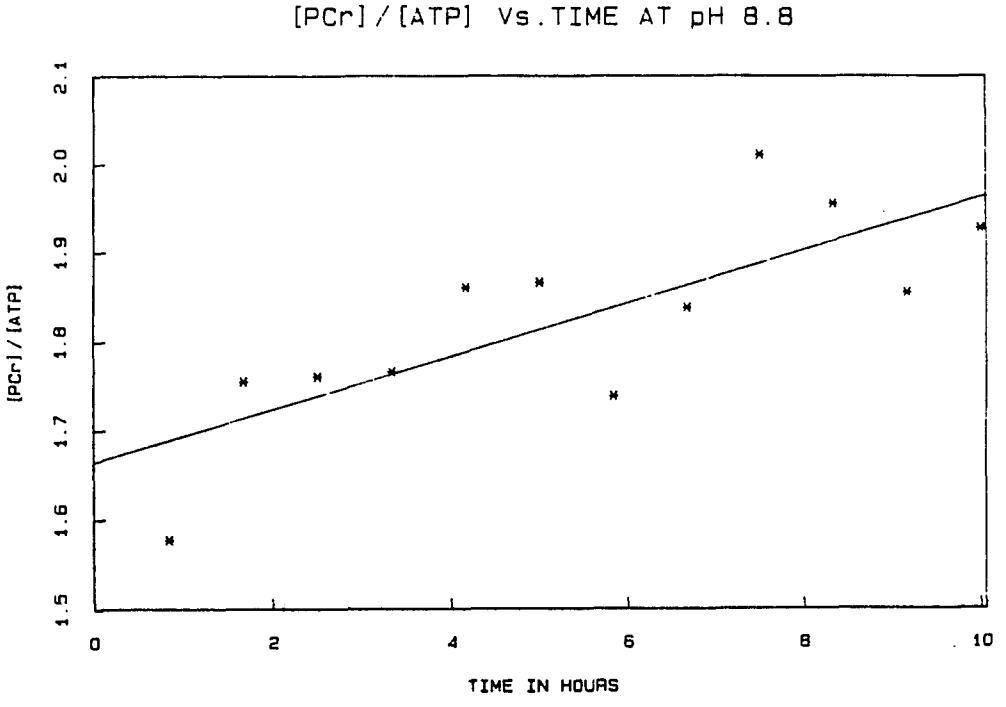
[PCr] / [ATP] Vs. TIME AT pH 8.8
[PCr] / [ATP]
1.5
1.6
1.7
1.8
1.9
2.0
2.1
0
2
4
6
8
10
TIME IN HOURS

(C)

FIG. 56 (C)

saturation transfer techniques the unidirectional flux from ATP to PCr has been measured for rat E. Coli (Brown et al., 1978) brain (Shoubridge, et al., 1982) heart (Brown, et al., 1978) and frog leg muscle, (Matthews, et al., 1982) and been expressed in moles per kg. tissue weight per second. This measurement reflects the combined measure of the efficiency of the enzyme and the copy number. It is possible to separate the two factors by extracting the enzyme and making a quantitative statement about the number of mg. of enzyme protein per kg. of tissue (effectively copy number), a substantial task. Here data are presented for the total flux.

4.3.5.1 Saturation transfer

Saturation transfer experiments were run on the undifferentiated neuroblastoma cells but not on differentiated cells. The saturation transfer experiment was done by saturating the ATP resonance at γ and observing at the PCr resonance. The results of four experiments run on NIE-115 cells showed that the effect was small, if any. The T_1^{sat} used was that value obtained under non-saturating conditions, an assumption deemed justifiable in light of the predominance of the unsaturated condition.

This set one limit on the activity of the enzyme, namely that it be greater than 15 seconds. The other limit was set by the observation that PCr levels go down either before or at the same time that the ATP levels go down when the cells were subjected to an ischemic reaction. This time is put on the order of minutes.

4.3.5.2 Dissociated rat brain cells

DRBC prepared as previously described were fed creatine-supplemented medium while in the magnet and when the PCr to ATPα ratio reached approximately 2:1, a saturation transfer experiment was run. The results are shown in Fig. 57-58. There was a distinct difference at the PCr chemical shift. The ratio of $\Delta M/M$ of 0.27 for DRBC is comparable to that of neonates of 0.2. A second independent experiment gave a value of 0.35. With T_1^{sat} approximately 4 sec., one can calculate k of .07 and .09 S^{-1} respectively (see Table 8).

In conclusion we can compare the k values of the undifferentiated N1E-115 and DRBC with the value obtained from neonates and adult rats with surface coils by S. Ogawa (Ogawa, S. et al. 1986) of .5 for $\frac{\Delta M}{M}$ or .13 S^{-1}, which is a combination of glia as well as neuronal cells, and is considered a good agreement.

4.3.6 PCr response to insult

PCr seems to act as a buffer to maintain ATP levels at a constant or near constant value in a number of tissue systems. A great deal of work has been done on creatine kinase activity in heart and leg muscle. There have also been reports on tissue slices and cultured cells, and the protection they receive from incubation in creatine solution (Matthews, et al., 1982). The experience in muscle shows that the ATP levels stay constant or nearly so during periods of high-energy demand at the expense of depleting the PCr pool, which is in turn

Figure 57

This figure is the result of a saturation transfer experiment on DRBC (E 19). The position of the on and off pulses are as indicated in panel (A). A) shows the spectrum with the ATPγ peak saturated. B) shows the spectrum irradiated at the off position. C) shows the difference spectrum. As can be seen, there is a definite effect on PCr.

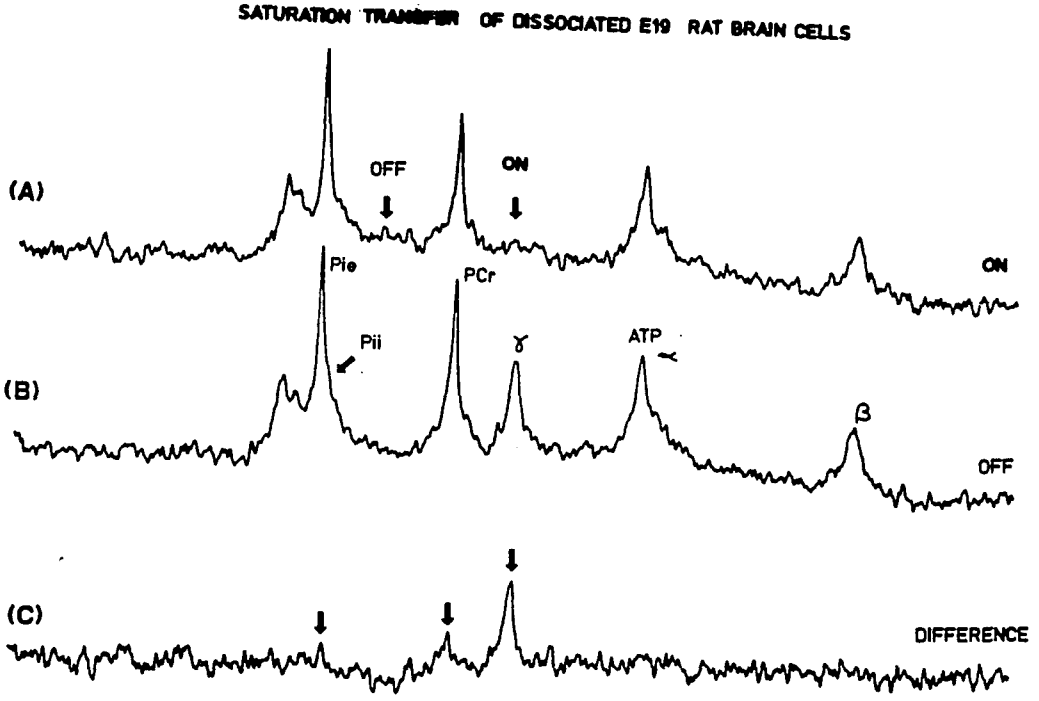
SATURATION TRANSFER OF DISSOCIATED E19 RAT BRAIN CELLS
(A)
OFF
ON
ON
(B)
Pie
Pii
PCr
γ
ATP
α
β
OFF
(C)
DIFFERENCE

FIG. 57

Figure 58

This figure shows an expanded view of the experiment in Fig. 57. Here we address the peak associated with the P_i inside the cells (P_{ii}). Using convolution difference processing on this spectra, this P_i peak at the chemical shift 2.51 (see panel B) can be resolved from the external P_i peak (P_{ie}). The different spectrum A) shows a peak at 2.51 PPM. Because this was a noisy, although real, signal and since the P_{ii} could not be obtained quantitatively from this experiment, a numerical figure cannot be given to the transfer rate of the terminal phosphate group of ATP to P_i in the cells.

However, qualitatively we know the P_{ii} contribution was small compared to P_{ie} in the fully relaxed spectrum and that this transfer represents a sizable percent of the total, possibly greater than 50%. In the neonate, using surface-coil saturation on the whole animal, (Ogawa et al., 1985) shows the P_i in the brain to be less than 25% of the ATP level. The saturation peak area in (A) is on the order of 15% of the ATPβ peak area and lends support to a large effect on P_{ii}.

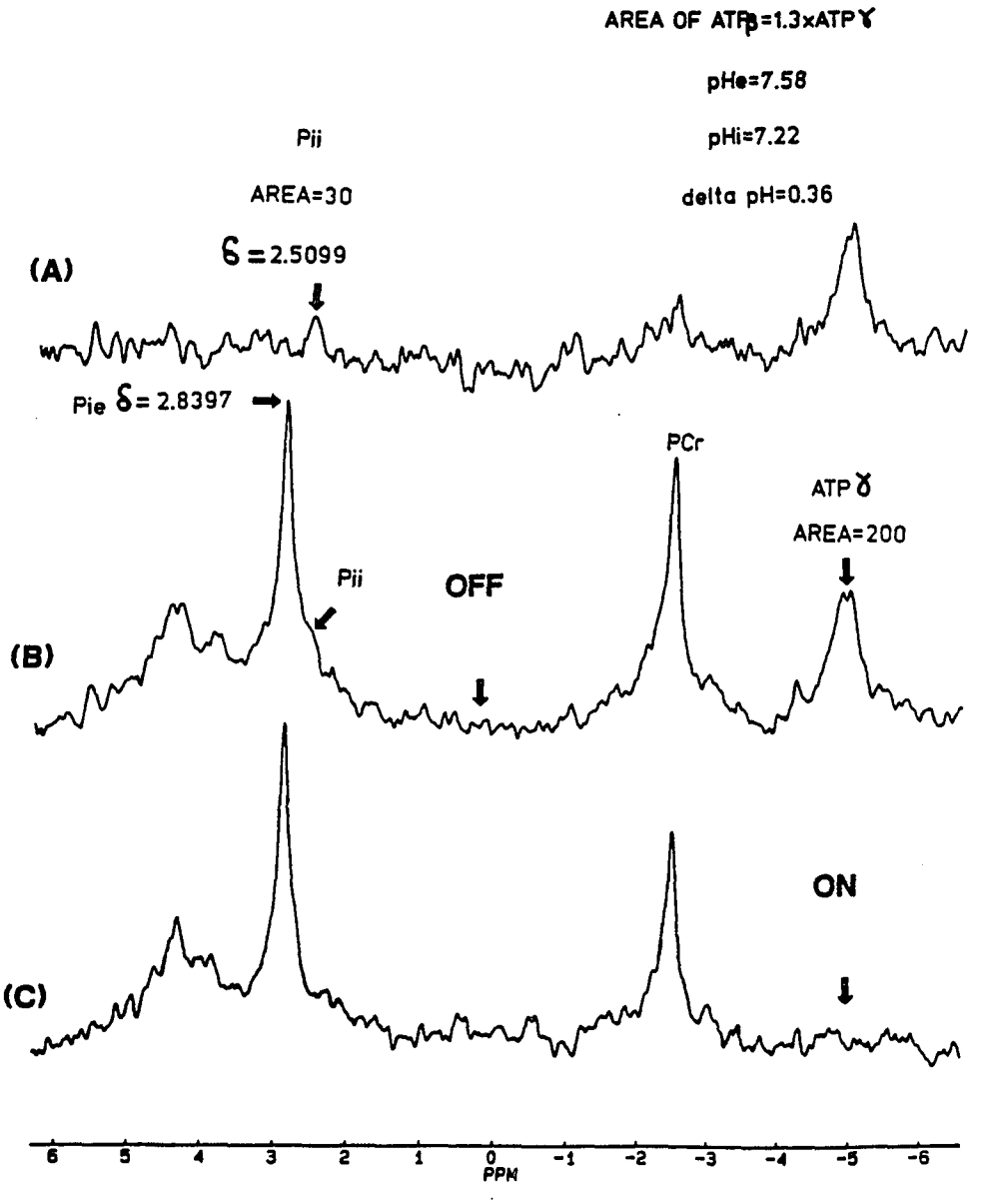
AREA OF ATPβ=1.3xATPγ
pHe=7.58
pHi=7.22
delta pH=0.36
Pii
AREA=30
δ=2.5099
(A)
Pie δ=2.8397
PCr
ATPγ
AREA=200
Pii
OFF
(B)
ON
(C)
6
5
4
3
2
1
0
PPM
-1
-2
-3
-4
-5
-6

FIG. 58

TABLE 8

FLUX RATE K1 (f+)

	$\Delta M/M^* \times 1/T_1^{Sat}$	pH
Undifferentiated Cells	0.0	7.6
DRBC	0.07 0.09	— —
IN VIOV Day P2 P10	 0.02 ≈ 0.10	 7.3 7.1

Undirectional flux rates defined as:

$$Cr\,P + APD + H^+ \underset{f-}{\overset{f+}{\rightleftarrows}} Cr + ATP$$

replenished during periods of low demand. The dynamics in muscle are such that there is a high flux through the creatine kinase reaction, so that substantial drains on the ATP pool can be offset quickly by the creatine kinase reaction. What is seen when muscle is stressed beyond its physiological limit is, first, a constant ATP level is maintained with a concomitant decrease in the PCr level, and then, when the PCr concentration reaches zero, the ATP pool starts to deplete. Similar results have been obtained for brain *in vivo* using NMR with surface coils (Ogawa, et al., 1986). These findings suggest questions concerning the role of creatine phosphate and its role in protecting neuroblastoma cells and DRBC from the kinds of external stresses encountered *in vivo*, such as anoxia, hypoglycemia, and an ischemic response. The following experimental results were obtained from experiments run to answer some of these questions while looking at one cell type when it does not have the privilege of support from glia cells, such as astrocytes or microglia.

Neuroblastoma were looked at under four conditions: 1) low oxygen, 2) low pH, 3) total ischemic conditions, 4) high oxygen. The experimental procedure to generate an ischemic condition was simply to shut off the pump and close the return valve to the reservoir so that the 6 ml of medium superfusing the cells which was present in the cell holder when the pump was turned off remained trapped in the holder. This experimental condition approximated what is generally considered to be an ischemic episode *in vivo*. In all experiments, the cells were grown as previously described, put into the sample holder and then the magnet, equilibrated in temperature and pH, and superfused with

creatine-supplemented medium for various periods of time, after which control spectra were taken.

4.3.6.1 Anoxic response

What contribution do each of the major factors of ischemia (i.e., changes in pH, low glucose and oxygen deprivation) make to the alteration of the cell's behavior? The changes in pH and low glucose have been discussed: here the contribution of oxygen deprivation is described.

Prior to running anoxic experiments, the rate of oxygen utilization was determined. N1E-115 cells were grown, seeded onto microcarriers, put into the sample holder and magnet and allowed to equilibrate for several hours with 100% air in the oxygen exchanger. The oxygen tension of the effluent from the cell holder was measured. The oxygen meter was switched from the standard calibration medium to the cells at time zero (see Fig. 59) and spectra were collected starting at plus ten minutes. (The medium was supplemented with 10 mM creatine.) When the effluent oxygen concentration had reached its lowest value, 5.5%, the input to the oxygen exchanger was switched to a mixture of 50% oxygen, 9.3% CO_2, the balance being air. The oxygen concentration of the effluent was checked at its steady state conditions at the end of the experiment, and found to be 9% at pH7.4. Figure 60 shows a stack plot, and in Fig. 61 the peak height of PCr, ATPβ and the pH over this ten-hour experiment on undifferentiated N1E-115 cells. During the first hour, the pH adjusted to 7.4 from a basic condition. This change was accompanied by

the decrease in the PCr peak to a steady state value at hour six, an expected shift with pH. These data provide a good base from which to judge changes.

The anoxic response of the neuroblastoma cells was looked at using DMEM medium with glucose and a mixture of 10% CO_2 and 90% N2 in the gas exchanger. The oxygen content of the effluent is plotted in time in Fig. 62 after the oxygen meter was switched from a standard to the cell circuit. The effluent oxygen concentration reached approximately zero in eighty to 120 minutes at the end of the tenth file, the time for the system to equilibrate. Figure 63 shows the spectra and peak height obtained over a 6.5 hour period. The most important point of this experiment is the fact that no ATP was lost and only 30% of the PCr was lost. Basically, at this pH under non-stress condition, the cells were almost capable of sustaining themselves indefinately via glycolysis. The data were presented in two figures. The first 100 minutes, during which time the oxygen is being purged from the cell and meter system, and the following 300 minutes, during which time anoxic conditions apply exclusively.

There is most assuredly some back leakage of oxygen across the Teflon tubing connecting the gas exchanger and cell sample holder. Even so there is no question that the cells, although not completely anaerobic, are in a very much reduced oxygen environment.

Anoxic glycemic experiments were run on DRBC without glucose and oxygen to see if they behaved in the same way as neuroblastoma cells. Figure 64 shows the results of these experiments. The cells were charged with PCr in ZAM

Figure 59

The oxygen content of the effluent of the sample holder when the holder contained a full sample of N1E-115 cells. The cells were superfused at a standard rate of 3.5 ml per minute. The meter was switched from a 20% oxygen standard into the cell effluent path at time zero. From time equals zero to 80 minutes, the gas exchanger contained 100% air with no CO_2 added. At 80 minutes, the exchanger was switched to 50% O_2 (by mixing pure O_2 with air), 9.3% CO_2 and the balance N_2. The curve is simply a point-to-point connection.

The 5% minimum represents a balance between the 20% O_2 supplied to the sample holder, the oxygen consumption due to the aerobic activity of the cells and a small amount of O_2 diffusion from the surrounding air back into the Teflon tubing connecting the sample holder to the oxygen meter. The increase in the O_2 content of the sample holder effluent when the gas exchanger had 50% O_2 demonstrates that there was residual O_2 left when 50%-100% O_2 was used in the gas exchanger, and therefore that the cells were not in an anoxic state.

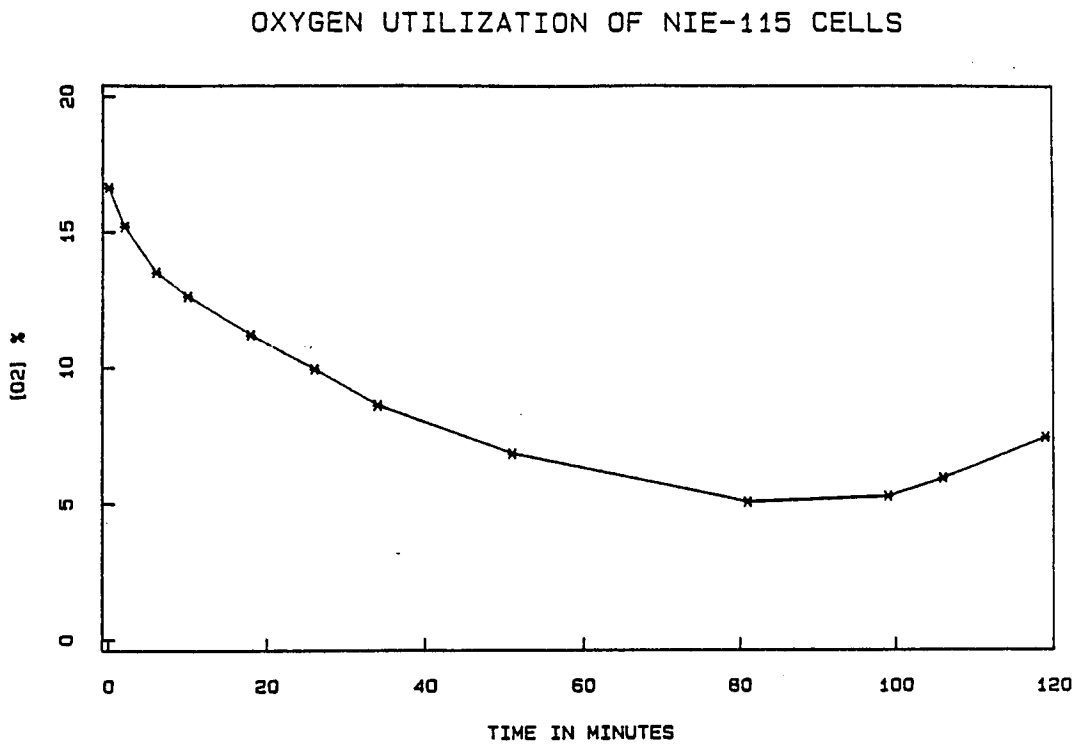
OXYGEN UTILIZATION OF NIE-115 CELLS
[02] %
0
5
10
15
20
0
20
40
60
80
100
120
TIME IN MINUTES

FIG. 59

Figure 60

This stack plot demonstrates control conditions and general stability of the N1E-115 undifferentiated cells with time. The file at 30 min is at a basic state just before the cells were switched to a more acidic condition. Note that the PEt peak is sharp in the basic condition and diminishes with the acidification of the cells. The profile at 90 minutes is during the transition period to a lower pH (see Fig. 61 for quantitative date). (Each file is the sum of 1700 FID is taken in 30 minutes. LB=2.5HZ).

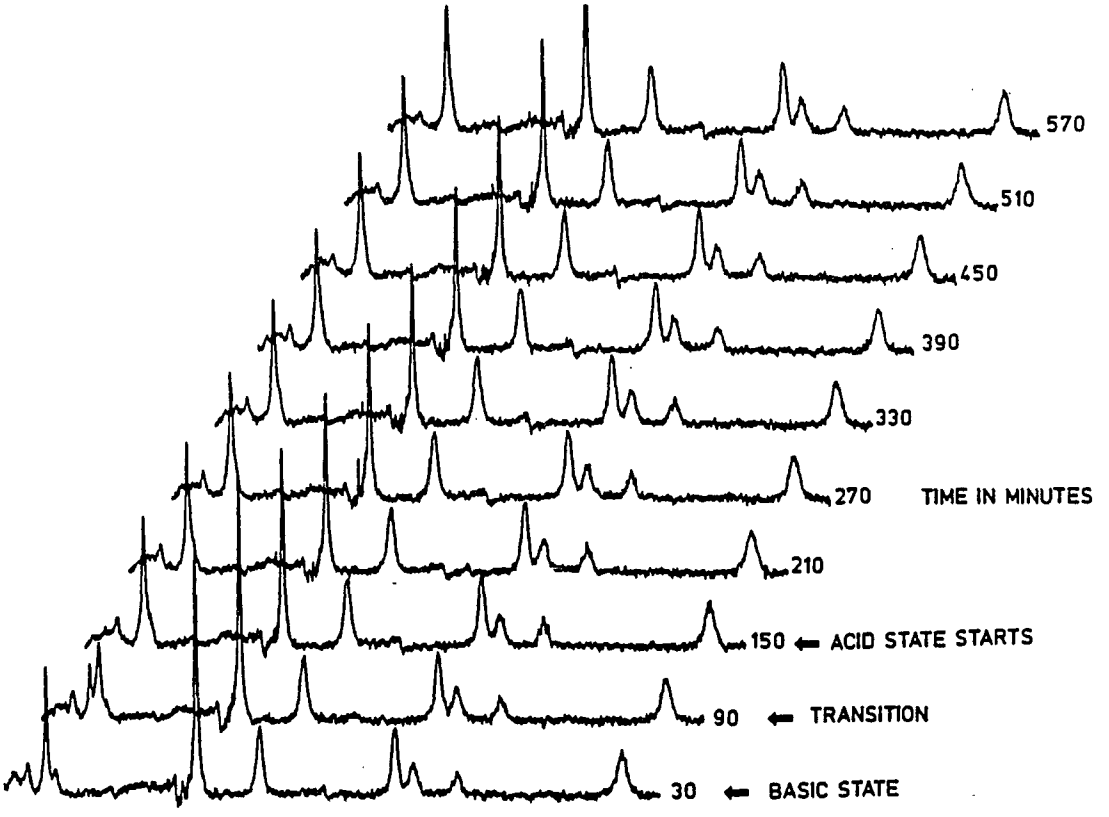
570
510
450
390
330
270
TIME IN MINUTES
210
150 ← ACID STATE STARTS
90 ← TRANSITION
30 ← BASIC STATE

FIG. 60

Figure 61

This is a 10-hour control. At 80 minutes the CO_2 of the gas exchanger was switched from 0 to 9.3% and the O_2 from 20 to 50%. A) shows the ratio of the PCr/ATPα peak heights. It took about one-and-one-half hours for the system to reach complete equilibrium with a distribution of this type. B) shows the pH of the extracellular medium measured from the chemical shift of the P_i external (P_i e). C) demonstrates that the ATPα peak height was stable over the 10-hour period. D) a plot of pH and the PCr/ATP ratio is presented for ease of comparison. The actual spectra are shown in Fig. 60 and at 2 hr. intervals in Fig. 61b.

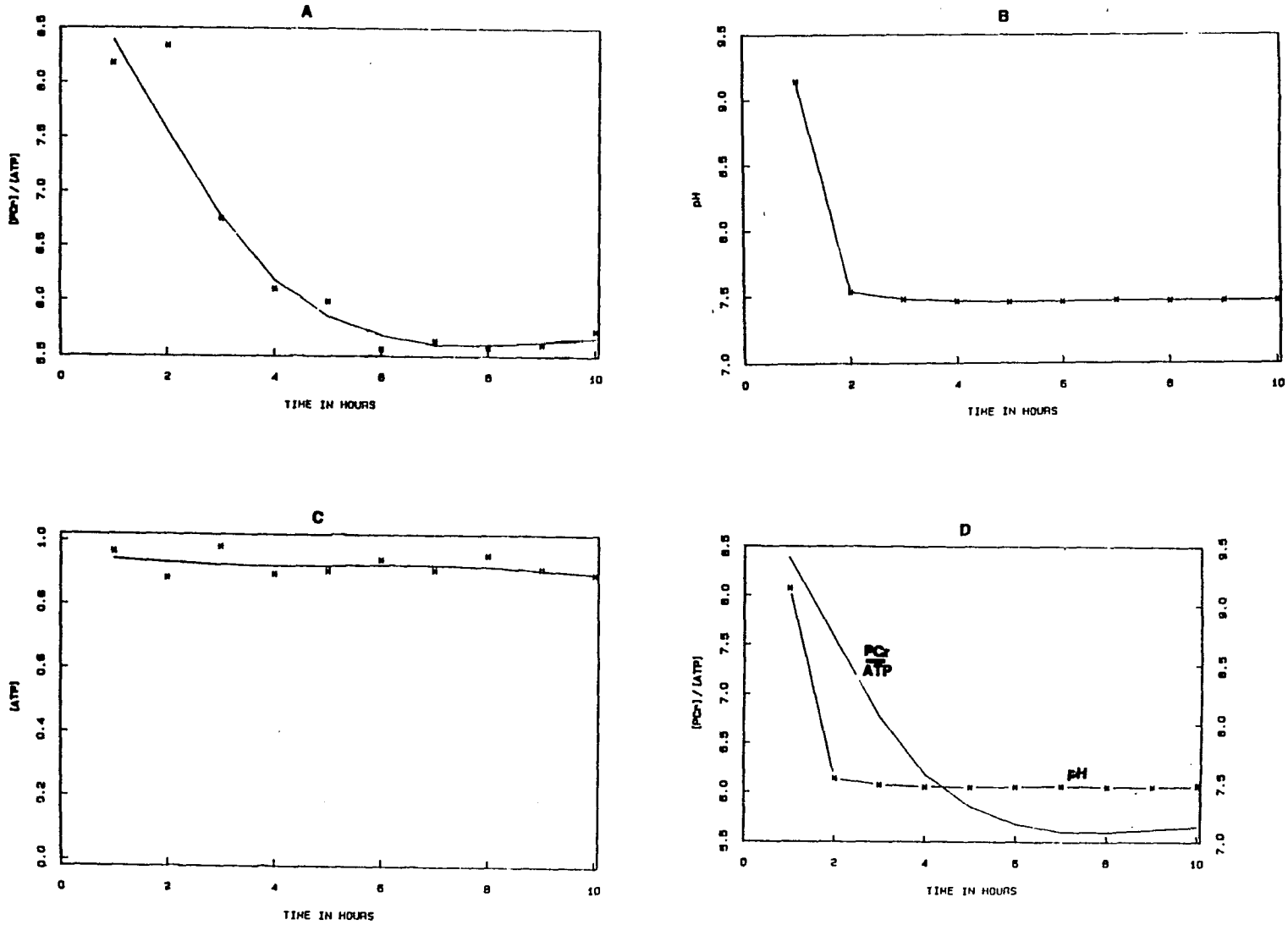
A
[PCr] / [ATP]
TIME IN HOURS
B
pH
TIME IN HOURS
C
[ATP]
TIME IN HOURS
D
[PCr] / [ATP]
PCr
ATP
pH
TIME IN HOURS

FIG. 61 (A)

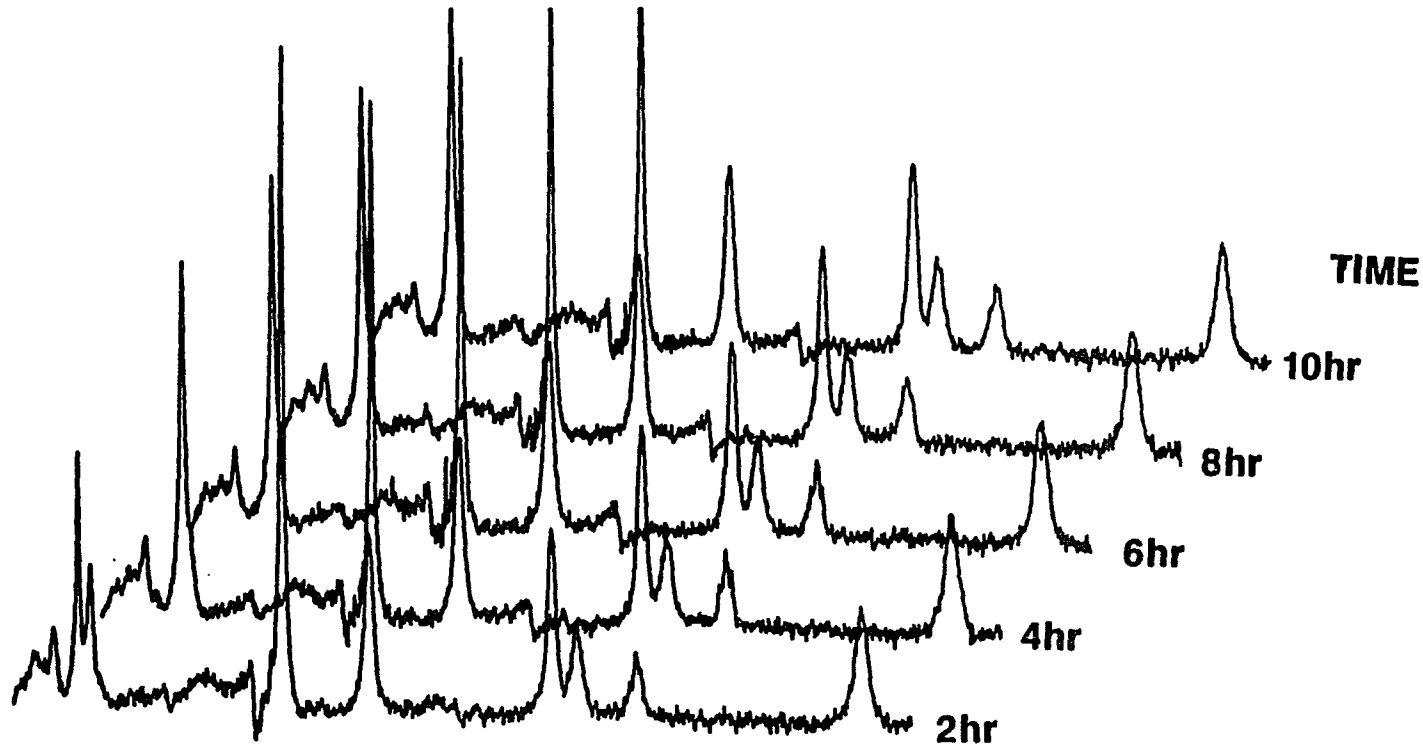

FIG. 61(B)

Figure 62

The oxygen content of the effluent from the undifferentiated N1E-115 cells in the sample holder was measured when the gas exchanger was switched from a normal condition of 90% air, 10% CO_2, to 90% N_2, 10% CO_2. In the first 250 minutes of this experiment, the decay was dominated by the equilibrium of the oxygen metering system which was switched from a 20% standard at time zero to the cell return circuit. The curve demonstrates that the O_2 content of the cell holder's effluent is small at 100 minutes. The steady-state level was less than 1%. Part of this residual O_2 may have been due to back diffusion of O_2 into the tubing between the gas exchanger and oxygen meter.

Since the length of the tubing connecting the gas exchanger to the sample holder was the same as that connecting the sample holder to the O_2 meter, we can be safe in saying the O_2 content immediately upon exiting the sample holder was zero. (This is reasonable because there is only N2 and CO_2 in the exchanger and the the cells used what little O_2 may have diffused back into the Teflon tubing during transport from the gas exchanger to the sample holder. We can set an upper-limit estimate of less then 1% back-diffusion of O_2 into the line between the exchanger and the sample holder. Although we can not say the cells were living completely anaerobically, we may infer that the cells under these anoxic conditions were very close to anaerobic conditions.

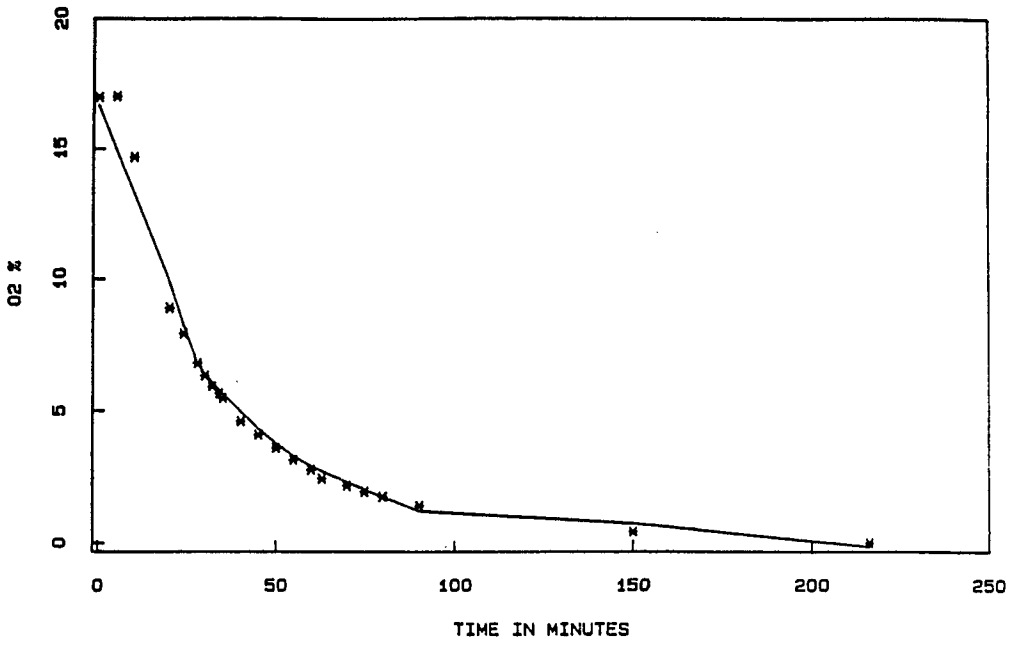

FIG. 62

Figure 63

A) This figure shows the first 100 minutes of the anoxic response of N1E-115 undifferentiated cells. A) shows that the pH remained constant. B) shows that the P_i peak height remained relatively constant. C) shows that the PCr went down approximately 30%. The ATPβ remained approximately constant at 5.55 units $\pm$0.62 n=9 (not shown). The units within the figure are consistent with one another. Each file is from 150 FID's taken with a repetition rate of 3 seconds.

B) This is a result of the anoxic response of the N1E-115 undifferentiated cells in the period 100 to 400 minutes after the onset of anoxia. The first 100 minutes was allowed for near equilibrium conditions to be reached. During the next 300-minute period, the PCr level dropped an additional 18% (B) while the pH (A) and ATPβ (C) peaks remained constant.

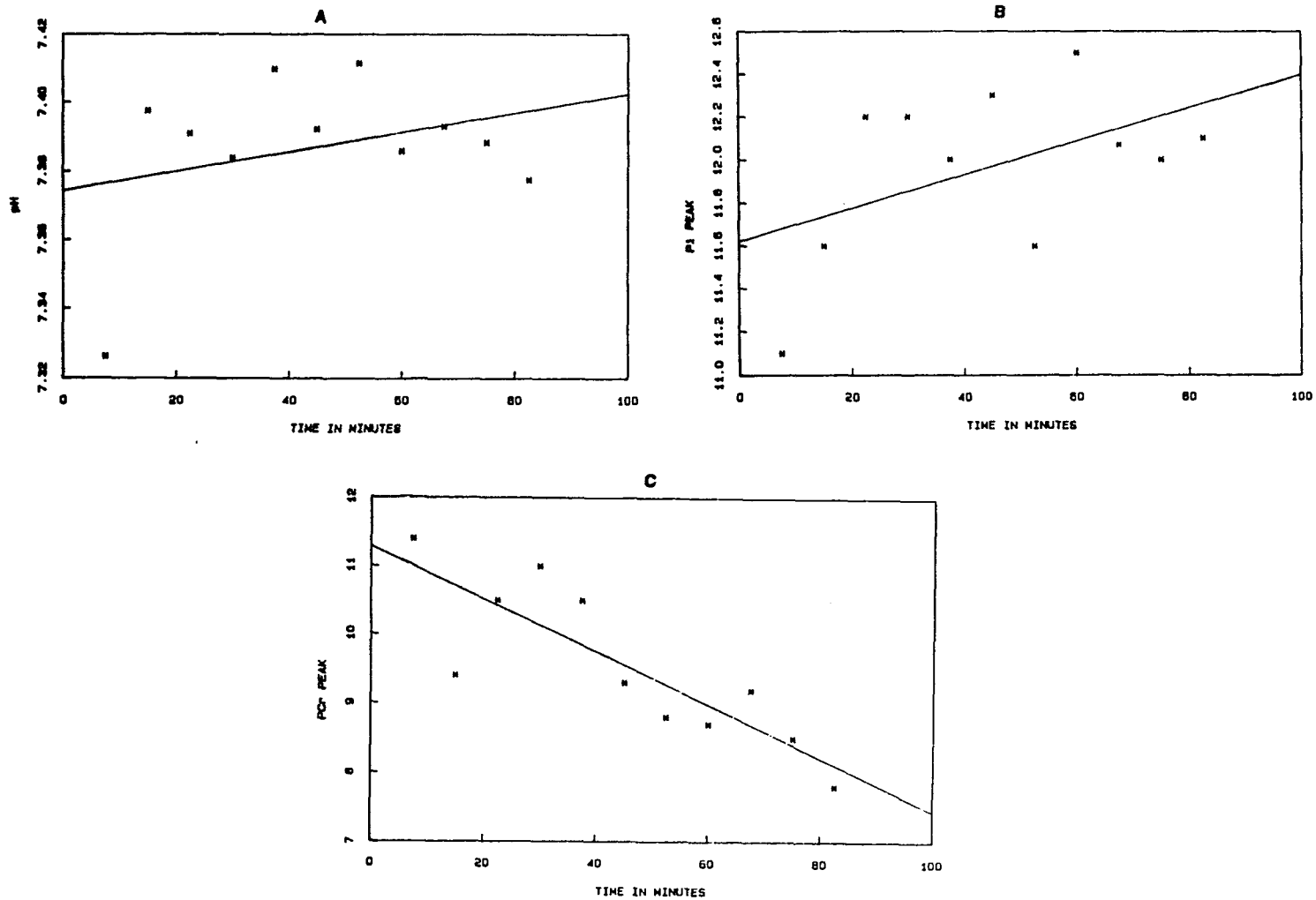
A
pH
7.42
7.40
7.38
7.36
7.34
7.32
0
20
40
60
80
100
TIME IN MINUTES
B
P1 PEAK
12.6
12.4
12.2
12.0
11.8
11.6
11.4
11.2
11.0
0
20
40
60
80
100
TIME IN MINUTES
C
PCr PEAK
12
11
10
9
8
7
0
20
40
60
80
100
TIME IN MINUTES

FIG. 63 (A)

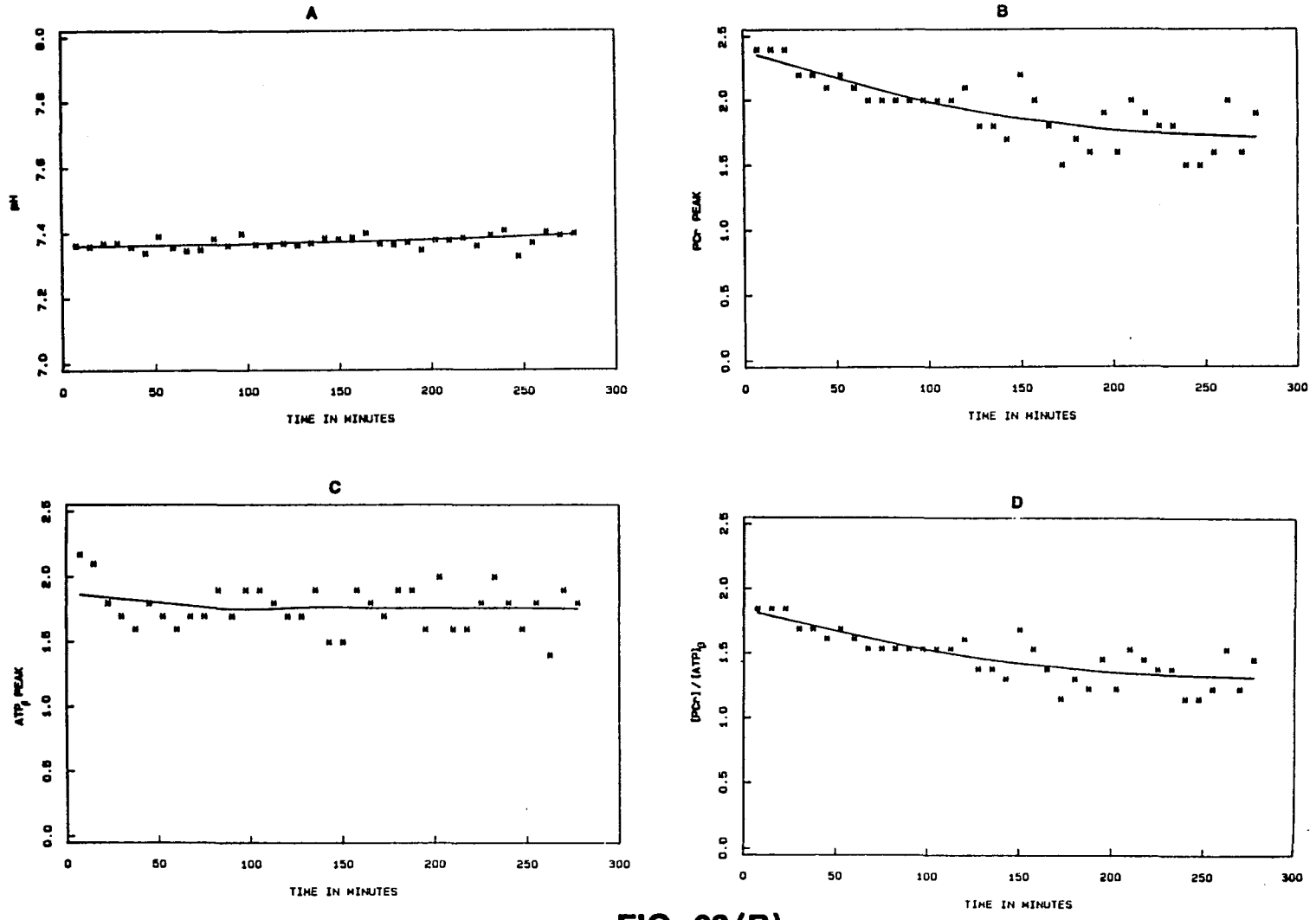
A
pH
7.0
7.2
7.4
7.6
7.8
8.0
0
50
100
150
200
250
300
TIME IN MINUTES
B
PCr PEAK
0.0
0.5
1.0
1.5
2.0
2.5
TIME IN MINUTES
C
ATP$_\beta$ PEAK
TIME IN MINUTES
D
[PCr] / [ATP]$_\beta$
TIME IN MINUTES

FIG. 63(B)

buffered with CO_2 and supplemented with 30 mM Cr, then maintained on ZAM with glucose, and without the creatine supplement, after which they were subjected to 2.5 hours on Hepes-buffered Ringers without glucose under anoxic conditions. During this time the pH outside the cells dropped from approximately 7.5 to 7.28 due to the change of the pH in the Hepes-buffered Ringer, the ATP dropped to 65% of the control, and the PCr dropped to 53% of its original value. When the oxygen was turned back on, the pH and PCr started recovering. Once it was evident that the PCr was recovering, the cells were switched to complete ZAM medium supplemented with 30 mM creatine.

These cells showed a high tolerance for oxygen glucose deprivation. By switching to complete ZAM medium supplemented with creatine it was established under the best recovery conditions what levels the cells could recover to. With this information the experiment was run again with a variation. Ringers without Cr was used in the first two phases of this experiment, although the cells had been previously charged with PCr (Fig. 65). In the first phase, the Ringers was supplemented with glucose oxygenated and buffered with Hepes. During this period (two hours) the PCr and ATP levels remained high and constant. In the second phase, the glucose and oxygen were withdrawn and as in the previous example, the PCr level dropped. When it reached 40% of its original level, the cells were switched to ZAM without Cr but with oxygen and glucose. In this phase the PCr reappeared within thirty minutes to 80% of its original value. These results tell us two things; first, the fact that PCr levels were not depleted during the first phase suggests that in

Figure 64

Anoxic pH jump experiment. This experiment was run on DRBC which were initially superfused with ZAM supplemented with 30 mM Cr, 90% oxygen and buffered with CO_2. The cells were switched to ZAM with O_2 and without creatine at time "A" (see panel B). The new medium with a slightly different sodium bicarbonate concentration had a slightly higher pH (see panel A) which is reflected in an increase in the PCr peak height. At time "B" the cells were switched to a Hepes Ringers pH 7.28 which contained no oxygen, glucose or Cr. At this point, the ATPβ peak started to decrease slowly to about 80% over the life of the experiment. At time "C" the oxygen was turned on. Once the recovery was assured, (time "D") the cells were switched to complete ZAM with 30 mM Cr, and complete recovery was obtained.

Panel (D) shows the PCr peak height and pH plotted together for ease of comparison. It is important to note that the pH shift was controlled and determined by buffer and CO_2 levels of the superfusate. The important experimental observations are 1) the PCr peak went down with the pH at the same time, but reappeared after the pH returned to normal. 2) the PCr returned in a time scale much shorter than that which it did when it initially took up Cr and 3) the cell can sustain a reasonably long period of anoxia (2.5 hours).

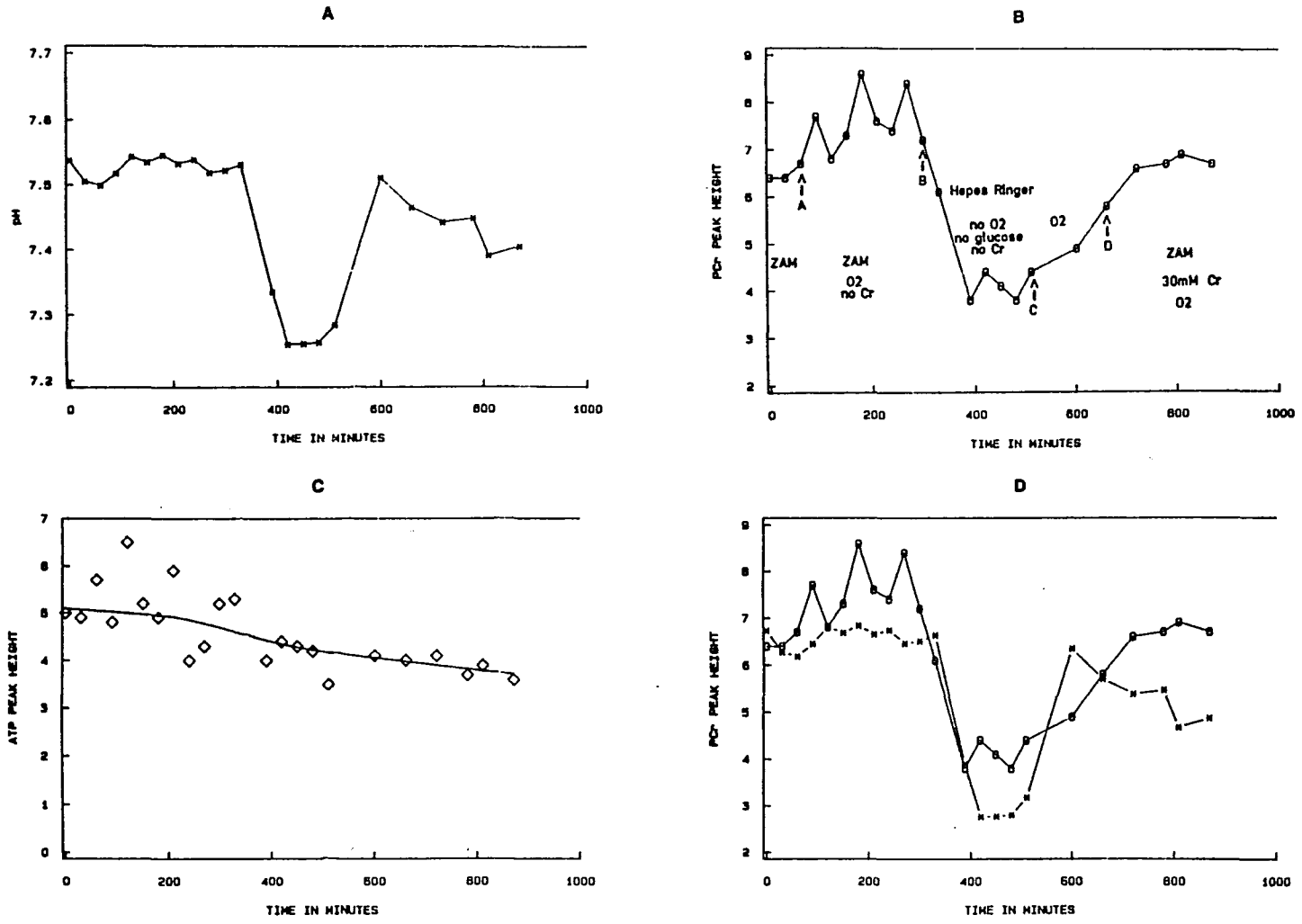
A
pH
7.7
7.6
7.5
7.4
7.3
7.2
0
200
400
600
800
1000
TIME IN MINUTES
B
PCr PEAK HEIGHT
ZAM
ZAM
02
no Cr
A
A
B
Hepes Ringer
no 02
no glucose
no Cr
02
C
D
ZAM
30mM Cr
02
TIME IN MINUTES
C
ATP PEAK HEIGHT
TIME IN MINUTES
D
PCr PEAK HEIGHT
TIME IN MINUTES

FIG. 64

Figure 65

DRBC subjected to an anoxic episode at a constant pH without external Cr. In this case the decrease in PCr was due to use of the PCr bond energy alone and not to a shift in the pH. There was no extracellular Cr in the medium at any time during this experiment.

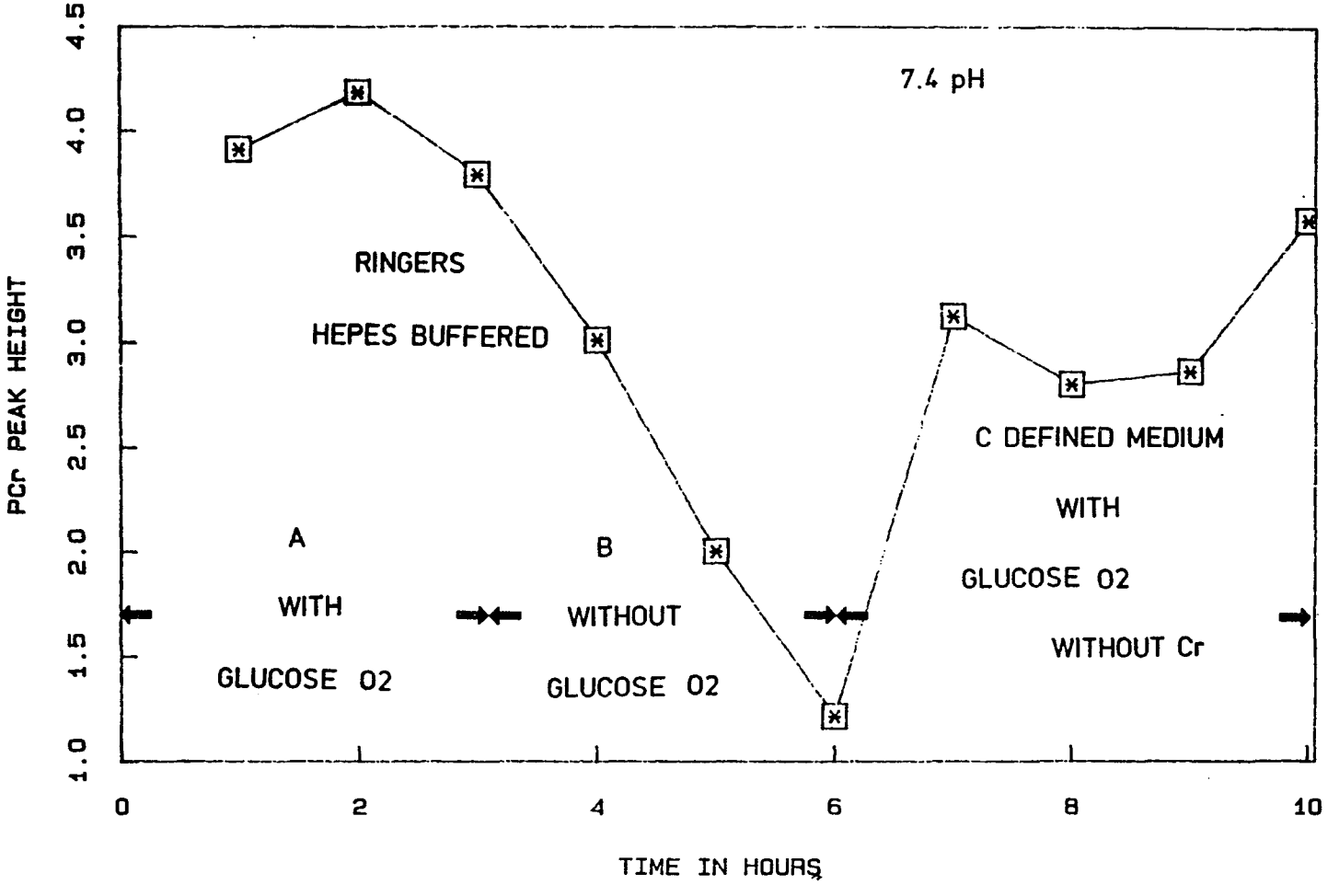
7.4 pH
RINGERS
HEPES BUFFERED
A
WITH
GLUCOSE O2
B
WITHOUT
GLUCOSE O2
C DEFINED MEDIUM
WITH
GLUCOSE O2
WITHOUT Cr
PCr PEAK HEIGHT
1.0
1.5
2.0
2.5
3.0
3.5
4.0
4.5
0
2
4
6
8
10
TIME IN HOURS

FIG. 65

this time frame the cells were not unduly stressed and were capable of maintaining reasonable metabolic activity in Ringers. The second is that the cells, when returned to normal growth conditions, but without extracellular creatine, regained high intracellular PCr levels within minutes, compared to the hours it took to reach these levels initially in the presence of high extracellular creatine. This second finding suggests that the creatine released from PCr in the cells during the three hours of hypoglycemic anoxic conditions did not leave the cells and was available for rapid rephosphorylation. This leads to the conclusion that the rate of appearance of phosphocreatine in cells superfused with medium supplemented with high concentrations of creatine was limited by the transport of creatine into the cells.

4.3.6.2 Ischemic response

Undifferentiated neuroblastoma cells were grown on 10 mM creatine-supplemented medium, then switched to creatine-free medium for more than five hours, during which time the PCr peaks remained stable. At the beginning of this experiment, time zero, the pump and return valve were shut off and spectra were collected in 7.5 minute blocks for 53 minutes. After this time the pump and valve were turned back on (see Figs. 66 and 67). Figure 66 shows a stack plot of the spectra over the 120 minutes of the experiment. The Pi peak was seen to increase linearly to more than 300% during the ischemic portion of the experiment with a upfield shift equivalent to a pH change of 0.6 units from 7.49 to 6.89. File number 8, recorded one hour after the start of the ischemic episode and just after return to normal perfusing conditions, is a

Figure 66

Undifferentiated neuroblastoma cells — 53 minute ischemic response. This shows a stack plot before, during and after an ischemic shock. Note: The PCr disappeared before the ATP and reappeared after the ATP. Each frame is 7.5 min from the next.

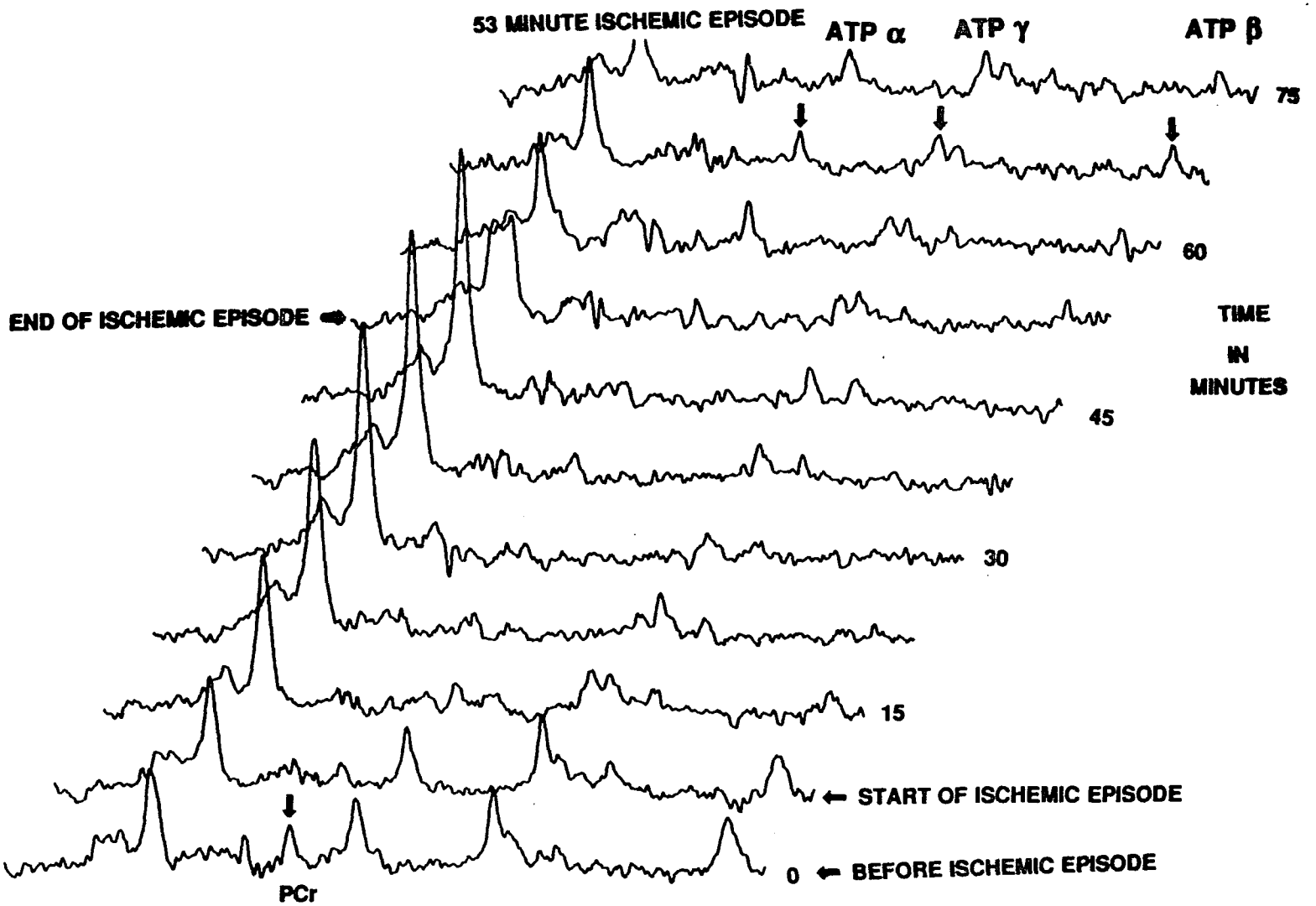
53 MINUTE ISCHEMIC EPISODE
ATP α
ATP γ
ATP β
75
60
END OF ISCHEMIC EPISODE
TIME IN MINUTES
45
30
15
START OF ISCHEMIC EPISODE
0
BEFORE ISCHEMIC EPISODE
PCr

FIG. 66

Figure 67

N1E-115 undifferentiated cells 53 minute ischemic response. (A) shows the changes in external pH "*", and internal, "0". (B) the peak height of the total free phosphate in the sample holder inside the cell as well as outside. (C) shows the ATPγ, "0", and the sum of α, β and γ "+". (D) the peak height of PCr. (E) plots the internal pH only, "*", the PCr peak height, "0", and the sum of the ATP peaks, "·". Note here that all three fell in value at the same time. The ATP came back first, but the PCr returned to normal levels only when the internal pH did so. The period of the ischemic episode started at 10 minutes, and was over at approximately 65 min.

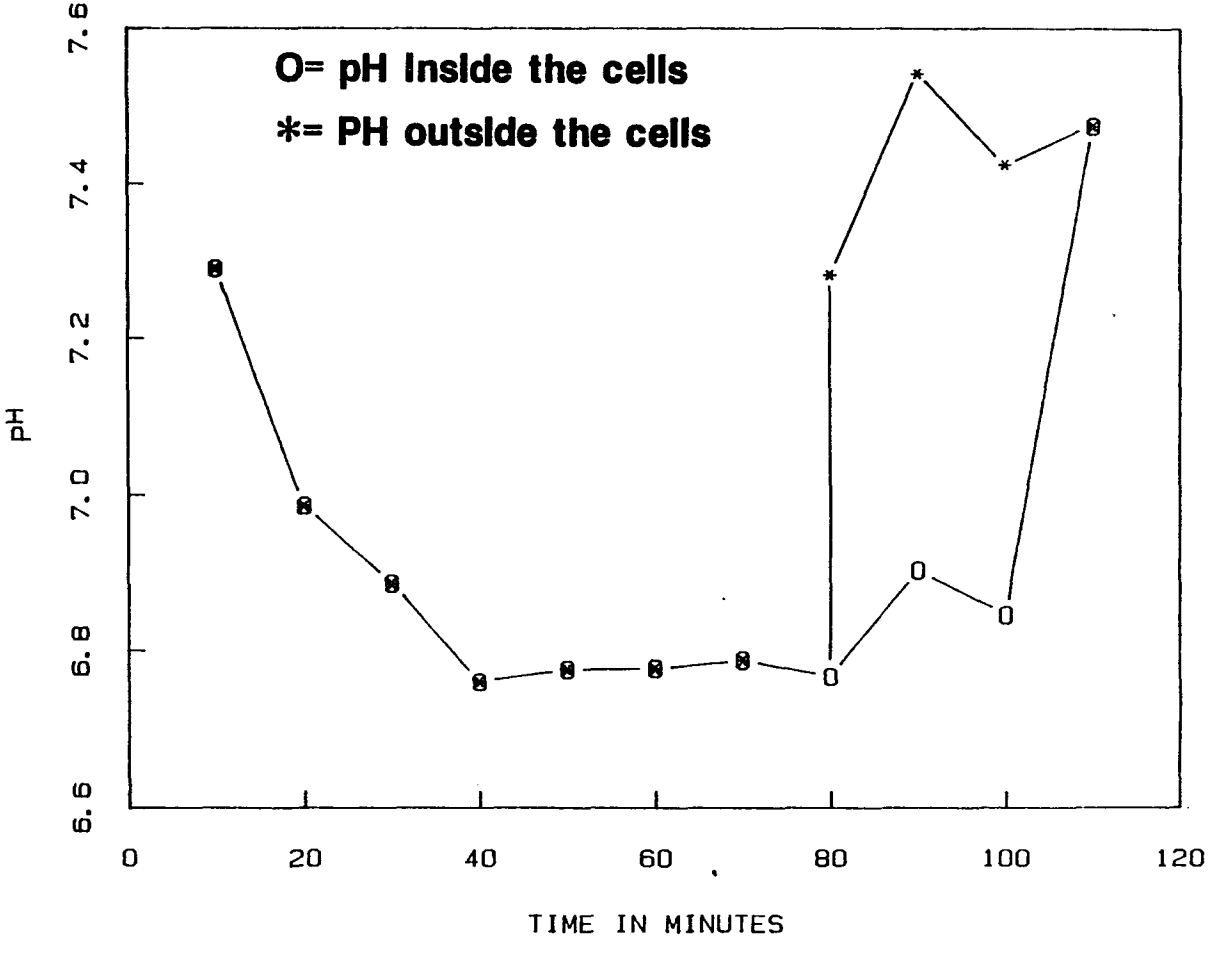
O= pH Inside the cells
*= PH outside the cells
pH
7.6
7.4
7.2
7.0
6.8
6.6
0
20
40
60
80
100
120
TIME IN MINUTES

FIG.67 (A)

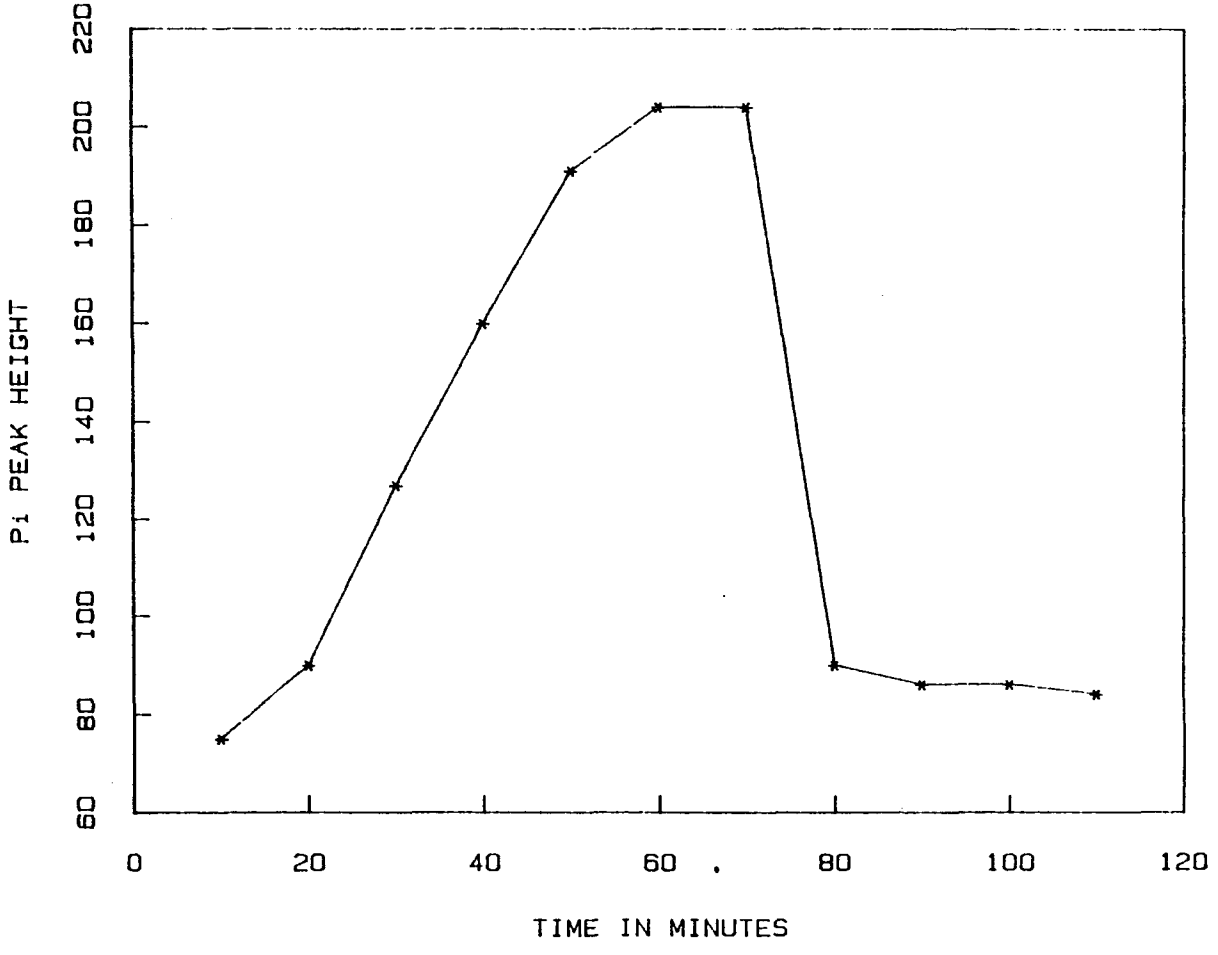
Pi PEAK HEIGHT
60
80
100
120
140
160
180
200
220
0
20
40
60
80
100
120
TIME IN MINUTES

FIG.67 (B)

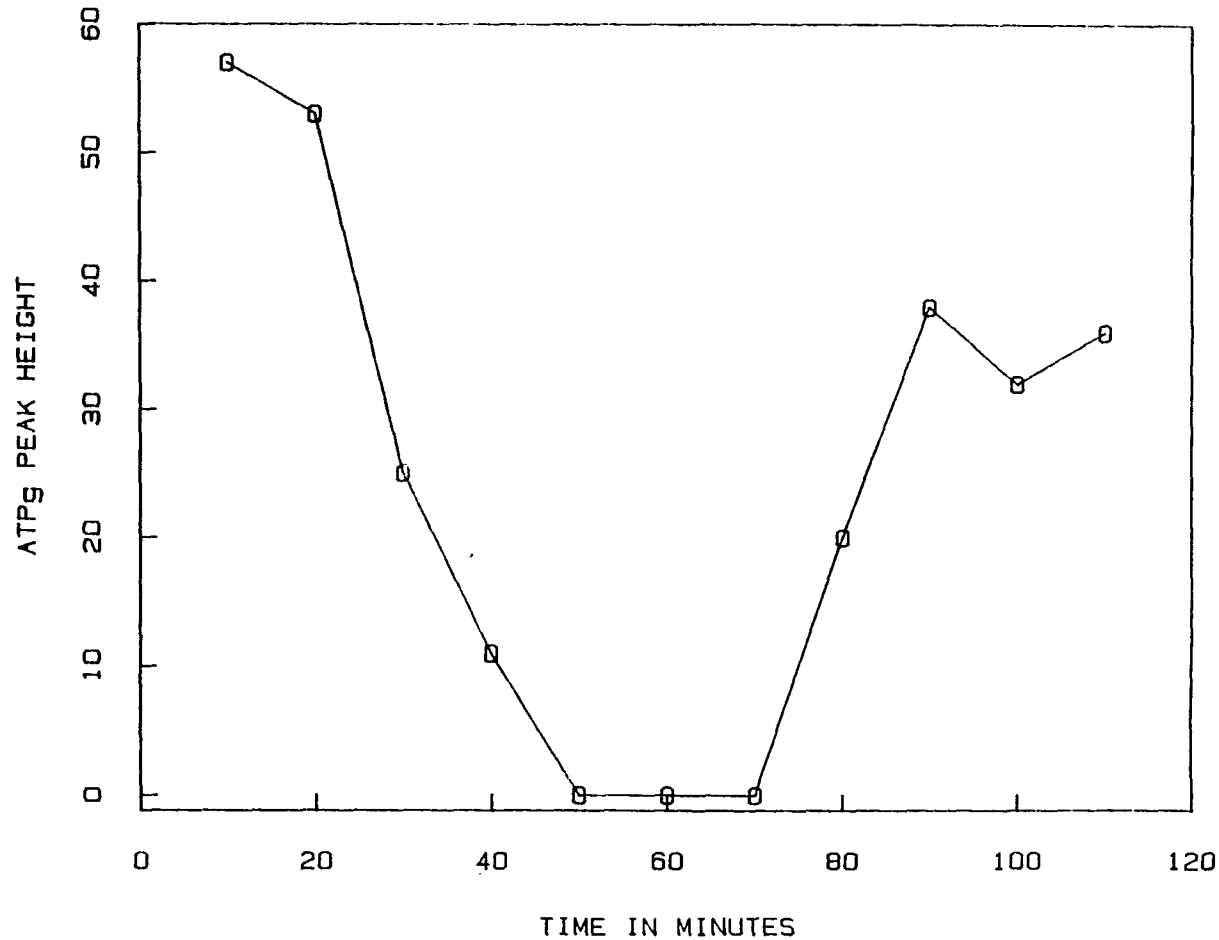
ATPg PEAK HEIGHT
0
10
20
30
40
50
60
0
20
40
60
80
100
120
TIME IN MINUTES

FIG.67 (C)

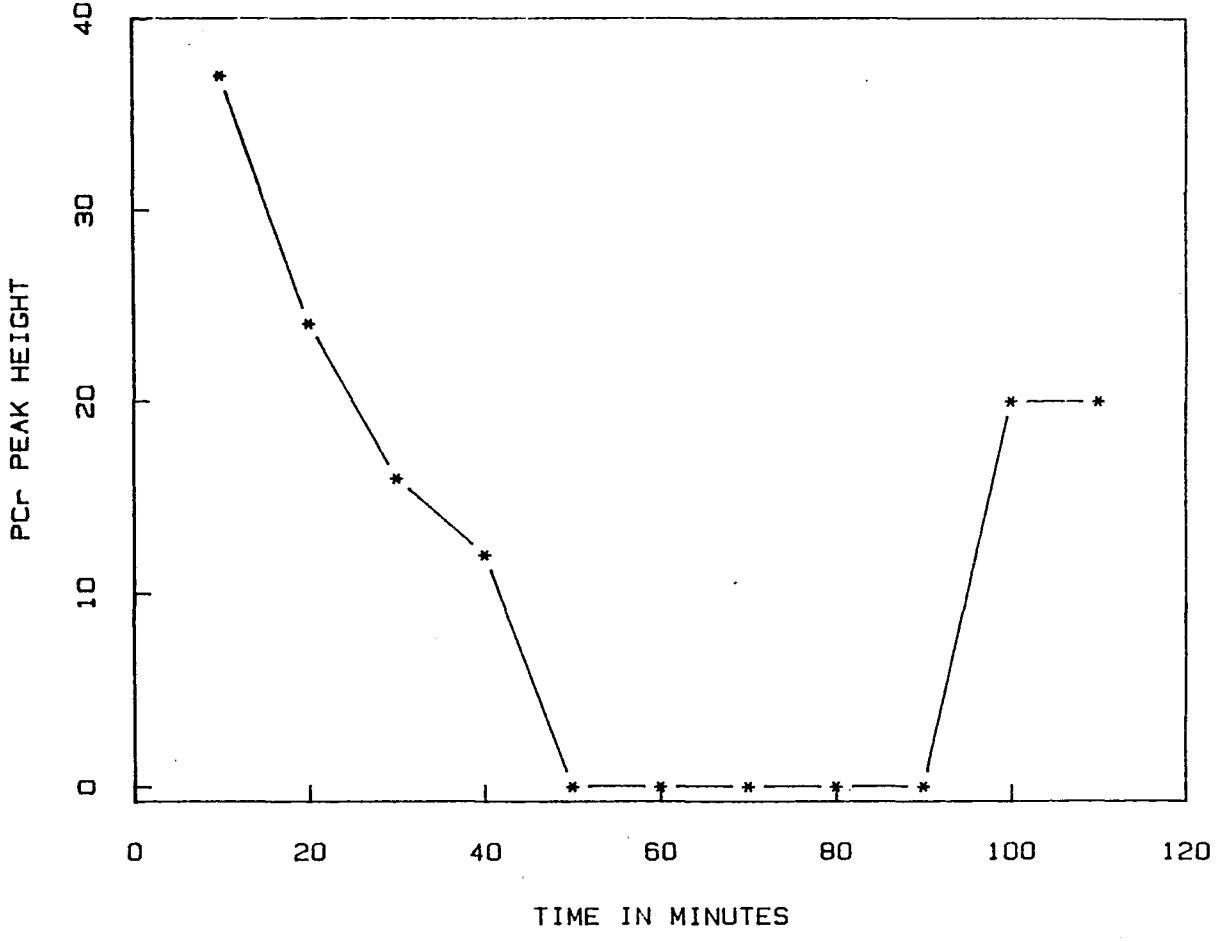
PCr PEAK HEIGHT
0
10
20
30
40
0
20
40
60
80
100
120
TIME IN MINUTES

FIG.67 (D)

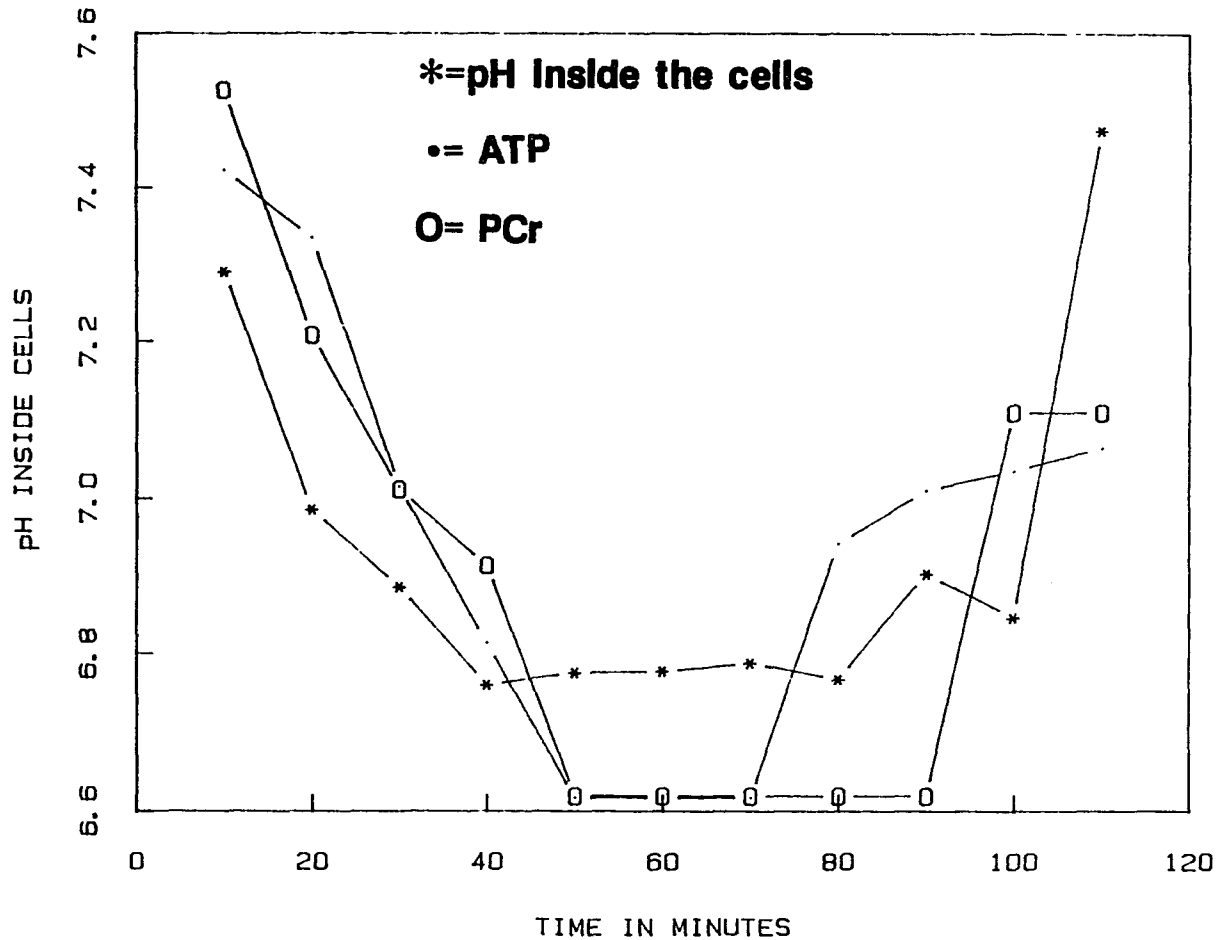
*=pH inside the cells
•= ATP
O= PCr
pH INSIDE CELLS
6.6
6.8
7.0
7.2
7.4
7.6
0
20
40
60
80
100
120
TIME IN MINUTES

FIG.67 (E)

transition spectrum. The Pi splitting was the result of Pi inside the cells and the outside acidic Pi, which had not been washed out yet (pH 6.89) and the peak from the fresh medium, which was just starting to go through (pH 7.49). Figure 67B shows a plot of the Pi peak height. At its zenith, this additional 200% increase comes from the almost complete hydrolysis of all the phosphoester bonds in the large pools in the cells. Since the volume of the cells is estimated to be no more than one-tenth that of the cell holder and the original concentration of Pi in the medium is 1 mM, and if the Pi liberated from the hydrolysis remained in the cells, its concentration was a minimum of 20 mM. Whether in reality it actually leaked out of the cells was not determined in this experiment but the ability of the cell to rapidly recover phosphorylated nucleotides, the persistence of an upfield peak at plus 15 minutes after resumption of pumping, and a continued presence of a shoulder on the Pi peak in the same spot at plus 23 minutes suggest that in the experimental conditions not all of the 20 mM P_i leaked out.

What happens to the loss of PCr and nucleotide phosphate is shown in Fig. 67D and C. They all declined at the same rate and within 33 minutes were all zero. This tells us that the flux through creatine kinase was not adequate to maintain the ATP levels at a constant level until all the PCr has been depleted. This is in keeping with the low phosphocreatine flux constant found with the saturation transfer techniques, and is not surprising. The simultaneous decrease of both PCr and ATP levels sets an upper limit on the flux through the kinase reaction and distinguishes it as being much faster than the transport of Cr into

the cells. In the recovery period, it is interesting to see a phase lag for the appearance of PCr behind the appearance of the other nucleotide phosphates. The fact that the PCr did come back in the time frame we see, however, gives evidence to the fact that the Cr released from the hydrolysis of PCr was retained in the cells for the most part during the ischemic episode, and was available for the rapid rephosphorylation of creatine. The CHI measured with a pulse repetition time of 3 s was 0.82 at the beginning of this experiment, and 0.42 at the end, which represents a recovered to 52% of the original value of ATP. The final long-term recovery after ten hours was 61%. The PCr/ATPα ratio was .60 before the experiment, .66 immediately after, and was .63 ten hours after the start of recovery. Within experimental error these are identical. On the basis of these results, the most probable scenario is that 60% of the cells survived, and of the surviving cells, no free creatine was lost. Support for this assumption comes with the increase in appearance of the unknown peak at approximately –.5 ppm, which was previously mentioned as correlating closely with cell death. (see Fig. 68a). Figure 68b shows the control before the experiment, after the experiment and the difference spectra which emphasizes the difference in the peak at –.5 ppm.

Two additional peaks of interest are the UDPH peak at –12.32 ppm and the NAD+ at –10.66 ppm. The peak height of UDPG was seen to remain relatively constant (17 $\pm$3.4). The NAD+ peak was not wholly resolved from the ATPα peak and as such a good quantitative assessment is not valid; however, to a first approximation, this peak was also constant throughout this experiment.

Figure 68

The difference in N1E-115 undifferentiated cells before and after being subjected to a 53-minute ischemic episode. A) before (2) after (3) and the difference (1). The noise is different in 2 and 3 because a different number of FID's were summed for each file; however, these are plotted to a corrected scale as is the difference spectrum. B) the peak height of the PDE region is plotted during the ischemic episode.

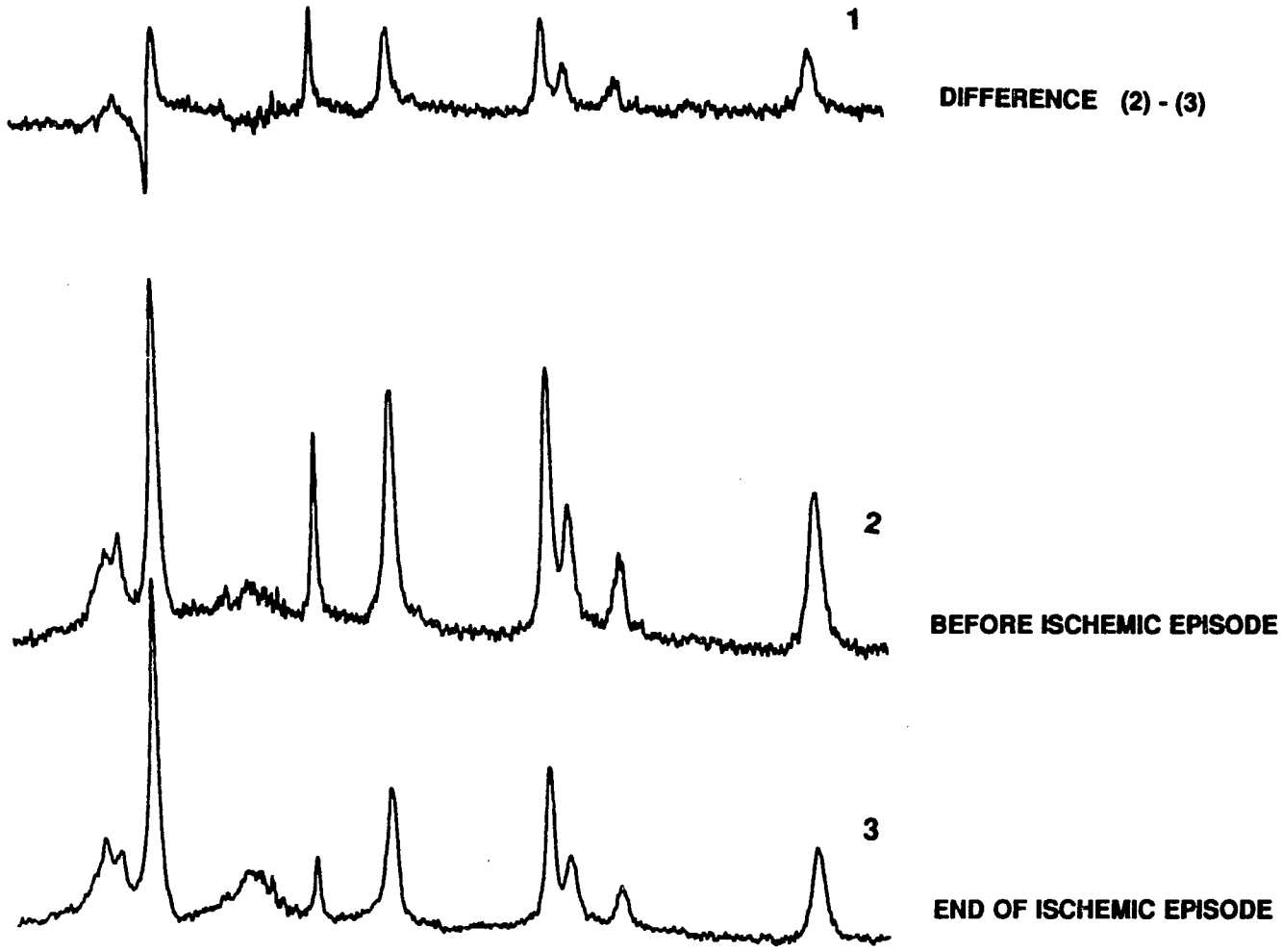
1
DIFFERENCE (2) - (3)
2
BEFORE ISCHEMIC EPISODE
3
END OF ISCHEMIC EPISODE

FIG. 68 (A)

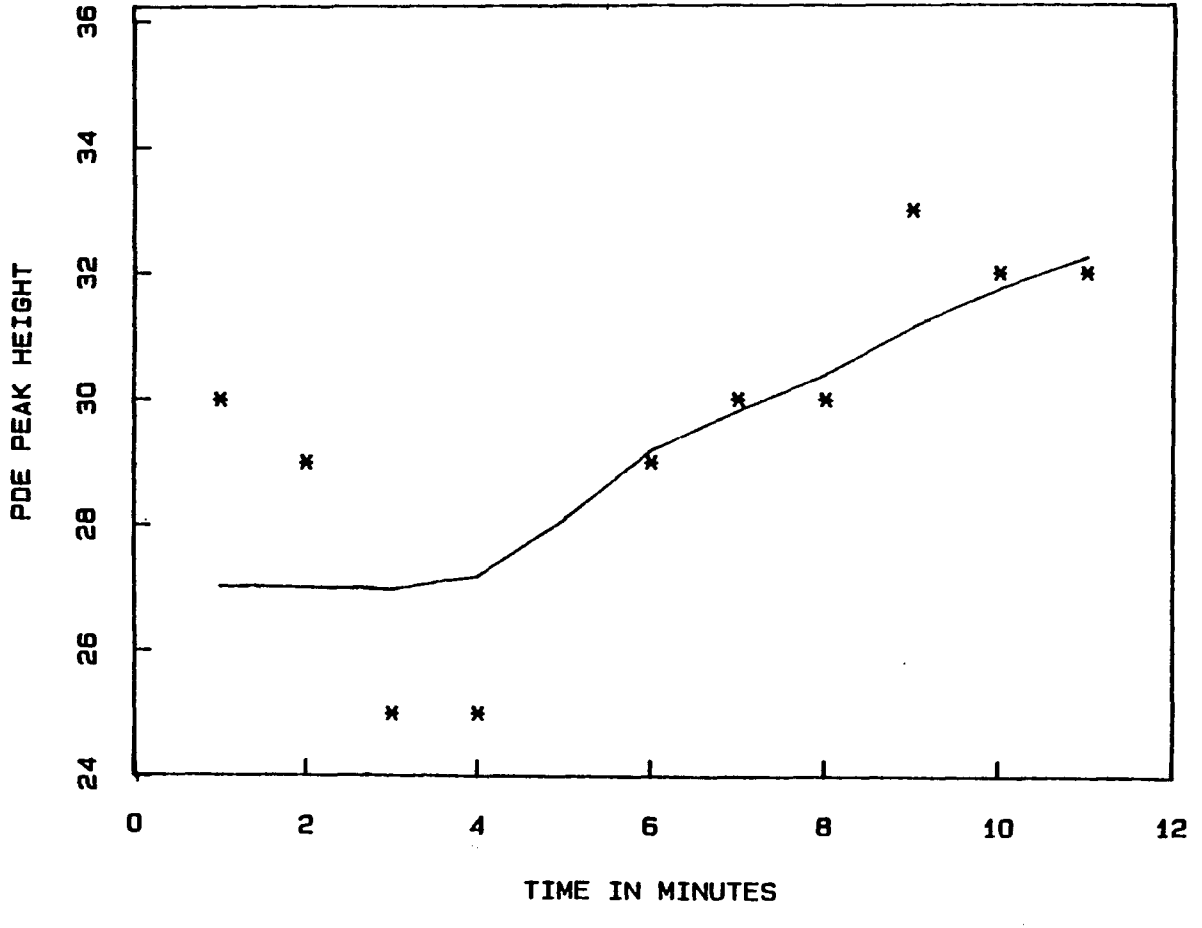

FIG. 68 (B)

The phosphomonoester region did change in a systematic way. The actual shape of this region prior to the ischemic episode was broad with a suggestion of two peaks. With the onset of ischemia, the upfield peak seemed to be shifting downfield into the peak closest to the Pi, sharpening it and increasing its amplitude. This was most likely the PEt peak titrating with the pH. The trend seemed to reverse with recovery. The peak height is plotted in Fig. 69. It is interesting to look at the phase relationship between the return of pH to normal conditions and restoration of the PCr and ATP to their maximum recovery levels. The pH inside and outside the cells vs. time are plotted in a composite figure (Fig. 67E) with PCr and the ATPβ peaks. The pH inside the cells during the recovery phase was determined as in section 4.3.4.1, but it was not possible to resolve the internal Pi peak in the acidic going phase, where the internal and external pH values are assumed to be close to equal.

The time course of the outside pH was identical with resumption of oxygenation of the cells and with restoration of normal glucose levels, and in this sense gives a benchmark from which to judge the time required for the cells to replenish their ATP and PCr stores. From these data we can see that there was a 15-minute delay between the time the external pH reached an equilibrium value, and the time the internal pH reached it. Throughout this fifteen minutes period, the ATP was continuously rising, but the PCr level remained at zero, and recovered precipitously exactly in phase with the internal pH, mimicking the results of the pH jump experiments in section 4.3.4.1. These results taken with the pH jump experiment suggest that during the recovery phase from

Figure 69

Changes in the phosphomonoester (PME) region of undifferentiated N1E-115 undifferentiated cells as compared to the Pi peak during an ischemia episode. A) PME B) Pi

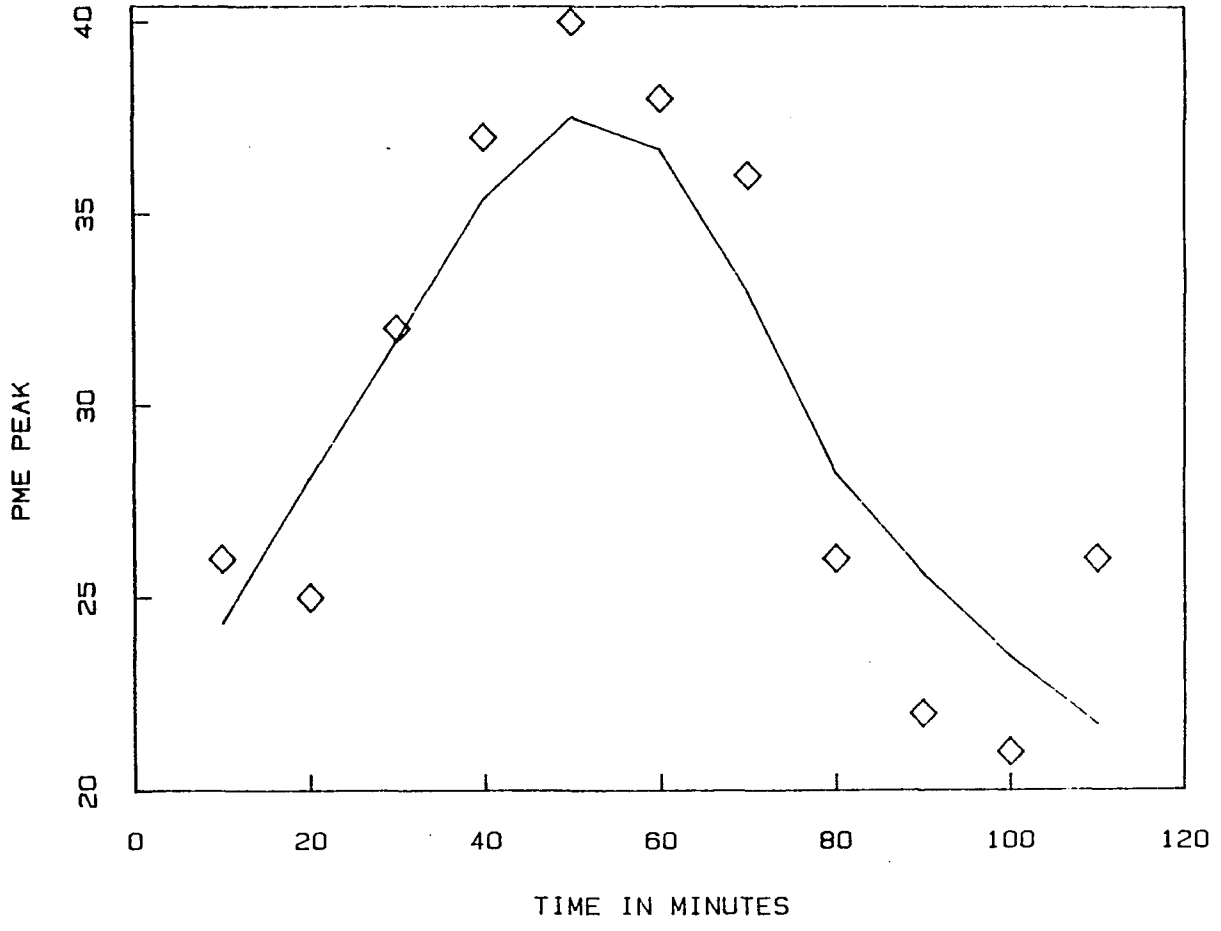

FIG. 69 (A)

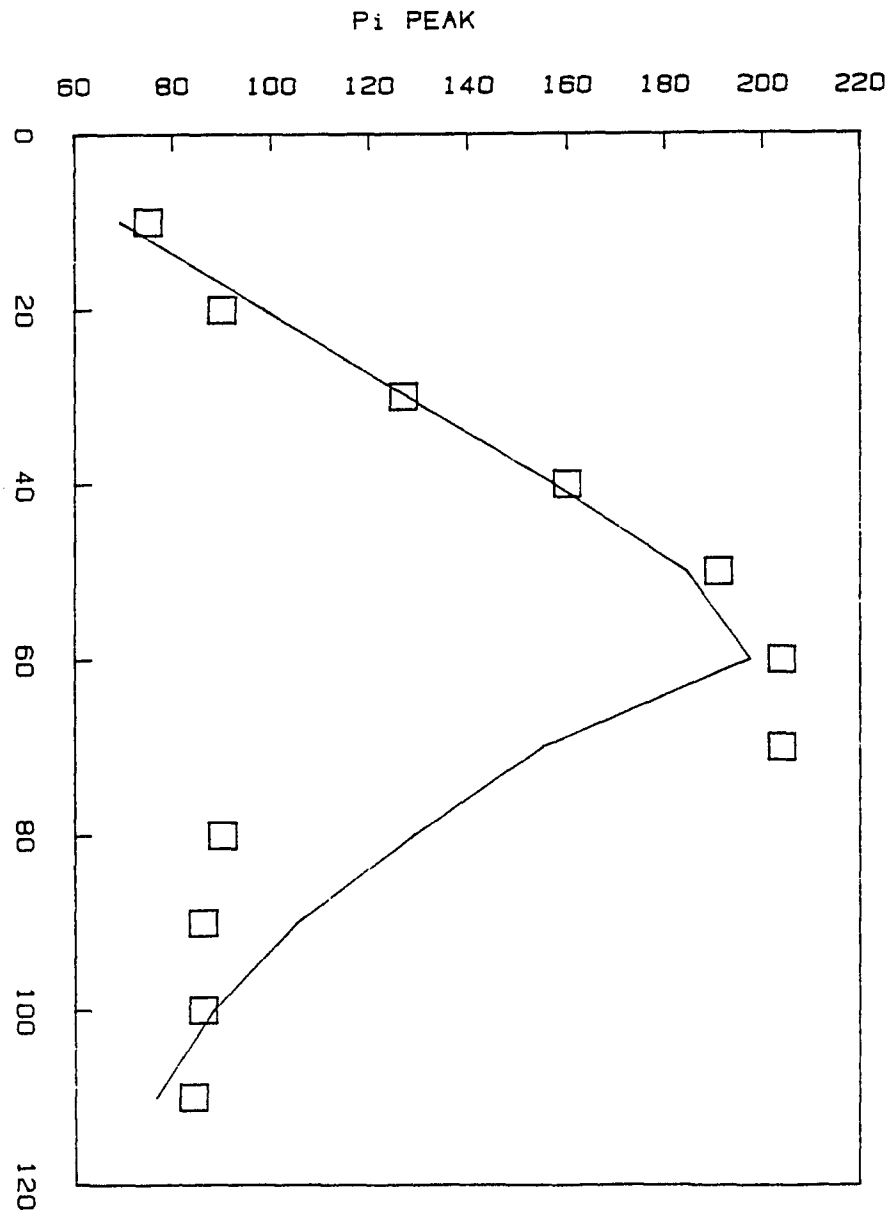
Pi PEAK
60
80
100
120
140
160
180
200
220
0
20
40
60
80
100
120
TIME IN MINUTES

FIG. 69 (B)

ischemia the high H+ concentration pushed the creatine kinase reaction in the direction of Cr where it stayed until a normal physiological ATP was reached, whereupon the pH and PCr concentrations jumped back to normal. The pH gradient sustained for 15 minutes suggested that interesting events concerning the proton gradient were taking place.

The duration of 55 minutes for an ischemic episode was a severe treatment. Therefore, cells were subjected to less demanding conditions of 10, 20 and 30 minutes of ischemia. These results are looked at individually below (see Fig. 70, 71. 72). In all of these experiments the cell systems were equilibrated at a basic medium condition to start with, and with the exception of the 10-minute experiment, all the pH's dip below the normal physiological 7.0 pH value. And with this same exception, all ATP and PCr levels fall with pH in the ischemic phase and rise with pH during the recovery phase. In all cases the pH and ATP recovery lead the PCr appearance. It was not possible to measure the internal pH versus the external pH with any degree of accuracy, and the pH values given are based on the chemical shift of the unresolved Pi peak. In the case of the 10-minute ischemic episode the ATP levels remained constant. The Pi peaks of all but the 10 mM case increased during the ischemic episode as expected. The exception was again the 10 minute case, but this result is open to interpretation because the peak heights of the signal were plotted, and this can be misleading, particularly when the peak had contributions from two sources, as in this case. The area under the Pi peak seems to be larger, although the peak is reduced in absolute peak height. The noisy conditions did not allow good quantitative

Figure 70

10 minute ischemic response of undifferentiated N1E-115 cells. Cells were in standard DMEM supplemented medium without creatine. The ischemic event took place between 10 and 20 minutes on this time scale. A) the extracellular pH leads the PCr recovery by approximately 10 minutes. In this case the pH did not drop below 7.0 in the time of the episode. The ATPβ and ATPα peaks (not shown) did not change. B) the P_i peak went down. This is a result of a pH gradient developing across the cell with a shift of the intracellular peak out from under the external P_i resulting in an apparent decrease in peak height.

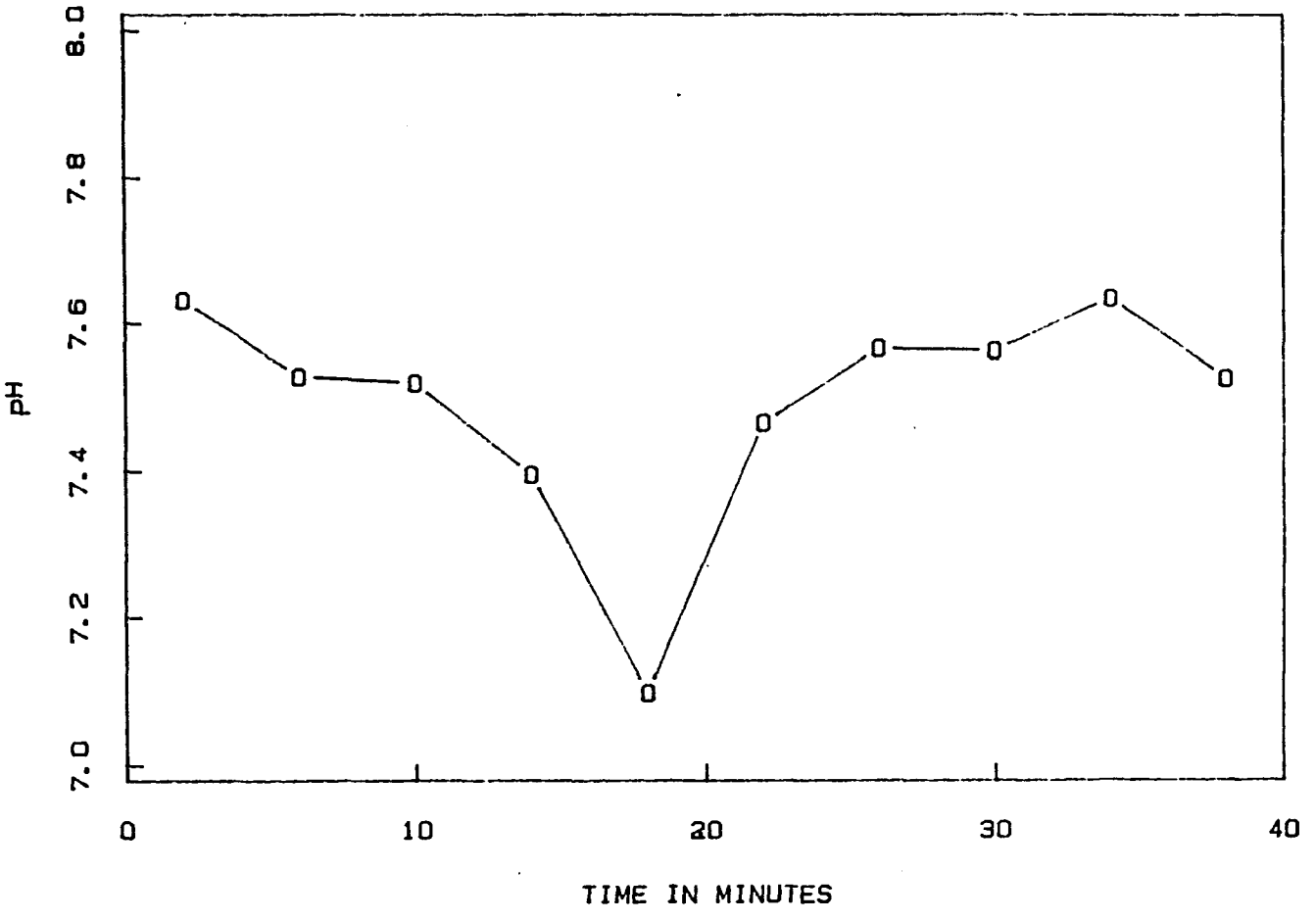

FIG. 70 (A)

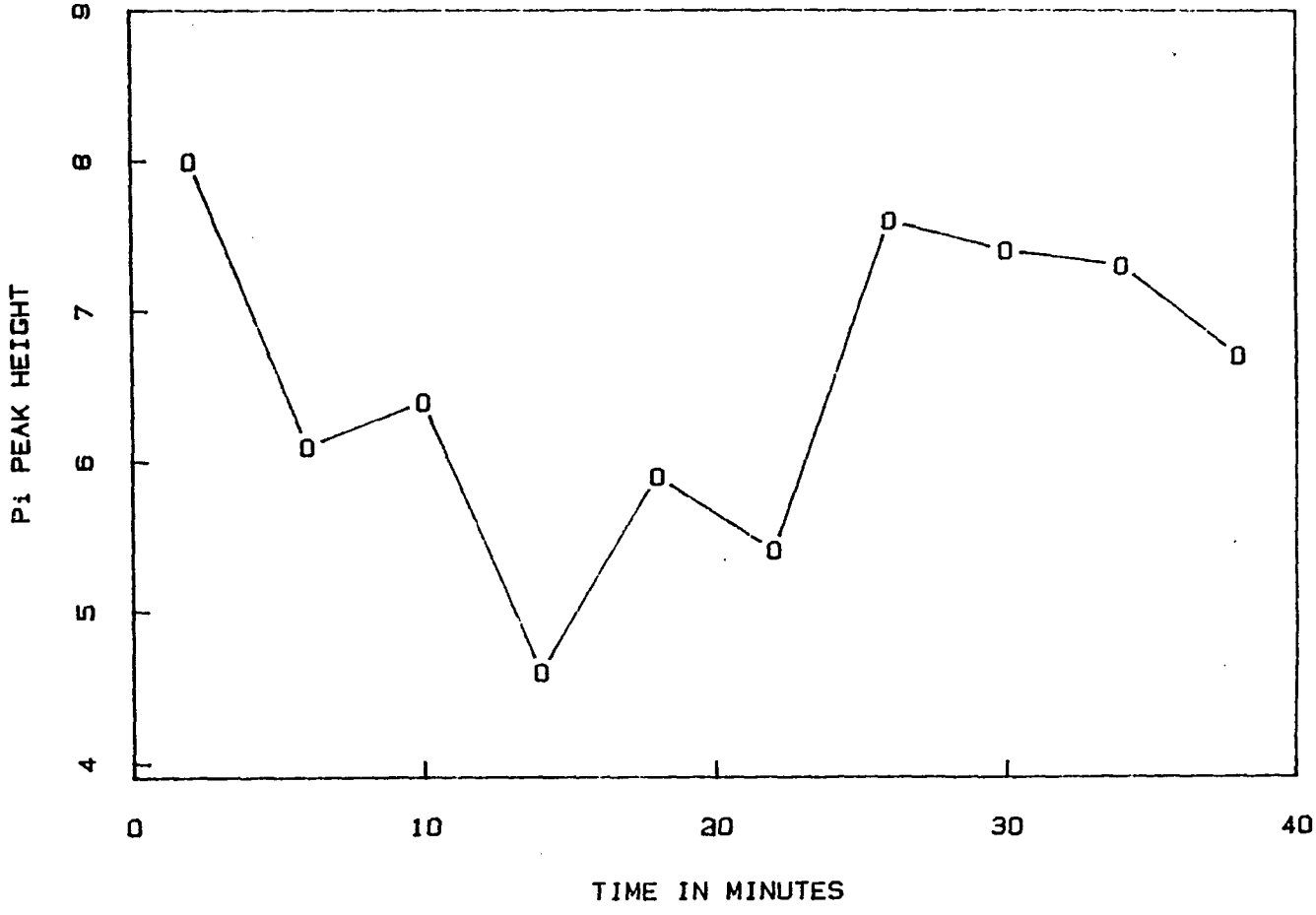

FIG. 70 (B)

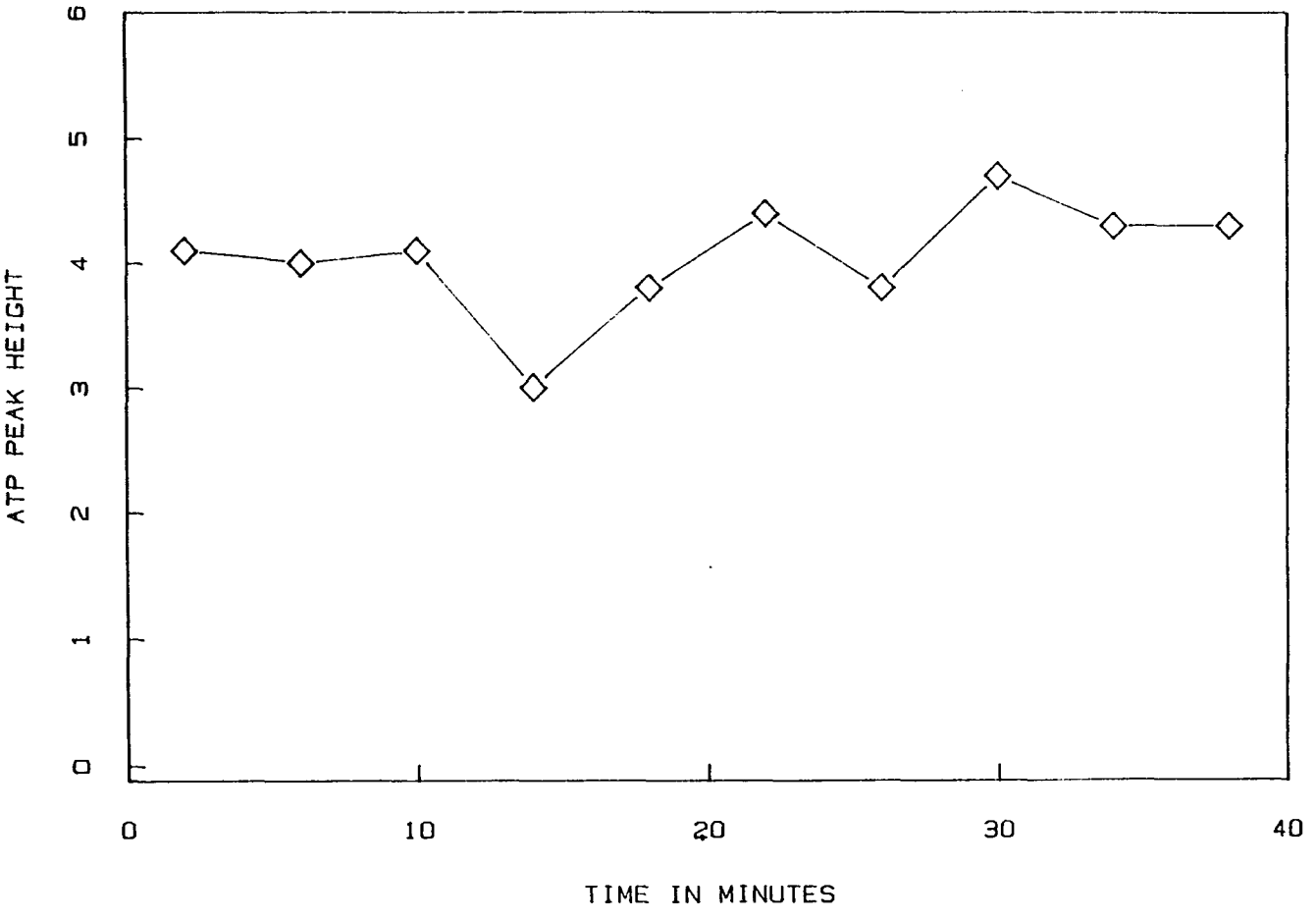

FIG. 70 (C)

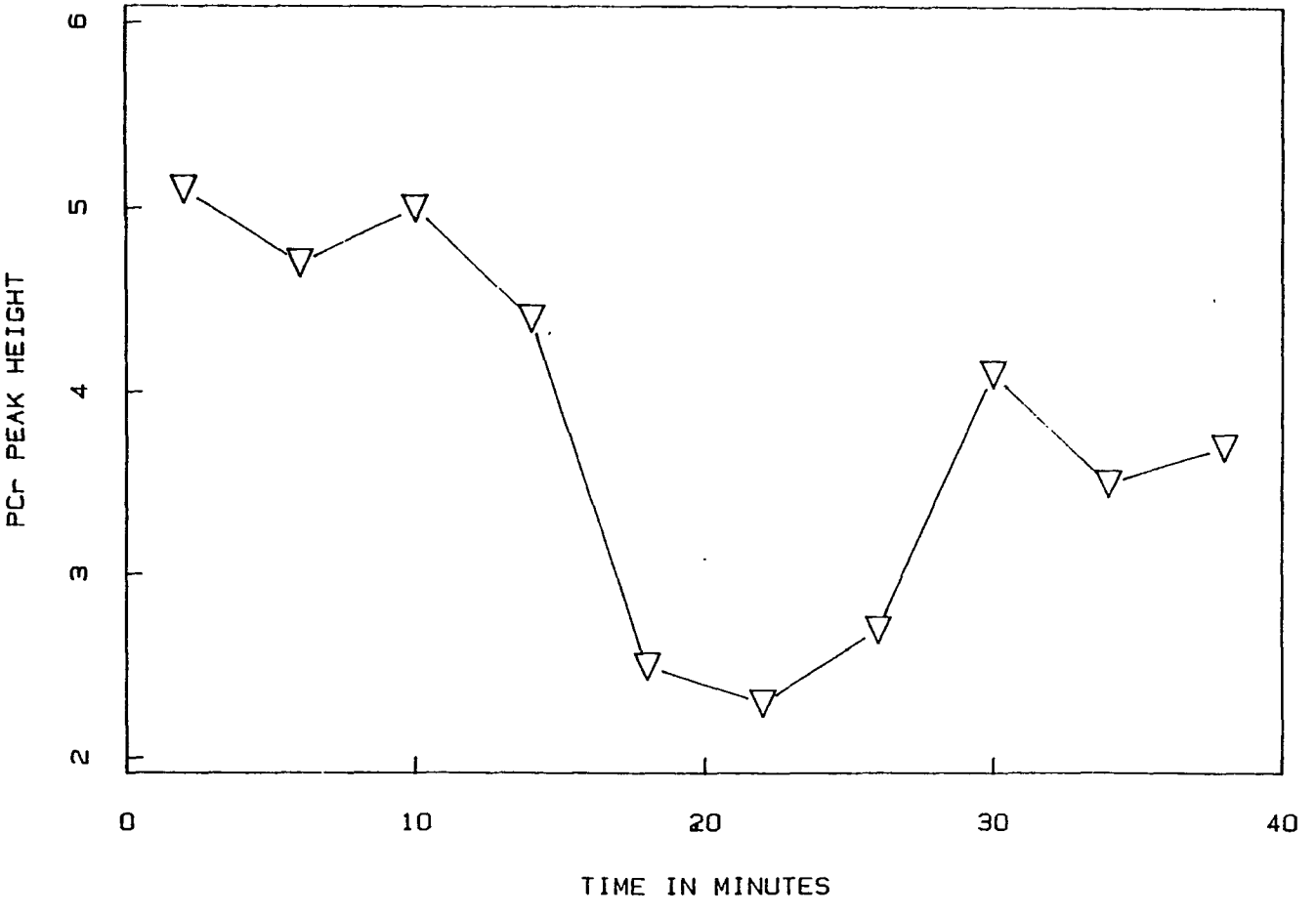

FIG. 70 (D)

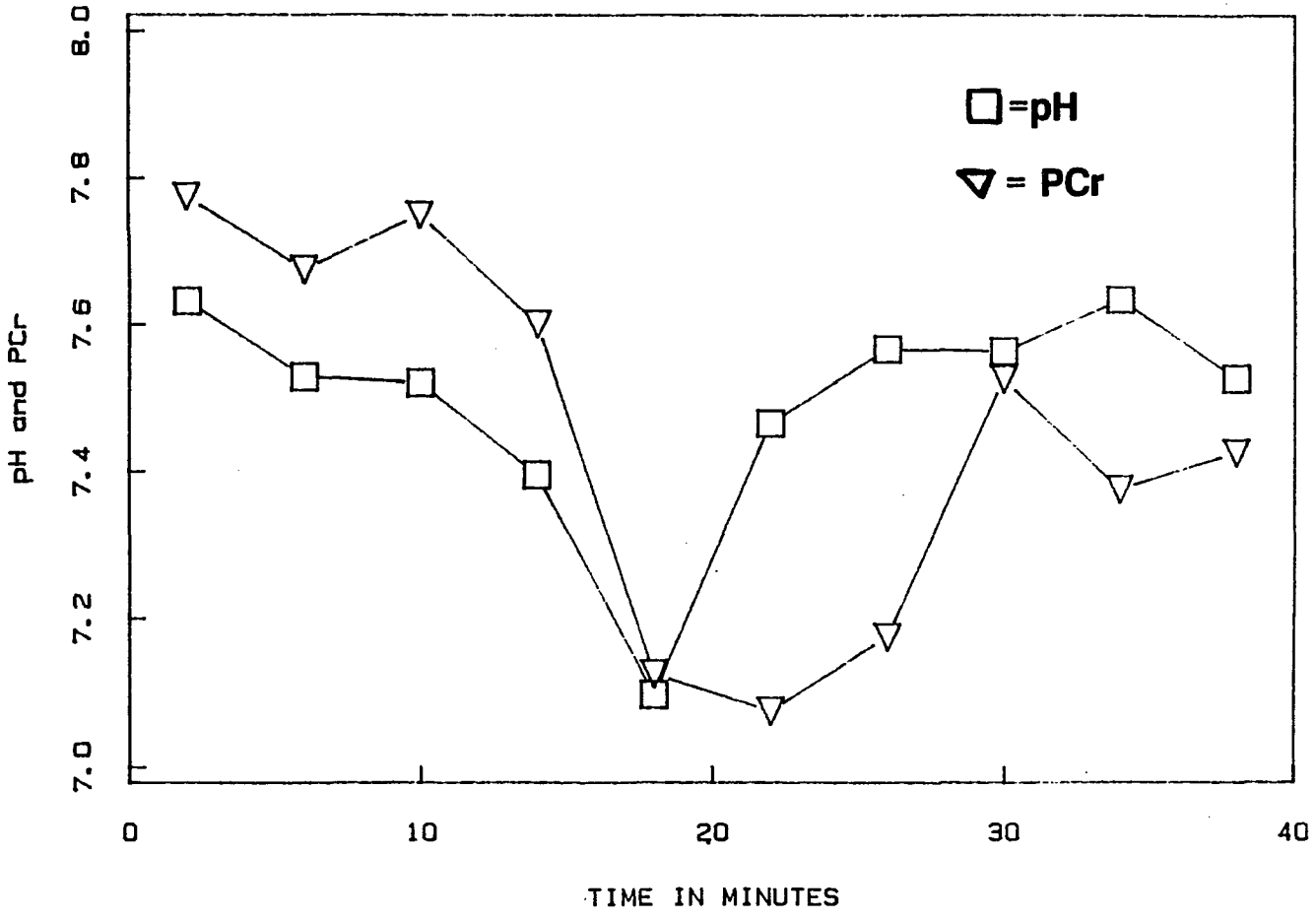

FIG. 70 (E)

Figure 71

20 minute ischemic response of undifferentiated N1E-115 cells. Cells in standard supplemented DMEM without creatine. The ischemic event took place between 0 and 20 minutes on this time scale. A) the extracellular pH, B) the total P_i in the cells and in the extracellular medium. C) shows the individual nucelotide peaks, and D) the PCr. E) For ease of comparison, the sum of the nucleotide peaks, pH and PCr, were plotted. Here, as in other ischemic experiments, the decrease of PCr, ATP and pH are in phase, however only the pH and ATP peaks were in phase upon recovery with the PCr lagging by approximately 30 to 40 minutes.

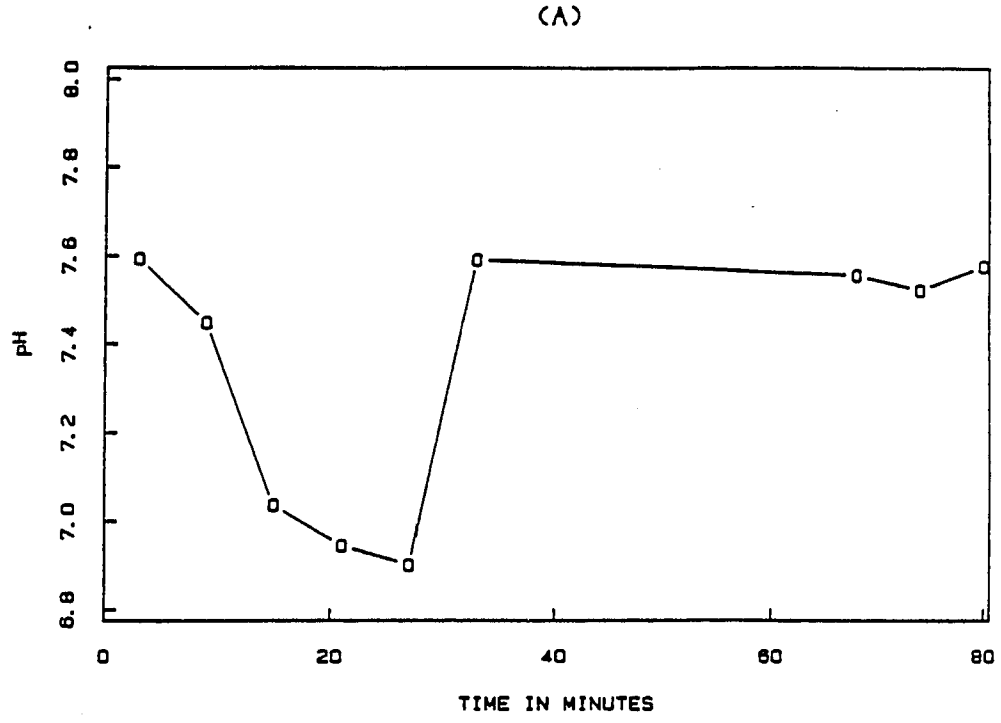
(A)
pH
8.0
7.8
7.6
7.4
7.2
7.0
6.8
0
20
40
60
80
TIME IN MINUTES

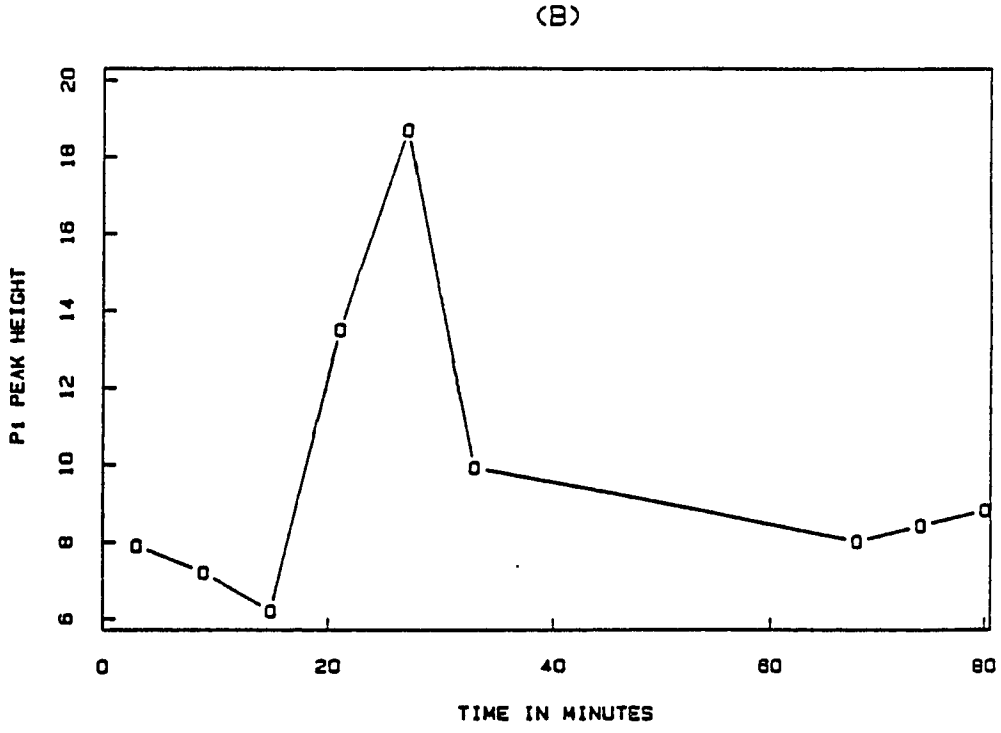
(B)
P1 PEAK HEIGHT
20
18
16
14
12
10
8
6
0
20
40
60
80
TIME IN MINUTES

FIG. 71 (A) (B)

(C)

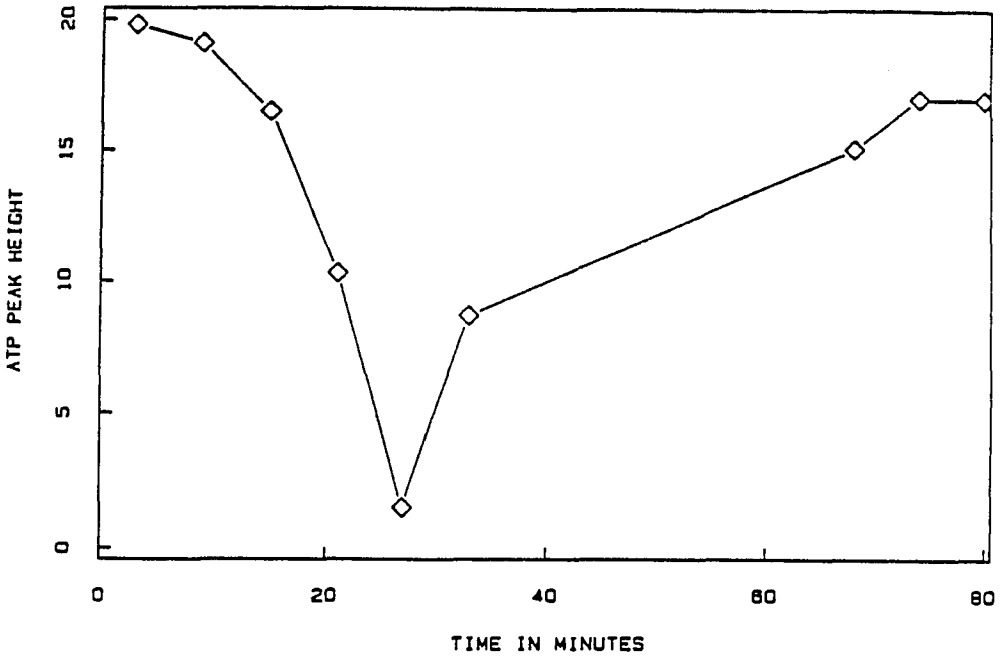
ATP PEAK HEIGHT
0
5
10
15
20
0
20
40
60
80
TIME IN MINUTES

(D)

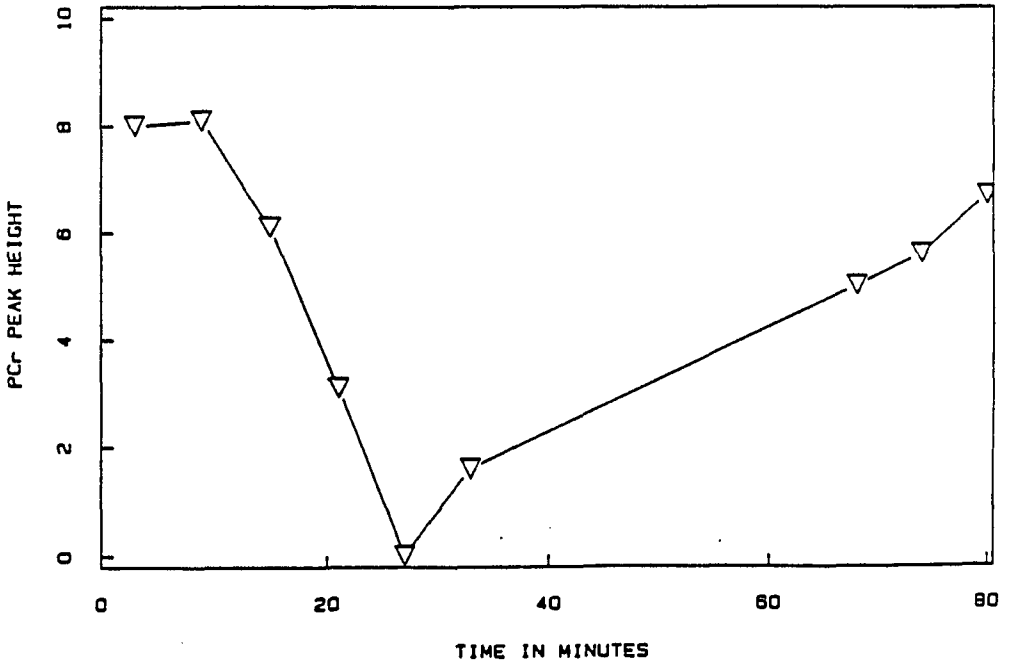
PCr PEAK HEIGHT
0
2
4
6
8
10
0
20
40
60
80
TIME IN MINUTES

FIG. 71 (C) (D)

Figure 72

30 minute ischemic response of undifferentiated N1E-115 cells. Cells were in standard DMEM supplemented medium without creatine. The ischemic event took place between 0 and 30 minutes. A) is the extracellular pH, B) the total P_i in the cell and in the extracellular medium. C) shows the individual nucleotide peaks. D) the PCr, and for ease of comparison, the sum of the nucleotide peaks, pH and PCr are plotted. Here the pH and ATP recovery led the PCr by 18 minutes.

(A)

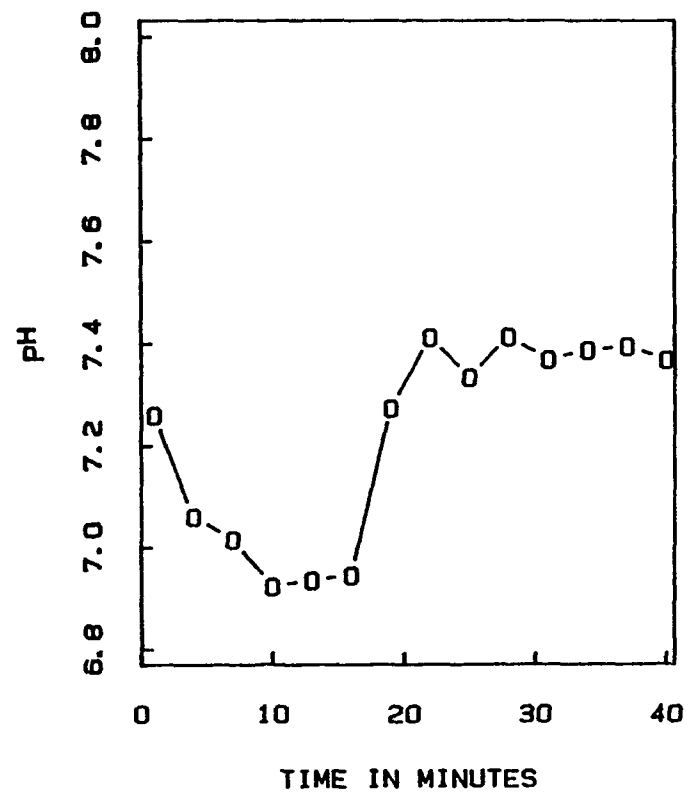

FIG. 72 (A)

(B)

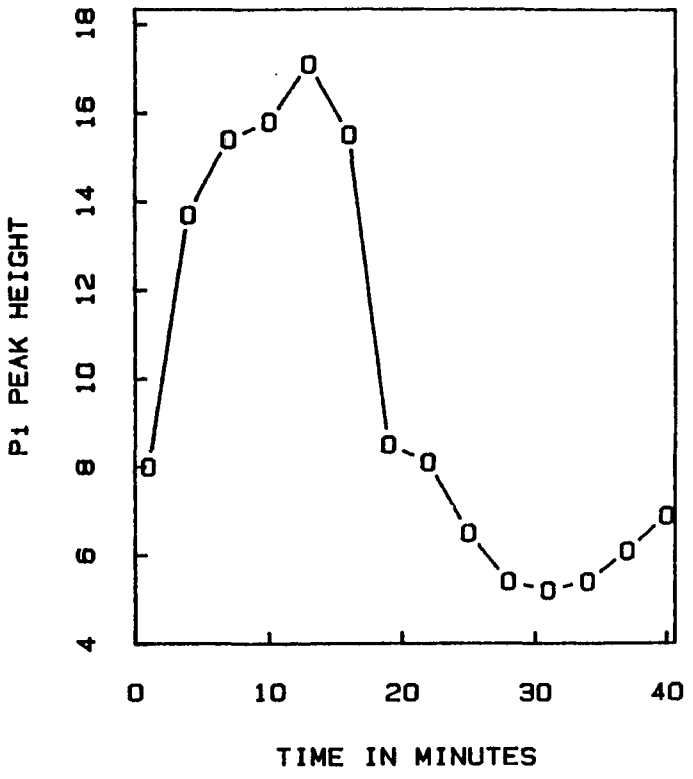

FIG. 72 (B)

(C)

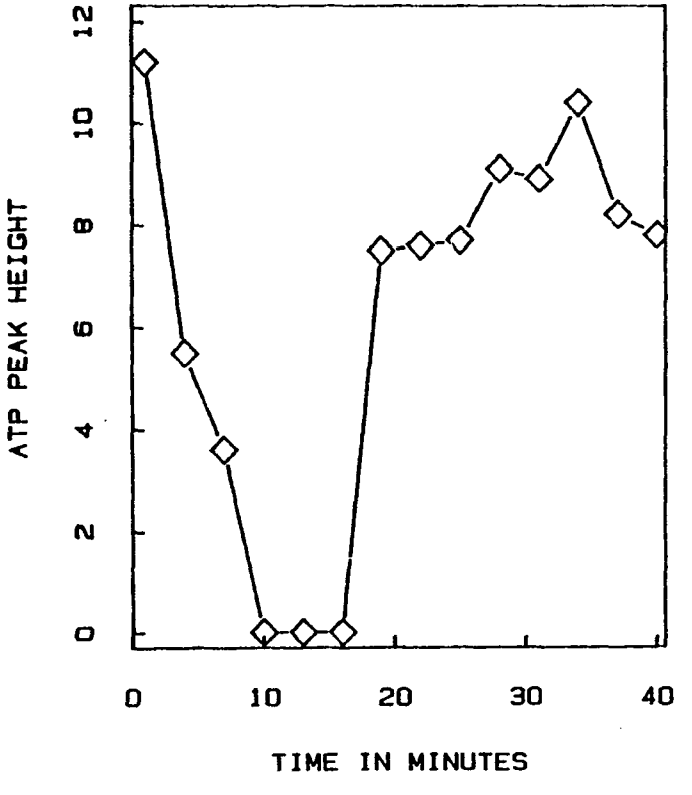

FIG. 72 (C)

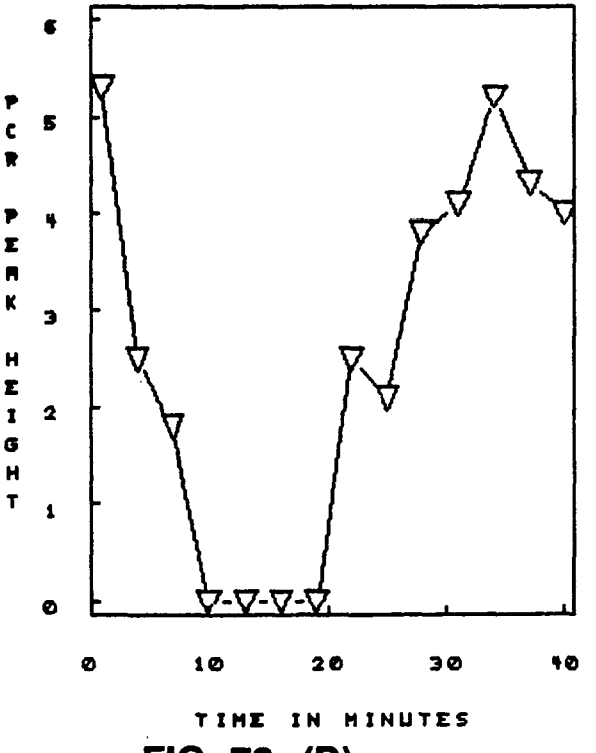

FIG. 72 (D)

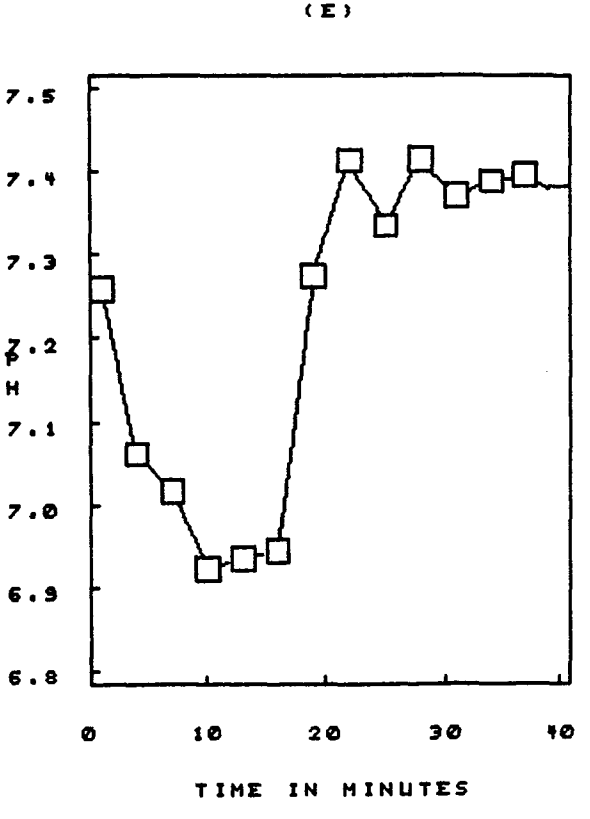

FIG. 72 (E)

evaluation of this result.

The degree of recovered of the ATP concentration was 100% for the 10 minute episode and substantially less for all longer times. In all respects, these shorter times of ischemia down to, but not including the ten minute condition, substantially correspond to the observations made above for the 55 minute condition.

When the time taken for the PCr to recover to one half of its final height was measured relative to the time the external pH recovered to $\frac{1}{2}$ its original value, and plotted against the time of the ischemic episode, what was found was a linearly increasing function of time of the ischemic episode (see Fig. 73). This suggests that the return of the intercellular pH to its normal value was also a linear function of time of the ischemic response.

Ischemic experiments were not run on DRBC, which were charged with PCr.

4.3.7 Stress on undifferentiated and differentiated cells as a result of the addition of extracellular potassium chloride

In order to test the effect of what can be considered normal stress on the cells, they were subjected to a higher than normal concentration of extracellular K^+, a high enough concentration to cause depolarization in fully differentiated neuroblastoma cells. For comparison, the same experiment was conducted on both differentiated cells and on undifferentiated cells.

Figure 73

This is a summary of the four ischemic response experiments. ΔpH is the total excursion experienced during the ischemic episode. 1/2 T recovery is the time for the PCr peak to recover to 1/2 of its final value relative to the return of the extracellular pH to 1/2 its final value.

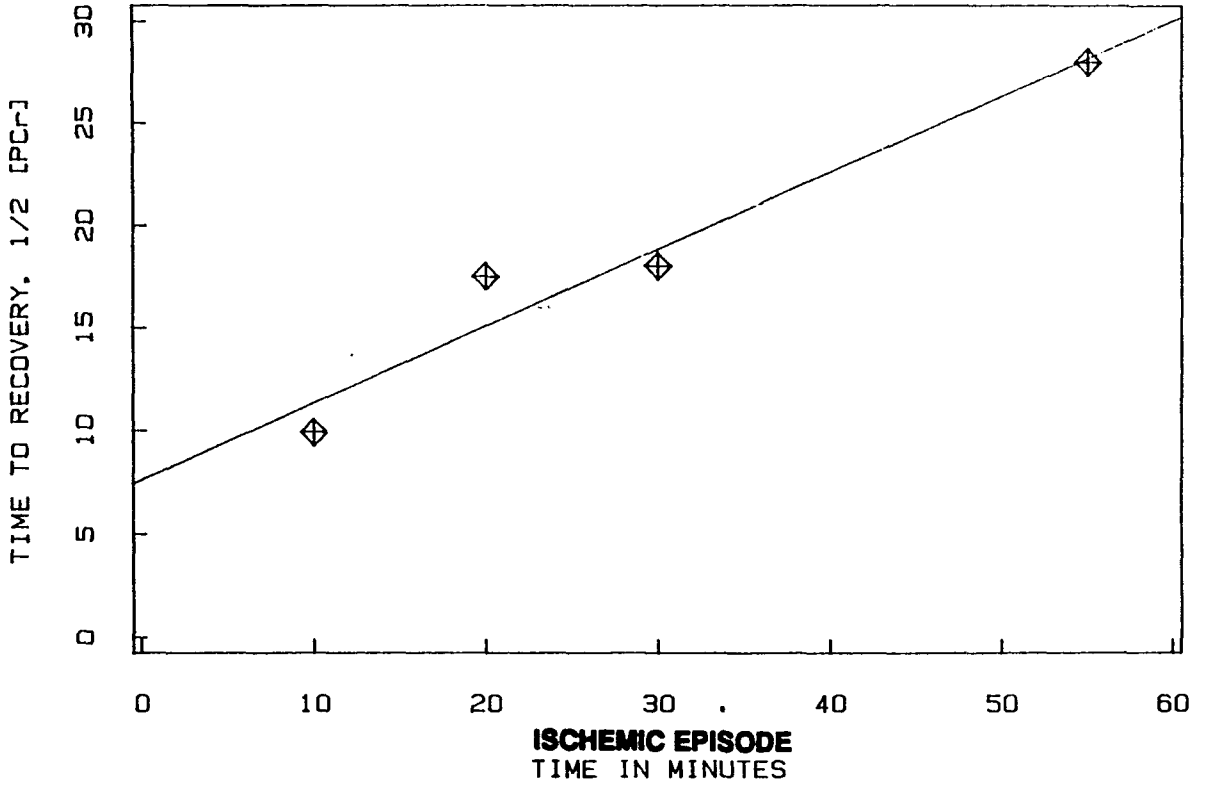
TIME TO RECOVERY, 1/2 [PCr]
0
5
10
15
20
25
30
0
10
20
30
40
50
60
ISCHEMIC EPISODE
TIME IN MINUTES

FIG. 73

As in previous experiments, N1E-115 cells were grown in standard tissue culture conditions in DMEM supplemented with 10% FBS, 1% penicillin-streptomycin and 0.2mM Cr (final concentration). The cells used in the NMR experiment which were not differentiated were continued in this medium; those to be looked at in the differentiated state were switched to DMEM supplemented with 2% DMSO, 2% FBS, 0.2 mM Cr (final concentration) and fed every other day for fourteen days, at the end of which time they were used in an experiment. In both cases the cells were seeded on Cytodex III, put in the life-support system, and superfused with the same medium on which they had been growing, but it was supplemented with 10 mM Cr for twenty-four hours, after which they were switched to identical medium, but with 0.2 mM Cr instead of 10 mM Cr, for an additional twenty- hour hours in the case of the undifferentiated cells, but kept on 10 mM Cr in the case of the differentiated cells. This insured that the cells were charged with PCr. At this time KCl was added to the recirculating superfusate of the life support system to a final concentration of 80 mM.

The undifferentiated cells showed no obvious difference between the two or three files before and after the addition of KCl.

Figure 74 shows the spectrum of undifferentiated N1E-115 cells at the beginning of the experiment and at the end. The pH was basic, above 8, the difference spectrum between the beginning and the end of the experiment showed no appreciable difference in the peak height as a result of the KCl addition. For the differentiated cells shown in Fig. 75, this is not the case.

Figure 74

Effect of KCl on undifferentiated N1E-115 cells. (A) is the 15 minute file before the KCl medium entered the sample holder. (B)is the average of the last fifteen minutes of the experiment 150 minutes later. The noise is relatively large, so the first four 15-minute files were added (C), and subtracted from the last four files (D) to give the difference (E). Each file is the sum of 300 FID with a separation of 3 seconds of 60 pulse was used. The superfusate pH was greater than 8.

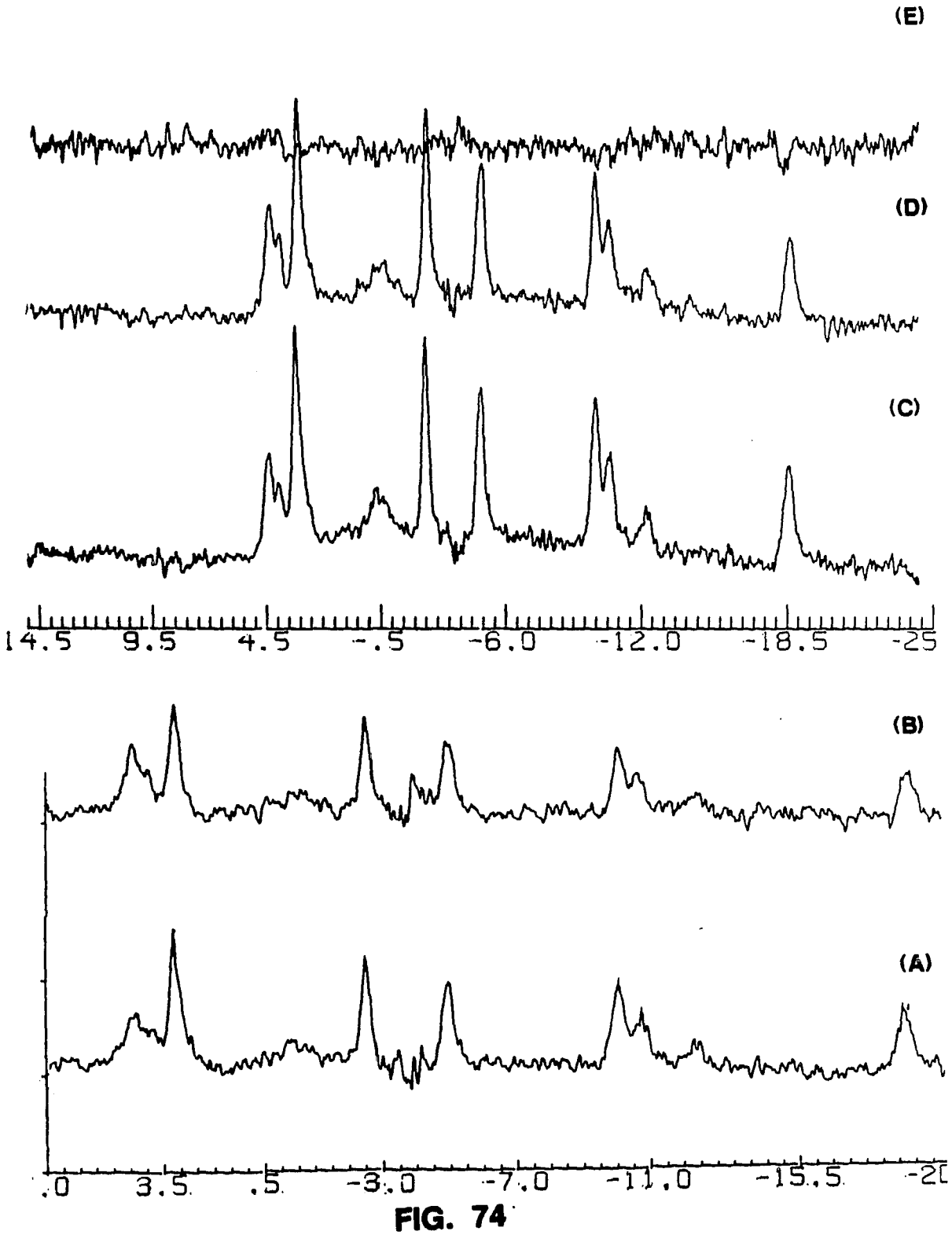

FIG. 74

Figure 75

Differentiated N1E-115 cells grown on DMEM + 2% DMSO + 2% FBS + 1% PS and 0.2 mM Cr fifteen days in standard tissue culture techniques were put in the life-support system and superfused with the same medium plus 10 mM Cr. KCl was added to the superfusate in a closed recirculating system to a final concentration of 80 mM. The KCl was added at the end of file one. At the end of 80 minutes after file eleven, the superfusate was switched to the original growth medium, i.e., with 0.2 mM Cr and low KCl. File one is the control. The high K+ reached the cell holder at the beginning of file two. Each file is the sum of 150 FID's obtained with a 70 pulse in a 7.5 minute interval. The peak height of the spectra, pH and difference in the chemical shift between PEt and PCh are presented in Fig. 76.

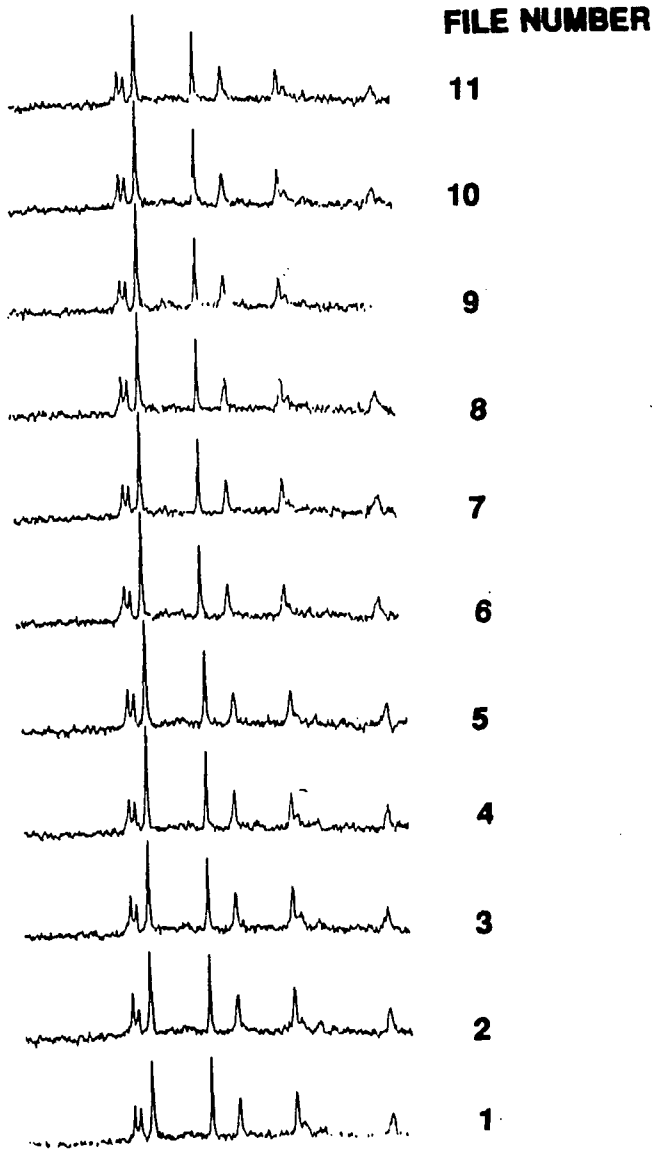

FIG. 75

These cells were kept on 10 mM Cr, and 80 mM KCl final concentration was added to the recirculating medium in the middle of the first file, and first reached the cell holder in the time file number two was being accumulated. In this 7.5 minute interval, the PCh decreased 12% and the PEt increased 15%, and within 15 minutes returned to their normal control values. This may be the result of the small external pH shift of -0.015 pH units, which accompanied the addition of the KCl and a titration of the PEt and PCh peaks. This estimate of the delta pH was based on the internal pH estimated from the PEt and the external pH measured from the Pi. The major effect is reflected in Fig. 76.

Pi in the sample holder increased 33% within 30 minutes and stayed high until the superfusate was switched to DMEM medium without KCl supplemented. There were comparable decreases in the PCr and nucleotide phosphates. The PCr started to decline in concentration about fifteen minutes before the nucleotide phosphates. The error in these measurements was large because of the short accumulation time, 7.5 minutes, and with the return of the PCr and nucleotide phosphates to their original concentrations, it is difficult to say if one proceeded the other. The medium of the superfusate during this recovery period had 0.2 mM Cr in it; therefore, the PCr recovery in the time frame of one hour demonstrated the Cr was not lost from the cells. These experiments show that upon depolarization with 80 mM KCl, the phosphate profile of the cells changed. It has been shown here that chronic depolarization of N1E-115 cells drains energy reserves at a rate faster than they can be restored by oxidative phosphorylation and glycolysis.

Figure 76

The data obtained from the spectra in Fig. 75 are presented here. (A) Pi vs. time. (B) pH vs time. (C) PCr vs time. (D) The sum of all the nucleotide peaks. (E) The ATPβ peak. (F) The difference between the PEt and PCh chemical shift. At the point indicated, the medium was switched from one containing .2 mM Cr and 80 mM KCl to one containing only DMEM, 2% DMSO, 2% FBS, 1% PS and 0.2 MM Cr.

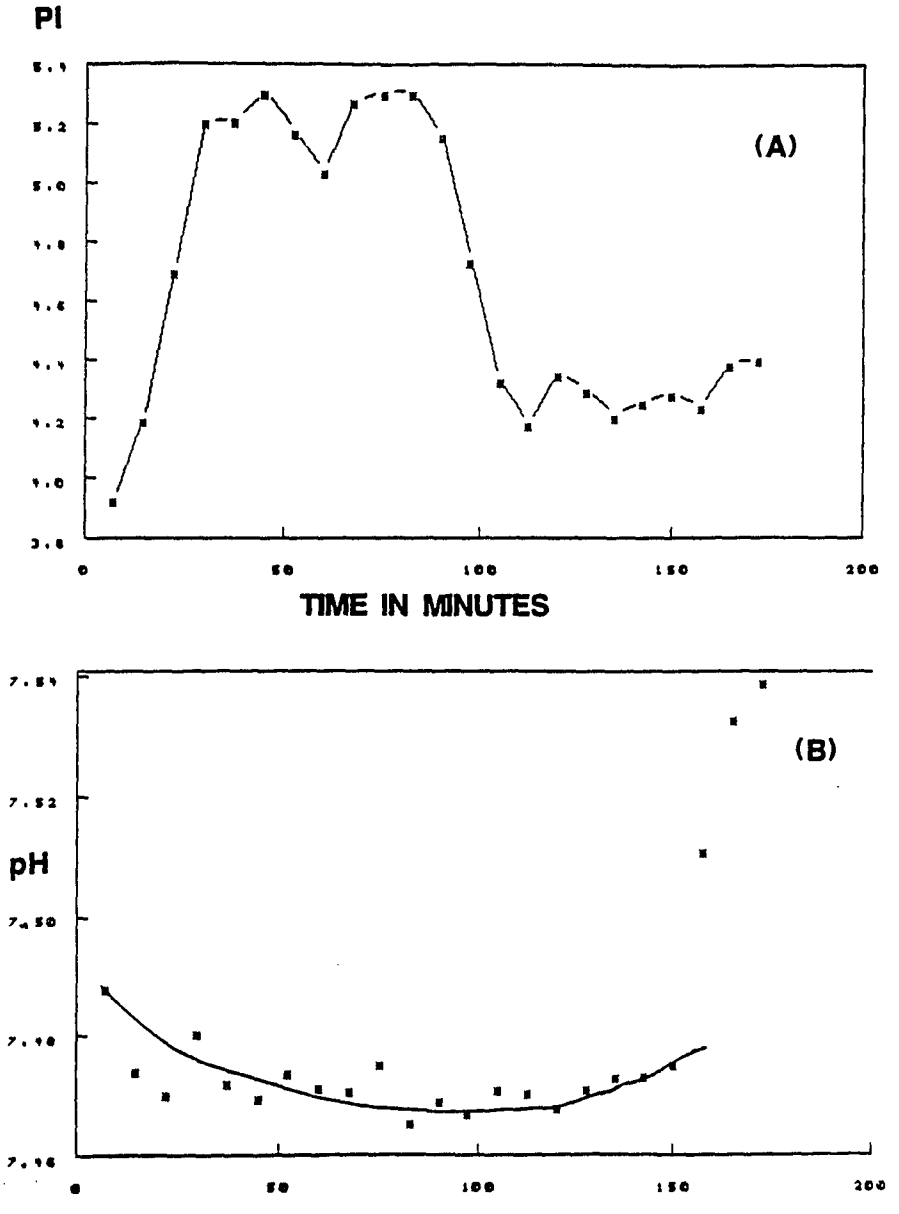

FIG. 76 (A) (B)

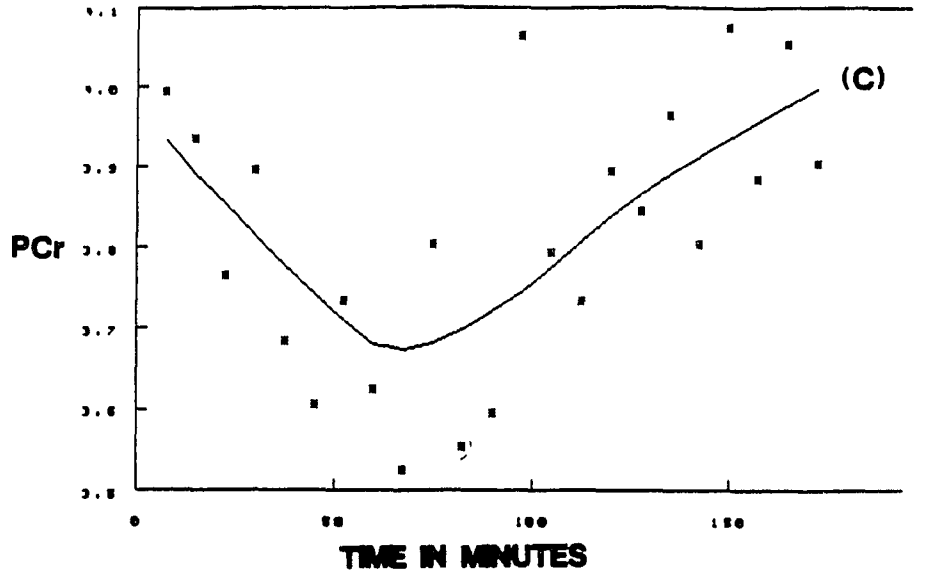

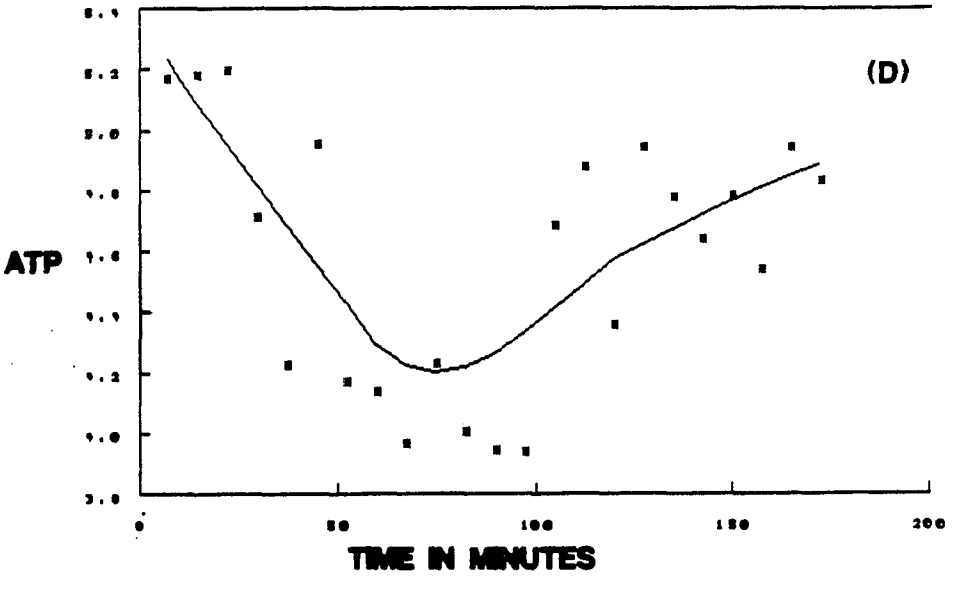

FIG. 76 (C) (D)

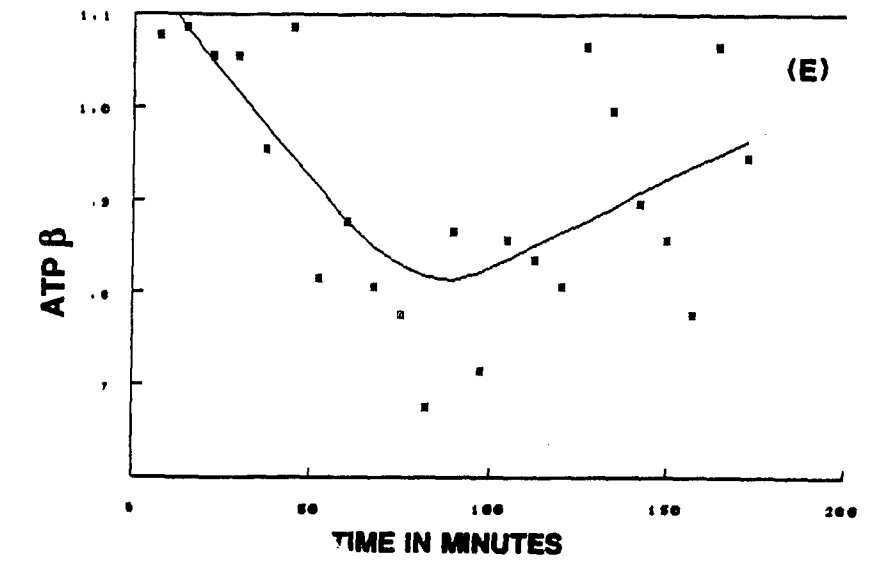
(E)
ATP β
TIME IN MINUTES

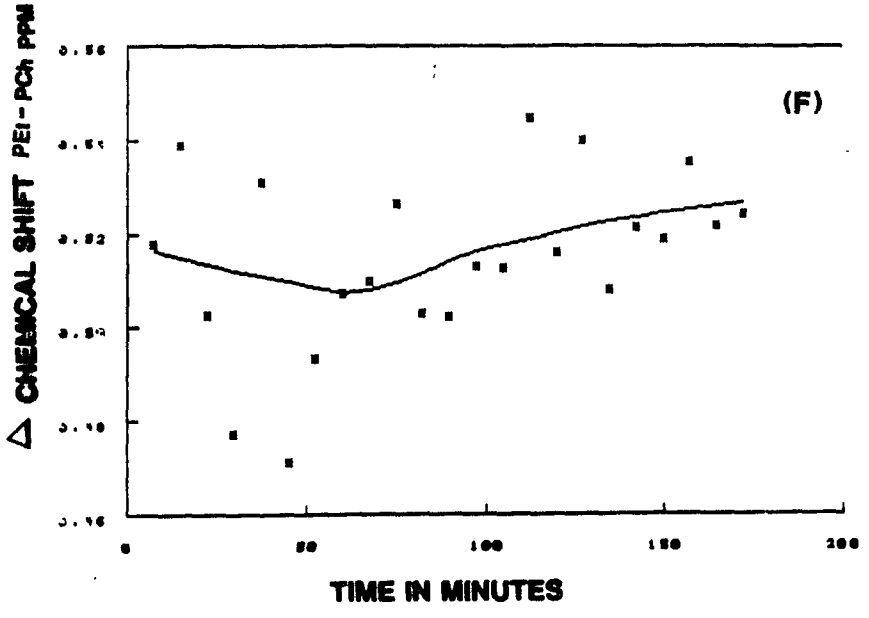
(F)
Δ CHEMICAL SHIFT PEt - PCh PPM
TIME IN MINUTES

FIG. 76 (E) (F)

5. DISCUSSION

The research presented in this work started as a result of asking the question: how can anchorage-dependent cells be looked at using NMR spectroscopy, and in particular, what happens to the ATP in cells of neuronal systems when they are stressed? The microcarrier-based system developed here and used to study four cell types has answered these questions and posed many more (Figs. 12, 16, 19).

There is no question that cells growing in high density and continuously superfused with medium are different from those raised in conventional tissue-culture dishes and incubators, where they are fed three times a week.

The most striking difference between cells raised in traditional tissue-culture conditions and those in the life-support system is the difference in the rate of growth. Cells taken in mid-to-late log growth from standard tissue culture conditions, when transferred to the microcarrier-based system, virtually stop dividing but remain viable, as judged by their ATP levels while in the life-support system, and by their morphology upon removal from the system. There is evidence based on DNA measurements that some growth continues in the case of C3T10½ cells. Evidence in the case of the undifferentiated N1E-115 cells suggests that there is a balance between slow cell multiplication and death such that the total number of viable cells does not change. These changes can be explored by measuring parameters such as changes in DNA and protein content of the sample holder, changes in cell count, and volume with time.

These factors surely vary with cell type and state of differentiation. The difference suggested above should pose some problems in translating experience gained on a cell system in the life-support system to standard tissue culture conditions and in vivo environment. These should be resolvable.

It seems more reasonable to use a life-support system than standard tissue culture conditions when the experimental protocol permits because it mimics the geometric constraints of the in vivo systems more closely than standard tissue culture conditions do. The major concerns in standard tissue culture conditions, other than adequate space for cell attachment and growth, are adequate oxygen and nutrient delivery, pH balance, removal of waste products and sterility. All of these have been addressed and resolved with the life-support systems.

The delivery of nutrients and removal of waste are done continuously with respect to the cells and periodically with respect to the reservoir. The reservoir was replenished in a one-shot process or partially drained and replenished, thus buffering the cells from medium shock. This is an improvement over three time a week feeding in standard tissue culture conditions. The cells are not subjected to a basic shock, which frequently accompanies standard tissue culture feedings. Experiments presented here show that adequate oxygen is supplied to the cells. It is possible under more demanding conditions, re-energized whole blood can be used. This is possible with mouse blood. This system, when loaded with neuroblastoma cells and superfused with medium containing mouse red blood cells, permitted the blood cells to continuously

circulate through the system, passing through the sample holder containing cells on microcarriers unhindered. This system was not needed for the protocols used here, and was not examined more closely.

Very tight control of the pH in terms of hundreds of pH units was obtained over periods of hours using a sodium bicarbonate system (Fig. 18). The crucial component in this regulation is the pressure regulation of the oxygen and carbon dioxide sources. It is essential to have a low pressure regulator in series with a two-stage high-pressure regulator to keep these tight tolerances.

Sterility, the major factor affecting the length of time cells can be kept viable in the life-support system, is the most crucial and sensitive aspect of any culture system. Without natural immunological systems, the culture systems are extremely sensitive to bacteria, fungus and yeast. The life-support system is more vulnerable at the sample-loading stage than spinner bottles or standard tissue culture conditions. Two protocols were used in sterilizing the system and loading the cells. The most stringent was to use a life-support system wrapped in aluminum foil and autoclaved at 15 psi and 120C for two hours. The life-support system was loaded in a hood with cells on microcarriers. The stoppers were removed with gloved hands washed in ethanol. The system was autoclaved with empty reservoir bottles in place. Bottles of fresh medium were substituted for these while the system was in the hood. The cells themselves were raised and passaged in T150 flasks up to the final passage, at which time they were transferred to fifteen or thirty 150 mm tissue-culture plates. When medium bottles were replaced it was done in a hood. This procedure is time

consuming and painstaking, and gives a life expectancy of greater than one month, the longest time a system was monitored, with a probability of success of 0.5 (n=4). Most of the experiments used a less stringent protocol.

In the second procedure, the system was not autoclaved, but was washed first with 500 ml of 0.1 N HCl, then 500 ml of 0.1N sodium hydroxide, followed with a final wash with 500 ml of autoclaved, doubly-distilled water, supplemented with 3% penicillin-streptomycin. The sample-holder stopper was sprayed with ethanol, as were the medium bottle caps and gloved hands. The cells on the microcarriers were pipetted into the sample holder in a conventional room without a hood. The life expectancy was 10 to 14 days for this system when the reservoir bottle was changed daily. Thus, the longevity of the system can be controlled, leaving the door open to do experiments on the same cells over a period of weeks or months, so that cells at different stages of development or maturity can be looked at. For example, undifferentiated cells were looked at over a five-day period, during which time they were induced to differentiate.

The cell-microcarrier complex is at the heart of the system. How the cells attach to various microcarrier surfaces is an important factor in determining how fast the superfusate can be pumped through the system and whether or not the cells will be sheared off the microcarrier, clogging the exit port of the sample holder. C3HT10½ cells were found to stick tenaciously to any of the Cytodex microcarriers. The C6 cells also stick very tightly to the Cytodex III microcarriers, and in the case of both of these cells lines, the seeding of a few

cells per microcarrier, followed by a ten-day to two-week incubation results in a good NMR sample. On the other hand, dissociated rat brain cells adhere best to a polylysine-coated Biosylon microcarrier, and N1E-115 undifferentiated cells adhere best to Cytodex III microcarriers having a collagen coating.

What has been found is that ideal coating of the microcarrier with cells may not give the best experimental system. In the extreme, small bits of tissue mixed with microcarrier acting as a matrix to separate the tissue, gives an excellent solution for looking at tissue minces. This has worked well for C1300 primary cultures. This solution is also good for dissociated rat brain cells, which have been allowed to aggregate into spheres of 100-300 μm in diameter in tissue culture. Some cells, the C6 glioma, for example, form mono-layers on the microcarrier, and since they have a cell volume one-fiftieth of the neuroblastoma, they give a proportionally smaller signal. It is therefore better from a signal-to- noise point of view, to have a mixture such as has been encountered with dissociated rat brain cells and undifferentiated N1E-115, namely, cells aggregating with themselves and also with the microcarriers, forming roughly spherical aggregates of cells 50-200 μm in diameter, which attach to each other and to cell-laden microcarriers, forming a labrinyth through which medium passes.

The observations made on the cell systems described here demonstrate the need for investigating the various microcarrier-cell systems for each cell type, keeping in mind diffusion length of oxygen, nutrient and waste products in cell aggregates, substrate adhesion factors, and cell volumes necessary for a

reasonable NMR signal. It was fortuitous that the neuroblastoma cell line was chosen as a neuronal model for these experiments over a PC12 or B50 cell line, which have a fraction of the volume.

With this system, the best pumping speed was found to be 3 ml per minute (Fig. 16 to 19). This value reflects the best balance between the factors which determine what the superfusate, pH, temperature, and gas content are when it reaches the cells, using the sample holder under the condition of insulation and plumbing lengths used. Because of the interactive nature of the various elements involved, pump speed was not altered. With the addition of a second independent temperature bath, the temperature of the input medium could be controlled independently. This would be an important modification, in that temperature cycling could be used to synchronize cell division, modify enzyme behavior or determine the effect of pharmicological agents as a function of cell temperature.

The washout time of the system is between 10 and 20 minutes. This sets a limit on the resolution of effects observed by washing an agent or drug into or out of a system in a one-shot experiment, but time resolution down to the order of magnitude of the applied pulse width are theoretically possible with a system which is cyclic and has a reasonably short refraction period, for example it should be possible to study an intact retina by stimulating it with a light pulse synchronized to the NMR computer, such that the probe pulse of the NMR spectrometer is generated, say, 100 μ second after the light stimulus is turned on, and the resulting FID stored, and then repeating the experiment for various

delay times after the light stimulus is turned on, after which the whole set of experiments could be repeated a number of times until sufficient signal-to-noise is obtained. The ability of the life-support system to keep the preparation in a healthy, stable state will determine the ultimate time resolution and signal-to-noise ratio. This synchronous approach to the visual system with optical stimulation or to the neuronal system with electrical stimulation will generate interesting results in the future.

The second half of the story in obtaining a good NMR signal is the design of the probe. The single-turn probe developed here and used with the microcarrier-based life-support system results in a homogeneous field, giving better than 10 HZ for the width of the PCr peak at 1/2 height. With a good cell sample, a spectrum of ATP can be observed in two minutes. With longer accumulation, differences in the intra- and extracellular pH can be made to 0.01 ph units of resolution.

The filling factor for cells is low, there being 0.6 ml of cell volume in a 6.0 ml sample holder, yet a good signal in reasonable times can be obtained. Although this system gives good results, there are problems maintaining a good flow profile through the sample. Frequently the interface between the medium and microcarriers slopes relative to the axies of the solenoid, interfering with homogeneous flow through the sample. Thus, the development of a solenoid coil configuration with vertical flow would be a great improvement. The testing of such a configuration is currently being done. This system is a first step in the development of a tissue culture system capable of using a number of nuclei such

as ^{13}C, ^{1}H, K, Na and ^{31}P in a variety of complementary ways, such as cross relaxation measurements between 31P and 1H, 2D NMR of protons (with appropriate water suppression) and other nuclei, and in synchronized manner mentioned above to investigate such events as are found in differentiation, development, growth and functional interactions between cells, which involved much smaller concentrations than the fractions of millimoles which are measured here. The long-term stability of a life-support system developed and demonstrated here are the necessary first step in this direction.

There were several major findings that were made while using the life-support system on cells. They center around the creatine kinase reaction in the N1E-115 cells and around changes in the PME and PCr content of these cells when they are induced to differentiate.

The undifferentiated cells were looked at first, and it was found that there was no PCr present (Fig. 30); in fact, its presence was not anticipated, nor were there any peaks in the PME region. The original question asked of the cells was, "How much ATP is there in them, and how is the pool degraded as the cells are subjected to adverse energy draining conditions?" The surprising answer came when the cells were subjected to such a treatment. The ATP reserves did not diminish in a gradual way as the energy drain was increased, but failed catastrophically. (These cells were without a Cr supplement.)

The amount of PCr in the undifferentiated cells was small because creatine is not made by N1E-115 cells and must come from the small amount of Cr in

the feeding medium. The small amount of creatine is derived from the FBS supplement of the growth medium, an amount estimated to be less than 0.2 mM. This small amount of Cr in the medium, the possible lack of a good transport system for Cr, and the rapid doubling time of the cells prevented any perceptible amount of PCr from accumulating. The presence of phosphocreatine was not suspected until an analogue of Cr was added to the cell growth medium and the product of the creatine kinase reaction was observed. By charging the undifferentiated cells up with PCr by the process of subjecting them to larger extracellular physiological concentrations of Cr, changes in the cell system were generated which allowed the general characteristics of the creatine kinase reaction in the intact cell to be evaluated (Fig. 45). Although this is an order of magnitude greater than the normal extracellular concentration, it generated important observations.

The slow PCr appearance when large concentrations of Cr were added to the growth medium allowed for the analysis of the creatine kinase reaction in the life-support system. The rate-limiting step was demonstrated to be the transfer of the Cr into the cells, which is much slower than the creatine kinase reaction. Thus, the pH jump experiments in combination with ^{1}H and ^{31}P NMR spectra of the cells' extract allowed for the calculations of the ATP/ADP and Cr/PCr ratio to be made (Fig. 36-44). The one complicating factor centered around the assumption that the ATP level and ADP levels remain substantially constant over the life of the experiment (Fig. 42).

In the short term, the period before, during and after the pH jump, this is a good assumption, and as long as the extract for the Cr and ADP determinations is made within a one-hour period after the pH jump, all assumptions are reasonable. However there is a substantial increase in the ATP in the hours after the jump to an acidic condition which is not reversed with the return of the cells to acidic condition. These cells at high extracellular pH values of 8 to 9 in tissue culture do not grow and divide. It therefore seems unlikely that they would do so in the life-support system. This leaves the possibility that the ATP concentration was raised in the cells, or that the concentration remained constant, and that for some reason the cell swells at these higher pH levels, and the number of moles per cell was increased by the cell regulating system to keep the cell ATP concentration constant. It is also possible that it is a combination of these reasons.

The constant concentration speculation seems most appealing in light of the importance the role the ATP concentration plays in many enzymatic reactions. It would be reasonable to maintain the ATP concentration constant, so as not to upset the delicate balance of the cells' machinery. As this study suggests, the big factor in doing this is creatine kinase.This is important to know since all excitable cells and some support cells (i.e., muscle and all nerve and glia) have high intermittent energy demands made on them. A good direction to look to in order to resolve the point regarding cell swelling vs. concentration change will be to search for small changes in cell volume with variation in external pH states using cell sorting techniques.

An interesting observation surrounding the cells' reaction to the pH transitions also include the shift in the internal Pi concentrations from approximately 7 mM to approximately 1 mM at the higher pH value (Fig. 42). The Pi washout experiments using Ringers solution showed the cells to be permeable to Pi by virtue of the fact that the Pi all washed out of the cells, yet here in the pH jump experiment at the low pH value of 7.2 to 7.3 (inside pH) the Pi concentration is 6 to 7 mM, while the outside concentration is only 1 mM. It is quite possible that the 1 mM internal Pi concentration at the high pH of 7.5 is a result of free exchange of Pi with the outside world, which is also 1 mM, and that under normal pH conditions, the membrane may be permeable to Pi, but have Pi actively pumped into the cells against the Pi gradient. In any case, the results of these pH jump experiments show the way intact cells can be studied in terms of their ATP/ADP ratio, and give a clear picture of where PCr goes in experiments which alter the cells pH.

The presence of PCr in these cells allowed the creatine kinase reaction to act as a buffer to maintain the ATP level of the cells at a constant level, but the activity of the creatine kinase enzyme was not sufficient to protect the ATP concentration under severe stress. In comparison, the creatine kinase activity in the dissociated rat brain cells was much faster (Table 8). So is the reaction in brains of intact animals (Ogawa, et al. 1986).

The difference could be accounted for by differences in the enzymes found in the two systems, or by the number of enzyme copies per unit cell volume. This question is not resolved here. A question which was asked was, "Does the

activity of the creatine kinase enzyme change when the N1E-115 cells are induced to differentiate with DMSO?" The answer here is no. But when turning to the dissociated neuroblastoma cells to answer this question, a large quantity of PCr was found in N1E-115 cells which had been kept in a differentiated state for two weeks (Fig. 23). What most likely happened to generate this high quantity of PCr is the cells, which are not dividing, and which are subjected to a low concentration of Cr, was that Cr was slowly transported to the inside of the cell and quickly phosphorylated, the reason being that with each cell being subjected to the Cr for several weeks, there was time for a considerable amount of Cr to enter the cells. The differentiated cells' ability to buffer the ATP pool was tested by subjecting the cells to several stress situations, reduced glucose, oxygen, high pH and a general ischemic state.

The general trend in ischemic experiments was for the PCr reserve to diminish slightly before or concomitant with the ATP.

In the dissociated rat brain cells, however, the trend was for the PCr level to diminish before any change was seen in the ATP levels, a situation which bespeaks of a real buffering condition (Fig. 64 and 65). It can be concluded, therefore, that the N1E-115 phosphocreatinekinase reaction mimics the same reaction in neurons of young rats without the same efficiency, and that in the N1E-115, the activity of the creatine kinase enzymatic reaction is most likely copy number limited, although the possibility exists that the enzyme itself could be less efficient and have a smaller specific activity. A practical aspect of this finding shows that it may be good to load up the cells with PCr by subjecting

them to, say, 30 mM extracellular creatine for several hours before using them in experiments which subject them to harsh conditions, such as those found while doing electrophysiological experiments.

The energetic parameters of the undifferentiated neuroblastoma cells observed in the present study can be compared with the values found in rat brain cells in vivo, keeping in mind that the neuroblastoma cell line is a model for a sympathetic neuron. There is a small amount of PCr present after ten days of feeding with 0.2 mM of creatine-supplemented medium, but this is still very small in comparison to the neonate brain. The estimated cytosolic ATP/ADP ratio, 63, was lower than the value of 100 in neonate brain. The cellular concentration of Pi (6mM) was high because of the high medium Pi concentration (1mM) and therefore, the phosphate potential was lower than in brain cells. In neuroblastoma cells which were undifferentiated, the value of the phosphate potential might not be as critical as it is in muscle cells, where the ATP hydrolysis is the major cellular reaction. These values of ATP/ADP and [ATP]/[ADP] - [Pi] are lower than those reported for young adult and neonate rat brains, (Ogawa, et al., 1986) and larger than those reported in adult rat brains (Veech, et al., 1979).

The present findings about neuroblastoma cells, such as their low creatine kinase activity, the extremely slow uptake of creatine in physiological environments, and a relatively low phosphate potential as compared with brain cells, are consistent with the notion that the undifferentiated N1E-115 cell should be looked at as a model cell of a neuroblast which is an immature

neuron. In an immature cell, one would expect various enzymes associated with the mature cell not to be expressed or be weakly expressed. Upon differentiation in tissue culture, these N1E-115 cells showed a capability for taking up creatine against the concentration gradient although the creatine kinase activity still seemed to remain low. Along this same line of in vitro studies in the future, one would expect to shed some light on interesting questions concerning the association of these neuronal type cells with glia cells. The activity of creatine kinase and various other enzymes may or may not change as a result of the cell-cell interaction when both neurons and glial populations are present.

With some understanding of how creatine kinase reactions behave, differentiated and undifferentiated N1E-115 cells and dissociated rat brain cells loaded with PCr were subjected to various insults in order to characterize their ability to recover. Undifferentiated neuroblastoma cells were the most extensively studied. First, they were subjected to the most severe stress, an anoxic condition (Fig. 66-73), and subsequently studied to determine their specific reaction to hypoglycemia, basic pH shock, anoxia (Fig. 62), the constituents of ischemia, as well as low sodium and a high potassium situation simulating electrical stimulation (Fig. 74 and 75).

An ischemic insult in the whole animal is a catastrophic event. It is an event in which the blood flow to and from the area of concern is stopped, resulting in an oxygen and glucose depletion, a pH drop and waste product buildup. In the absence of oxygen, the cells are forced to use glycolysis to generate ATP with a

concomitant buildup of lactic acid. When the episode is over and normal flow resumes, cells can regain their original status or die. In vivo the percentage of cells which die is dependent upon the length of the episode and possibly on post-ischemic treatment. In tissue culture experiments, superoxide produced after an ischemic episode has been implicated in cell death, an event which has been alleviated in part by elevating the concentration of superoxide dismutase in the cells (Saez, J. C. et al., 1984).

With this system it was possible to look first at the effect of the ischemic insult itself, and then to dissect out the various elements, such as hypoglycemia and anoxia events, in order to evaluate their contribution to the morbidity rate.

Undifferentiated neuroblastoma cells with large PCr stores subjected to ischemic events for various times between 10 and 55 minutes were found to vary considerably in their response (Fig. 66-72). The parameters monitored during these episodes were Pi concentration of the whole sample holder, pH, ATP and PCr concentrations. The general trend for all the experiments involved was for the pH to go down. In all cases the ischemic episode was started from a basic pH condition so that a range of observations could be made without pushing the cells to extremely low pH values and total death. The range of pH values was between 7.6 and 6.6. In all cases, the PCr and ATP declined. The break in the length of time of the ischemic episode dictating the point between partial and total recovery was someplace between ten and twenty minutes. The recovery of cells subjected to a 10 minute episode is almost complete (Fig. 70). It was complete for the ATP, which returned to normal from a 25% reduction, and

there was an 80% recovery for PCr 20 minutes after return to normal conditions (Fig. 73). This was interpreted to mean that there was no cell death, but that some of the Cr leaked from the cells.

In the first few minutes of this short ischemic episode, the pH dropped from 7.6 to 7.1 and the concentrations of PCr dropped 50%. Knowing the character of creatine kinase reaction, it was concluded that most of the PCr disappearance was due to an adjustment in the equilibrium condition of the reaction and that some was used to synthesize ATP which was in turn drained off to maintain the homeostasis of the cells.

The net loss of the PCr (20-25%) gave an estimate of the minimum energy required above the cells' aerobic and anaerobic production capacity in the 30-minute period coinciding with the ischemic and post-ischemic events. In none of the cases of 20 minute through 53 minute lengths of ischemic periods did the ATP or PCr return to their pre-ischemic conditions (Fig. 66, 71, and 72). In all of these cases the ATP level returned in phase with the external pH, and the PCr level lagged the return of the pH with a time which was proportional to the length of the ischemic episode.

There are several curious aspects to this data. First, the ATP which had been hydrolized, was quickly reformed. It followed the same time course as the return of the pH of the external medium, to pre-ischemic levels, even in the 53 minute ischemic case, where there was a marked pH gradient across the cell membrane during the recovery phase. The ATP was still in phase with the

external pH. In contrast, the PCr did not recover until minutes after. This cannot be attributed to the speed of readjustment of the equation:

$$ATP + Cr \rightleftharpoons ADP + PCr + H+$$

due to the H+ concentration because, as seen at the onset of ischemia, the PCr concentration adjusts rapidly with the fall in pH, setting a lower limit on the flow through the enzyme, and in the case of the 10, 20 and 30 minute episode (Fig. 70, 71 and 73), the exterior and interior cellular pH were indistinguishable from one another, and one would expect the PCr equilibrium to readjust equally as fast upon normalization of conditions as it did at the onset of the ischemic conditions. Since it didn't, there must have been another factor involved.

It can also be argued that most, if not all, of the Cr stayed in the cells, otherwise the reappearance of PCr would take hours. This leaves the alternative, that the ADP concentration must have been forced to very high levels, thus forcing the reaction to the left, and keeping the PCr low until the ADP concentration reached some reasonable value. This, of course, assumes that there is adequate Pi to go around. The creatine kinase is a cystolic enzyme and the ATP is made in the mitochondria.

The data here show that the total Pi in the sample holder intra- and extracellular during the ischemic event went up in a graded way with the time since the pump was off.

It is not possible to tell if the Pi is intra- or extracellular; if it is extracellular,

it was washed out of the sample holder upon resumption of pumping. Since continuous mixing of old and new medium in the sample holder is going on, one can consider that one-half the peak Pi concentration is present on average during the wash-out phase, that period during which the pH returns to normal. If this Pi is in free exchange with the cells' cytosol, it could account for at least ½ the quantity necessary for phosphorylating the ADP to ATP.

If it were not for the data in the fifty-three minute episode, one could speculate that the lag in PCr appearance was tied to changes in the internal pH in some way. The data for the fifty-three minute episode sets it apart from the lower timed episodes and may represent the case where the glucose trapped in the sample holder at the beginning of the episode was used up during the ischemic episode. Using a value of glucose consumption for rat brain cells in culture of 0.25 μ mole glucose consumed/min-mg protein (Honeggar, 1985) and knowing there are approximately *25* 10^{-3}g of protein in the sample, the glucose needs of the cells for fifty- three minutes would be 33 μ mol. The sample holder had 33 μ moles when filled with low glucose medium, in this case, and 150 μ moles when high glucose medium is used.

It has been reported (Guroff, 1980) that the glucose utilization can go up by a factor of 20 or more during periods of ischemia. Because of the large variation of the glucose consumption in the literature, one can only say at this juncture, without measuring the glucose in the cell, that it is possible for the glucose in the high glucose medium to be completely consumed in 53 minutes and that the 33 μ mol. glucose in the low glucose medium was completely used. One can

only speculate at this point that periods of ischemic events here fall into three categories. The first one, the complete recovery period for zero to ten minutes of ischemic conditions; the second from ten minutes to some time less than fifty-three minutes following which there is a partial recovery of cell integrity with some cell death, and a third period where integrity of the cells has been substantially altered in a fashion which does not allow for the pH of the cells' interior to recover at the same rate as the extracellular pH, a situation suggestive of the suspension of glycolysis, as well as oxidative phosphorylation.

Some major factors to the ischemic episodes were investigated separately. 2DG was used to compete with glucose, thus representing a hypoglycemic condition and interfering with glycolysis (Fig. 30 and 31). Oxygen deprivation was used to assess the anoxic contribution (Fig. 63). The pH was varied, but only in the basic direction from the neutral pH of 7.0. In undifferentiated neuroblastoma cells which had been grown without creatine and therefore had no phosphocreatine in the cells, the reaction to the addition of 10 mM 2DG to the superfusate medium containing 5 mM glucose was pronounced; at least 30% of the cells died in the first hour, as judged by the ATP levels of the sample, which decreased 30% in the first hour and remained constant at these levels for the next ten hours.

The 2DG-6-P peak appears in the PME region and gives a marker for its presence. The results of these 2DG experiments are interesting in light of recent interest in glucose 6 phosphates (G6Pase) (Nelson et al., 1986; Deuel, et al., 1985), and its affect on the validity of the deoxyglucose method for

estimating glucose utilization in the brain devised by Sokoloff, et al. (1977, 1982).

Nelson in the technical comments column in Science (Nelson, et al., 1986; Deuel, et al., 1985), compared the time course of deoxyglucose-6-phosphate (DG6P) concentration in a rat brain as measured by Deuel et al., (1977) using NMR spectroscopy after administration of an intravenous dose of deoxyglucose at 500 mg/kg where it was found after an initial period of 40-60 minutes that the 2DG-P signal diminished, reaching the half peak value in 120 minutes. These results were in excellent agreement with a similar time course calculated from cerebral glucose utilization made by Sokoloff et al. (1982). This is the more surprising in that Sokoloff's method only trace amounts of ^{14}C 2DG were used. Nelson supported Sokoloff's contention that G6Pase has little if any effect in the first forty-five minutes after administration of 14C-labeled 2-deoxyglucose by suggesting that this is understandable in light of experiments by Fishman et al. (1985) which showed that there was a lag in appearance of G6Pase activity in normal brain due to the absence of a carrier for G6P, thus delaying the 2DG-6P entry into the microsomal compartment which contains the G6Pase.

I have measured the appearance of 2DG-6P and found it to have a dependence on the extracellular concentration (Fig. 31 and 32), and have also found that the rate of appearance was at least twice that of its disappearance once the extracellular medium was replaced with 2DG-free medium. This value was slow enough to be affected by the degrative processes of the G6Pase, the

transport of the substrate into the microsomal volume; therefore a quantitative statement cannot be made concerning this uptake process based on these data. Once an equilibrium state had been established, however, and the extracellular 2DG removed from the feeding medium, a time which took less than 20 minutes, the disappearance of 2DG-6P was purely the result of the process of G6Pase. This was a clean experiment and gave a rate of 2DG-6P degradation, which was twice that which is described above. This rate was for undifferentiated N1E-115 cells which are not fully developed, neuron-like cells and in general are more like sympathetic cells than central nervous system cells. Caution should also be exercised here in comparing in vitro and in vivo results. What can be said is that within the confines of this experiment, ^{14}C lab 2DG estimates of glucose utilization will be seriously compromised in experiments requiring forty-five minutes to execute.

The experiments described here suggest a protocol for determining 2DG uptake and degradation and can be used to explore G6Pase actively in differentiated neuroblastoma, dissociated rat brain cells, glia, glioma and astrosites, or mixes thereof, to gain a better understanding of these process in vitro with possible inferences for *in vivo* systems.

When differentiated N1E-115 cells maintained in tissue culture conditions for thirty days and containing PCr were fed 2DG medium, the PCr gave protection against the low glucose availability. In this case the ATP level stayed at its original level and the PCr concentration level decreased over a period of several hours.

Experiments run on the undifferentiated neuroblastoma cells to see what effect low oxygen had on the cells showed that cells superfused under standard conditions with standard glucose, DMEM medium, could exist with no oxygen for five hours with a small, 20%, diminuation of their PCr store (Fig. 62). One can conclude from this that the major effect of the ischemic events is primarily due to a low glucose and or to the lowering of the pH but not to anoxic conditions.

With an understanding of how the N1E-115 cells responded to ischemic conditions the experiments were run on dissociated rat brain cells to estimate the effect of glucose and O_2 on the cells. The PCr peak decreased 75% in a 2.5 hour period when the cells in this 7.4 pH Hepes buffered system were superfused with O_2 free Ringers A without glucose (Fig. 64 and 65). ATP decreased 20% without recovering when the cells were eventually returned to ZAM medium.

These results suggest that although lowering of the pH may be an accelerating catalayst, the reduction of glucose and O_2 to zero is an adequate condition to kill 20% of the cells.

The extracellular K+ concentration was varied to simulate what happens when these cells were depolarized during the firing of an action potential (Fig. 74 and 75). This was done by adding 80 mM KCl to the superfusate of the medium for a period of eighty minutes and then washing it out. The shortest time period which could be observed was one minute and this was with a poor signal-to-noise ratio. The best results were obtained with a file accumulation of

7.5 minutes. The long-term depolarization appeared to have little effect on the undifferentiated cells. Only one experiment was done for the undifferentiated cells and this was frustrated by a low signal-to-noise ratio. Depolarization of the differentiated cells, however, resulted in a decrease in the PCr and nucleotide phosphate concentration and a build up of the cellular Pi. There was a shift in the internal pH relative to the outside pH which was measured by taking the difference in extracellular pH as measured from the chemical shift of the Pi peak and the intercellular pH as measured from the chemical shift of the PEt peak.

There is no question that the simulated depolarization of the cells is energy demanding and that the ATP pool is drained. It is also clear that the high concentration of PCr helps to alleviate this condition. This persistent depolarized condition is an extreme stress. It is quite possible that the creatine kinase reaction would be able to maintain ATP concentrations if the cells could be synchronously depolarized with a period comparable to their refactory period, which for normal neuronal cells would be comparable to a seizure condition.

A second major observation concerns the PME and PCr region of the spectra after the cells were induced to differentiate. Once the undifferentiated cells had been studied with respect to the creatine kinase reaction, the questions naturally arose concerning what happens to this reaction when the cells are induced to differentiate. What was observed in cells induced to differentiate with DMSO was the appearance of extremely large pools of PEt, PCh and PCr

(appendix B Fig. 1 and 2).

The mechanism governing the rate of appearance of these large pools is different. PEt and PC synthesis may depend on endogenous substrate synthesis as well as transport of substrate into the cells. It certainly is dependent upon enzyme copy number and specific activity. How any of these factors change with development has yet to be determined.

In cells held in a differentiated state for 20 days, the concentration of PEt and PCh are equal and in excess of 10mM, as it is in the PCr concentration. When either ethanolamine (EA) or choline are added individually to undifferentiated cells or cells which have or are differentiated, the phosphorylated compound increases with respect to the other, i.e., when the 0.2 mM EA is added to differentiated and undifferentiated cells, the amount of PEt increased fourfold and the PCh increases twofold respectively in a seven hour period (see appendix B). Since EA is expected to cross the cellular membrane easily (Sundler, et al. 1975, Zelinski, and Choy, 1982) it was concluded that a change in the flux through the enzyme and or intracellular substate synthesis was responsible for the increase in the monoesters. The flux through the enzyme is the best candidate. Recent work has lent strong support to this conclusion (Glynn, et al., 1987, appendix B).

These observations are important because high concentrations of PEt have been reported to be present in various brain cells, such as mouse and human neuroblastoma, human glioblastoma, and rat glioma (Maris, et al., 1986, Naruse,

et al., 1985) and the 31P in vivo changes in these peak heights to chemo and radiation therapies have been used as a marker of effectiveness. The PEt peak has also been shown to be present in developing brains of neonates and near-term fetuses of several animals (Bolinger, et al., 1984, Ogawa, et al., 1986) The PEt content in these brains has been shown to decrease during the course of brain growth.

The biological value of these high level pools is not clear. One speculation is that normal tissue containing post mitotic cells ready to grow and develop into mature neurons needs a large pool of membrane building blocks to allow for a rapid assembly of vesicles and cell membranes without being limited by a slow rate of synthesis of PEt and PC at the time PEt and PC are needed.

Why the pools develop in neuroblastoma cells, and why they persist well after the morphological, chemical and electrophysiological differentiation of the cells are interesting questions, and answering them should give some insight into normal and aberrant development. A good second step in investigating these processes would be to use ^{13}C labelled EA to follow the synthetic process.

In the case of the PCr, the rate-limiting step for the appearance of PCr is the transport of the creatine into the cells. This was demonstrated by comparing the quick rephosphorylation rate (within minutes) of creatine which had been generated in the cell by the hydrolysis of PCr during an ischemic episode with the long (in terms of hours) time required to accumulate PCr originally. The explanation for the appearance of a large pool of PCr in

differentiated vs undifferentiated cells is twofold. Differentiated cells, which had been maintained in a low (0.2mM) concentration of Cr growth medium had enough time (14-20 days) to transport the Cr into the cells, where dividing cells have only 3 to 4 days.

6. SUMMARY AND CONCLUSIONS

An NMR probe and life-support system was built to measure anchorage-dependent cells in a tissue culture type of environment. Its utility was demonstrated using a hardy cell line, C3HT10½.

This system is a good system for studying anchorage-dependent neuronal cells. The proven system was used to study the metabolic processes of several neural-type cells, and to study changes in the development of the N1E-115 neuroblastoma cell line, a model cell for a sympathetic neuron, that was induced to differentiate with DMSO. The metabolic studies centered around the creatine kinase activity, the response of the cells' high-energy reserves of ATP to the severe stress of an ischemic episode, and the effects of the various components of an ischemic response, hypoglycemia, pH change and anoxia. Studies were made with less severe stress, that of depolarizing the cells with high extracellular potassium. The emphasis on the design of the system was to be able to make experimental measurements in a nonintrusive way, either intermittently or continuously over a long period of time, i.e. days to weeks.

When used to study undifferentiated neuroblastoma cells, the following were found:

1. It was possible to measure intercellular and extracellular pH in the extracellular pH range of 7.2 to 9.0 pH units. At an extracellular pH of 7.4, the normal pH for tissue culture growth, the pH gradient was 0.01 pH units with the outside basic.

2. These cells have creatine kinase activity.

3. The unidirectional flux rate (f+) of PCr to ATP is very slow in undifferentiated neuroblastoma cells and not measurable with the saturation transfer technique.

4. The results of ischemic episodes show the flux rate to be less than several minutes, thus placing the value between 15 seconds and several minutes.

5. Creatine must be supplied from outside the cell.

6. The rate of appearance of PCr once Cr is put in the medium outside the cells in limited by the transport of Cr into the cells. The Km of the transport is 100 mM and the V max is 1.1 h^{-1} and 72 $\mu M - min^{-1}$ if it is assumed that the ATP level is 3.9 mM (Ogawa, S. et al., 1986) where V is in units of d(PCr/ATP)/dt and the PCr and ATP are the peak heights of phosphocreatine and adenisinetryphosphate peaks respectively.

   The uptake of undifferentiated neuroblastoma cells is almost double that of differentiated neuroblastoma cells, dissociated rat brain cells and C6 cells.

7. Inorganic phosphate is capable of being washed out of the cells at high

extracellular pH, i.e., 8 - 9, but is capable of being as high as 8 mM inside the cell when the external Pi concentration is only .98 mM if the external pH is in the range of pH 7.4.

8. The Pi concentration inside the cells was found to be different under different conditions of external pH.

9. The phosphate potential was calculated for the cells in vivo using data from pH jump experiments and values for Cr obtained from cell extracts made after the experiment. This is an important measure of the energy state of the cell, particularly when measured continually in a non-intrusive way.

10. Creatine kinase in these cells provides some protection against ischemic insult, hypoglycemia, anoxia, low extracellular sodium and high extracellular potassium.

11. The depleted ATP and PCr concentrations recover after an ischemic episode to some percentage of their preischemic value in a fixed pattern.

    a) The PCr returns to 1/2 its final value some minutes after the pH inside the cells reaches 1/2 its final value. The time lag is linearly proportional to the time of the ischemic response.

    b) The ATP and pH recover at the same time

    c) ischemic episodes less than ten minutes result in full recovery; those episodes longer than ten minutes result in partial recovery of PCr

and ATP due to cell death.

12. Of all the microcarriers tested, these cells grew best on Cytodex III in DMEM medium supplemented with FBS.

N1E-115 cells induced to differentiate with DMSO in standard tissue culture conditions showed marked differences in other 31P profiles when compared to those of undifferentiated neuroblastoma cells as follows:

1. Differentiated N1E-115 cells cultured in standard tissue culture conditions for fourteen days had large PEt and PCh peaks in addition to a large PCr peak not seen in undifferentiated neuroblastoma cells. Cells cultured for thirty days had even larger peaks at PEt and PCh resonances. The changes in the PEt and PCh reflect developmental changes in the activity of the enzymes making them. The increase in the PCr reflects a longer period in the growth medium which contains low concentration of Cr, 0.1 - 0.2 mM, which is transported slowly into the cells, and not an increase in the activity of the enzyme.

2. N1E-115 cells induced to differentiate while in the life- support system in the magnet showed an increase in the PEt and PCh stores with time. Addition of EA resulted in an increase in the rate appearance of PEt. The addition of Ch resulted in an increase rate of appearance of the PCh. In contrast, when EA was added to undifferentiated cells there was a much smaller effect. This was the same case as for the addition of Ch to the undifferentiated cells.

3. Differentiated N1E-115 cells behaved similarly to undifferentiated neuroblastoma cells when stressed.

Dissociated rat brain cells showed the following characteristics:

1. The activity of the creatine kinase was measurable with saturation transfer technique and was found to be between 0.07 $-0.09\ S^{-1}$. The value in the intact animal is $0.13\ S^{-1}$. Considering experimental error, these are in close agreement.
2. The cells showed a high tolerance for oxygen-glucose deprivation, up to three hours, without a large permanent loss of ATP, Cr, or PCr.
3. The PCr pool goes before the ATP levels start to go in stress conditions. Thus, the activity of the creatine kinase offers more protection against stress in dissociated rat brain cells than it does in neuroblastoma cells.
4. The PME's, PET and PCh concentrations are large, similar to differentiated neuroblastoma.

From undifferentiated C6 glioma cells it was found:

1. They have creatine kinase activity.
2. The rate of appearance of PCr when the cells are supplemented with Cr is similar to differentiated neuroblastoma and dissociated rat brain cells.
3. They have small concentrations of PME comparable to undifferentiated neuroblastoma cells, but do have a prominent peak at a chemical shift of

4.3782, the PEt position.

4. There are two prominent peaks at —0.255 and 0.505 and a third peak near the PCr peak, which is a good candidate as a cell marker (origin unknown).

C3T10 1/2 were used to develop the life-support system described here.

The N1E-115 is a good model system for a neuron from the point of view of energetics when it is kept in mind that the creatine kinase activity is slower in differentiated neuroblastoma cells than it is in DRBC.

From the point of view of development, N1E-115 and dissociated rat brain neurons are similar in that they build up large concentration of PEt and PCh, but unlike N1E-115 cells, rat brain neurons use up or degrade this pool within 15 to 20 days after birth.

There is no question the system developed and proven here is the system of choice for studying homogeneous populations of anchorage-dependent cells and combinations of different cell populations. Continued innovation in terms of synchronized electrical or optical stimuli of specific cell systems should yield interesting insights into neuronal and visual systems with a time resolution of one second. It is also ideally suited for studying developmental changes in the short term as well as long term and during therapy.

APPENDIX A

Procedure for Obtaining Dissociated Rat Brain Cells

I. **SOLUTIONS.** All solutions should be filtered and placed in autoclaved bottles that have unbroken seals, or sterile test tubes. This was done under the hood. Filter at 0.2 μm, except for trypsin inhibitor, which was filtered because at 0.45 μm it won't go through 0.2, and DNAse. This can't be filtered at all, so use sterile - packaged DNAse dH_2O filtered at 0.2 μm. Do not keep any solution more than 4 wks.

II. **MEDIUM:**

A. Refrigerate, don't freeze.

1. Trace elements stock: 5×10^4 fold, so add 20 $\mu\ell$ per 1ℓ medium stock. Store *at room temperature.*

	for 1ℓ	conc.[in stock]
cupric sulfate, $CuSo_4 \cdot 5H_2O$	12.5 mg	5.00×10^{-5}M
manganese sulfate, $MnSC_4$	7.5 mg	4.97×10^{-5}M
molybric acid, MoO_3	7.2 mg	5.00×10^{-5}M
chromium chloride, $CrCl_3 \cdot 6H_2O$	13.3 mg	4.99×10^{-5}M
zinc sulfate, $ZnSo_4 \cdot 7H_2O$	14.4 mg	5.01×10^{-5}M

2. Biotin stock: 5×10^3 fold, so add 200 $\mu\ell/\ell$ medium stock. Store at 4° C.

	for 100 mℓ	conc.
d-biotin	12 mg	4.91×10^{-4}M

This will not go into solution unless heated/stirred for at least 15 min.

3. Nucleotide stock. 25C fold, so add 4 mℓ/ℓ medium stock, store at 4° C.

	for 1ℓ	conc.
adenosine	107 mg	6.25×10^{-4}M
quanosine	15.2 mg	5.37×10^{-5}M
cytidine	30.5 mg	1.25×10^{-4}M
uridine	35.4 mg	1.45×10^{-4}M

4. Amino acid/vitamin stock a.a./v. stock. Add the entire 500 mℓ to 5ℓ medium stock, i.e. 100 mℓ/ℓ.

	for 500 mℓ	1L	conc.
aspartic acid	16.68 mg	33.36 mg	2.50×10^{-4}M
alanine	11.1 mg	22.2 mg	2.50×10^{-4}
asparagine	18.8 mg	37.6 mg	2.84×10^{-4}
proline	43.0 mg	86.0 mg	7.48×10^{-4}
lipoic [a.k.a. thioctic] acid	6.0 mg	12.0 mg	5.82×10^{-5}
taurine	31.0 mg	62.0 mg	4.96×10^{-4}
B_{12}	6.8 mg	13.6 mg	1.00×10^{-5}

This takes about 2 hrs. to go into solution. Wrap flask with foil to keep fluorescent lights out.

5. Defined medium stock.

	for 5 ℓ
DMEM	66.9g [=1 packet]
	Rinse packet with dH_2O
$NaHCO_3$	18.5g
t.e. stock	100 μℓ
biotin stock	1 mℓ
nuc. stock	20 mℓ
a.a./v. stock	500 mℓ
pH 7.2	

Store in 500 mℓ [for primary] and 100 mℓ [for feeding] aliquots. Use bottles that have been autoclaved with stir bars in them.

B. Store frozen — thaw only once.

1. Insulin. You want 4 μg/mℓ medium as final concentration

	For 50 mℓ	conc.
insulin	50 mg	8.25×10^{-5}M

add acid oil NHCl dropwise until it goes into solution. Add 0.4 mℓ to 100 mℓ medium. It is easiest to store insulin in tubes of 0.4 mℓ and 2 mℓ; then you can take the pre-measured amount out depending on whether you're making 100 or 500 mℓ of medium.

2. Transferrin. Should be 40 μg/mℓ of medium in final concentration.

	for 50 mℓ	conc.
transferrin	500 mg	7.50×10^{-5}M

Add 0.4 mℓ to 100 mℓ medium. Store in the same as insulin.

3. Selenium. Needs *two* dilutions.

	100 mℓ	*conc.*
sodium selenite	21.6 mg	6.25×10^{-6}M Takes 15 min to dissolve
		to dissolve

Then take 0.5 mℓ of this solution and add it to 99.5 mℓ dH_2O.

Store in 2 mℓ fractions in polypropylene tubes (will stick to polystyrene). Add 0.4 mℓ to per 100 mℓ medium.

4. Putrescine.

for 60 m ℓ	conc.
125 mg	1.29×10^{-2}M

Store in 2 mℓ fractions like Se. Add 0.4 mℓ/100 mℓ medium — gives a final concentration of 8.3 μg/mℓ.

5. Albumin—fatty acids. First make up chloroform stocks of the fatty acids:

   (a) *arachiotonic acid* (20:4): 50 mg in 10 mℓ $HCCl_3$.

   (b) *linolenic acid* (18:3): 100 mg in 10 mℓ $HCCl_3$.

   (c) *linoleic acid* (18:2): 1g in 20 mℓ $HCCl_3$.

   Store these in freezer in amber bottles that have tops you can stick a syringe through to extract them [they are very easily oxidized by air].

6. Albumin—fatty acid.

   (a) Add 10 g fatty—acid free albumin to ~100 mℓ dH_2O.

   (b) Decant after stirring into another beaker. Do not let foam come as well. The foam is denatured albumin since albumin is very fragile unless complexed with fatty acids.

   (c) If you feel like it, recalibrate the albumin concentration by using Lowry's method on 10 μℓ.

(d) Bring 2 beakers of H_2O to a boil:
one with 400 mℓ double distilled water (dH_2O)
one with 50 mℓ double distilled water

7. Do the following under N_2 to prevent oxidation.

(a) Rinse glass [plastic would dissolve] syringe with $HCCl_3$. Also rinse after each addition below:

(b) Set up round-bottomed flask under N_2 stream:

(c) Add, using syringe, 5 mg arachidonic acid. With the stock described above, that would be 1 mℓ.

(d) Add 10 mg linolenic acid [1 mℓ], (2.5 mℓ/250 mℓ)

(e) Add 15 mg linoleic acid [300 μℓ] 50 mg + 0.3 = 15 mg (750 μℓ/250 μℓ).

(f) Let $HCCl_3$ evaporate until flask bone dry. If the sediment turns yellowish, through out, because the fatty acids have oxidized.

(g) Add 1-2 mℓ NaCH (1N) to flask. Swirl until saponified, when it will smell like soap and look slightly yellow. The yellow is from arachiotonic acid. If you used tocohexaonic acid, it will smell like fish at this point.

(h) Add ~5 mℓ boiling dH_2O from the 50 mℓ beaker

(i) Put to flask [still under N_2] in the 400 mℓ beaker of H_2O for a short time.

8. Using another pasteur pipet, add the fatty acid mixture to the beaker or albumin at a rate of 1 drop/sec. If it is added too fast, it will form micelles. The fatty acids should never be exposed to air until they are thoroughly mixed with the albumin.

9. pH adjust to 7.2, and filter under the hood.

10. Calculate total volume of liquid and using that, the volume that contains 1g albumin — divide into aliquots such that fractions made up for 500 mℓ medium contain 1g albumin and those for 100 mℓ medium contain 0.2 g albumin.

11. ZAM-DEFINED MEDIUM. Do this under the hood on a stirring plate. Take a 100 or 500 mℓ bottle of medium stock and bring to 37° C. pH adjust if it looks off-color. Take out and thaw appropriately-sized premeasured frozen aliquots:

(a) insulin (0.4 mℓ for 100 mℓ; 2 mℓ for 500)/ml for 250

(b) transferrin (0.4 mℓ for 100 mℓ; 2 mℓ for 500) 1 ml for 250

(c) selenium. These aren't premeasured; there's only a 2 mℓ size 1 ml for 250 ml ZAM

(d) putrescine 1 mℓ for 250 ml ZAM

(e) albumin/fatty acid 10 mℓ for 500 ml ZAM; 5 mℓ for 250 ml ZAM

Add all the contents of insulin, transferrin and albumin tubes. It may be a good idea to rinse them with medium as well. Pipet out 0.4 mℓ each of selenium and putrescine if making 100 mℓ of medium. If making 500 mℓ, you can add the entire tubes contents.

III. SOLUTIONS NEEDED FOR PRIMARY

SOLUTION D. Freeze in 200 mℓ fractions.

	for 2ℓ		conc.	
NaCl	16.01	g	137	mM
KCl	0.81	g	5.4	mM
Na_2HPC_4	0.048	g	0.2	mM
KH_2PO_4	0.06	g	0.2	mM
glucose	1.98	g	5.5	mM
sucrose	40.39	g	59.0	mM
Phenol red	1.5	mℓ 4% soln.	0.02	mM

Ajust the pH to pH 7.2 (or higher, since freezing lowers pH), filter, and divided into 200 mℓ and 500 mℓ fractions.

Then add antibiotic/antimycotic agents such that final concentration is:

penicillin 10,000 μ/mℓ
streptomycin 10 mg/mℓ

A. Solution + Trypsin. Make this at same time as solution D.

Add 500 mg trypsin to 500 mℓ solution D. Freeze 25 mℓ fractions.

B. Poly-d-lysine. Freeze 100 mℓ aliquots.

	for 330 mℓ	for 1ℓ	conc.
boric acid	5 mg	6.18 g	0.1 M
pH 8.4			
poly-d-lysine hydrobromide	15 mg		0.15 mM

C. Hepes-Buffered Saline. Don't freeze. Store ~500 mℓ/bottle; this can be reused for several primaries as long as it is opened only in sterile conditions.

	for 4ℓ	conc.	for 1L
KCl	0.81 g	2.7 mM —	0.202 gm
NaCl	32.00 g	137 mM —	8.00 gm
glucose	3.96 g	5.5 mM —	1.00 gm
HEPES	1.00 g	1 mM —	0.25 gm
NaH_2PO_4	0.2 g	0.4 mM —	0.05 gm
pH 7.2			

D. Trypsin Inhibitor. Freeze in 2 mℓ aliquots. Remember to filter at 0.45 μm, not 0.2. 1 mg trypsin inhibitor inhibits approximately 1.8 mg trypsin.

Add 1g into 40 mℓ dH_2O.

E. Dnase. Mix up under hood. Use 20 mℓ filtered dH_2O and 5 mg DNAse. Since DNAse comes in 5 mg bottles, just add the whole bottle and rinse it a few times.

Freeze, 1 ml per tube.

IV. RECORDING SOLUTIONS

Don't freeze or keep more than a day.

A. Krebs-Hepes

	conc.
NaCl	145 mM
KCl	4.7 mM
glucose	5.5 mM
HEPES	10.0 mM
pH to 7.4	
$CaCl_2$	2.5 mM
$MgCl_2$	1.2 mM

B. KAc INTERNAL SALINE

	conc.
KAc	140 mM
HEPES	10 mM
pH 7.2	Use KOH, not NaOH to balance pH
$MaCl_2$	2 mM

C. KCl Internal Saline

	conc.
KCl	140 mM
HEPES	10 mM
pH 7.2	Use KOH to balance pH
$MaCl_2$	2 mM

V. ADDITIONS TO MEDIUM

A. Tri—iodthyronin (T_s). Final concentration should be 10 picomolar in medium. Make stock through two solutions:

	for 1ℓ	conc.	
T_s	6.5 mg	10 μM	saponify with NaOH over heat to dissolve.

Add 0.1 mℓ or 10 μM stock to 100 mℓ to give 10 nM. Filter and store in sterile bottle at 4° C. Do not freeze.

Add 1 mℓ of this stock per liter medium.

B. Thyroxin (T_4). 40 pM in medium.

	for 1ℓ	conc.	
T_4	3.1 mg	4 μM	saponify with NaOH over heat.

Add 1 mℓ of 4 μM solution to 99 mℓ H_2O to give 40 nM. Filter.

Add 1 mℓ of this stock per ℓ medium.

C. Progesterone. Want 50 mM in medium. Dissolve in acetone.

	for 10 mℓ	conc.
progesterone	7.8 mg	2.5 mM
acetone	10 mℓ	—

Add 1 μℓ of this stock per 50 mℓ of medium. Acetone concentration in medium should never exceed 20 μℓ/ℓ.

D. Estradiol. Dissolve in acetone. 10 mM concentration in medium.

	for 100 ℓ	conc.
17-β-estradiol	13.6 mg	0.5 mM
acetone	100 mℓ	

Add 1 μℓ of this stock per 50 mℓ medium. Keep estradiol and progesterone in freezer.

E. KCl. For cells from fetuses more than 19 days old at time of primary, 25 mM KCl [filtered] in medium is needed to promote differentiation. Needed only for approximately the first week in culture.

VI. PROCEDURE FOR PRIMARY.

A. Much primary, get these ready:

1. Cheesecloth. Put 6" × 6" square, 5 layers thick, in aluminum foil packet, and seal edges with autoclave tape. Autoclave them a week before use.
2. Cover slips. 12 mm for 24 well dishes; 18 mm for 12-well dishes.
   (a) Soak in concentrated H_2SO_4 for 10 min.
   (b) Rinse with dH_2O until pH of H_2O is back to normal.
   (c) Put in small widemouthed bottle, cover with dH_2O, and autoclave.
3. Autoclave some 125 mℓ Ehrlenmeyer flasks with caps.

4. Make sure you have:
   (a) sterile hood
   (b) sterile hood with dissecting microscope
   (c) 10% CO_2 incubator
   (d) shaker bath with clip for 125 mℓ flask
   (e) microscope with 10X - 50X objectives
   (f) autoclave
   (g) hemacytometer
   (h) macro and microdissection tools
   (i) preplugged Pasteur pipets, autoclaved
   (j) 10, 5 and 1 mℓ serological pipets
   (k) 24-well or 12-well culture dishes
   (l) 12 mm or 18 mm cover slips
   (m) small widemouth jars (for autoclaving cover ships)
   (n) 125, 250 and 500 mℓ autoclavable bottles (for medium, etc.)
   (o) screw-top Ehrlenmeyer flask, 125 mℓ
   (p) sterile polypropylene tubes, 12 × 75 mm
   (q) sterile polypropylene centrifuge tubes, 50 mℓ
   (r) 35 mm sterile Petri dishes
   (s) 100 mm sterile Petri dishes
   (t) defined medium, solution D, etc. (see list below).
   (u) Five 150 mm Sigma Coat dishes

B. The Primary

1. Polylysine. For cells on plates for biochemical assay. Polylysine can be put on coverslips and microcarriers as much as 2-3 days before primary; but must be at least 12 hours before.
   (a) Thaw a bottle of polylysine
   (b) Under hood, put some autoclaved cover slips in Petri dish of polylysine.
   (c) Place 1 slip per well of culture dish.

(d) Soon (<10 sec) after, put 0.5 mℓ polylysine in that dish. If you wait too long, slip will try and polylysine surface will crack and peel.

(e) Let sit for at least 24 hours so polylysine forms enough coating on slip.

(f) Three 24-well dishes are probably enough for 1 primary (if you do only 1 brain area).

2. For cells to be attached to microcarriers for NMR experiments. 2-3 days before experiment.

(a) Thaw a bottle of polylysine.

(b) Under hood put 10g of Biosylon microcarriers in a sterile 50 nl centrifuge tube (polypropylene with cap, corning catalogue number 25331)

(c) pipette enough polylysine into tube to cover the microcarriers with 5 cm of polylysine.

(d) vortex three times for 30 seconds.

(e) let set in tissue culture hood for at least 24 hours.

(f) Drain off polylysine from tube. Rinse them four times with Hepees-buffered saline at room temperature.

(g) Do not allow the microcarriers to dry.

(h) Rinse a fifth time and leave the saline in the tube covering the microcarriers with 1 cm of saline.

3. Clean, polish, sterilize dissection tool.

4. Check you have enough sterile cheesecloths [1 per brain area], sterile 125 mℓ flasks, and plugged Pasteur pipets.

5. Check the following:

(a) 500 mℓ medium

(b) solution D

(c) solution D + trypsin

(d) DNAse

(e) trypsin inhibitor

(f) insulin

(g) transferrin

(h) selenium

(i) putrescine

(j) albumin/fatty acids

(k) any others:

(l) plug UV light on in dissection hood, check took, etc.

(m) cheesecloth

(n) 70% ethanol in water

(o) ice plates — 4 & 5

(p) 125 ml flask — 3

(q) H_2O shaker

(r) 10% CO_2 incubator

(s) coated glass plates

(t) 4 or more sterile 50 mℓ plastic tubes — 6 or more

(u) Petri dishes
60 mm with 6 mℓ of solid Sylgard 184 silicone elastomer in it
100 mm with 20 mℓ of solid Sylgard 184 silicone elastomer in it

(v) Pasture pipettes, cotton plugged

(1) tri-iodothyronin

(2) thyroxin

(3) progesterone

(4) estradiol

(5) sterile KCl

C.

1. *1 hr. before anesthetizing the rat*

(a) Bring frozen solution D to room temperature using bath.

(b) Take 500 mℓ medium stock out of refrigerator and set it at room temperature [*not* using bath].

(c) Take HEPES-saline out of refrigerator and bring to room temperature using bath.

(d) Take tube of solution D + Trypsin and put it at room temperature. [As soon as it's completely thawed, put it in refrigerator to retard auto-digestion.]

(e) Put macro-dissection tools in beaker and EtOH in hood. [Leave micro-tools and scissor in the dissection hood under UV.]

(f) Make sure the shaker bath is at 37° C.

2. Right before anesthesia, put solution D and the following in the hood:

(a) Ten 35 mm Petri dishes [sterile] with 3 mℓ solution D each

(b) Three 100 mℓ Petri dishes [sterile] with 20 mℓ solution D each Push these out of the way so you can do the gross dissection here.

(c) Lay 3 paper towels on tinfoil to dissect on.

3. Anesthesia

(a) Bring rat to room with anesthetic chamber.

(b) Put 6 ml of ether in chamber

(c) Put paper towel in bottom of a 100 mℓ beaker; splash some ether on it.

(d) Use tail pinch to see if rat is out. If so, take her out and put it on the towels/tinfoil. Stick ether breaker over her nose to keep her down.

(e) Place her in hood

4. Macro-Dissection. In regular hood.

(a) Spray alcohol on rat's abdomen.

(b) Flame scissors/forceps before use. Make sure flame is gone and all the EtOH has burnt off or you'll light the EtOH on rat's belly when you cut. Let tools cool a bit.

(c) Make longitudinal, incision, find uterus.

(d) Remove fetuses:

(1) Cut through uterus

(2) Cut through placenta

(3) Cut through amnion, umbilical cord, etc.

(e) Place fetuses in one of the 100 mm dishes

(f) Make sure you've cleaned out *both* horns of the uterus. There should be 8-10 fetuses if 1st pregnancy; more if this is a 2nd pregnancy.

(g) Kill rat, e.g., sever aorta.

(h) Chop heads off fetuses and place the heads in another 100 mm Petri as a rinse.

(i) Place 1-3 heads per dish in as many of the 35 mm dishes as you need.

(j) Put the 35 mm dishes that have heads in them in the refrigerator.

5. Micro—dissection

(a) Don't forget to turn off UV in dissection hood.

(b) Fill three 100-mm Petri's with ice [you might want to make extras and keep them in the freezer].

(1) One goes under the Sylgard® dissection dish.

(2) One will go under the heads when they are taken them from the refrigerator.

(3) One will go under the dish of brain area you dissect out

(c) Take one of the extra solution D filled 35 mm Petri dishes from the hood and put it in the dissection hood on the third ice pack.

(d) Take a dish of brains at a time from the refrigerator; set it on ice.

(e) Take two of the extra solution D-filled 35 mm dishes and pour them into the Sylgard® dissection dish.

(f) Put a head in the Sylgard® dissection dish.

(g) Dissect it:

(1) Remove skin from dorsal skull and pull off. Scissors are not needed for this.

(2) Remove cartilage from dorsal brain. It is very tough. One can see the brain bulge through the rip if it is done right.

(3) Pull away skin, cartilage, etc., along side of neck until you can see the side. The back has too much tissue. You should be able to see where cranial nerves attach brain to head.

(4) Gently stick forceps between cerebrium and skull, and push brain out of skull until the brain is held only by cranial nerves. You must pinch off optic nerves to do this. Then pinch off cranial nerves and remove skull entirely. Put skull and any other floating debris in a

wash dish somewhere.

(5) Take off meninges.

(6) Turn brain dorsal. Peel meninges forward from brainstem and back from cerebrum, till all of them are collected at the junction between cerebrum and cerebellum. Then take them off completely. Make sure you pull them from beneath the overhang of the cerebrum.

(7) Turn brain again. Push back the cerebral hemispheres a bit so you can see the corona radiata:

(8) Cut off the brain area you want with small scissors:

(a) For cerebral cortex, cut outside the hippocampod-amygoaloid complex ridge, and save only the hemispheres.

(b) For brainstem, cut along corona radiata. Discard hemispheres. Cut off spine below pons. Finally, cut off cerebellum. This is most easily done if you split the brain like a french loaf — then can see the folds of the cerebellum: If you wanted cerebellar cells, you'd save what you cut off here.

If you want only supratentorial brainstem (SES), cut at *base* of thalamus. The rest is infra-tentorial brainstem (IBS).

(9) Take the brain area you want and put it in the dish on the ice pack.

(10) Repeat till you run out of heads.

(h) Medium and plate rinsing: *NB*: If there is only one person doing the primary, both these steps must be done before anesthetizing the rat. Otherwise, the second person does these steps in the hood while the first person is doing the microdissections:

(a) Rinsing cover slips.

(1) Bring a bottle of Hepes-buffered saline to room temperature.

(2) Drain off the polylysine, a few wells at a time and rinse them twice with the saline. For 24 well dishes, rinse with 1 mℓ/well.

(3) Don't allow dishes to dry out between rinses.

(4) Rinse a third time and leave the saline in the wells.

(b) Make up 500 mℓ medium. Leave at room temperature.

(i) Dissociation

Take 2 sterile 50 mℓ centrifuge tubes. Add to one, then divide equally between the two tubes.

(a) Take the dish with the brain areas, with its cover on, into the regular hood. Bring fine scissors along.

(b) Rinse brain areas with solution D once or twice. Using a pipet line, to suck off solution. Don't use the vacuum line or you'll suck the brains up too.

(c) Dip the fine scissors in etOH and flame them.

(d) Mince the brains in their dish.

(e) Suck them up and down a pipet (1 mℓ serological, or Pasteur] once, to further break up the big chunks.

(f) Pipet the chunks into one of the autoclaved flasks.

(g) Rinse the mincing dish a few times with solution D; add these to flask too.

(h) Trypsin. For fetal day 16-17, 12 fetuses' brain stems, you'd want to use total of 16-20 mg trypsin (=16-20 mℓ solution D+trypsin) over all the trypsinizations. Adjust proportionally for larger or smaller number of fetuses, and for larger or smaller brain areas. This amount of trypsin will be spread over several applications of trypsin in the following way:

(1) first trypsinization: 5 mg trypsin in 16-20 mℓ total volume [bring to volume with solution D].

(2) second: 4-5 mg in 12-15 mℓ

(3) third: 3-4 mg in 10-12 mℓ

(4) fourth: 3-4 mg in 10-12 mℓ

(5) fifth: (if necessary): 3-4 mg in 10-12 mℓ

See the following for greater detail.

(i) After adding the chunks to the flask, add solution D and then solution D+trypsin (5 mℓ) such that total volume is 12-15 mℓ.

(j) Close bottle and place in 37° C shaker bath at 100 rpm, for 5 minutes.

(k) Pipet off supernatant, leaving all chunks, and put half the supernatant into each of the 2 centrifuge tubes containing trypsin inhibitor and medium.

(l) Add enough solution D 4-5 mℓ solution D+trypsin to bring total volume to 12-15 mℓ [it's best to add trypsin last).

(m) Shaker bath for 2 minutes.

(n) After 2 minutes, add ~0.2 mℓ DNAse [more if chunks are very clumped together] and return to shaker bath for 5 minutes. Do not pipet off supernatant.

(o) Pipet off supernatant into the two tubes of trypsin inhibitor.

(p) Add 3-4 mℓ solution D+trypsin and bring volume to 10-12 mℓ.

(q) Put in shaker bath for 2 minutes.

(r) Add 0.2 mℓ [or more or less if needed — all these figures are approx.] DNAse, and return to bath for 5 minutes.

(s) Pipet off supernatant into the 2 tubes.

(t) Repeat steps through until the two centrifuge tubes are nearly full of supernatant.

(u) Then pipet the entire contents of the flask, chunks and all, into the tubes. Try to make sure the chunks are evenly divided between the two tubes.

(j) Resuspension

(a) Centrifuge the two tubes of supernatant/trypsin inhibitor at ~750 rpm for 10 minutes.

(b) Take out a third 50 mℓ sterile tube, and a packet of sterile cheesecloth.

(c) Bring the centrifuged tubes back under the hood, and suck off supernatant, leaving only the pellet of cells.

(d) Add 5 mℓ medium to each tube with pellet.

(e) Resuspend pellet by gently sucking it up and down a pipet ~10 times [use 5 or 10 mℓ pipet]:

(f) Combine the 2 tubes into one.

(g) Touching it only by the edge, take cheesecloth out of packet and place it over the mouth of the third [empty] tube. Poke it into the mouth of the tube with a clean

pipet and then pipet 10 mℓ medium thru the cheesecloth to wet it.

(h) Pour the resuspended cells and chunks through the cheesecloth.

(i) Rinse the centrifuge tube with 10 mℓ medium and pour that through too.

(k) Cell count.

(a) Combine 0.25 mℓ cells and 0.25 mℓ trypan blue at room temp in a cell count tube. Up to the step with trypan blue the system is sterile, but after that, nothing in the count has to be sterile.

(b) Place clean, dust-free coverslip on equally clean hemacytometer.

(c) Put on drop of cells/trypan blue on each edge of hemacytometer.

(d) Count the number of live cells i.e., cells which haven't absorbed trypan blue within the 5×5 grid on each side of the hemacytometer. That number $\times 10^4$ = number of cells per mℓ.

A typical brainstem sample from 12 fetuses will have 99% live cells, 1% of which have short processes. Density is $\sim 100 \times 10^4$ cells/mℓ. Cortical samples would have $\sim 500 \times 10^4$ cells/mℓ.

(e) Multiply number cells/mℓ by total volume of cells [here, 25 mℓ].

(f) Divide by optimum plating density of 5×10^5 cells per well. This gives the number of wells you should plate. This gives the number of wells you should plate.

(g) Multiply number of wells you should plate by 0.5 to get total number of mℓ needed.

(h) Dilute the tube of cells to this volume with medium. (If you did a poor dissociation and 25 mℓ is already too dilute, simply plate more than 0.5 mℓ per well — just keep number of cells per well as close to 5×10^5 as possible.

(l) Plate the cells.

(a) Remove the Hepes-saline from a few wells at a time [no more than 10] and replace with 0.5 mℓ cells per well.

(b) Continue until you run out of cells or wells [you will usually run out of wells first].

(c) Place the plates of wells in the 10% CO_2 incubator for ~30 minutes. This allows live cells to attach to cover slips. Also put medium in 37° C bath.

— If plating is too dense leave the dishes in only 30 minutes.

— If plating density is low or if you added more than 0.5 mℓ per well, leave cells in longer: 45-60 minutes. You can even leave them in overnight.

(d) Take dishes out, suck off original medium [fewer than 10 wells at a time] and replace with fresh (37° C) medium 0.4 mℓ per well, unless very low density — then give 0.3 mℓ. This rinses off dead cells and debris.

(e) Put cells back in incubator. Do not feed until two days from date of primary, since cells need time to condition their medium.

VII. FEEDING

Feeding is roughly the same as the rinse step described above in the primary.

A. Take out 100 mℓ medium stock and tubes of insulin, transferrin, albumin [all premeasured for 100 mℓ medium], selenium, and putrescine.

B. pH adjust medium stock if necessary. There should be no purple tinge. pH adjusting must be done now; it cannot be done after proteins are added since HCl concentration will denature them. Make sure HCl is sterile. Do this in a hood over stirring plate.

C. Bring medium stock to 37° C in bath.

D. Add thawed aliquots to medium [see I.C.(1-5)].

E. Feeding:

1. Take one or two dishes from incubator at a time. Push rapid inject button when shutting door to keep CO_2 at 10%.

2. Tilt dish and suck off medium from 6-8 wells at a time, then replace with 0.4 mℓ new medium. Make sure you have the pipet flamed and ready *before* you drain the wells. Do not let wells dry out.

3. Flame pipe after each group of wells. Make sure it's cool before you stick it back in the medium.

4. Also flame vacuum line after each group and make sure it's cool.
5. Don't keep dishes out of the incubator too long.

F. Changes in defined medium since the Ahmed-Walker-Fellows paper [o.f. its Table I].

DELETED	*ADDED*
HEPES	taurine
KCl	adenosine
$MgCl_2$	cytidine
	quanosine
	uridine
	arachidonic acid

APPENDIX B

The following represents the sum of what has been presented at the New York Academy of Sciences, 1987 (Glynn, P. et al., 1987a), and the Neuroscience Meeting, 1987 (Glynn, P. et al., 1987b), concerning the effect of extracellular ethanolamine and choline on differentiated and undifferentiated cells. This work was done by T. M. Lee, S. Ogawa, R. L. Chappell and myself.

Introduction

High concentrations of phosphoethanolamine (PEt) have been reported to be present in various brain tumor cells, such as mouse and human neuroblastoma, human glioblastoma and rat glioma.[1,2] It was also shown earlier by Navon et al.[3] that lymphoid cells contained a large amount of PEt. In *in vivo* 31P NMR studies of these tumors, the PEt peak has been used as a monitor of the response that these tumor cells show to various chemo and radiation therapies. Similarly high levels of PEt have been observed in developing brains of neonates and near term fetuses of various animals,[4,5] ranging from rat to man. However, the PEt content in these brains decreases along the course of the brain growth.

Although PEt is a common metabolite present in many types of cells as an intermediate compound for phospholipid synthesis, the biological reason for its high level in these cells mentioned above is not clear. We observed, in 31P NMR spectra, varying amounts of PEt and phosphocholine (PCh) in neuroblastoma cells (N1E-115), a model cell line of sympathetic neurons, and therefore we have examined some conditions which affected cellular levels of PEt, in order to find the controlling factors which determine the high level of PEt in these cells.

Materials and Methods

N1E-115 neuroblastoma cells were obtained from Dr. E. Richelson of the Mayo Clinic. They were grown in tissue culture as previously described.[6] After they grew to a confluent stage, they were transferred from the culture dishes to a suspension of microcarriers (cytodex III) for NMR experiments.[6]

A sample holder, a 20 mm diameter tube, was placed vertically in a probe coil and the flow of the medium was directed from the top to the bottom of the tube. The major advantage of this vertical setting relative to the horizontal one in the solenoid coil used earlier[7] was that it was not affected by air bubbles occasionally trapped in the sample holder. Because of the flat horizontal boundary of the microcarrier beads at the top, the flow of the medium was homogeneous in the horizontal plane. The color of the medium due to phenol red was uniform along the length of the sample holder tube, indicating the homogeneous pH of the medium in the whole sample and therefore, adequate

oxygen supply. When the medium flowed from the bottom to the top, it was uneven due to channel formation. The sensitivity of the coil, a double turn parallel connected Helmholtz coil, was comparable to, or better than the solenoid coil arrangement. The 90° pulse width was 34 μsec with the sample. NMR spectra were taken at 145.8 MHz for 31P resonance with a Bruker wide bore 360 spectrometer.

Results

N1E-115 neuroblastoma cells were grown in tissue culture to a confluent stage and were attached to the microcarrier beads as described earlier.[6] A volume of 6 ml of the packed beads carrying about 70 million cells was put into a NMR sample tube through which the medium was superfused. A typical 31P NMR spectrum is shown in Fig. 1a. The peak assignments are given in the figure legend. The major part of the Pi peak intensity came from the Pi in the medium (1 mM) and the intracullular Pi resonance was hidden in the peak. With a peak narrowing signal processing procedure, the two Pi resonances could be resolved. In the case of the spectrum of Fig. 1a, the chemical shift difference was 0.1 ppm which corresponded to a pH gradient of 0.1 with the internal pH being lower. The amount of the Δ pH was dependent on the medium pH. In the region of the phosphomonoester resonances in Fig. 1a, the PCh peak (peak 2) was clearly observable, but the PEt resonance was not distinct from other phosphomonoester resonances (peak 1). The pattern of these resonances in this region showed a slight variation among samples under similar conditions. The intensities of peaks 8 and 9 (diphosphodiesters) relative to peak 10 (ATPβ)

varied to some extent depending on the conditions these cells were exposed to.

In the medium, superfusing around the cells, there was about 10 μM of ethanolamine (EA), which came from the 10% fetal bovine serum added to the medium. Since the level of PEt should be dependent on the phosphorylation of cellular ethanolamine, EA was added to the medium so that the cellular EA could be increased. The spectrum taken several hours after the EA addition (200 μM) is shown in Fig. 1b. There was a slow increase in the PEt peak intensity. The peak at 13 ppm was due to 1 mM phenylphosphonic acid added to the medium with EA in order to follow the rapid change (in a few minutes) of the medium by NMR spectra. The insert in Fig. 1b is the difference between Fig. 1b and 1a, and it also shows a slight increase of PCh.

Neuroblastoma cells can be induced to differentiate when the serum supply in the medium is withheld and dimethylsulfoxide (DMSO) is added to the medium.[8] This is one of many ways to induce cell differentiation. They differentiate morphologically, biochemically (transmitter synthesis) and electrophysiologically. After neuroblastoma cells were grown to confluency in tissue culture, the medium was changed to the one in which the fetal bovine serum was reduced from 10% to 2%, and DMSO (2%) was added. The cells were kept in the tissue culture for several days. They showed morphological changes by sending out processes. When these cells were attached to microcarriers for NMR measurements, they stuck to each other, forming clusters on the microcarriers. Some processes were still visible under an optical microscope. The spectrum of these cells is shown in Fig. 2. The difference in

the phosphomonoester region from Fig. 2a was notable. The peak intensities of PEt and PCh relative to the NTP peak were higher than those in undifferentiated cells. The peak 5 (phosphocreatine) increased in intensity. When 200 μM of EA was added to the medium, the PEt peak increased with time as shown in Fig. 2. Figure 2c is the spectral difference between Fig. 2a and 2b (before and 7 hours after the addition of EA). There were no other changes in the spectra except peak 4 (glycerophosphocholine). The ATP peak intensities stayed constant during this incubation. The time course of the intensity change in the PEt resonance was plotted (Fig. 3) together with the one observed in undifferentiated cells. The difference between the two cases was striking. The differentiated cells showed a faster and larger accumulation of PEt than the undifferentiated cells.

Since the PEt seemed stable in these cells once it accumulated to a high level (see later descriptions), the cellular content was measured in perchloric acid extracts by high pressure liquid chromatography. When 200 μM EA was added to the culture medium at the same time that cells were induced to differentiate, the PEt slowly increased to a high level over a period of several days. This was the same time required for the cells to complete differentiation.

To take advantage of *in situ* NMR measurements, responses of the PEt peak to various medium conditions were examined. After neuroblastoma cells had accumulated PEt they were subjected to an EA wash out, pH changes and stoppage of medium flow (an ischemic condition). When the EA concentration in the medium was reduced from 200 μM to less than 10 μM, the PEt peak did

not show any appreciable decrease for more than several hours. Since the EA was expected to cross the cellular membrane rather easily,[10,11] the observation that there was no decrease of the PEt peak indicated that the PEt usage rate in these cells was slow under the conditions of these measurements and also the ethanolamine kinase reaction did not proceed backward at the reduction of EA. There were small changes in the PEt peak intensity with the medium pH change (from 7.0 to 8.0), a slight increase at basic pH and a slight decrease at an acidic pH. When the flow of the medium was stopped, the medium and cellular pH became acidic. The phosphocreatine peak disappeared and then ATP peaks showed a decrease. Soon after the acidification was seen by the two Pi peaks, they overlapped each other and the Δ pH was no longer observable. The pH, which the medium Pi peak indicated, went down to 6.6. During this period the PEt and PCh peaks were still resolved and they moved upfield indicating the acidified environments as the Pi peak showed. Under the ischemic condition the Δ pH was expected to be essentially zero, due to a large amount of lactate formation. The correlation of the chemical shift changes among these phosphate compounds indicated that these intracellular phosphate compounds shared the same pH environment. When the flow of the medium was resumed, the intracellular pH immediately followed the change in the medium pH as indicated by the changes in the peak positions of these phosphate compounds. It was interesting to note that the intracellular Pi peak emerged from the medium Pi peak about 15 minutes after the change of the medium pH. In other words, it required some time to rebuild the Δ pH. The peak shape suggested

that the intercellular Pi peak was not broad, due to a transient distribution of intracellular pH values among the cells. It remained to be seen whether this delayed Δ pH formation was due to the time required for the complete removal of lactate from the cell environment or from some process coupled to the pH gradient which reestablished itself after the ischemic insult (some ion gradient across the cell membrane could be a candidate).

Discussion

The major pathway of phospholipid synthesis which involves phosphoethanolamine is well known as depicted in the following diagram.

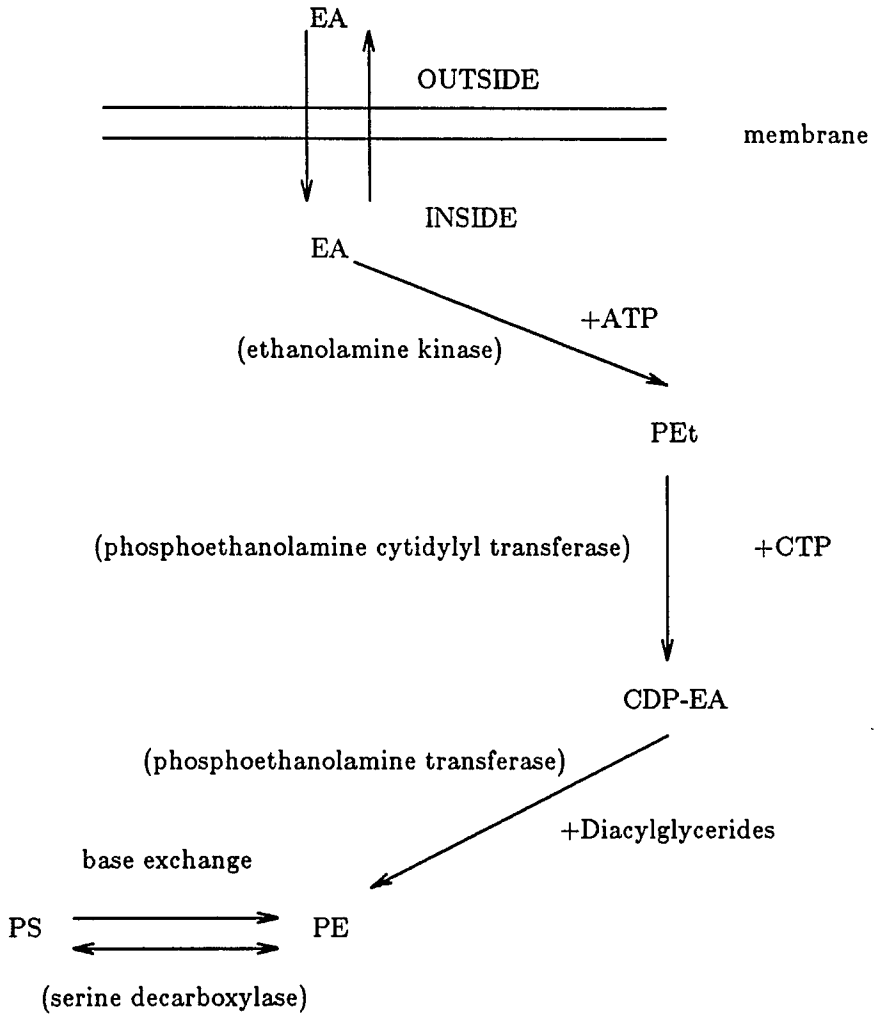
EA
OUTSIDE
membrane
INSIDE
EA
+ATP
(ethanolamine kinase)
PEt
(phosphoethanolamine cytidylyl transferase)
+CTP
CDP-EA
(phosphoethanolamine transferase)
+Diacylglycerides
base exchange
PS
PE
(serine decarboxylase)

Among the processes of the above pathway to synthesize phosphatidyl ethenolamine (PE), the process to make CDP-EA from PEt and CTP is said to be the controlling step.[13] The process is catalized by phosphoethanolamine cytidylyl transferase and is essentially irreversible due to the hydrolysis of pyrophosphate, the reaction product, to 2 Pi's. The process is kinetically controlled through the product inhibition by CDP-EA. The pathway from EA to PE is the dominant pathway of the PE synthesis and the conversion of phosphatidylserine (PS) to PE by decarboxylation of serine or exchange of serine with EA on PS is a minor pathway. The synthesis of phosphatidylcholine (PC) is similar to the PE synthesis starting with choline.

At a steady state the level of PEt is constant and therefore the net flux rates of the production and the consumption of PEt is the same. The net flux of the consumption should be a sum of the PE synthesis for cell growth and for cell maintenance to balance lipid degradation. The metabolite usage rate (the net flux rate) for the cell growth in neuroblastoma cells in tissue culture could be estimated from the cell doubling time (one and half days) during the log phase of growth and the lipid compositions of neuroblastoma cells.[13] The estimated value was a few mM/hr in terms of a cellular concentration and could be compared with the steady state levels of PEt in the cells (a few mM to 10 mM).

Under the standard medium conditions in the present experiments, the EA concentration was low (about 10 μM). By raising the EA concentration, the process by the ethenolamine kinase could be perturbed and some change in the PEt level might be expected. The response to a 200 μM EA addition in the

undifferentiated cells at confluence was only a slight increase of the PEt level with time as shown in Fig. 1. The rate of increase was about 0.15 mM/hr (the cellular ATP concentration was assumed to be 4 mM). On the contrary, in the differentiated cells the response was quite dramatic. The rate of PEt accumulation was about 0.7 mM/hr and much higher than the estimated rate of PE synthesis in the growing cells. The process of EA uptake is known to be much faster than the time scale of these responses. Their difference was likely due to the difference in the kinase activity rather than in the later processes of PE synthesis. In either state of these cells, there was no cell multiplication and the PE synthesis for cell growth was minimal In the tests of EA washout from the medium, the PEt resonance did not lose its intensity for several hours after the washing of EA, indicating that the PEt usage rate was quite slow. In the differentiated cells, (Fig. 3) the accumulation of PEt slowed down when the PEt concentration reached a high level. Since the PEt usage rate did not seem to have increased, the likely cause of this saturation was the inhibition of the kinase, possibly by the product of the enzyme, PEt itself. Although the steady state level of PEt varied among various samples, it was higher with higher EA, indicating the competition between the substrate (10 - 200 μM) and the product (several mM).

In the undifferentiated cells the response to the EA addition was much smaller and therefore the kinase activity appeared to be lower. Consistent with this, the PEt and PCh levels before the addition of extra EA were also lower (Fig. 1). It has not been determined whether this lower kinase activity was due

to a lower enzyme concentration or due to a stronger inhibition of the enzyme in these undifferentiated cells. When undifferentiated cells at confluence were subjected to a condition which induced cell differentiation in the presence of 200 μM EA, the increase of the PEt level was slow. The time scale of the PEt increase was days, not hours as in the case shown in Fig. 3 and the PEt level increased with the morphological changes of these cells which took several days to complete. This observation excluded the possibility that the presence of some substances or the lack of them, which caused differentiation, removed the enzyme inhibition, inducing an increase of the enzyme activity instantly. Either the enzyme concentration was increased by protein synthesis during cell differentiation, or there was a gradual removal of the enzyme inhibition along with the morphological changes. Since cell differentiation is known to be associated with active protein synthesis, the former possibility is more likely.

We have shown here that the usually high level of PEt can be accumulated in neuroblastoma cells *in vitro* if the cells are subjected to a condition of cell differentiation and an elevated level of EA. The ethanolamine kinase activity becomes high in the differentiated cells. Since the high level of PEt reached a steady state without increasing much in the usage of PEt, the inhibition of the ethanolamine kinase by PEt was a good possibility. In various brain tumors, where such high levels of PEt have been observed, tumor cells are probably quite heterogenous in their population. Similar kinds of cell status dependence in PEt contents could be present as we have observed in neuroblastoma cells. As another control, an *in vivo* study is under way of a tumor mass generated by

implanting these neuroblastoma cells into mice, of the same strain from which the cell line was originally obtained.

UNDIFFERENTIATED
BEFORE AND AFTER ETHANOLAMINE ADDITION

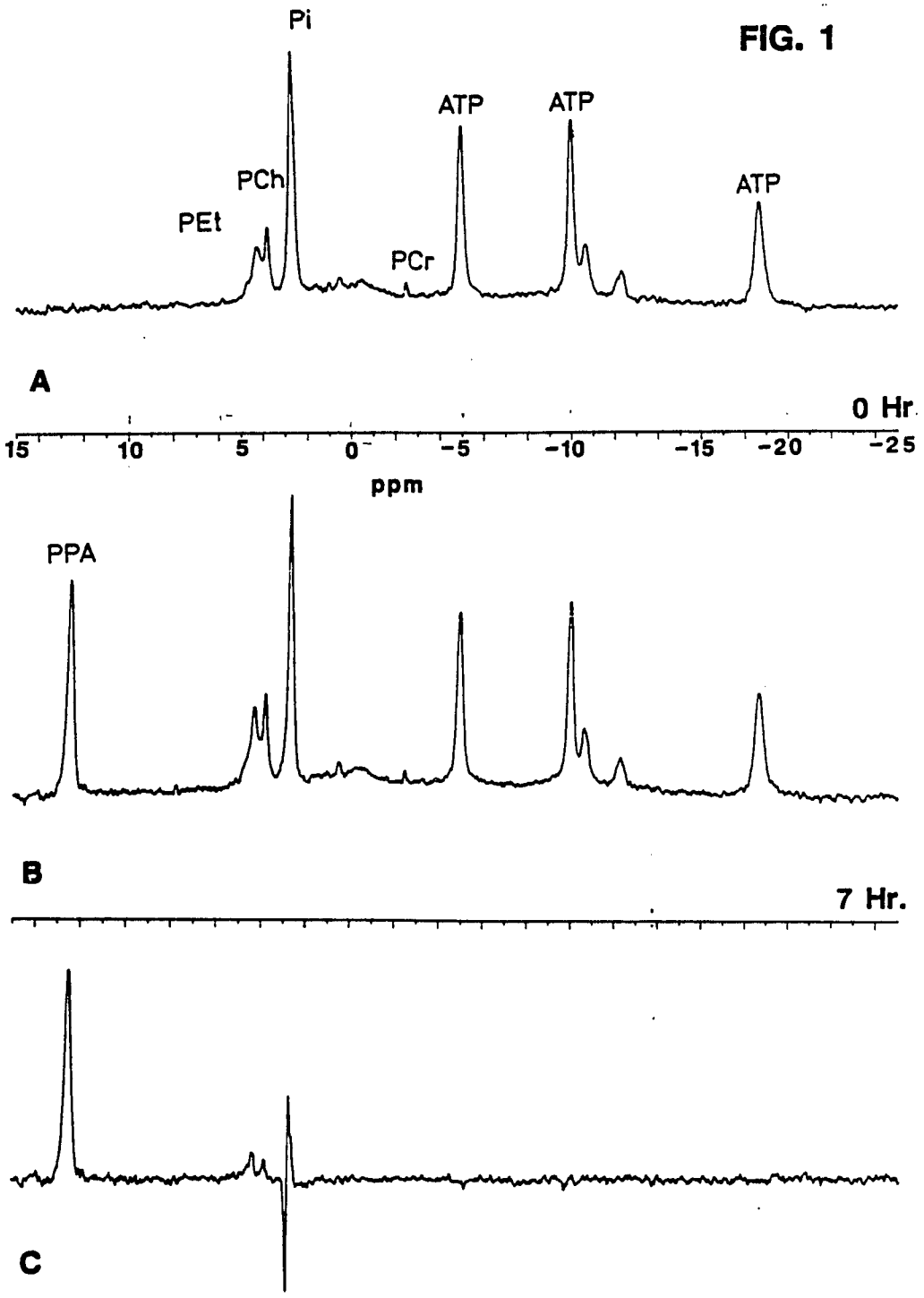

FIG. 1

DIFFERENTIATED

BEFORE AND AFTER ETHANOLAMINE ADDITION

FIG.2

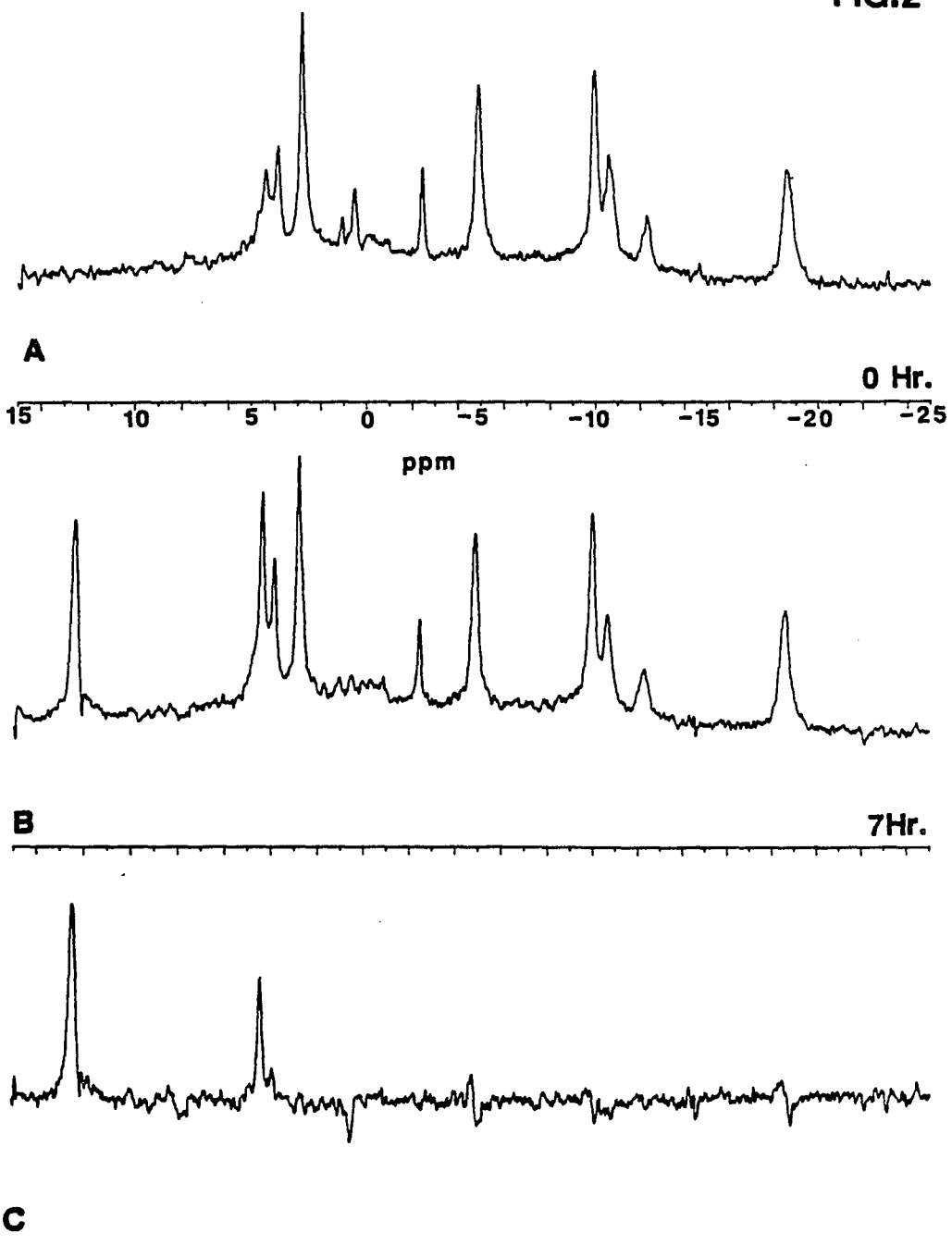

FIG.3

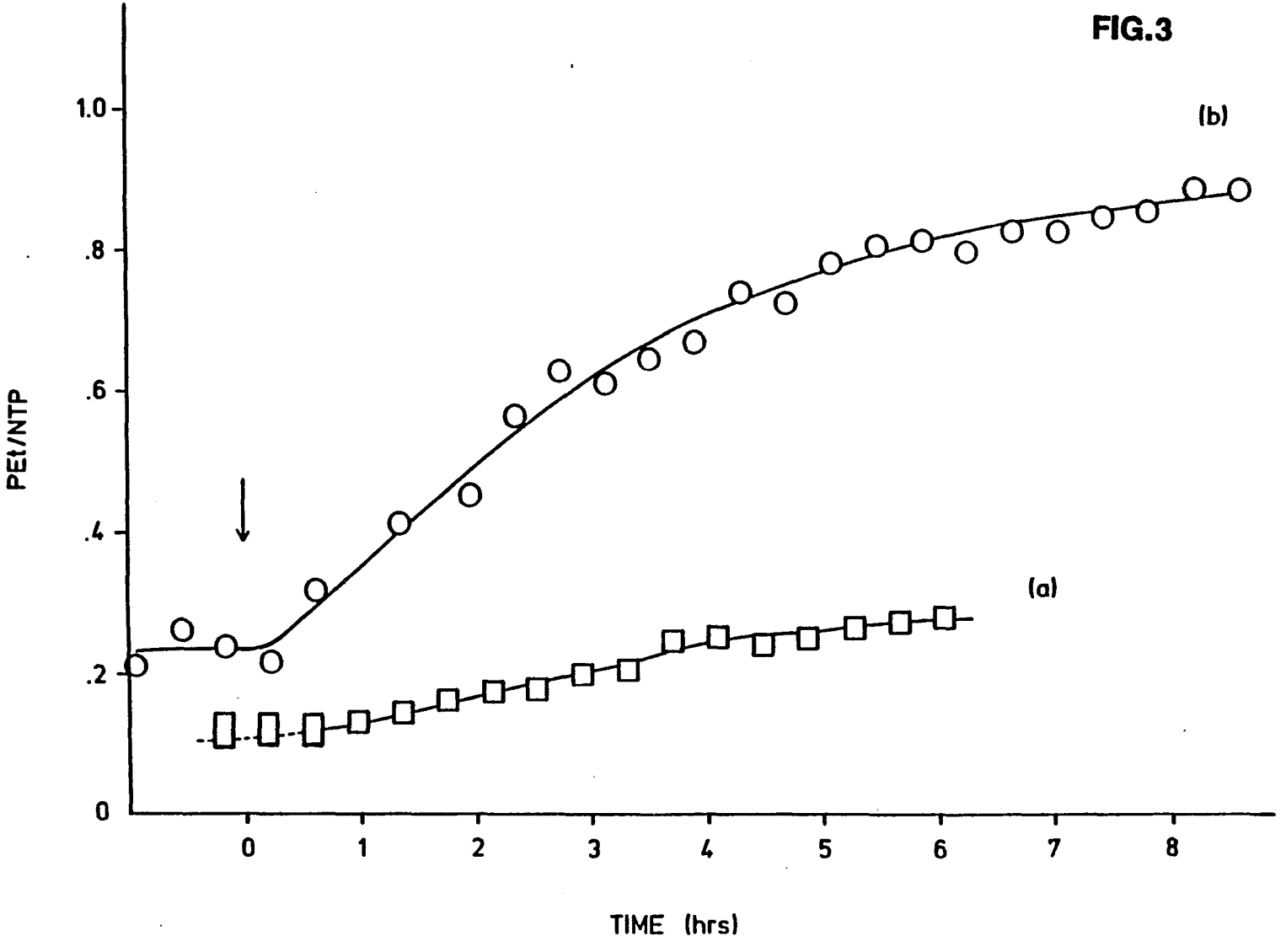

FIGURE CAPTIONS

Fig. 1. Undifferentiated cells on microcarriers at a higher density were put in a life support samples holder system, and placed in a 360 wide bore NMR spectrometer, operated at 145.8 MHZ. The total N1E-115 cells volume of 70×110^{-6} cells was on the order of .6 ml. 31P spectra of 1024 FID's were obtained in 51 minute blocks. The repetition time was 3 seconds. a) shows the spectrum collected just before the addition of 200 μM ethanolamine. (b) is the spectrum 7 hours after the addition of ethanolamine, and (c) shows the difference spectrum. The spectra have been processed with 10 Hz line broadening.

Fig. 2. Differentiated cells were seeded onto Cytodex III microcarriers and loaded into the same chamber of the life-support system, and placed in the magnet. Data were collected, as in Fig. 1. (a) shows the 31P profile prior to addition of 200 μM ethanolamine. (b) shows the spectrum 7 hours after the addition of ethanolamine, and (c) shows the difference spectrum. The spectra have been processed with 10 Hz line broadening.

Fig. 3. The spectrum peaks typified in Fig. 1 and Fig. 2 were corrected for differences in the relaxation times for PEt, and ATP. The ratios of PEt/ATP were then calculated and plotted. (a) is a plot of PEt/ATP for undifferentiated cells. The arrow indicates the point at which ethanolamine was added. The dotted line indicates estimated values. (b) is a plot of PEt/ATP for

differentiated cells.

REFERENCES

1. Maris, J. M., Evans, A. E., Bolinger, L., McLaughlin, A. C. and Chance, B. (Pub. 1986). Analysis of the metabolism of lipid precursors in human neuroblastoma by phosphorus-31 NMR spectroscopy. *Magn. Reson. Cancer, Proc. Int. Conf.*, pp. 83-90.

2. Naruse, S., Hirakawa, K., Tanaka, C., Higuchi, T., Ueda, S., Nishikawa, H. and Watari, H. (1985). Measurements of *in vivo* ^{31}P Nuclear Magnetic Resonance Spectra in Neuroectodermal Tumors for the Evaluation of the Effects of Chemotherapy. *Cancer Res.* **45**, 249-2433.

3. Navon, G., Navon, R., Shulman, R. G., and Yamane, T. (1978). Phosphate Metabolites in Lymphoid, Friend Erythroleukemia, and HeLa cells observed by high-resolution ^{31}P Nuclear Magnetic Resonance. *Proc. Natl. Acad. Sci. USA*, **75**, No. 2., 891-895.

4. Bolinger, L, Gyolai, L., Chance, B., and Leigh, J. S. (1984). Abstracts for 3rd Annual Meeting, Society of Magnetic Resonance in Medicine, pp. 59-60.

5. Ogawa, S., Lee, T. and Glynn, P. (1986). Energy Metabolism in Rat Brain *in vivo* Studied by ^{31}P Nuclear Magnetic Resonance: changes during Postnatal Development. *Arch. Biochem.*. Biophys. **248**, 43-52.

6. Glynn, P., Lee, T., and Ogawa, S. (1986). The Presence of Creatine Kinase Activity in Neuroblastoma NIE-115 Cells in Tissue Culture as

Measured by ^{31}P NMR. (In Preparation).

7. Ugurbil, K., Guernesey, D. L., Brown, T. R., Glynn, P., Tobkes, N., and Edelman, I. S. (1981). ^{31}P NMR Studies of Intact Anchorage-dependent mouse embryo fibroblast. *Proc. Acad. Sci.* USA, **78**, 4843-4847.

8. Kimhi, Y., Palfrey, C., Spector, I., Barak, Y., and Littauer, U. Z. (1976). Maturation of Neuroblastoma Cells in the Presence of Dimethylsulfoxide. *Proc. Nat. Acad. Sci. USA*, **73**, No. 2, 462-466.

9. Burmeister, D. W., (1982). Process Formation in the Human Neuroblastoma clone SK-N-SH-SY5Y *In Vitro*. PhD. dissertation submitted to the Graduate Faculty in Biology at The City University of New York.

10. Sundler, R., and Akesson, B. (1975). Regulation of Phospholipid Biosynthesis in Isolated Rat Hepatocytes. *J. Biol. Chem.* **250**, No. 9, 3359-3366.

11. Zelinski, A. T. and Choy, P. C. (1982). Phosphatidylethanolamine biosynthesis in isolated hamster heart. *Can. J. Biochem.*, **60**, 817-823.

12. Sundler, R. (1975). Ethanolaminephosphate Cytidylyltransferase. *J. Biol. Chem.*, **250**, No. 22, 8585-8590.

13. Robert, J., Rebell, G., Mandel, P. and Yavin, E. (1978). Polar Head Groups Manipulation of Phospholipids in Cultured Neuroblastoma Cells. *Life Sci.*, **22**, 211-216.

APPENDIX C

At an early stage of this research it was hoped that neuroblasoma cells could be studied while being superfused with Ringers "B" solution with or without glucose. This Ringers is sodium and Pi free. The results of the experiments with C3T101/2 cells suggested this possibility. However, when the undifferentiated cells were superfused with Ringers B by itself or when supplemented with 10% FBS or 20% complete DMEM, the cells responded with major changes in their PME, PDE and ATP concentrations. The PME peak was quite sensitive to a pH shift, which was not simply a titration even where the peak shifted into the Pi region, as has been observed with PCh and PEt. The events are not explained here, but their unusual nature and their relevance to future experiments utilizing Ringers B and possibly other Ringers or modified medium is important enough to justify the characterization of these events. The undifferentiated neuroblastoma cells used did not have a PCr store and had not been grown with any extracellular Cr supplement, and therefore had no appreciable ATP buffering capacity. Cells which were superfused with Ringers B supplemented with 10% FBS, maintained their ATP levels constants and were seen to have a large peak appear in the PME region. The cells did well for at least two hours. When they were switched to Ringers B without supplement, the cells lasted 30 minutes, at which time the ATP was down 80%. The broad peak in the PME region was the most persistent, dropping 50% in 80 minutes. A most interesting observation was that the pH had a very strong effect when

undifferentiated neuroblastoma cells were superfused with Ringers B supplemented with 20% complete DMEM, which is 10% FBS at pH 6.8. There was no appreciable change in the PME region, although a peak seen at higher pH and similar conditions appeared. However when the pH was shifted to 7.3 concurrently, a very large PME peak appeared. The requirements for this event most likely involved low level glucose. The PME peak is quite possibly a sugar phosphate. It is possible further study of these events will give insights into glucose utilization, and should be pursued further.

RINGERS B PLUS 10% FBS

Figure C-1

N1E-115 cells in low glucose, sodium and P_i Ringers. A) control spectra taken over a three-hour period. The cells were in DMEM, 10% FBS and 1% PS. The extracellular pH was approximately 8.0. B) these spectra were taken after the cells were switched to ringers "B" (see table 4.5-1B) supplemented with 10% FBS and 1% PS in the recirculating mode. The 60 ml portion of unswitched or dead volume of the system together with the FBS and Ringers "B" account for the final low sodium, glucose and phosphate in the superfusate the system was run in a non recirculative mode for 50 minutes. Estimates for these are 0.3-0.4 mM for P_i, 0.6 mM for glucose and 12 mM for Na. The pH went from 8 in the control period to 7.3 during this series in Ringers "B". C) Spectrum of cells switched to Ringers without a supplement of FBS. Note that the P_i peak washed out in part. This spectra represents the average values from the start (a) to end (c) of the wash out. (a) is the control from panel A. (b) is the last of panel B. These are put together for ease of comparison. D) The peak heights of P_i, ATPβ and PME are plotted for one control and the next six files. The peak height of P_i includes intracellular and extracellular P_i. The extracellular P_i includes P_i from the FBS in the ringers, the contribution from the unswitched DMEM and 10% FBS, and the underlying base role. When these have been taken into account, the estimated 30% remaining in P_i is attributed to a 60%-

70% decrease in the superfusate P_i concentration.

The repetition time for all the above spectra was 1 second and each file is the sum of 1000 FID (16.7 min per file). Note the enormous increase in its PME and the increase in the phosphodiester region. Because of differences in the buffers, the external pH changed to pH 7.2 i.e., going from Ringers B to Ringers A.

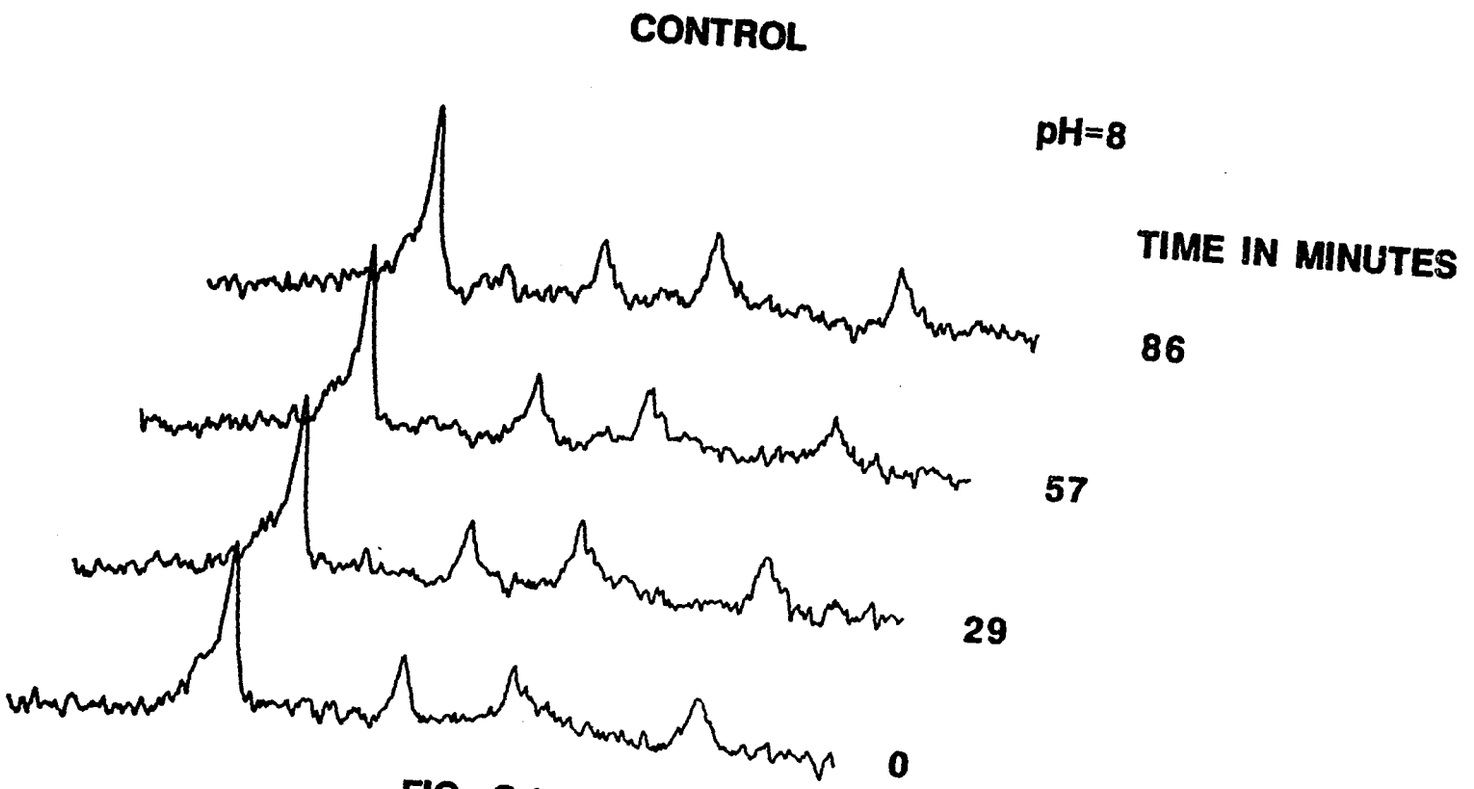

FIG. C.1 (A)

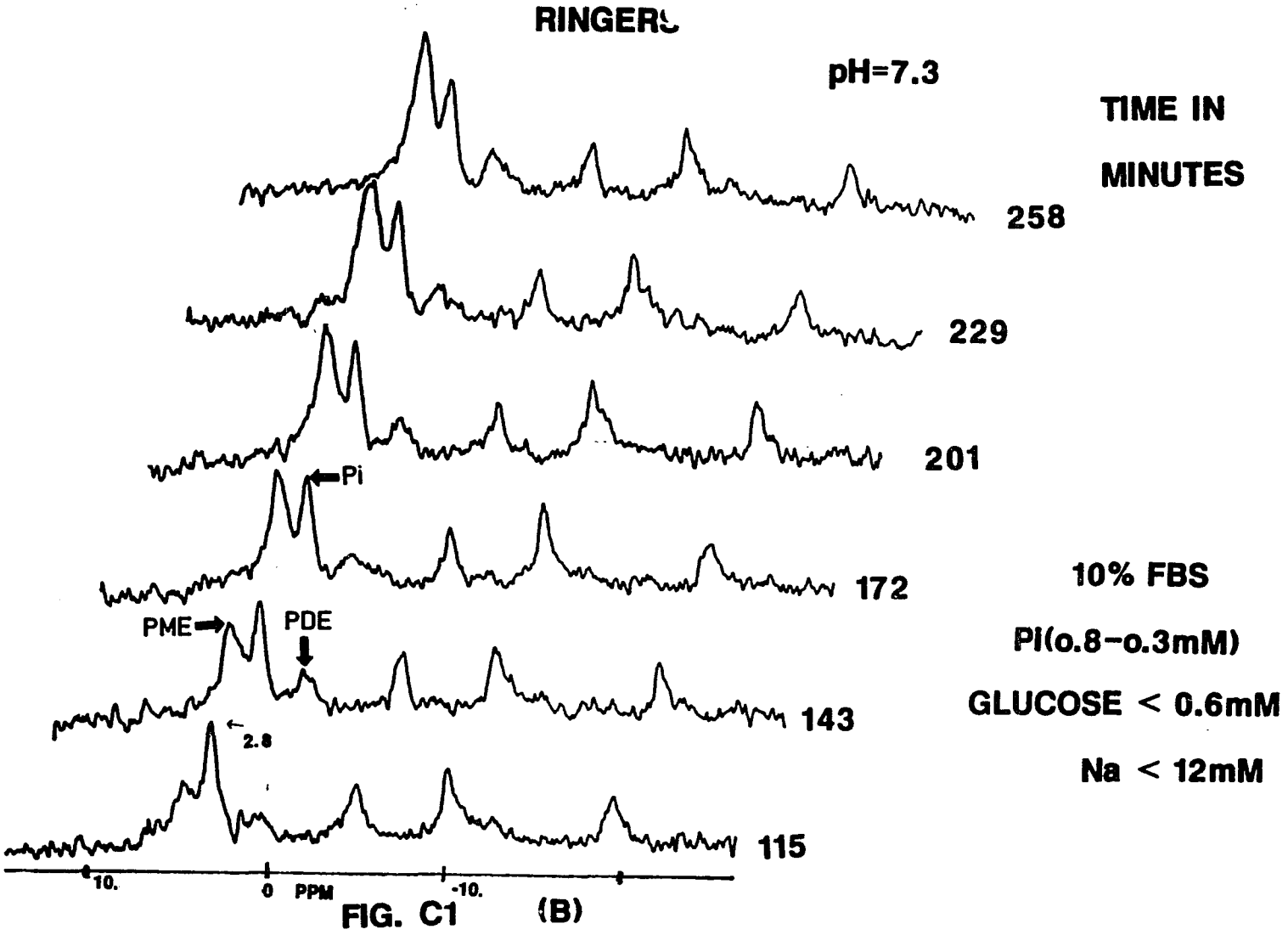
RINGER
pH=7.3
TIME IN
MINUTES
258
229
201
Pi
172
PME
PDE
143
2.8
115
10.
0 PPM
-10.
10% FBS
Pi(o.8-o.3mM)
GLUCOSE < 0.6mM
Na < 12mM

FIG. C1 (B)

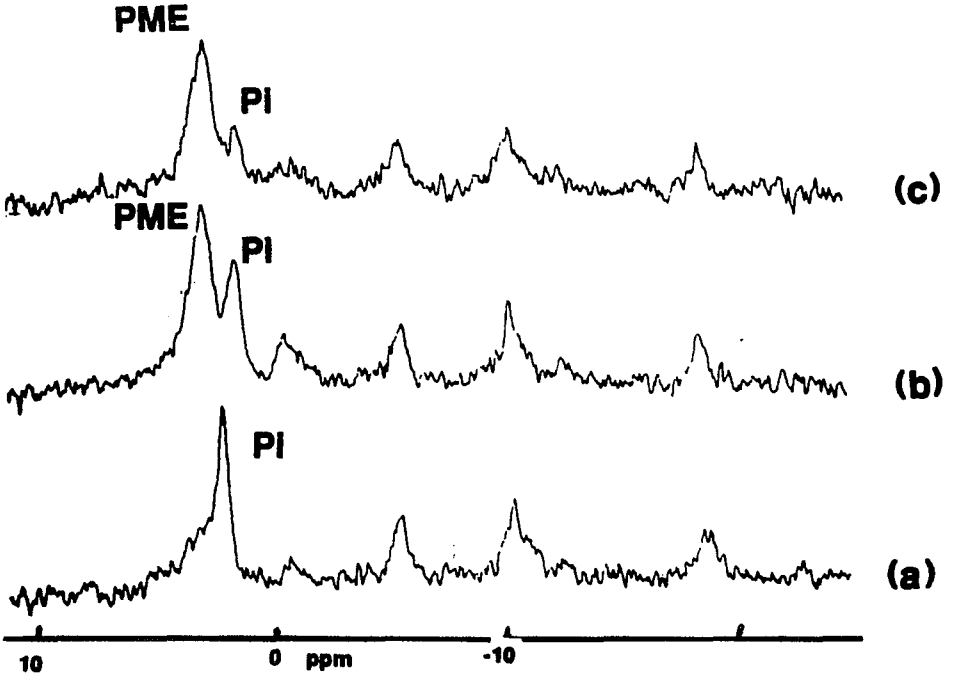

FIG. C1 (C)

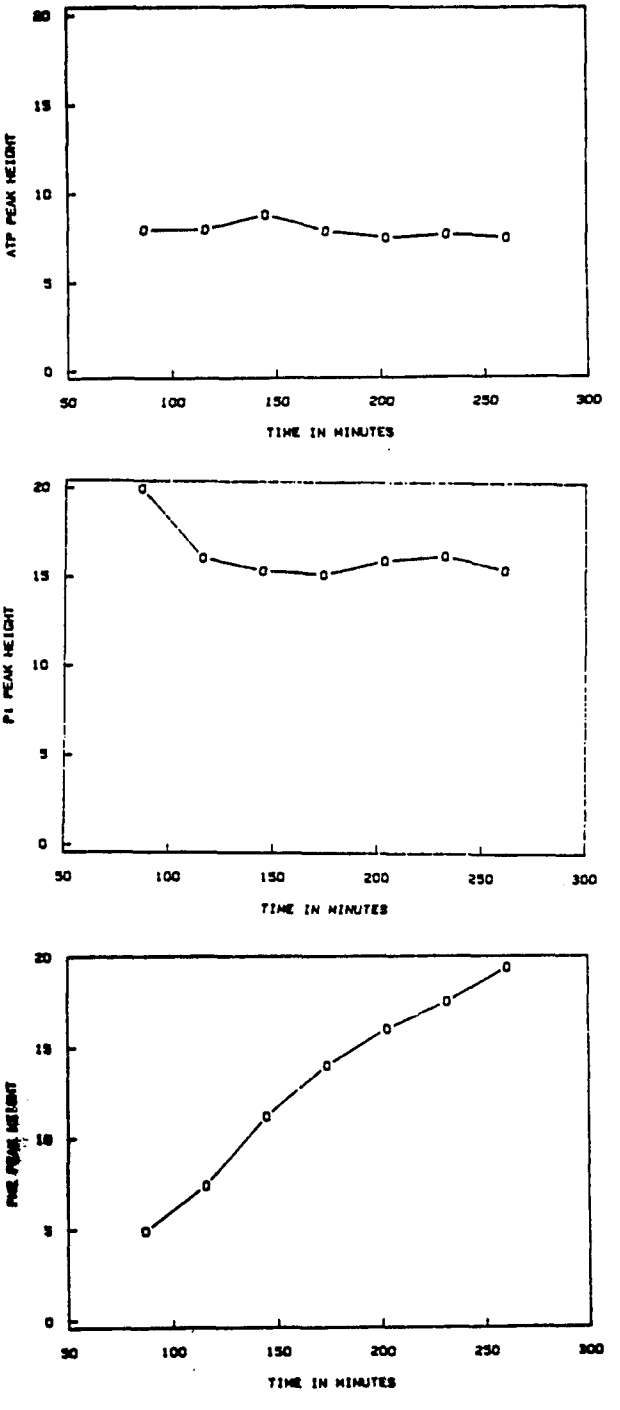
ATP PEAK HEIGHT
0
5
10
15
20
50
100
150
200
250
300
TIME IN MINUTES
Pi PEAK HEIGHT
0
5
10
15
20
50
100
150
200
250
300
TIME IN MINUTES
0
5
10
15
20
50
100
150
200
250
300
TIME IN MINUTES

FIG. C1 (D)

RINGERS B PLUS 20% DMEM

Figure C-2

N1E-115 cells in low glucose, sodium and P_i ringers. A) The cells at pH 7.4 as measured with a pH meter at the exit of the sample holder. This is the control in DMEM supplemented with 10% FBS and 1% PS. B) cells after being switched to 300 ml of ringers "B" with 10% FBS and 1% PS. The total volume of the recirculating medium and unswitched DMEM was 360 ml. (Note the pH dropped to 6.8 as a result of CO_2 in the gas exchanger and returned to 7.3 when the CO_2 was turned off (see c). C) The cells in the same ringers as (B) but at pH 7.3. Note the difference in time scale. The number of scans per file in (A) and (B) is 1000 and for (C) it is 5000 repetition time is 1 sec., and the line broadening is 20 Hz. D) Shows the difference between the spectra from file 1 and 9. Note that the difference in the P_i region is small, that is, this total of the inter and extracellular P_i remains approximately constant at pH 7.3. However files 6, 7 and 8 show a much smaller P_i peak. This is in part due to pH heterogeneity.

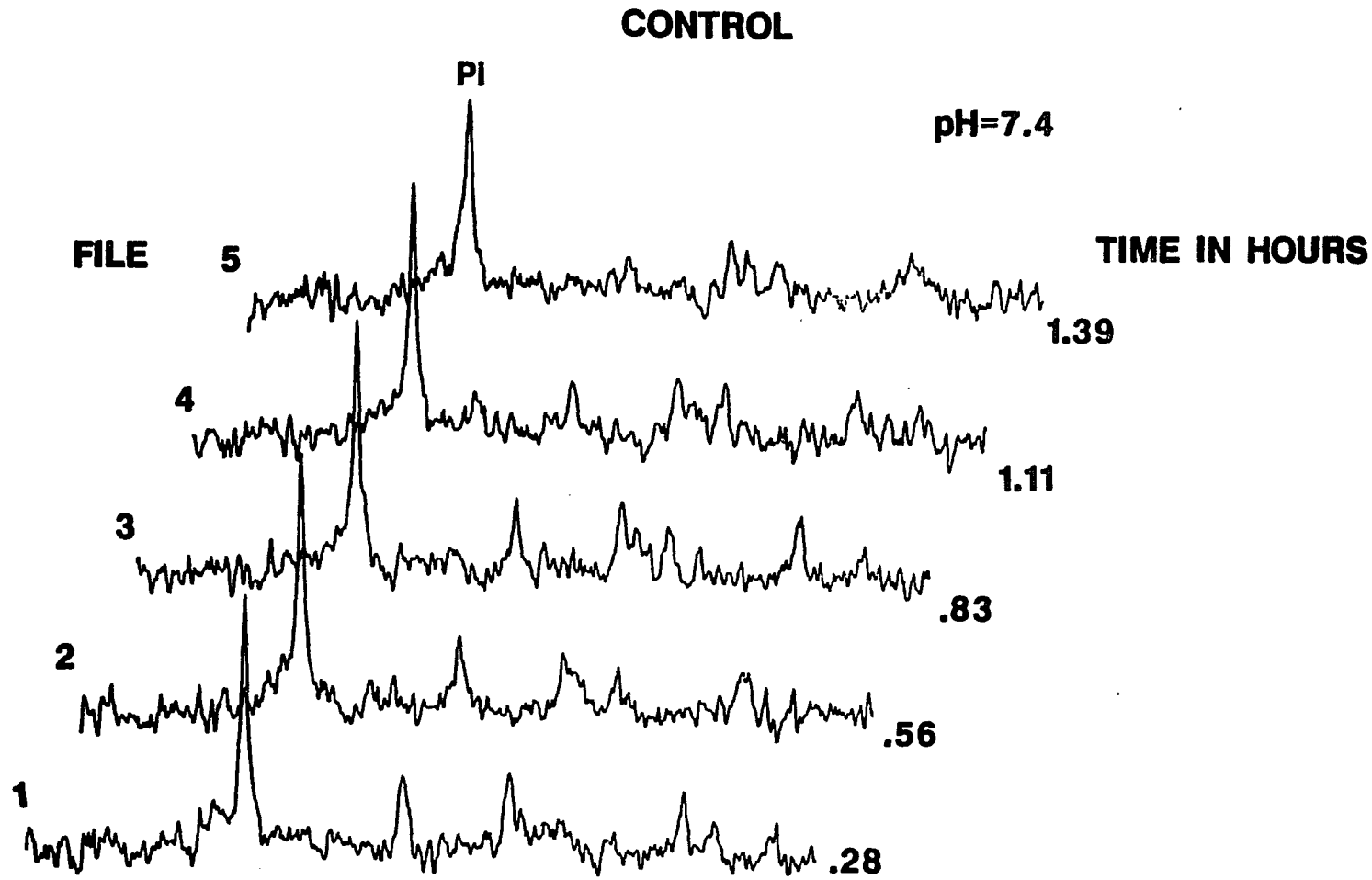

FIG. C2 (A)

RINGERS B

pH=6.8

CO2 ON

TIME IN HOURS

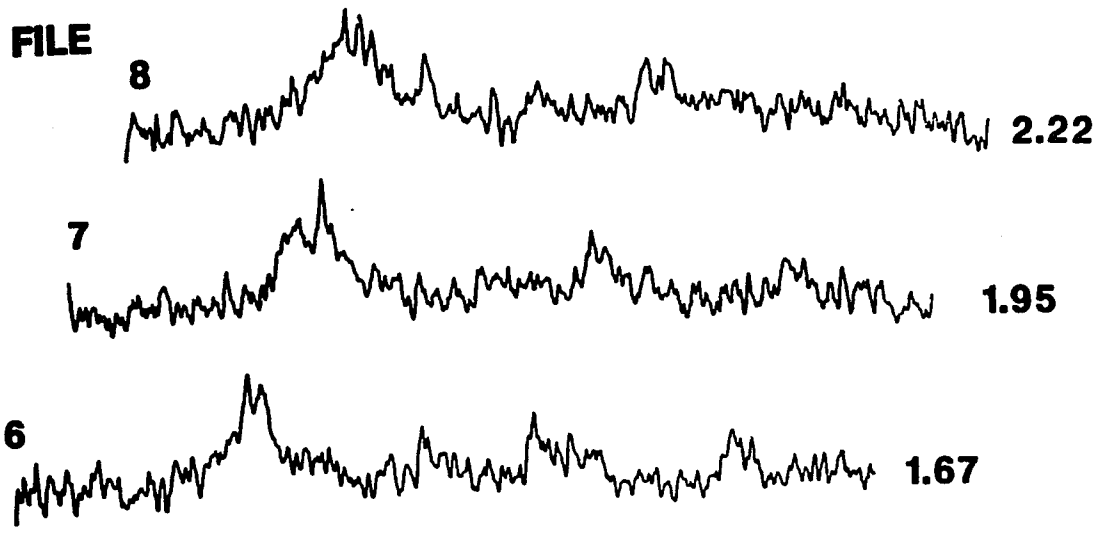

FIG. C2 (B)

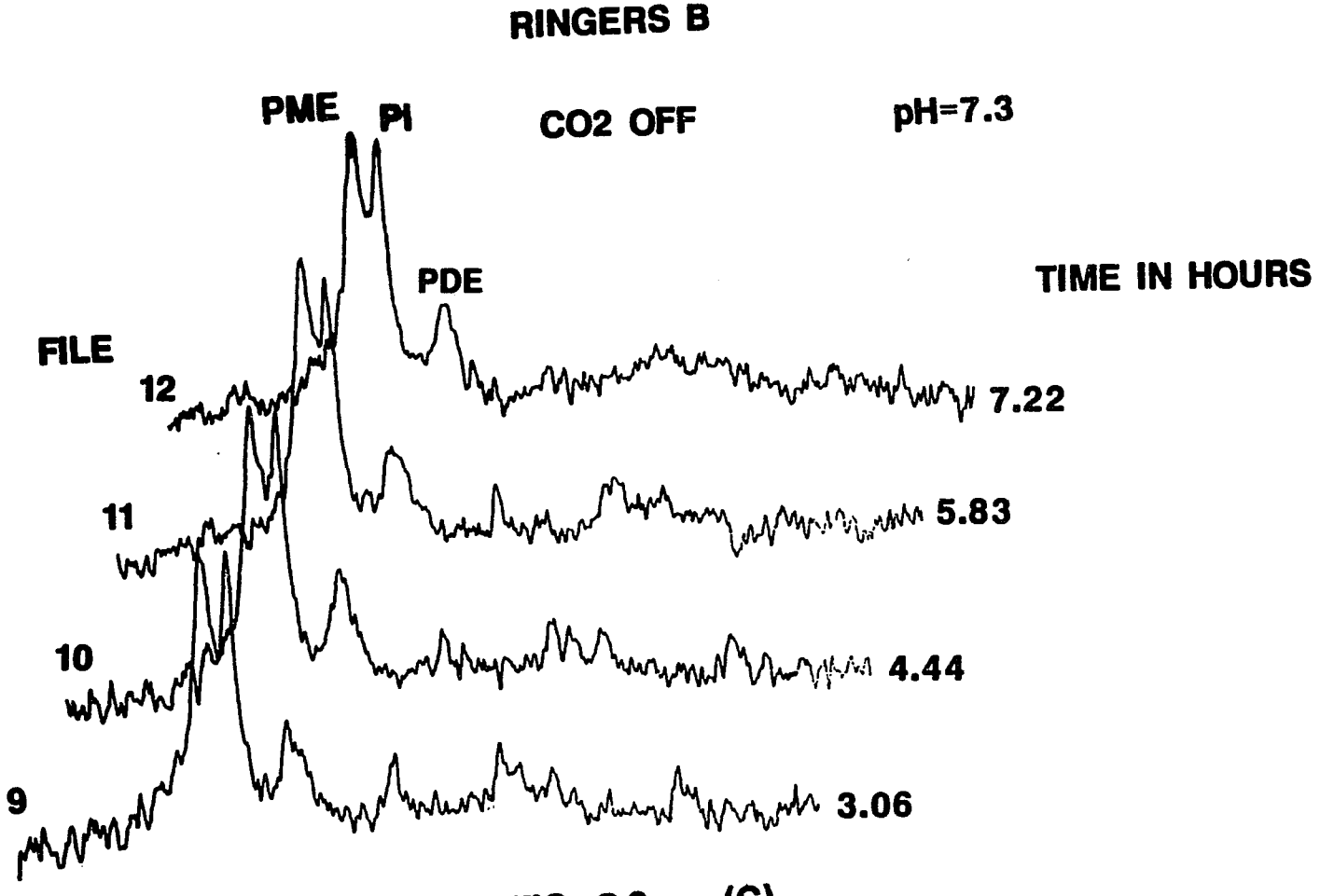
RINGERS B
PME
PI
CO2 OFF
pH=7.3
PDE
TIME IN HOURS
FILE
12
7.22
11
5.83
10
4.44
9
3.06

FIG. C2 (C)

DIFFERENCE

BETWEEN

FILE 1 AND FILE 9

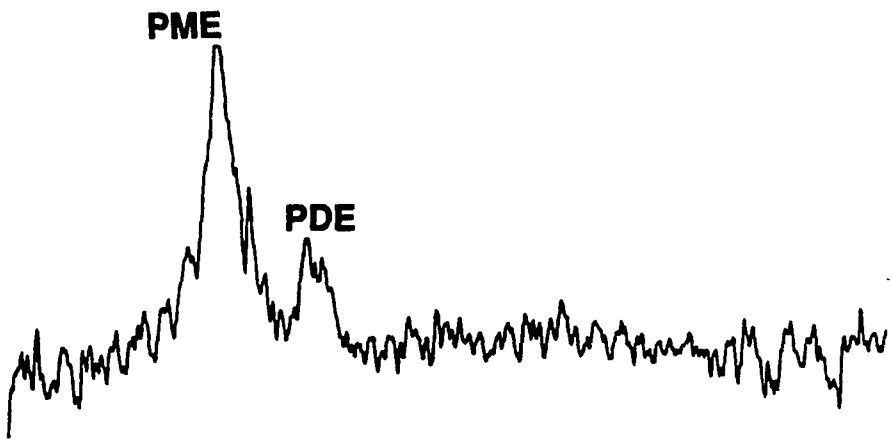

FIG C2 (D)

Fig. C-3

RINGERS B ONLY

N1E-115 cells were superfused with complete medium (files 1 and 2) and then switched to a Ringers B with FBS but without glucose, Pi or Na (files 3 to 5). The superfusing Ringers B solution was not recirculating. After 50 minutes the cells were switched to Ringers without Pi, Na or FBS (files 6, 7 and 8). After another 50 minutes, an 8 mM final concentration of Na was added to the same Ringers and the system was switched to recirculating (files 9, 10 and 11) for another 50 minutes. Finally the cells used returned to complete the medium (not shown). Each file is from 1000 FID with a repetition time of 1 second.

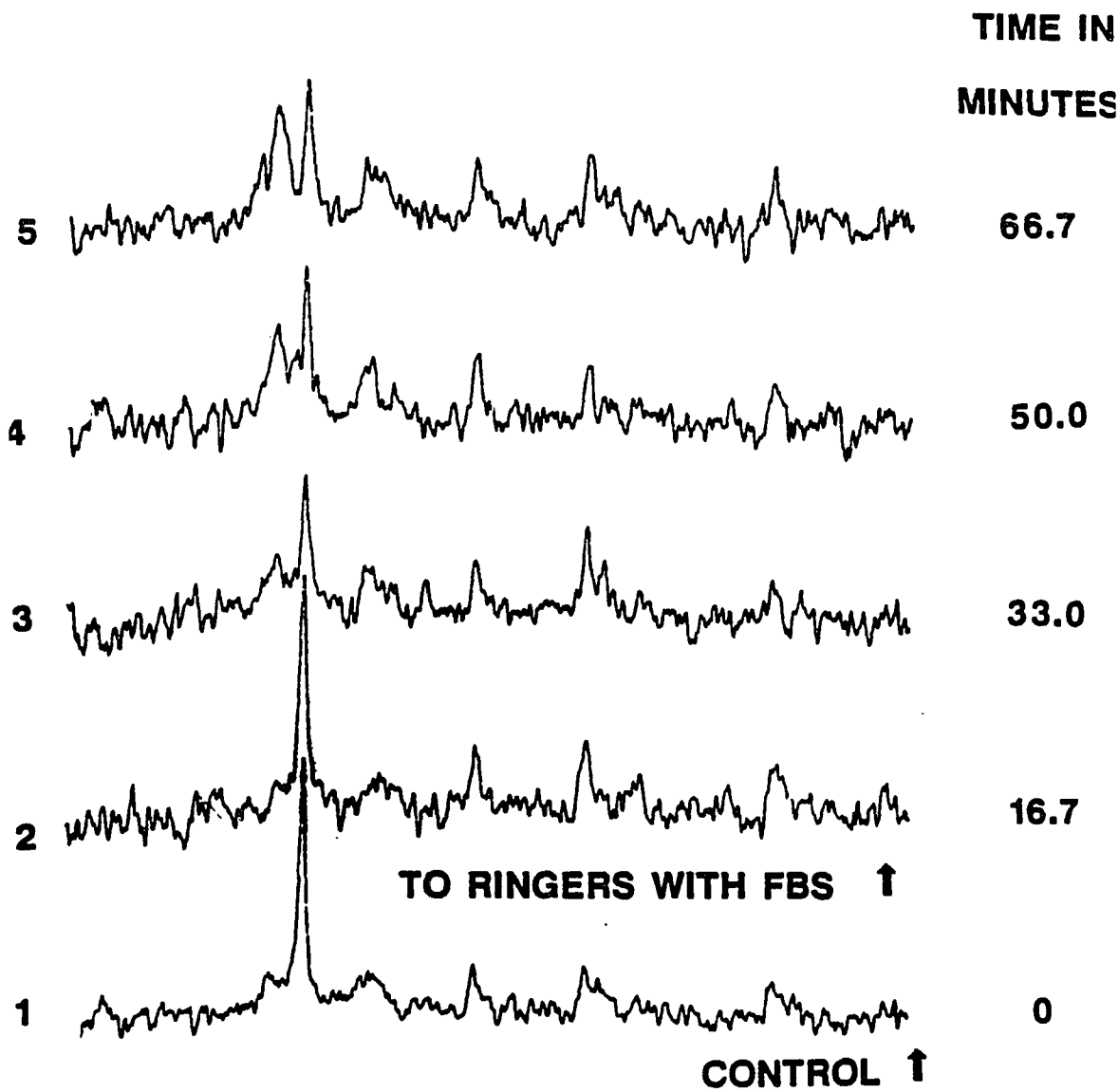
TIME IN
MINUTES
5
66.7
4
50.0
3
33.0
2
16.7
TO RINGERS WITH FBS
1
0
CONTROL

FIG. C3 (A)

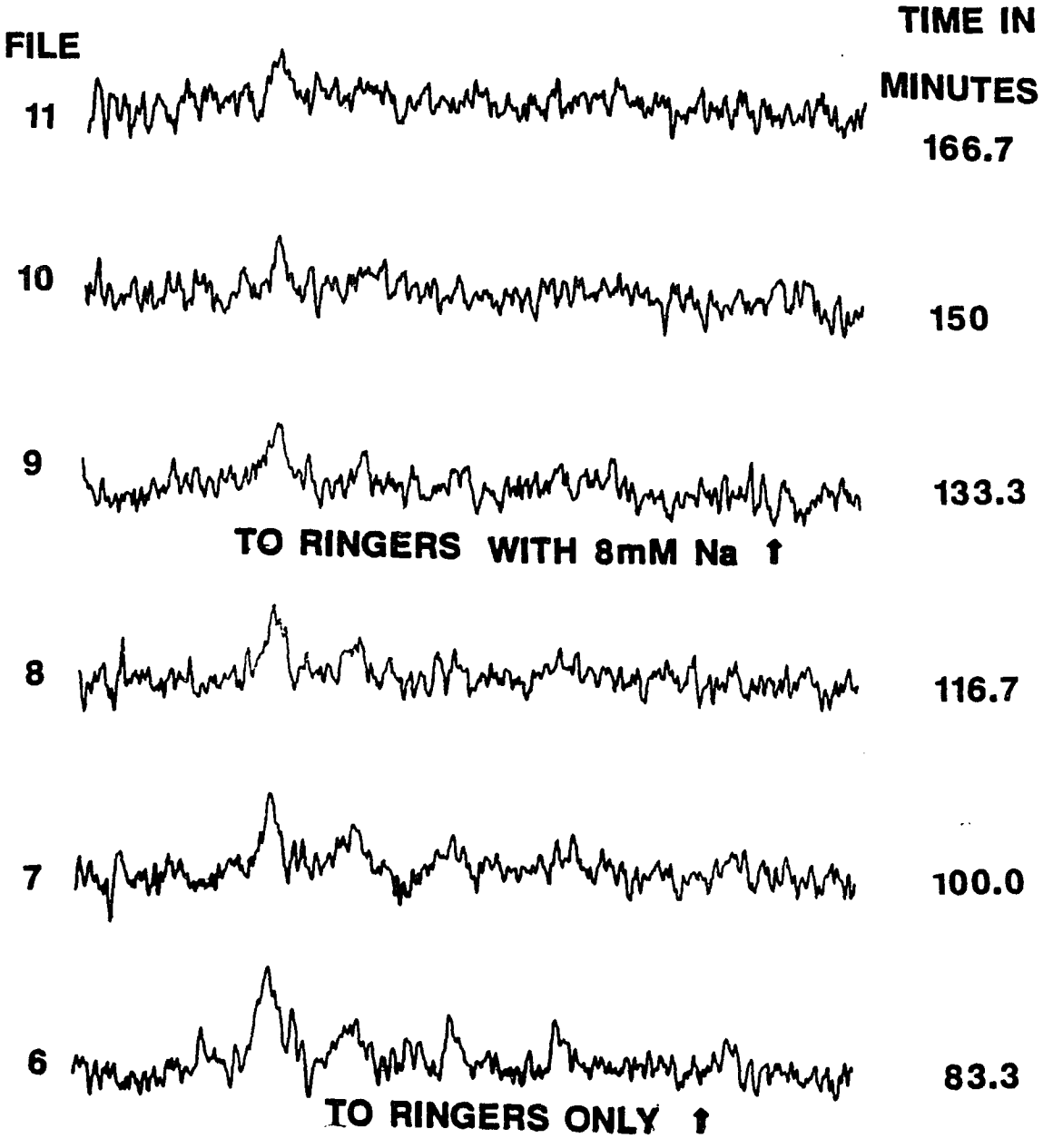
FILE
TIME IN MINUTES
11
166.7
10
150
9
133.3
TO RINGERS WITH 8mM Na ↑
8
116.7
7
100.0
6
83.3
TO RINGERS ONLY ↑

FIG. C3 (B)

Fig. C-4

a) N1E-115 cells. The control was superfused with DMEM + 10% FBS. 2000 FID per file were collected in a 33.3 minute period.

b) The cells were switched to Ringers with a glucose supplement with no Pi and no FBS. The system was operated in a non recirculating mode until 105 ml of medium had been flushed out. This took approximately 30 minutes. The system was then put back in the recirculating mode. Files 2, 3, and 4 show a small PME and Pi profile. File 5 shows a small increase in both of these regions. (D) shows subsequent files taken in 67 minute blocks. These spectra show a gradual increase in the PME, PDE and Pi regions with a concomitant decrease in the ATP.

What was not known at the time this experiment was run was that the warm, (33° C) medium returning from the sample holder formed an unmixed layer on top of the cold medium (4° C) in the medium resevoir and mixed with the bulk of the medium in a gradual way. Thus the data in panel (B) and (C) can be interpreted in the following way. When the control cells were switched to Ringers without Pi, the Pi peak appeared to wash out and the cells remained energized for up to 2.5 hours. During this time the residual FBS and Pi mixed with the resevoir of glucose supplemented Ringers and brought about the changes seen (C). The system was washed through with a volume of Ringers (105 ml) equal to

twice that of the unswitched volume before circulating with approximately 400 ml of Ringers was started.

The magnitude of Pi in the sample holder at the time recirculating started had to be less than that of file 1 in (B) which is much less than the (A) File 4, at most 1/10 (the value of Pi in (A) 4). This dilution compounded with a 1/10 dilution of the dead volume with the Ringers resevoir brought the dilution factor down to 1/100. This suggests that the effects seen in (C) are highly amplified reactions of, say, small quantities of hormones present in the residual FBS, or an unusual mix of inorganic factors, i.e., salts acting on the cells. The source of the large increase of Pi was probably due to the hydrolized ATP with some of the Pi being retained in the cells, some used to form PME and PDE and some spilled into the medium. These results have not been unraveled.

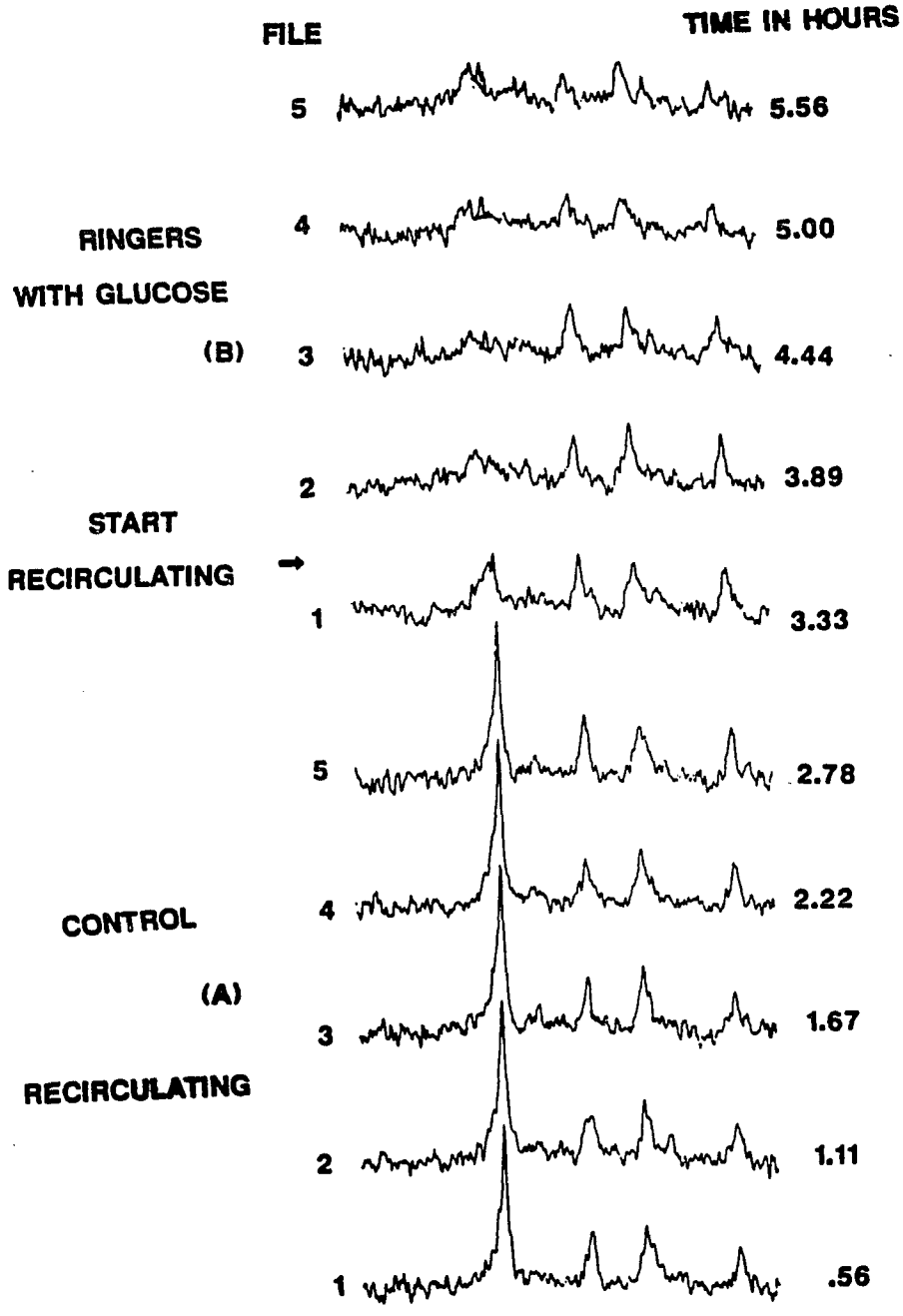
FILE
TIME IN HOURS
5
5.56
RINGERS
WITH GLUCOSE
(B)
4
5.00
3
4.44
2
3.89
START
RECIRCULATING
1
3.33
5
2.78
CONTROL
(A)
4
2.22
3
1.67
RECIRCULATING
2
1.11
1
.56

FIG. C4 (A)–(B)

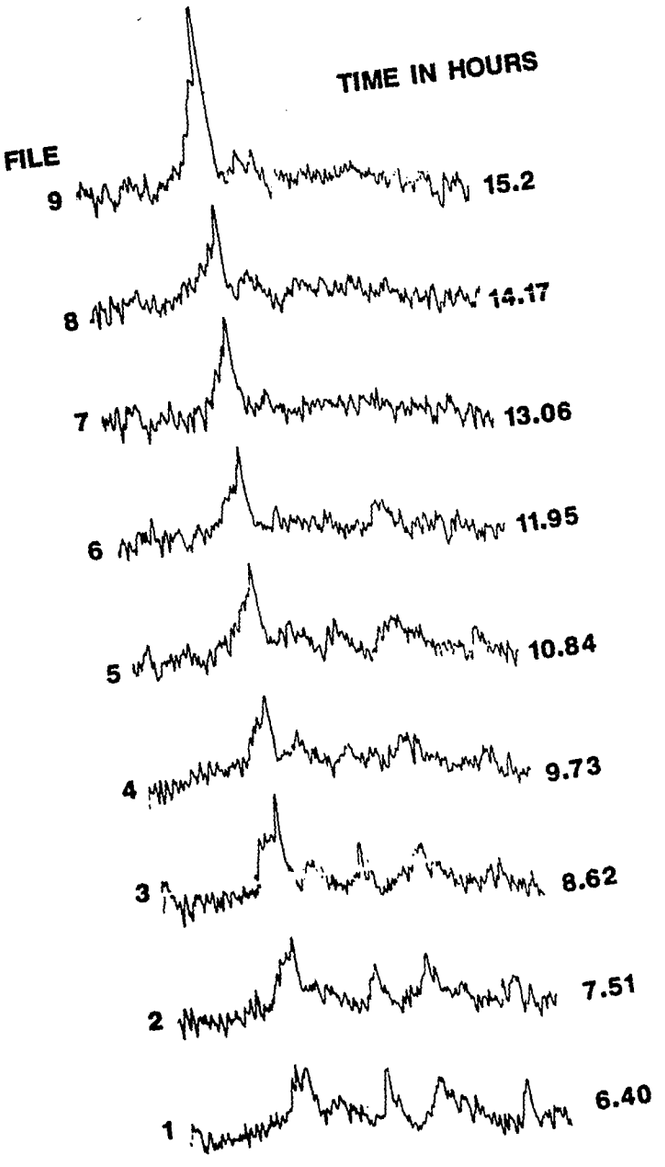
TIME IN HOURS
FILE
9
15.2
8
14.17
7
13.06
6
11.95
5
10.84
4
9.73
3
8.62
2
7.51
1
6.40

FIG. C4 (C)

APPENDIX D

Properties of N1E-Cells

Cell Lineage:

C1300, mouse neuroblastema cells, were found in an A/J mouse and were first reported in 1959 (Stewart, et al., 1959). The establishment of a functional clonal line was reported in 1969, (Augusti-Tocco and Sato, 1969). N1E-115, a clone of the C1300, was obtained and reported on by Amano, (Amano, et al., 1972).

Physical Characteristics:

The modal number of chromosomes is 192. Cells grown in suspension are tetraploid (Augusti-Tocco and Sato, 1969). Cells grown on a substrate are 50% octaploid (Augusti-Tocco and Sato, 1969). Giemsa stains show C1300 cells grown in suspension to be round and 40 μm in diameter - they contain 1-3 nuclei. Cells attached to a substrate vary from 40 to 150 μm in diameter and contain 1-8 nuclei. Cells have a diffused system of endoplasmic reticulum and associated virus particles. Two populations of mitochondria exist, one normal to slightly shrunken in size and the other one swollen (Schubert, et al., 1969). There are multivesicular, lysosomal bodies, and dense-core vesicles which have homogeneous contents. These are found in the cytoplasm with a maximum diameter of 0.4 μm (Augusti-Tocco and Sato, 1972).

Undifferentiated cells in normal growth medium:

In a confluent state, the population is a heterogeneous population of mostly round cells, some cells with poorly developed neurites and a small number of well-differentiated cell with cell bodies greater than 40 μm in diameter. When replated these cells have a doubling time of 4-6 days. Two to four days after replating there is a transient increase in the number of cells bearing neurites (Augusti-Tocco, G. and Sato, G., 1969). Exponentially growing cells when replated have a doubling time of 24 hours. Three major enzymes have been looked at in these cells when they have not differentiated but are in stationary growth phase (Augusti-Tocco, G. and Sato, G., 1969).

Tyrosine hydroxylase - specific activity in stationary cells is 40-fold that of logarithmically dividing cells, and is 980 pmol/minute/mg protein in stationary phase cells (Amano, T. et al., 1972; Guroff, G., 1980).

Acetylcholinesterase - specific activity in stationary cells is 25-fold that in logarithmically dividing cells. The value is 256,000 pmol/minute/mg protein (Amano, T. et al., 1972).

Cholineacetyltransferase - specific activity is 4-fold that of logarithmically growing cells. The value is 0.1 pmol/minute/mg protein in undifferentiated cells (Amano, T. et al., 1972).

Differentiation:

In the first reports of C1300 cells grown *in vitro* there were observations and characterizations of some of the cells which appeared to be differentiated (Augusti-Tocco and Sato, 1969). Burmeister reviewed 59 agents which had been used to induce various neuroblastoma cell lines to differentiate, nineteen of which were used on C1300 cells and five of these specially for N1E-115 cells (Burmeister, 1982). The cells differentiated in terms of their morphological, biochemical and electrophysiological profiles. To date 2% DMSO + 10% FBS supplemented DMEM has been the best characterized (Kimhi, et al., 1976). Their work suggested that cell morphology, the induction of neurospecific enzymes and electrical differentiation were not necessarily linked and that all three modes of differentiation could be expressed independently.

Cells differentiated via addition of 2% DMSO from replated confluent cells results in:

1) Proliferation being completely inhibited.

2) A lag period (2-4 days) for process formation.

3) The presence of long processes by day 4-8.

4) A stable condition for a period of over 4 weeks.

The longer the cells were in a confluent state prior to replating in DMSO, the higher the percentage of differentiated cells and the shorter the lag in process formation. 25% of the cells remained round in aggregates (Kimhi, et al., 1976).

DMSO removal result in:

1) Resumed growth after a delay of one to two weeks.

2) Cells which exhibit malignancy when injected into A/J mice.

It was unclear whether this is due to a small yet undifferentiated subpopulation or not. (Kimhi, et al., 1976).

Biochemical measurements from confluent cells which were induced to differentiate:

AChE activity:

1) decreases 90% on trypsinization of confluent cells.

2) when plated with 2% DMSO it returns toward pretrypsinization rate in the same way that the control (0% DMSO) does. In 12 days it has recovered to 50%. (400 nmol/mg protein/min at day 0, 200 nmol/mg protein/min at day 12.).

TH activity:

1) decreases to 10% of its original value before trypsinization of confluent cells.

2) The control returns slowly. At day 12 it is back to 40% of its original value. Those plated with 2% DMSO remain at the 10% value and do not return.

cAMP

1) decreases 10% in first 2 days after replating in 2% DMSO. The level is down 20% relative to control by day 5 to 12 pmol of CAMP/mg of protein (Kimhi 1976).

2) adenosine when added to cells leads to a 2-fold increase in cAMP and the R020-1724, a phosphodiesterase inhibitor, has the same effect. The two

together, however, lead to a 27-fold increase in the cAMP level (Blume, A. J., et al., 1973).

Glycoproteins:

2% DMSO induces a glycoprotein (Mr = 200,000). The protein is in the neurites of differentiated N1E-115 cells but not in the cell body or undifferentiated cells (Littauer, et al., 1980).

Enolase, neuron-specific:

There is a significant increase in the γgene product expressed as $X\gamma$ enolase during differentiation. A specific event at differentiation of most neurons is the transition of the enolase from the XX form to the $X\gamma$ and then to the $\gamma\gamma$ form (Lamande, et al., 1985).

Electrophysiological Properties:

The rest potential after 8 days in 2% DMSO is -45.1 ± 3 mV. There is a 25% increase between day 3 to day 8. The rate of change of voltage of the action potential dV/dt evoked from a standard resting potential of -90 mV/second generated by a hyperpolerization current was 78.4 ± 11, a prolonged depolarizing current (500 μsec.) resulted in a repetitive action potential numbering 4 to 5 in this time interval (Kimhi, et al., 1976). Several ions have been identified as contributing to currents generated by voltage-dependent channels.

Na^+:

There is a fast inward Na^+ channel, which is blocked by tetrodotoxin (Hugues, et al. 1981). Single Na^+ channels have been observed by the patch clamp technique. They are reversibly blocked by pancuronium, modulated by BTX, and are present in low density (maximum of $20/\mu m^2$, a value consistent with slow kinetics). The mean sodium channel conductance is $\simeq 15$ pS. Inward currents generated in response to a membrane depolarization of -40 mV have a normal amplitude but also have a prolonged open time, $i = 1.3 \pm 0.3$ pA with an open time of 16.7 ± 0.9 μsec (Quandt and Yeh, 1986).

DPH (diphenylhydantoin) has been found to enhance inactivation and induce a block of Na^+ channels which develop in response to repetitive depolarization (Matsuki, et al., 1984). Voltage dependent channels have also been reported by Aldrich and Gellen (1983).

K^+:

There is a delayed outward Et_4N^+ sensitive, and a slow Ca^{++} dependent, Et_4N^+ insensitive current in differentiated N1E-115 cells. The undifferentiated cells do not have this Ca^{++} dependent conductance (Hugues et al., 1981).

Ca^{++}:

Calcium channel density in the growth cone and cell soma are about the same and are higher than in the neurite. The existence was shown by elicting an action potential in the soma and observing changes in the calcium concentrations in the soma, neurite and growth cone. In addition it has been shown that the amplitude of the prolonged after-hyperpolarization (AHP) reflected the change in magnitude of the cytosolic Ca^{++} (Bolsover and Spector, 1986).

Stretch Activated-Channels:

Falk (1986) reported a stretch-activated cation specific, non-selective channel. It is sensitive to voltage, membrane deformation and may be sensitive to calcium.

Amino acid transport and receptors:

phenylalamine:

The K_T (the concentration at 1/2 V_{max}) is nearly the same for all amino acids. The range is 1×10^{-4} to 1×10^{-5} M and is not dependent on Na^+ or energy (Breakefield 1976).

tyrosine:

Tyrosine is inhibited by agents which attack sulfhydryl groups. dbcAMP increases long term uptake (Breakefield 1976).

choline:

Choline has a high affinity uptake $K_T = 5 \times 10^{-6}$ to 10^{-7} M, V_{max} ranges .3 to 70 pmoles/min/mg protein only 0.1-0.5% goes into acetylcholine; the rest goes into phosphatidylcholine (Breakefield 1976).

Taurine:

The uptake of taurine into N1E-115 cells has a K_T of 2.1×10^{-5} M and a V_{max} of 127 pmoles/min/mg protein (Breakefield 1976).

GLOSSARY

2DG	=	2-deoxyglucose
2DP	=	adenosine diphosphate
AMP	=	adenosine 5^1-monophosphate
ATP	=	adenosine triphosphate
BME	=	Basal medium Eagle
CPK	=	Creatine phosphokinase (also known as creatine kinase)
Cr	=	Creatine
DG6P	=	deoxyglucose-6-phosphate
DMEM	=	Dulbecco's modified Eagle's medium
DMO	=	5,5-dimethyl-2,4-oxazdiolinedione
DMSO	=	dimethylsulfoxide
DPG	=	diphosphoglycerate
DRBC	=	dissociated rat brain cells
DBS	=	fetal bovine serum
FFT	=	fast Fourier transform
FID	=	free induction decay
GPC	=	glycerophosphorylcholine
IBS	=	isotonic buffer solution
NAD, NADH	=	nicotinamide adenine dinucleotide (diphosphopyridine

nucleotide)

NAD, NADPH = nicotinamide adenine dinucleotide phosphate (triphasphopyridine nucleotide) and its reduced form

NCS = newborn calf serum

PCh = phosphocholine

PCr = phosphocreatine

PDE = phosphodiester

PEt = phosphoethanolamine

pHi = intracellular pH

Pii = Pi internal

PME = phosphomonoester

PPA = phenylphosphonic acid

RF = radio frequency

ZAM = A completely defined serum-free medium.

BIBLIOGRAPHY

Ahmed, Z., Walker, P. S., Fellows, R. E., 1983. Properties of neurons from dissociated fetal rat brain in serum-free culture. J. Neurosci. 3: 2448-2462.

Akeson, R. and Herschman, H. R., 1974. Modulation of cell-surface antigens of a murine neuroblastoma. Proc. Natl. Acad. Sci. U.S.A. 71:187-191.

Amano, T., Richelson, E., Nirenberg, M., 1972. Neurotransmitter synthesis by neuroblastoma clones. Proc. Natl. Acad. Sci. U.S.A. 69: 258-263.

Augusti-Tocco, G. and Sato, G., 1969. Establishment of functional clonal lines of neurons from mouse neuroblastoma. Proc. Natl. Acad. Sci. U.S.A. 64:311-315.

Barton, J., Den Hollander, J. A., Lee, T. M., MacLaughlin, A., Shulman, R. G., 1980. Measurement of the internal pH of yeast spores by ^{31}P nuclear magnetic resonance. Proc. Natl. Acad. Sci. U.S.A. 77: 2470-2473.

Block, F., Hansen, W. W., and Packard, M., 1946. Nuclear induction. Phys. Rev. 69:127.

Blume, A. J., Dalton, C., Sheppard, H., 1973. Adenosine-mediated elevation of cyclic 3':5" -adenosine monophosphate concentrations in cultured mouse neuroblastoma cells. Proc. Natl. Acad. Sci. U.S.A. 70: 3099-3102.

Bolinger, L., Gyulai, L., Chance, B., Leigh, J. S., 1984. Identification of a major component of the monoester region of the phosphorus NMR spectra of neonate and puppy brain.

Boonstra, J., Mummery, C. L., van Zoelen, E. J. J., van der Saag, P. T., de Laat,

S. W., 1982. Monovalent cation transport during cell cycle (review). Anticancer Res. 2: 265-274.

Brown, T. R., Gadian, D. G., Garlick, P. B., Radda, G. K., 1978. In: *Frontiers in biological energetics.* Dulton, L., Leigh, S., Scarpa, A., eds Vol. 2, Academic Press, New York.

Brown, T. R. and Ugurbil, K., 1984. Nuclear magnetic resonance. In: *Structural and resonance techniques in biological research.* Rousseau, D. L., ed. Academic Press, Orlando, Fla., pp. 1-88.

Burmeister, D. W., 1982. Process formation in the human neuroblastoma clone SK-N-SH-SY5Y *in vitro.* Thesis, City University New York.

Campbell, I. D., Dobson, C. M., Williams, R. J. P., Xavier, A. V., 1973. Resolution enhancement of protein NMR spectra using the difference between a broadened and a normal spectrum. J. Mag. Res. 11: 172-181.

Casey, R. P., Njus, D., Radda, G. K., and Sehr, P. A., 1977. Active proton uptake by chromaffin granules: observations by amine distribution and phosphorus - ^{31}P NMR techniques. Biochem. 16:972-976.

Chalzonitis, A., Greene, L. A., and Nirenberg, M., 1974. Electrophysiological characteristics of chick embryo sympathetic neurons in dissociated cell culture. Brain Res. 68:235-252.

Cohen, S. M., Ogawa, S., Rottenberg, H., Glynn, P., Yamane, T., Brown, T. R., Shulman, R. G., and Williamson, J. R., 1978. ^{31}P NMR nuclear magnetic

resonsance studies of isolated rat liver cells. Nature 273:554-556.

Cohen, S. M., Ogawa, S., and Shulman, R. G., 1979. ^{13}C NMR studies of gluconeogenesis in rat liver cells: utilization of labeled glycerol by cells from euthyroid and hyperthyroid rats. Proc. Natl. Acad. Sci. USA 76:1603-1607.

Cohn, M. and Hughes, T. R., Jr., 1962. Nuclear magnetic resonance spectra of adenosine di- and triphosphate. J. Biol. Chem. 237: 176-181.

Daly, M. and Seifter, S., 1980. Uptake of creatine by cultured cells. Biochem. Biophys. 203: 317-324.

Dennis, E. A. and Pluckthun, A., 1984. Phosphorus-31 NMR of phospholipids in Micelles. In: *Phosphorus-31 NMR principles and applications.* Academic Press, Orlando, Fla., pp. 423-4460.

Deuel, R. K., Yue, G. M., Sherman, W. R., Shickner, D. J., and Ackerman, J. J. H., 1985. Monitoring the time course of cerebral deoxyglucose metabolism by ^{31}P nuclear magnetic resonance spectroscopy. Science 228:1329-1331.

Deutsch C., Taylor, J. S., and Wilson, D. F., 1982. Regulation of intracellular pH by human peripheral blood lymphocytes as measured by ^{19}F NMR. Proc. Natal. Acad. Sci. USA 79:7944-7948.

Fishman, R. S. and Karnovsky, M. L., 1983. J. Neurochem. 46:371.

Folbergrova, J., MacMillan, V., Siesjo, B. K., 1972. The effect of moderate and marked hypercapnia upon the energy state and upon the cytoplasmatic

NADH/NAD+ ratio of the rat brain. J. Neurochem. 19: 2497-2505.

Foxall, D. L. and Cohen, J. S., 1983. NMR studies of perfused cells. J. Mag. Res. 52: 346-349.

Gadian, D. G., 1982. *Nuclear magnetic resonance and its applications to living systems.* Clarenden Press, Oxford.

Gadian, D. G., 1982b. Nuclear magnetic resonance and its applications to living systems. Clarenden Press, Oxford, p. 157.

Gadian, D. G., Hoult, D. I., Radda, G. K., Seeley, P. J., Chance B., and Barlow, C., 1976. Phosphorus nuclear magnetic resonance studies on anoxic and ischemic cardiac tissue. Proc. Natl. Acad. Sci. USA 73:4446-4448.

Glynn, P., Brown, T. R., Ugurbil, K., and Chappell, R., 1983. Intracellular pH, 2 deoxyglucose and sugar phosphate profile changes in morphologically differentiated neuroblastoma N1E-115 cells. Biophys. J. 41:72a.

Glynn, P., Lee, T. M., Ogawa, S., 1987. The levels of phosphoethanolamine and phosphocholine in intact neuroblastoma cells. Annals N.Y. Acad. Sci., pp. 474-475.

Gupta, R. K. and Gupta, P., 1984. NMR studies of intracellular metal ions in intact cells and tissues. Ann. Rev. Biophys. Bioeng. 13: 221-246.

Gupta, R. K. and Yushok, W.D., 1980. Noninvasive ^{31}P NMR probes of free MG2+, MgATP, and MgADP in intact Ehrlich ascites tumor cells. Proc. Natl. Acad. Sci. U.S.A. 77: 2487-2491.

Guroff, G., 1980. *Molecular Neurobiology*, Marcel Dekker, Inc. New York.

Haffke, S. C. and Seeds, N. W., 1975. Neuroblastoma: The e. Coli of neurobiology? Life Science 16: 1649-1657.

Honeggar, P., 1985. Biochemical differentiation in serum-free aggregating brain cell cultures. In: *Cell Culture in the Neurosciences*, Bottenstein, J. E., and Sato, G., eds., Plenum Press, New York, pp. 223-244.

Horton, R. W., Meldrum, B. S., Bachelard, H. S., 1973. Enzymic and cerebral metabolic effects of 2-deoxy-D-glucose. J. Neurochem. 21: 507-520.

Hoult, D., Busby, S. J. W., Gadian, D. G., Radda, G. K., Richards, R. R., and Seeley, P. J. 1974. Observation of tissue metabolites using ^{31}P NMR nuclear magnetic resonance. Nature 252:286-289.

Hoult, D. I., 1978. The NMR receiver: A description and analysis of design. In: *Progress in Nuclear Magnetic Resonance Spectroscopy*, Emsley, J. W., et al., eds Pergamon Press Ltd., Oxford, pp. 41-77.

Iles, R. A., Stevens, A. N., Griffiths, J. R., 1982. NMR studies of metabolites and living tissue. In: *Progress in Nuclear Magnetic Resonance Spectroscopy*, Emsley, J. W., et al., eds. Pergamon Press, Ltd., Oxford, pp. 49-199.

Jacobus, W. E., Taylor, G. J., Hollis, D. P., and Nunnally, R. L. 1977. Phosphorus nuclear magnetic resonance of perfused working rat hearts. Nature 265:756-758.

Karczmar, G. S., Koretsky, A. P., Bissell, M. J., Klein, M. P., Weiner, M. W., 1983. A devise for maintaining viable cells at high densities for NMR studies. J. Mag. Res. 53: 123-128.

Kass, I. S. and Lipton, P., 1982. Mechanisms involved in irreversible anoxic damage to the in vitro rat hippocampal slice. J. Physiol. 332:459-472.

Kimhi, Y., Palfrey, C., Spector, I., Barak, Y., Littauer, U. Z., 1976. Maturation of neuroblastoma cells in the presence of dimethylsulfoxide. Proc. Natl. Acad. Sci. U.S.A. 73: 462-466.

Kuby, S. A., Noda, L., Lardy, H. A., 1954. Adenosinetriphosphate-creatine transphosphorylase: Isolation of the crystalline enzyme from rabbit muscle. J. Biol. Chem. 209: 191-201.

Kuby, S. A. and Noltmann, E. A., 1962. ATP - Creatine transphosphorylase. In: *The Enzymes*, Vol. 6, 2nd ed., Boyer, B. D., ed., Academic Press, New York, pp. 515.

Lamande, N., Zeitoun, Y., Gros, F., Legault, L., 1985. Regulation of neuron-specific enolase isozyme levels during differentiation of murine neuroblastoma cell cultures. Neurochem. Int. 7: 867-874.

Littauer, U. Z., Giovanni, M. Y., Glick, M. C., 1980. A glycoprotein from neurites of differentiated neuroblastoma cells. J. Biol. Chem. 255: 5448-5453.

Mabe, H., Glomgvist, P., Siesjo, B. K., 1983. Intracelluar pH in the brain

following transient ischemia. J. Cereb. Blood Flow Metab. 3: 109-114.

MacMillan, V. and Siesjo, B. K., 1973. The influence of hypocapania upon intracellular pH and upon some carbohydrate substrates, amino acids and organic phosphates in the brain. J. Neurochem. 21: 1283-1299.

Matthes, P. M., Bland, J. L., Gadian, D. G., Radda, G. K., 1982. A ^{31}P-NMR saturation transfer study of the regulation of creatine kinases in the rat heart. Biochim. Biophys. Acta. 721: 312-320.

Maris, J. M., Evans, A., McLaughlin, A., Bolinger, L., Chance, B., 1984. *In vivo* ^{31}P studies of human neuroblastoma. Soc. Mag. Res. in Medicine. Abstr. 3rd annual meeting.

Maris, J. M., Evans, A. E., Bolinger, L., McLaughlin, A. C., Chance, B., 1986. Analysis of the metabolism of lipid precursors in human neuroblastoma by phosphorus-31 NMR spectroscopy. Mag. Res. Cancer, Proc. Int. Conf., pp. 501-502.

Martin, M. L., Martin, G. J., Delpuech, J. J., 1980. ***Practical NMR Spectroscopy.*** Heyden and Sons, Ltd., London.

Meldrum, B. S. and Horton, R. W., 1973. Cerebral functional effects of 2-deoxy-D-glucose and 3-0-methylglucose in rhesus monkeys. Electroencephalogr. Clin. Neurophys. 35: 59-66.

Microcarrier cell culture principles and methods, 1981. Pharmacia Fine Chemicals, Uppsala, Sweden.

Moolenaar, W. H., Tsien, R. Y., van der Saag, P. T., de Laat, S. W., 1983. Na+/H+ exchange and cytoplasmic pH in the action of growth factors in human fibroblasts. Nature 304: 645-648.

Moon, R. B. and Richards, J. H., 1973. Determination of intracellular pH by ^{31}P magnetic resonance. J. Biol. Chem. 248: 7276-7278.

Morrison, J. F. and White, A., 1967. Isotope exchange studies of the reaction catalyzed by ATP: creatine phosphotransferase. European J. Biochem. 3: 145-152.

Naruse, S., Hirakawa, K., Horikawa, Y., Tanaka, C., Higuchi, T., Ueda, S., Nishikawa, H., Watari, H., 1985. Measurements of *in vivo* ^{31}P nuclear magnetic resonance spectra in neuroectoermal tumors for the evaluation of the effects of chemotherapy. Cancer Res. 45: 2429-2433.

Navon, G., Ogawa, S., Shulman, R. G., and Yamane, T. 1976. ^{31}P NMR nuclear magnetic resonance studies of Ehrlich ascites tumor cells. Proc. Natl. Acad. Sci. USA 74:87-91.

Nelson, T., Lucignani, G., Sokoloff, L., 1986. Measurement of brain deoxyglucose metabolism by NMR. Science 232: 776.

Noda, L., Kuby, S., Lardy, H. A., 1954. Adenosinetriphosphate-creatine transphosphorylase: equilibrium studies. J. Biol. Chem. 210: 83-94.

Ogawa, S., Lee, T. M., 1982. Proton stoichiometry of Adenosine 5'-triphosphate synthesis in rat liver mitochondria studied by phosphorus-31 nuclear

magnetic resonance. Biochem. 21: 4467-4473.

Ogawa, S., Lee, T. M., Glynn, P., 1986. Energy metabolism in rat brain *in vivo* studied by ^{31}P nuclear magnetic resonance: changes during postnatal development. Arch. Biochem. Biophys. 248: 43-52.

Ogawa, S., Rottenberg, H., Brown, T. R., Shulman, R. G., Castillo, C. L., Glynn, P., 1978. High-resolution ^{31}P nuclear magnetic resonance study of rat liver mitochondria. Proc. Natl. Acad. Sci. U.S.A. 75: 1796-1800.

Ogino, T., den Hollander, J. A., and Shulman, R. G., 1983. ^{23}Na and ^{31}P studies of ion transport and intracellular pH in yeast. Biophys. J. 41:283a.

O'Sullivan, W. J. and Cohn, M., 1966. Magnetic resonance investigations of the metal complexes formed in the manganese-activated creatine kinase reaction. J. Biol. Chem. 241: 3104-3115.

Perrin, D. D. and Sharma, V. S., 1966. The stability constants of metal-adenosine triphosphate complexes. Biochem. Biophys. Acta. 127: 35-41.

Prasad, K. N., Hsie, As. S. 1977. Morphologic differentiation of mouse neuroblastoma cells induced *in vitro* by dibutyryl adenosine 3':5"-cyclic monophosphate. Nature New Biol. 233: 141-142.

Prichard, J. W., Alger, J. R., Behar, K. K., Petroff, O. A. C., Shulman, R. G., 1983. Cerebral metabolic studies *in vivo* by ^{31}P NMR. Proc. Nat. Acad. Sci. U.S.A. 80: 2748-2751.

Prichard, J. W. and Shulman, R. G., 1986. NMR spectroscopy of brain metabolism *in vivo*. Ann. Rev. Neurosci. 9:61-85.

Quandt, F. N. and Yeh, J. Z., 1986. Slow inactivation of single Na channels induced by diphenylhydantoin. Soc. Neurosci. Abstr. 12: 45.

Rabi, I. I., Zacharias, J. R., Millman, S., Kusch, P., 1938. A new method of measuring nuclear magnetic moment. Phys. Rev. 53:318.

Richelson, E., 1975. The culture of established clones for neurobiologic investigation. In: *Metabolic compartmentation and neurotransmission*, Ber. S., eds Plenum Press, N.Y.

Ross, B. D., 1972. *Perfusion techniques in biochemistry*. Oxford Univ. Press., London.

Saez, J. C., Hall, D. H., Kessler, J. A., Benett, M. U. L., Spray, D. C., 1984. Superoxide dismutase (SOD) increases survival of cultured sympathetic neurons exposed to a brief period of starvation. Soc. Neurosci. Abstr. 10: 886.

Salhany, J. M., Yamane, T., Shulman, R. G., Ogawa, S., 1975. High resolution ^{31}P NMR nuclear magnetic resonance studies of intact yeast cells. Proc. Nat. Acad. Sci. USA 72:4966-4970.

Schubert, D., Humphreys, S., Baroni, C., Cohn, M., 1969. *In vivo* differentiation of a mouse neuroblastoma. Proc. Natl. Acad. Sci. 64: 316-323.

Shulman, R. G., 1979. *Biological Applications of Magnetic Resonance.*

Academic Press, New York.

Shoubridge, E. A., Briggs, R. W., Radda, G. K., 1982. ^{31}P NMR saturation transfer measurements of the steady state rates of creatine kinase and ATP synthetase in the rat brain. FEBS Letters 140: 288-292.

Siesjo, B. K., 1978. Metabolism of substrates in the brain. *Brain Energy Metabolism*, John Wiley & Sons, Chichester, p. 180.

Smith, G. A., Hesketh, R. T., Metcalfe, J. C., Feeney, J., Morris, P., 1983. Intracellular calcium measurements by ^{19}F NMR of fluorine-labeled chelators. Proc. Natl. Acad. Sci. USA 80:7178-7182.

Sokoloff, L., 1984. *Metabolic probes of central nervous system activity in experimental animals and man.* Magnes Lecture Series Vol. I. Sinauer Assoc., Sunerland, MA, pp. 5-6.

Sokoloff, L., 1977. Relation between physiological function and energy metabolism in the central nervous system. J. Neurochem. 29:13-26.

Sokoloff, L., 1982. The radioactive deoxyglucose method. In: *Advances in neurochemistry*, Agranoff, B. W. and Aprison, M. H., eds. Plenum, New York, pp. 1-82.

Spector, I., Kimhi, Y., and Nelson, P. G., 1973. Tetrodotoxin and cobalt blockage of neuroblastoma action potentials. Nature New Biol. 246:124-126.

Stewart, H. L., Snell, K. C., Dunham, L. J. Schlyen, S. M., 1959. *Transplantable*

and transmissible tumors of animals. Armed Forces Inst. of Pathol., Wash, D.C., pp. 337.

Sundler, Roger and Akesson, B., 1975. Regulation of phospholipid biosynthesis in isolated rat hepatocytes. J. Biol. Chem. 250: 3359-3366.

Sundler, R., 1975. Ethanolaminephosphate cytidylytransferase. Purification and characterization of the enzyme from rat liver. J. Biol. Chem. 250: 8585-8590.

Tuttle, J. B. and Richelson, E., 1974. Regulation of electrical activity in mouse neuroblastoma clone N1E-115, Soc. Neurosci. (Abstr.), p. 455.

Ugurbil, K., Guernsey, D. L., Brown, T. R., Glynn, P., Tobkes, N., Edelman, I. S., 1981. ^{31}P NMR studies of intact anchorage-dependent mouse embryo fibroblasts. Proc. Natl. Acad. Sci. U.S.A. 78: 4843-4847.

Ugurbil, K., Brown, T. R., den Hollander, J. A., Glynn, P., and Shulman, R. G., 1978. High resolution ^{13}C nuclear magnetic resonance studies of glucose metabolism in escherichia coli. Proc. Natl. Acad. Sci. USA. 75:3742-3746.

Watts, D. C., 1973. Creatine kinase. In: *The Enzymes.* Vol. 6, 2nd ed. Boyer, B. D., ed., Academic Press, New York. p. 383.

Wu, S. T., Pieper, G. M., Salhany, J. M., Eliot, R. S., 1981. Measurement of free magnesium in perfused and ischemic arrested heart muscle. A quantitative phosphorous-31 nuclear magnetic resonance and multiequilibria analysis. Biochem. 20: 7399-7403.

Zelinski, T. A. and Choy, P. C., 1982. Phosphatidylethanolamine biosynthesis in isolated hamster heart. Can. J. Biochem. 60: 817-823.